1994

Adamantane-like Clusters Of The Zinc-group Elements

Yuyang Wu

ADAMANTANE-LIKE CLUSTERS OF THE ZINC-GROUP ELEMENTS

by

Yuyang Wu

Department of Chemistry

Submitted in partial fulfilment
of the requirements for the degree of
Doctor of Philosophy

Faculty of Graduate Studies
The University of Western Ontario
London, Ontario
March, 1994

ISBN 0-315-90560-3

Canada

ABSTRACT

Three new types of chalcogenate-bridged adamantane-like clusters of the zinc-group elements have been studied in detail: those with alkylthiolates as bridging ligands, formulated as $[(\mu\text{-SAlk})_6(MX)_4]^{2-}$ (Alk = Me, Et, 1-Pr, 2-Pr, 1-Bu, 2-Bu, *c*-C_6H_{11} (Cy), or CH_2Ph (Bz); M = Zn, Cd, or Hg; X = Cl, Br, or I); those with phosphines as terminal ligands, formulated as $[(\mu\text{-ER})_6(CdPPh_3)_{4-n}(Cd)_n]^{2+}$ (E = S or Se; R = 1-Pr, 2-Pr, 1-C_5H_{11} (1-Pe), Cy, or Ph; n = 0, 1, or 2); and those with halides as bridging ligands, formulated as $[(\mu\text{-ER})_{6-m}(\mu\text{-X})_m(MX)_4]^{2-}$ (E = S or Se; R = Et, 1-Pr, 2-Pr, 1-Bu, Cy, or Ph; m = 0, 1, or 2; X = Cl, Br, or I; M = Cd or Hg). In total, seventy-one new clusters have been isolated analytically pure; more than one hundred species have been characterized in solution by multinuclear magnetic resonance; and three representative crystal structures have been obtained by X-ray analysis (carried out by others).

In general, for the adamantane-like species, the metal chemical shift, δ_{Cd} or δ_{Hg}, varies with R in the order primary alkyl > secondary alkyl > phenyl, with X in the order Cl > Br > I, and with temperature in the order reduced T > ambient T. In a study of the mixed-metal clusters, $[(\mu\text{-SAlk})_6(MX)_{4-n}(M'X)_n]^{2-}$, (M/M' = Cd/Zn, Cd/Hg, or Hg/Zn), δ_{Cd} varies with n in the order 0 > 1 > 2 > 3 in $Cd_{4-n}Zn_n$ or $Cd_{4-n}Hg_n$ mixtures, while δ_{Hg} varies with n in the order 0 < 1 < 2 < 3 in the $Hg_{4-n}Cd_n$ mixture, but in the order 0 > 1 > 2 > 3 in $Hg_{4-n}Zn_n$ mixture. For the mixed-halide clusters, $[(\mu\text{-SPr}^i)_6(CdX)_{4-n}(CdX')_n]^{2-}$ (X/X' = I/Br, I/Cl, or Br/Cl), it has been shown that when X is heavier than X', δ_{Cd} varies with n in the order 0 < 1 < 2 < 3 for CdX site, and in the order 1 < 2 < 3 < 4 for CdX' site. In $[(\mu\text{-ER})_6(Cd_APPh_3)_{4-n}(Cd_B)_n]^{2+}$, δ_{Cd} varies with n in the order 0 < 1 < 2 for Cd_A or Cd_B.

Importantly, for Cd_B, the PPh_3-free site, the terminal position can be occupied by $OClO_3^-$ giving tetrahedral coordination geometry about the Cd. In $[(\mu\text{-}ER)_{6-m}(\mu\text{-}X)_m(MX)_4]^{2-}$, halides participate in bridging. When m = 2, the two bridging halides prefer to form a trans-$(\mu\text{-}X)_2$ structure. These results provide model data for studies on metallothioneins and other biological systems with metal-cysteine sites.

ACKNOWLEDGMENT

I would like to thank my supervisor, Dr. Philip A.W Dean, for his guidance, patience, and constant encouragement during the course of this study. Without his help and support, this work would not have been possible.

I would also like to thank my step-supervisor, Dr. R.J. Puddephatt, for his concerns and for making arrangement for my thesis defence while Dr. Dean is spending his sabbatical time in Australia.

I am grateful to my many friends and to the staff in this Department for their help and friendship. My special thanks go out to Dr. J.J. Vittal and Dr. N.C. Payne for their assistance in providing single crystal X-ray analyses, and to Susan England for expert technical assistance with the NMR facilities.

My thanks are also extended to my parents for their emotional support and encouragement during my years at Western, and to my wife Tracy for her love and support.

TABLE OF CONTENTS

LIST OF FIGURES

LIST OF TABLES

ABBREVIATIONS

Alk	alkyl
Ar	aryl
Bu	butyl
Bz	benzyl
cat	cation
Cy	cyclohexyl
Cys	cysteine or cysteinyl
δ	chemical shift
Δ	difference
E	chalcogenate element
edt	ethane-1,2-dithiolate
Et	ethyl
J	coupling constant
L	ligand
M	metal
Me	methyl
MT	metallothionein
μ	bridging
NHD	normal halogen dependence
$\nu_{1/2}$	line width
pdt	propane-1,3-dithiolate
Pe	pentyl
Ph	phenyl
Pr	propyl
R	alkyl or aryl
S_2-dur	durene-α,α'-dithiolate
S_2-xyl	xylene-α,α'-dithiolate
σ	screening constant
X	halogen or halide

CHAPTER 1 INTRODUCTION

1.1 General Comments

The study of adamantane-like clusters is a specialized area in inorganic chemistry. The interest in this area is mainly due to: (1) the specific structure and coordination geometry; (2) the dynamics of metal exchange and ligand exchange; (3) the stability of the cluster with variation in temperature, atmosphere, solvent and/or reaction medium; (4) mutual influence of thiolate coordination and metal oxidation state; finally and most importantly (5) the use of the clusters as models for biological systems. The basic adamantane cage structure of $M_4E_6L_4$ is shown in Fig. 1.1.

Not many reviews have been concerned with this area in detail. There was only one published in 1992.[1] A few reviews have brief coverage of this chemistry.[2-5]

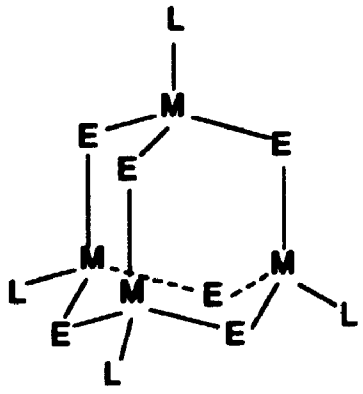

Fig. 1.1 Structure of adamantane-like $M_4E_6L_4$. M = metal ions, E = chalcogenated bridged ligands, L = terminal ligands (E, or P, or X, or empty).

The adamantane-like structure of $M_4E_6L_4$ was first described for $[Co_4(SPh)_{10}]^{2-}$ in the mid-1970s.[6,7] Since then numerous other adamantanoid cage compounds have been discovered. Most of the complexes have zinc group elements as their metal ions. For non-zinc group metals in the II oxidation state, only about eight clusters have been structurally characterized. They are $[Mn_4(SPh)_{10}]^{2-}$ [8], $[Fe_4(SPh)_{10}]^{2-}$ [9], $[Fe_4(SEt)_{10}]^{2-}$ [10], $[Fe_4(SPh)_6Cl_4]^{2-}$ [11], $[Fe_4(SCH_2Ph)_6Br_4]^{2-}$ [12], $[Co_4(SPh)_{10}]^{2-}$ [6,7], $[Co_4(SPh)_6Cl_4]^{2-}$ [13], and $[Co_4(SPh)_6Cl_2(PPh_3)(OPPh_3)]$ [13]. Besides these M^{II}_4 clusters, some M^{I}_4 and M^{III}_4 clusters have been subjected to X-ray analysis: $[Cu_4(SPh)_6]^{2-}$ [14], $[Cu_4(SMe)_6]^{2-}$ [14b], $[Cu_4(o\text{-}\{SCH_2\}_2C_6H_4)_3]^{2-}$ [15a], $[Cu_4(SC_3H_6S)_3]^{2-}$ [15b], $[Cu_4(SC_2H_4S)_3]^{2-}$ [15b], $[Ag_4(o\text{-}\{SCH_2\}_2C_6H_4)_3]^{2-}$ [16a], $[Ag_4(Te\{C_4H_3S\})_6]^{2-}$ [16b], $[Al_4I_4(SCH_3)_4S_2]$ [17a], and $[Ga_4I_4(SCH_3)_4S_2]$ [17b]. The clusters of Al and Ga have the same structure like those of M^{II}_4 (see Fig. 1.1), however, the clusters of Cu and Ag are somewhat different. M^{I}_4 clusters have the adamantane-like skeletons, but they do not have terminal ligands.

Adamantane-like clusters of the zinc group elements were first reported in the early 1980s[18-20]. Soon after, a lot of zinc group clusters were studied in the solid state and/or, especially, in solution by the multi-nuclear NMR techniques. These clusters could be divided into 3 types.

Type 1. $[(\mu\text{-}ER)_6(MER)_4]^{2-}$ (R = Ph)

E = S, M = Zn [9,21-23]

E = S, M = Cd [9, 21-25]

E = Se, M = Zn [26,27]

E = Se, M = Cd [27, 28, 31]

Type 2. $[(\mu\text{-}ER)_6(MX)_4]^{2-}$ (R = Ph)

E = S or Se, M = Zn or Cd, X = Cl, Br or I [29,30]

E = S or Se, M = Zn or Cd, X - NCO or NCS [31]

E = S, Se or Te, M = Hg, X = Cl, Br or I [32]

Type 3. $[(\mu\text{-ER})_6(ML)_4]^{2+}$ (M = Hg)

E = S or Se, R = Ph or alkyl, L = PPh_3, PEt_3 or $AsPh_3$ [33]

E = Te, R = Ph or alkyl, L = PPh_3, PEt_3, PBu^n_3, $P\{4\text{-}C_6H_4Cl\}_3$ or $P\{4\text{-}C_6H_4Me\}_3$ [34]

E = S, Se or Te, R = Ph or alkyl, L = $SPPh_3$, $SePPh_3$, $SPCy_3$ or $SePCy_3$ [35]

It is worthwhile to mention that very close to type 3, there is another group of mercury complexes, formulated as $[(\mu\text{-TePh})_6(HgL)_n(HgL')_{4-n}]^{2+}$, where n = 3; L = PPh_3, $P\{4\text{-}C_6H_4Cl\}_3$ or $P\{4\text{-}C_6H_4Me\}_3$; L' = DMF or "empty" (probably ClO_4^- coordinated).[34]

1.2 Biological Connections

Many of the clusters of zinc group elements have thiolate ligands. Complexes of this type are of interest as models for the chemical and spectroscopic properties of metallothionein(s) (MT) and other metal binding proteins MT was first reported in a 1957 study that was concerned with the distribution of cadmium in horse kidney tissue.[36] The protein contains unusually high proportions of cysteinyl residues that are able to provide the bridging and terminal thiolate coordination required for formation of clusters $M_x(S\text{-}Cys)_y$. Aromatic amino acids, histidine and disulfide are usually absent. Generally, there are seven moles of M^{2+} per 20 to 21 SH groups of MT.[4] For example, the proteins M_7-MT (M = Zn, Cd) from mammals have two discrete clusters, $M_4(S\text{-}Cys)_{11}$

and M_3(S-Cys)$_9$, in which the cluster M_4(S-Cys)$_{11}$ bears a close resemblance to the various $M_4E_6L_4$ that are described in this thesis. Structural details of M_7-MT are known from ^{113}Cd NMR[37] and X-ray analysis[38], so they will not be discussed here. The study of these model clusters is potentially of help in modelling those biological systems which have metal-cysteine coordination sites, such as {Zn(S-Cys)$_4$} and {Zn(S-Cys)$_2$(His)(OH)$_2$} in liver alcohol dehydrogenase (LADH)[39].

1.3 Structural Properties

The structure of the $(\mu\text{-ER})_6(ML)_4$ cluster is very interesting. For each M, the metal coordination is tetrahedral, $(\mu\text{-ER})_3ML$. For each bridging ER, the chalcogenate coordination is a trigonal pyramid, M_2ER (not including the lone pair). The four M atoms are arrayed as a tetrahedron. Each of the six edges of the M_4 tetrahedron is bridged by a chalcogenate ligand (see Fig. 1.1). Another point of view is that the six bridging chalcogenate atoms are arrayed as an octahedron. The four M atoms are at the midpoints of, and outside, the four faces of the octahedron. (see Fig 1.2)

Considering the whole cage structure, commonly known as the "adamantanoid" cage structure, $(\mu\text{-ER})_6(ML)_4$ contains four fused six-membered rings, $(\mu\text{-ER})_3M_3$, each in a chair conformation. For this *octahedro*-$(\mu\text{-E})_6$-*tetrahedro*-M_4-*tetrahedro*-L_4 core, T_d symmetry is possible, but the substituent R groups usually break this high symmetry, even for a simpler model of $(\mu\text{-ER})_6M_4$ core cage. Configurational isomerism can occur through the substituent R groups attached to the E atoms adopting either axial (a) or equatorial (e) dispositions with respect to the E_3M_3 chairs. This possibility was first recognized by Dance *et al* in 1983[14], then completed by Vittal *et al* in 1987[30]. Each

substituent R is common to two six-membered rings. Thus, although there are a total of six axial and six equatorial possibilities for the substituents on the six bridging atoms of $(\mu\text{-ER})_6M_4$, it needs to pointed out that R being axial in one ring must lead to the same R being equatorial in another. Therefore only four configurational isomers are possible. They are isomer I [aaa, aae, aee, eee], isomer II [aae, aae, aae, eee], isomer III [aae, aae, aee, aee], and isomer IV [aaa, aee, aee, aee]. Thus, the symmetries of $(\mu\text{-ER})_6M_4$ are much lower than $(\mu\text{-E})_6M_4$ or $(\mu\text{-E})_6(ML)_4$. The symmetries of isomers I and III are C_1, and II and IV are C_3. (see Fig. 1.3)

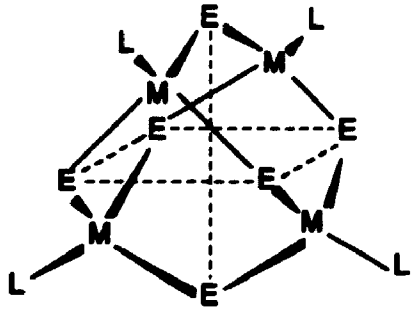

Fig. 1.2 Structure of $M_4E_6L_4$, emphasizing the octahedral E_6

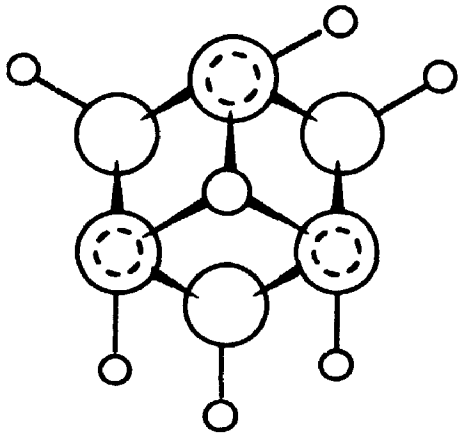

Isomer I

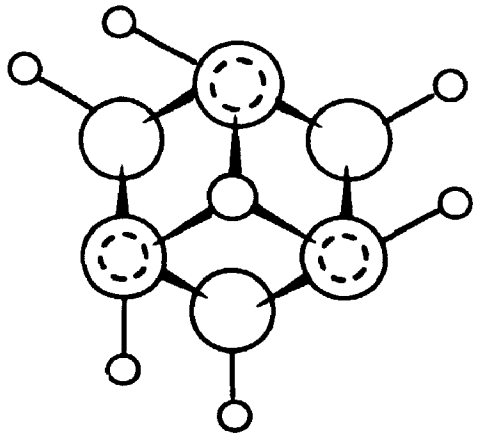

Isomer II

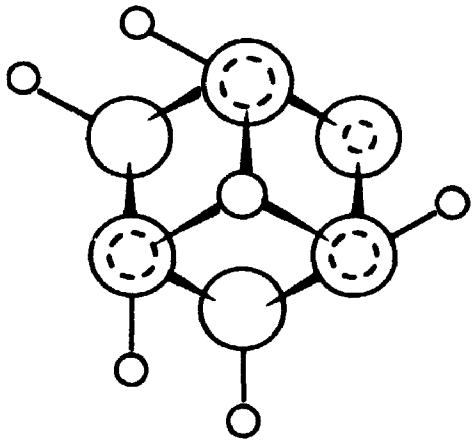

Isomer III

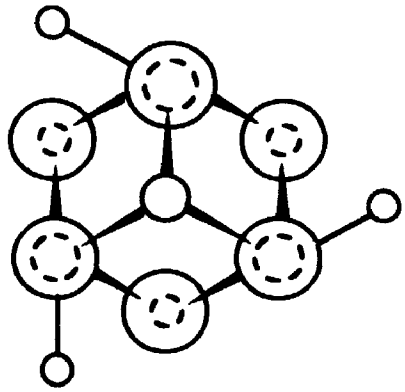

Isomer IV

Fig. 1.3 Configurational isomerism in adamantanoid $(\mu\text{-ER})_6M_4$. All isomers are represented as projectional drawings. The largest circles stand for E atoms; the medium circles stand for M atoms; the smallest circles stand for the carbon atoms in R groups.

1.4 NMR Properties

The zinc group elements have $d^{10}s^2$ electronic structures, and the cations M(II) have d^{10} structures. There is no d-d spectrum for M(II) and this property determines that Vis-UV spectroscopy is not suitable for studying the clusters. X-ray diffraction is a very good method for their study, but this application is limited by two facts: (1) not all compounds can be developed into single crystals suitable for X-ray diffraction; (2) the structure of the cluster in the solid state may not always be the same as it is in solution. Therefore, the NMR technique has become a very important and powerful method for the study of adamantane-like clusters also.

The NMR technique has the following advantages: (1) it can be applied both in solid state and in solution, with solution state measurements being much more common; (2) multi-nuclei are now available for NMR measurement as a result of recent rapid development of this technique; (3) it is a relatively simple method compared to X-ray analysis; (4) dynamic information can be obtained; and (5) the NMR properties of model clusters are very helpful for the study of the more complex situations found at biologically occurring binding sites for metals.

The nuclei that have been useful for NMR in the present study are ^{1}H, ^{13}C, ^{31}P, ^{77}Se, $^{111/113}Cd$, and ^{199}Hg. Especially useful are those at the metal centre and those at bridging or terminal atoms that coordinate directly to the metals. The NMR properties of these nuclei are shown in Table 1.1.[40] Considering metal NMR, ^{67}Zn is not suitable for this study, because of its relatively low natural abundance (4.11%), low sensitivity relative to proton (0.00285), and its quadrupolar nature, which ensures that broad resonances are observed in many chemically interesting situations.[41] However, $^{111/113}Cd$

and ^{199}Hg are convenient probe nuclei, as are ^{77}Se in selenolate (bridging ligand) and ^{31}P in phosphine (terminal ligand). In addition, ^{1}H and ^{13}C NMR provide information about the nature of hydrocarbon residues and ^{1}H NMR provides information about stoichiometry. All of the nuclei listed in Table 1.1 have been measured in this thesis and the NMR spectroscopic details will be seen in separate chapters.

Table 1.1 NMR Properties of Some Nuclei [40]

Nucleus	Spin I	Natural Abundance(%)	Relative Sensitivity to ^{1}H
^{1}H	1/2	99.985	1.00
^{13}C	1/2	1.108	0.0159
^{31}P	1/2	100	0.0663
^{77}Se	1/2	7.58	0.00693
^{111}Cd	1/2	12.75	0.00954
^{113}Cd	1/2	12.26	0.0109
^{199}Hg	1/2	16.84	0.00567

1.5 Statistical Distribution of Isotopes

In NMR studies (especially $^{111/113}$Cd and ^{199}Hg), the statistical distribution of magnetically-active isotopes should be considered. In general, the population of isotopes $^{A}l_{x}{}^{B}l_{y}{}^{C}l_{n-x-y}$ is given by the following formula:[42]

$$P = n!a^{x}b^{y}c^{n-x-y} / x!y!(n-x-y)!$$

where a = fractional abundance of isotope ^{A}I, and so on,

x = number of isotope ^{A}I in the compound, and so on,

n = total number of sites involved.

Take ^{111}Cd in $Cd_4E_6L_4$ as an example (see Fig. 1.1 or Fig. 1.2). The natural abundance of ^{111}Cd is 12.75% (see Table 1.1). The population of isotopomers having one ^{111}Cd in $Cd_4E_6L_4$ (abbreviated as $^{111}CdCd_3$) is: $4!(0.1275)(0.8725)^3 / 1!3! = 0.3387$ Similarly, all ^{111}Cd populations in Cd_4 can be calculated by this method. Some values are listed in Table 1.2.

Table 1.2 Statistical populations of ^{111}Cd in Cd_4 †

Cluster	Calculation	Population
$^{111}Cd_0Cd_4$	$4!(0.1275)^0(0.8725)^4 / 0!4!$	0.5795
$^{111}Cd_1Cd_3$	$4!(0.1275)^1(0.8725)^3 / 1!3!$	0.3387
$^{111}Cd_1{}^0Cd_3$	$4!(0.1275)^1(0.7499)^3 / 1!3!$	0.2151
$^{111}Cd_1{}^{113}Cd_1{}^0Cd_2$	$4!(0.1275)^1(0.1226)^1(0.7499)^2 / 1!1!2!$	0.1055
$^{111}Cd_1{}^{113}Cd_2{}^0Cd_1$	$4!(0.1275)^1(0.1226)^2(0.7499)^1 / 1!2!1!$	0.0172
$^{111}Cd_2Cd_2$	$4!(0.1275)^2(0.8725)^2 / 2!2!$	0.0743
$^{111}Cd_2{}^0Cd_2$	$4!(0.1275)^2(0.7499)^2 / 2!2!$	0.0549
$^{111}Cd_2{}^{113}Cd_1{}^0Cd_1$	$4!(0.1275)^2(0.1226)^1(0.7499)^1 / 2!1!1!$	0.0179

† Cd represents all isotopes other than that which is specifically mentioned.

^0Cd represents all isotopes except ^{111}Cd and ^{113}Cd

In the case of $^{111}Cd_1Cd_3$, the ^{111}Cd in a tetrahedral Cd_4 cluster is chemically equivalent, but magnetically inequivalent, to the other three cadmium atoms, whether these three are ^{113}Cd or ^{0}Cd (^{0}Cd stands for nonmagnetically-active atoms). If the cluster is $^{111}Cd_1{}^{0}Cd_3$, the ^{111}Cd NMR will show only one line; but if it is $^{111}Cd_1{}^{113}Cd_1{}^{0}Cd_2$, the spectrum will show two lines caused by $^2J(^{111}Cd\text{-}^{113}Cd)$ coupling. Similarly, if the cluster is $^{111}Cd_1{}^{113}Cd_2{}^{0}Cd_1$ or $^{111}Cd_1{}^{113}Cd_3{}^{0}Cd_0$, the ^{111}Cd NMR spectrum will show three or four lines As can be seen from Table 1.2, the fractional population of $^{111}Cd_1{}^{113}Cd_2{}^{0}Cd_1$ is too small (0.0172; of course, that of $^{111}Cd_1{}^{113}Cd_3{}^{0}Cd_0$ is much smaller), therefore, such a contribution to the spectrum can be neglected. Following this analysis, the other contributions, such as $^{111}Cd_2{}^{113}Cd_2$, can be neglected also. Considering all possibilities, the theoretical ^{111}Cd NMR spectrum for the Cd_4 cluster should be a central line with two satellites, if some weak lines are neglected. Actually, not all the ^2J values are observed in practice, due to the broadness of the Cd NMR signals.

In some other cases, such as $Cd_4S_5X_5$, the four cadmium atoms may be chemically inequivalent. The ^2J coupling is caused not only by neighbouring ^{113}Cd, but also by chemically-inequivalent ^{111}Cd. Details will be seen in separate chapters.

If the measured isotope is ^{113}Cd, the method for calculation of isotope populations is the same for ^{111}Cd. The two bond coupling now is written as $^2J(^{113}Cd\text{-}^{111}Cd)$ or $^2J(^{113}Cd\text{-}^{111\ 113}Cd)$, depending on the chemical environment.

The treatment for ^{199}Hg is similar to ^{111}Cd, but simpler because ^{199}Hg, natural abundance = 16 84, is the only magnetically-active isotope in mercury.

1.6 Statistical Distribution of $[(\mu\text{-SR})_6(MX)_{4-n}(M'X)_n]^{2-}$ and $[(\mu\text{-SR})_6(MX)_{4-n}(MX')_n]^{2-}$

In this project, mixed-metal clusters $[(\mu\text{-SR})_6(MX)_{4-n}(M'X)_n]^{2-}$ (abbreviated by $M_{4-n}M'_n$) and mixed-halide clusters $[(\mu\text{-SR})_6(MX)_{4-n}(MX')_n]^{2-}$ (abbreviated by $(MX)_{4-n}(MX')_n$) have been studied in solution by metal NMR. If the mixtures start with 1:1 ratio of reactants and redistribution occurs statistically, the equilibrium amounts can be expressed by eqns. [1] and [2]. The skeletons of these mixed clusters are shown in Fig. 1.4.

[1] $$8\ M_4 + 8\ M'_4 = 1\ M_4 + 4\ M_3M' + 6\ M_2M'_2 + 4\ MM'_3 + 1\ M'_4$$

[2] $$8\ (MX)_4 + 8\ (MX')_4 = 1\ (MX)_4 + 4\ (MX)_3(MX') + 6\ (MX)_2(MX')_2 + 4\ (MX)(MX')_3 + 1\ (MX')_4$$

Consider M = Cd, M' = Zn and E = S as an example for the study of $M_{4-n}M'_n$. It can be seen from Fig. 1.4 that the four cadmiums in skeleton (b) are chemically equivalent. The chemical environment for each cadmium is $(\mu\text{-S})_3CdX$ (abbreviated by S_3CdX). However, the three cadmiums in (c) have the same chemical environment, $S_2S'CdX$ (S' stands for the S atom bridging between Cd and Zn), but they are chemically inequivalent to the cadmiums in skeleton (b). Similarly, in skeleton (d), two cadmiums are equivalent to each other with kernel SS'_2CdX, but they are inequivalent from that in both (b) and (c). In skeleton (e), there is only one cadmium with the coordination structure S'_3CdX, and of course this cadmium is chemically inequivalent to those in all (b), (c) and (d).

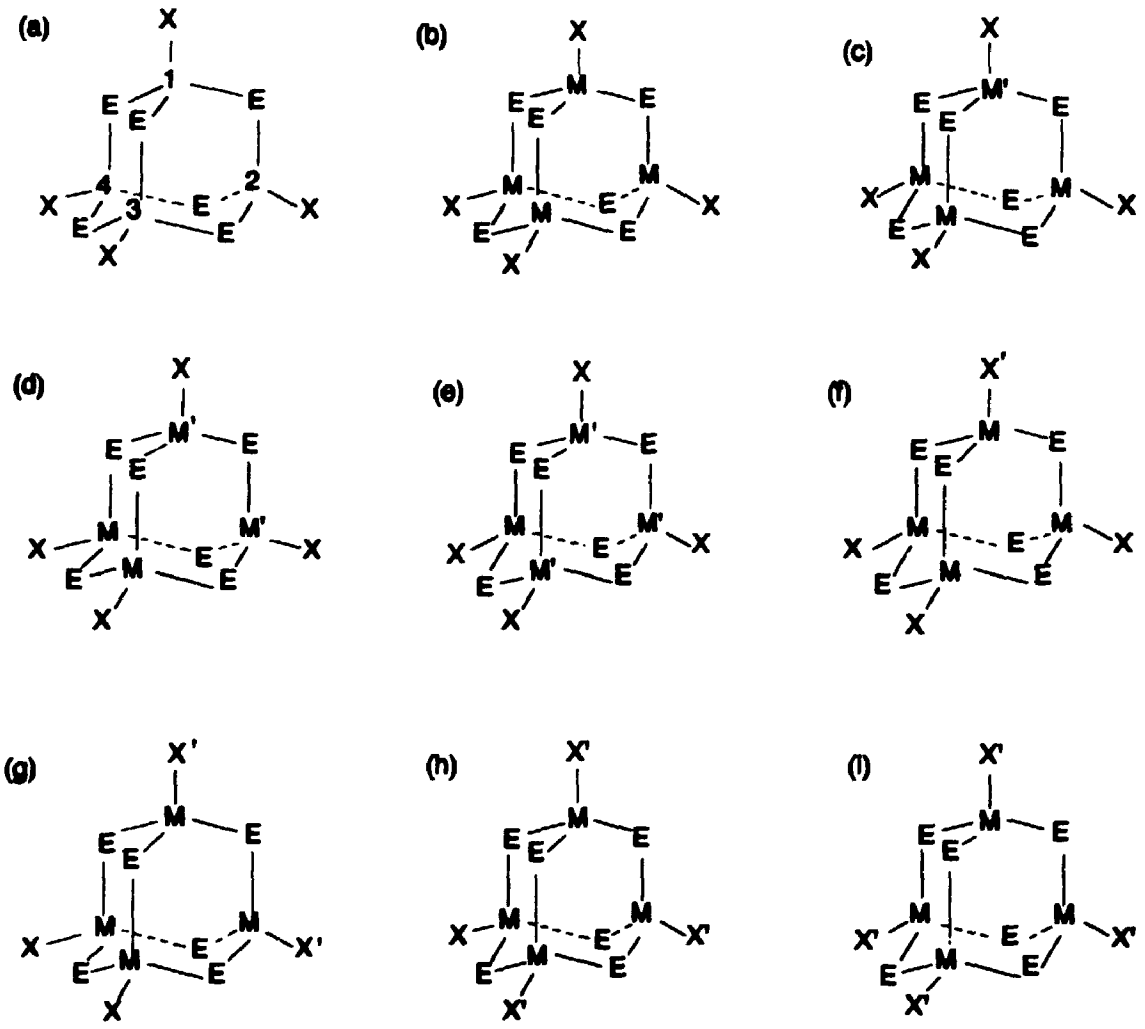

Fig. 1.4 The skeletons of $[(\mu\text{-ER})_6(MX)_{4-n}(M'X)_n]^{2-}$ and $[(\mu\text{-ER})_6(MX)_{4-n}(MX')_n]^{2-}$ (a): emphasizing four positions of metals; (b) - (e): showing structures of $M_{4-n}M'_n$, n = 0, 1, 2, 3; (f) - (i): $(MX)_{4-n}(MX')_n$, n = 1, 2, 3, 4.

According to the preceding analysis, there should be four signals in the metal NMR spectrum, when the samples are mixtures of Cd_4 and Zn_4. In addition, the intensity of the four signals could be 1:3:3:1, if the redistribution is a random process. This statistical phenomenon can be illustrated by Fig. 1.4. In the tetrahedral skeleton, there are four positions for the metals. For the cluster Cd_4, there is only one possibility to arrange these four cadmiums. Let it be labelled 1234. Therefore, the number of cadmiums with coordination kernel S_3CdX which contribute to the Cd NMR signal is $1\times4 = 4$. However, for Cd_3Zn, the three cadmiums can occur at positions 123, 124, 134, and 234 with equal probability. Thus, the total cadmium probability contribution is $4\times3 = 12$. Following this analysis, the number of probability contributions to NMR for all mixture formations is included below:

Cluster	Combination	No. of Cd
Cd_4	1234	$1\times4 = 4$
Cd_3Zn	123, 124, 134, 234	$4\times3 = 12$
Cd_2Zn_2	12, 13, 14, 23, 24, 34	$6\times2 = 12$
$CdZn_3$	1, 2, 3, 4	$4\times1 = 4$

In practice, the intensity ratio may not be 1:3:3:1, when one species in the mixture is more stable than the others, *i.e.* the redistribution is not statistical. In this case, the NMR spectrum will show an unexpectedly intense signal for the more stable species.

If the M/M' mixture is Cd/Hg or Hg/Zn, the result will be similar to that discussed above.

For the mixture $(MX)_{4-n}(MX')_n$, the possible skeletons are drawn in Fig. 1.4(b, f-i). Again take M = Cd and E = S as an example. In skeleton (f), it can be seen that the three cadmiums at positions 2, 3, and 4 are equivalent to each other, but inequivalent to that at position 1. Therefore, the cadmium at position 2 or 3 or 4 is labelled as $S_2S'CdX$ (S' stands for the S atom bridging between CdX and CdX') and the cadmium at position 1 is labelled as S'_3CdX'. The equally probable combinations of the three cadmiums ($S_2S'CdX$) are 123, 124, 134, and 234, *i.e.* 4×3 = 12. Correspondingly, the cadmium with coordination kernel S'_3CdX' can occur at positions 1, 2, 3 or 4 with equal probability, *i.e.* 1×4 = 4. However, the cadmium at position 3 or 4 in skeleton (f) is slightly different from that at the same position in (g). The latter two cadmiums are labelled SS'_2CdX and the probability combinations are 12, 13, 14, 23, 24, and 34. Meanwhile, the cadmium at position 1 in (f) is different from that at position 1 and 2 in (g). The latter two cadmiums are labelled as $S'_2S''CdX'$ (S'' stands for the S atom bridging between two CdX') and the probability combinations are the same to those two SS'_2CdX. Logical analysis in this way leads to the number of cadmium species in all different skeletons, as be tabulated below (Note: here there are two regions of interest, corresponding to Cd-X and Cd-X', and their difference in chemical shift is normally relatively large compared with those between S_3CdX and S'_3CdX where the coordination kernel of Cd is unchanged).

Skeleton	Species	Probabilty No. in Cd-X region	Species	Probabilty No in Cd-X' region
(b)	S_3CdX	1×4 = 4		
(f)	$S_2S'CdX$	4×3 = 12	S'_3CdX'	4×1 = 4
(g)	SS'_2CdX	6×2 = 12	$S'_2S''CdX'$	6×2 = 12
(h)	S'_3CdX	4×1 = 4	$S'S''_2CdX'$	4×3 = 12
(i)			S''_3CdX'	1×4 = 4

According to the analysis result above, we expect to see that in Cd NMR spectra of a 1:1 mixture of $(CdX)_4$:$(CdX')_4$ there are two groups of signals, corresponding to the regions of Cd-X and Cd-X', at intensity of 1:1. Within each region, there should be four signals with intensity ratio 1:3:3:1, if the linewidth is narrow enough. The real spectra and detailed discussion will be seen in following chapters.

1.7 Purpose of This Thesis

1.7.1 Looking for new clusters

Although more than a hundred adamantanoid clusters have been isolated and more than ten X-ray structural analyses have been reported, there are still a lot of gaps left in our knowledge of adamantane-like clusters of zinc group elements. Most of the clusters that are known have arylthiolates as bridging ligands; very few clusters with alkylthiolates have been studied.[1-5] For the purpose of comparison with metallothionein, clusters with alkylthiolates may be the better model compounds. Therefore, the search for new clusters that are better models for biochemical applications is the main purpose of this subject.

1.7.2 Collecting NMR data for model complexes

NMR is a very important tool in this research project. Without it, we could not fully characterize the new compounds, the metal coordination situations, the structures of the clusters in solutions, the redistribution of mixed metals or mixed terminal ligands or mixed bridging ligands between two different clusters, or the factors influencing cluster formation or decomposition (temperature, concentrations, solvents, *etc.*). Therefore, multi-NMR techniques must be applied in the study of zinc group clusters. Metal NMR plays a particularly important role in this study, because the results reflect directly the coordination spheres around the metal centres.

Through NMR studies, a lot of NMR data have been obtained. These data are helpful not only in the current context but also as model data for further investigation of metallothioneins.

1.7.3 Crystal structure studies

Complete information about coordination geometries in the clusters can be obtained directly by X-ray structural analysis (provided a solution of the structure can be made). The results give strong support to the existence of the adamantane-like clusters in solution. Also, comparison of these results with those of previous work may allow the discovery of natural "rules" governing the clusters. The significance of related crystal structures will be discussed later in separate chapters.

1.7.4 Specific Objectives

When this thesis work was started, we had some unsolved questions.

(1) Do clusters with alkylthiolates as bridging ligands exist in the solid state and/or solution? Do they exist for all the zinc group metals? Are they more stable than those with bridging arylthiolates?

(2) When phosphines act as terminal ligands in cadmium clusters, what is the coordination behaviour of those terminal ligands? Are vacancies in terminal coordination possible, and, if so, what is the maximum number that can occur, and under what conditions do they occur? Do other solvent molecules and/or anions in solution occupy "empty" positions?

(3) When halides take part in the coordination in adamantane-like clusters, can they act as bridging ligands, and, if so, what is the maximum number of bridging halides? Do the cadmium and mercury complexes behave in the same way in this case?

These questions will be answered in chapters 2-5.

1.8 Scope of Thesis

In this thesis, 71 new adamantane-like clusters have been isolated. More than one hundred cluster species have been characterized in solution by multi-NMR. Single crystals have been obtained of four representative compounds and these have been subjected to single crystal X-ray structural analysis by Drs. Vittal and Payne of this department. The chemistry of these adamantane-like clusters has been studied and some new properties are found.

The thesis is divided into six chapters:

Chapter 1. This chapter provides background information about adamantane-like clusters, especially those of zinc group elements, their biological connections, their NMR

and structural properties, their statistical distributions of the isotopes, and their probability formations of mixed clusters. A brief outline of this thesis is also presented.

Chapter 2. The results of a synthetic and multi-NMR study of the clusters of zinc and cadmium with alkylthiolates as bridging ligands are given. The existence of such alkylthiolate-bridged species is confirmed by the single crystal structural analysis of $(Et_4N)_2[(\mu\text{-}SPr^i)_6(CdBr)_4]$. The reaction of several cadmium complexes with elemental S and Se, as followed by multi-NMR, is described.

Chapter 3. Cadmium clusters with phosphines as terminal ligands are studied. The occurrence of phosphine-free cadmium centres is discovered both in the solid state and solution. This result is strongly supported by a structural analysis of $[(\mu\text{-}SPr^i)_6(CdPPh_3)_2(CdOClO_3)_2].EtOH$. In addition, some possible precursors to Cd_4 clusters have been found in solution by multi-NMR.

Chapter 4. Mercury clusters with alkylthiolates as bridging ligands and halides as terminal ligands are studied. Evidence is presented to show that halides can behave as bridging ligands in adamantanoid complexes, too. Metal NMR data are given for all the new species and the crystal structure of $(Ph_4P)_2[(\mu\text{-}SEt)_5(\mu\text{-}Br)(HgBr)_4]$ is described and discussed.

Chapter 5. Cadmium clusters containing both thiolates and halides in bridging positions have been studied. Their isolation and metal NMR spectra are reported. The results suggest that in the clusters $[(\mu\text{-}SR)_{6-n}(\mu\text{-}X)_n(MX)_4]$, when n = 2, the two halides prefer to occupy the *para*-bridged positions.

Chapter 6. A general summary and suggestions for future work are presented.

1.9 References

1. P.A.W. Dean and J.J. Vittal, in *Metallothioneins*, M.J. Stillman, C.F Shaw III and K.T. Suzuki, eds., VCH press, New York, 1992, ch. 14.
2. I.G. Dance, *Polyhedron*, 5 (1986) 1037.
3. P.J. Blower and J.R. Dilworth, *Coord. Chem. Rev.*, 76 (1987) 121.
4. R.H. Prince, in *Comprehensive Coordination Chemistry*, G. Wilkinson, R.D. Gillard, and J.A. McCleverty, eds., Pergamon Press, Oxford, 1987, V.5, p.972-3.
5. I.G. Dance, K. Fisher, and G. Lee, in *Metallothioneins*, M.J. Stillman, C.F. Shaw III and K.T. Suzuki, eds., VCH press, New York, 1992, ch. 13.
6. I.G. Dance and J.C. Calabrese, *J. Chem. Soc., Chem. Commun.*, (1975) 762.
7. I.G. Dance, *J. Am. Chem. Soc.*, 101 (1979) 6264.
8. T. Costa, J.R. Dorfman, K.S. Hagen, and R.H. Holm, *Inorg. Chem.*, 22 (1983) 4091.
9. K.S. Hagen, D.W. Stephan, and R.H. Holm, *Inorg. Chem.*, 21 (1982) 3928.
10. K.S. Hagen and R.H. Holm, *Inorg. Chem.*, 23 (1984) 418.
11. D. Coucouvanis, M. Kanatzidis, E. Simhon, and N.C. Baenziger, *J. Am. Chem. Soc.*, 104 (1982) 1874.
12. M.A. Whitener, J.K. Bashkin, K.S. Hagen, J.-J. Girerd, E. Gamp, N. Edelstein, and R.H. Holm, *J. Am. Chem. Soc.*, 108 (1986) 5607.
13. D. Fenske, J. Meyer, and K. Merzweiler, *Z. Naturforsch.*, 42 (1987) 1207.
14. (a) I.G. Dance, G.A. Bowmaker, G.R. Clark, and J.K. Seadon, *Polyhedron*, 2. (1983) 1031. (b) D. Coucouvanis, C.N. Murphy, and S.K. Kanodia, *Inorg. Chem.*, 19 (1980) 2993.

15. (a) J.R. Nicholson, I.L. Abrahams, W. Clegg, and C.D. Garner, *Inorg. Chem.*, 24 (1985) 1092. (b) M. Baumgartner, H. Schmalle, and E. Dubler, *Inorg. Chim. Acta*, 208 (1993)135.

16 (a) G. Henkel, P. Betz, and B. Krebs, *Angew. Chem. Int. Ed. Engl.*, 26(1987) 145. (b) J. Zhao, D. Adcock, W.T. Pennington, and J.W. Kolis, *Inorg. Chem.*, 29 (1990) 4360.

17. (a) A. Boardman, R.W.H. Small, and I.J. Worrall, *Inorg. Chim. Acta*, 120 (1986) L23. (b) (a) A. Boardman, S.E. Jeffs, R.W.H. Small, and I.J. Worrall, *Inorg. Chim. Acta*, 83 (1984) L39.

18. I.G. Dance, *J. Am. Chem. Soc.*, 102 (1980) 3445.

19. I.G. Dance, *Inorg. Chem.*, 20 (1981) 2155.

20. J.L. Hencher, M. Khan, F.F. Said, and D.G. Tuck, *Inorg. Nuclear Chem. Lett.*, 17 (1981) 287.

21. A. Choy, D. Craig, I.G. Dance, and M.L. Scudder, *J. Chem. Soc., Chem. Commun.*, (1982), 1246.

22. (a) I.G. Dance, A. Choy, and M.L. Scudder, *J. Am. Chem. Soc.*, 106 (1984) 6285; (b) I.G.Dance and J.K.Saunders, *Inorg. Chim. Acta*, 96 (1985) L71.

23. J.L. Hencher, M. Khan, F.F. Said, and D.G. Tuck, *Polyhedron*, 4 (1985) 1263.

24. P.A.W. Dean and J.J. Vittal, *J. Am. Chem. Soc.*, 106 (1984) 6436.

25. K.S. Hagen and R.H. Holm, *Inorg. Chem.*, 22 (1983) 3171.

26. P.A.W. Dean and J.J. Vittal, *Inorg. Chem.*, 26 (1987) 278.

27. J.J. Vittal, P.A.W. Dean, and N.C. Payne, *Can. J. Chem.*, 70 (1992) 792.

28. P.A.W. Dean and J.J. Vittal, *Inorg. Chem.*, 25 (1986) 514.

29. P.A.W. Dean and J.J. Vittal, *Inorg. Chem.*, 24 (1985) 3722.

30. P.A.W. Dean, J.J. Vittal, and N.C. Payne, *Inorg. Chem* , 26 (1987) 1683.

31. P.A.W. Dean and J.J. Vittal, *Can. J. Chem.*, 66 (1988) 2443.

32. P.A.W. Dean and V. Manivannan, *Inorg. Chem.*, 29 (1990) 2997

33. P.A.W. Dean, J.J. Vittal, and M.H. Trattner, *Inorg. Chem.*, 26 (1987) 4245

34. P.A.W. Dean, V. Manivannan, and J.J. Vittal, *Inorg. Chem.*, 28 (1989) 2360.

35. P.A.W. Dean and V. Manivannan, *Can. J. Chem.*, 68 (1990) 214.

36. M. Margoshes and B.L. Vallee, *J. Am. Chem. Soc.*, 79 (1957) 4813.

37. *(a)* J.D. Otvos and I.M. Armitage, *Proc. Natl Acad. Sci. USA*, 77 (1980) 7094; *(b)* J.D. Otvos, H.R. Engeseth, and S. Wehrli, *Biochem.*, 24 (1985) 6735.

38. A.H. Robbins, D.E. McRee, M. Williamson, S.A. Collett, N.H. Xuong, W F. Furey, B.C. Wang, and C.D. Stout, *J. Mol. Biol.*, 221 (1991) 1269.

39. H. Eklund and C.-I. Branden, *Zinc Enzymes*, T.G. Spiro, ed., Wiley, New York, 1983.

40. E.D. Becker, *High Resolution NMR*, Academic Press, London, 1980, Appendix B.

41. R.J. Goodfellow, in *Multinuclear NMR*, J. Mason, ed., Plenum Press, New York, 1987, ch. 21.

42. G. Calingaert and H.A. Beatty, *J. Am. Chem. Soc.*, 61 (1939) 2748.

CHAPTER 2 STUDIES ON ZINC AND CADMIUM CLUSTERS $[(\mu\text{-SAlk})_6(MX)_4]^{2-}$

2.1 Introduction

As described in Chapter One, adamantane-like clusters involving phenylthiolates as bridging ligands, of the general type $[(\mu\text{-SPh})_6(MX)_4]^{2-}$, are well-established for M = zinc-group elements, and X = halides.[1-8] However, very little attention has been paid to the analogous adamantanoid clusters containing alkylthiolates as bridging ligands. It seems reasonable to suggest that the type of cage $(\mu\text{-SAlk})_6M_4$ may provide a better model for the study of metallothionein. When the work that provides the basis for this chapter was started, the cage system $(\mu\text{-SAlk})_6M_4$ (M = zinc group elements) was known for only one cluster, $(Et_4N)_2[(\mu\text{-SPr}^n)_6(CdI)_4]$, which had been isolated with a satisfactory elemental analysis in our laboratory.[4] This cadmium complex as well as the Zn(II) and Hg(II) analogues were also characterized in solution by multi-NMR methods.

In this chapter is described the synthesis of a much wider series of clusters of the type $[(\mu\text{-SAlk})_6(MX)_4]^{2-}$ (M = Zn or Cd; X = Cl, Br or I). In total, 27 new clusters have been isolated by the self-assembly method. These clusters and related complexes with mixed metals or mixed terminal halides have been studied in solution by multi-NMR technique. The interesting NMR results obtained provided information about the properties of the clusters. A single crystal analysis of $(Et_4N)_2[(\mu\text{-SPr}^i)_6(CdBr)_4]$ has been carried out by Dr. Vittal of this department. This salt contains the first representative $(\mu\text{-SAlk})_6Cd_4$ cage to be characterized crystallographically, supporting the proposed structure of this type of cluster. In addition, the reaction of $[(\mu\text{-SPr}^i)_6(CdX)_4]^{2-}$ with elemental sulfur or selenium has been investigated. The results show the existence of a new type

of octa-nuclear clusters with bridged-alkylthiolates in solution

2.2 Experimental

Materials and general procedure

The compounds $M(SR)_2$ (M = Zn or Cd; R = Me, Et, 1-Pr, 2-Pr, 1-Bu, 2-Bu or benzyl) were synthesized by the literature method[9] for the preparation of $Zn(SR)_2$, except that Me_2CO:H_2O (1:5) was used instead of water and the metal nitrates instead of the sulphates. The compound $(Et_4N)_2[(\mu\text{-}SPr^n)_6(CdI)_4]$ was obtained as reported earlier[4]. The $(Pr^iS)_2Se$ was prepared by the literature method[10]. Red selenium was synthesized by the reduction of Na_2SeO_3 with $Na_2S_2O_4$ in strongly acidic aqueous solution. The Se_8 was separated by filtration, washed with water then alcohol, dried in vacuo at room temperature, and stored in the dark in a refrigerator at about 273K. All other starting materials were from commercial sources and were used as received. The solvents for use in synthesis and the preparation of NMR samples were stored over 3-A molecular sieves and deoxygenated by sparging with argon. All syntheses and preparations of NMR samples were carried out under an atmosphere of argon or nitrogen.

Synthesis

Method A

$(Et_4N)_2[(\mu\text{-}SMe)_6(ZnBr)_4]$. A mixture of $ZnBr_2$ (0.225g, 1.0mmol), $Zn(SMe)_2$ (0.48g, 3.0mmol), and Et_4NBr (0.42g, 2.0mmol) was stirred in CH_2Cl_2 (8mL) for 30min., producing a colorless solution with a small amount of insoluble material which was removed by filtration. The volume of the filtrate was reduced to ca. 4 mL by gentle

heating under a flow of N_2(g). The solution was layered with Et_2O (1mL), then was placed in the refrigerator (ca. 0°C) overnight. Colorless crystals were so formed. These were separated by filtration, washed with Et_2O, and dried in vacuo at room temperature. The yield was 0.80g (71%). Anal. Calcd. for $C_{22}H_{58}Br_4N_2S_6Zn_4$ (mol wt 1124.18): C, 23.50; H, 5.20, N, 2.49. Found: C, 23.42; H, 5.08; N, 2.87.

This synthesis was generally similar to that reported for $(Et_4N)_2[(\mu\text{-}SPr^n)_6(CdI)_4]$[4]. The preparations of the other compounds were made similarly (except as indicated).

$(Et_4N)_2[(\mu\text{-}SMe)_6(ZnI)_4]$, as a white solid. The yield was 61%. Anal. Calcd. for $C_{22}H_{58}I_4N_2S_6Zn_4$ (mol wt 1312.18): C, 20.14; H, 4.46; N, 2.14. Found: C, 20.37; H, 4.33; N, 2.47.

$(Et_4N)_2[(\mu\text{-}SEt)_6(CdCl)_4]$, as a white solid. The yield was 41%. Anal. Calcd. for $C_{28}H_{70}Cd_4Cl_4N_2S_6$ (mol wt 1218.62): C, 27.60; H, 5.79; N, 2.30. Found: C, 27.50; H, 5.57; N, 2.58.

$(Et_4N)_2[(\mu\text{-}SEt)_6(ZnI)_4]$, as a white solid. The yield was 36%. Anal. Calcd. for $C_{28}H_{70}I_4N_2S_6Zn_4$ (mol wt 1396.34): C, 24.08; H, 5.05; N, 2.01. Found: C, 23.72; H, 4.82; N, 2.16.

$(Et_4N)_2[(\mu\text{-}SPr^n)_6(ZnI)_4]$, as white crystals. The yield was 68%. Anal. Calcd. for $C_{34}H_{82}I_4N_2S_6Zn_4$ (mol wt 1480.50): C, 27.58; H, 5.58; N, 1.89. Found: C, 27.28; H, 5.45; N, 2.06.

$(Et_4N)_2[(\mu\text{-}SBu^n)_6(ZnI)_4]$, as a white solid. The yield was 45%. Anal. Calcd. for $C_{40}H_{94}I_4N_2S_6Zn_4$ (mol wt 1564.65): C, 30.70; H, 6.06; N, 1.79. Found: C, 30.54; H, 6.08; N, 1.79

$(Et_4N)_2[(\mu\text{-}SBu^t)_6(CdI)_4]$, as colorless crystals. The yield was 57%. Anal. Calcd.

for $C_{40}H_{94}Cd_4I_4N_2S_6$ (mol wt 1752.73): C, 27.41; H, 5.41; N, 1.60. Found: C, 27.56; H, 5.52; N, 1.96.

$(Et_4N)_2[(\mu\text{-}SPr^i)_6(ZnCl)_4]$, as a white solid. The yield was 81%. Anal. Calcd. for $C_{34}H_{82}Cl_4N_2S_6Zn_4$ (mol wt 1114.70): C, 36.63; H, 7.42; N, 2.51. Found: C, 35.49; H, 7.47; N, 2.39.

$(Et_4N)_2[(\mu\text{-}SPr^i)_6(CdCl)_4]$, as a white solid. The yield was 84%. Anal. Calcd. for $C_{34}H_{82}Cd_4Cl_4N_2S_6$ (mol wt 1302.78): C, 31.34; H, 6.34; N, 2.15. Found: C, 31.60; H, 6.15; N, 2.36.

$(Et_4N)_2[(\mu\text{-}SPr^i)_6(ZnBr)_4]$, as colorless crystals. The yield was 62%. Anal. Calcd. for $C_{34}H_{82}Br_4N_2S_6Zn_4$ (mol wt 1292.50): C, 31.59; H, 6.40; N, 2.17. Found: C, 31.35; H, 6.53; N, 2.16.

$(Et_4N)_2[(\mu\text{-}SPr^i)_6(CdBr)_4]$, as colorless crystals. The yield was 74%. Anal. Calcd. for $C_{34}H_{82}Br_4Cd_4N_2S_6$ (mol wt 1480.58): C, 27.58; H, 5.58; N, 1.89. Found: C, 27.09; H, 5.45; N, 1.60.

$(Et_4N)_2[(\mu\text{-}SPr^i)_6(ZnI)_4]$, as a white solid. The yield was 74%. Anal. Calcd. for $C_{34}H_{82}I_4N_2S_6Zn_4$ (mol wt 1480.50): C, 27.58; H, 5.58; N, 1.89. Found: C, 27.51; H, 5.23; N, 2.04.

$(Et_4N)_2[(\mu\text{-}SPr^i)_6(CdI)_4]$, as a white solid. The yield was 78%. Anal. Calcd. for $C_{34}H_{82}Cd_4I_4N_2S_6$ (mol wt 1668.58): C, 24.47; H, 4.95; N, 1.68. Found: C, 24.25; H, 4.99; N, 1.61.

$(Et_4N)_2[(\mu\text{-}S\text{-}2\text{-}Bu)_6(ZnCl)_4]$, as a white solid. The yield was 83%. Anal. Calcd. for $C_{40}H_{94}Cl_4N_2S_6Zn_4$ (mol wt 1198.85): C, 40.07; H, 7.90; N, 2.34. Found: C, 39.49; H, 7.82; N, 2.26.

$(Et_4N)_2[(\mu\text{-S-2-Bu})_6(CdCl)_4]$, as white crystals. The yield was 79%. Anal. Calcd. for $C_{40}H_{94}Cd_4Cl_4N_2S_6$ (mol wt 1386.93): C, 34.64; H, 6.83; N, 2.02. Found: C, 34.87; H, 6.51; N, 2.18.

$(Et_4N)_2[(\mu\text{-S-2-Bu})_6(ZnBr)_4]$, as a white solid. The yield was 80%. Anal. Calcd. for $C_{40}H_{94}Br_4N_2S_6Zn_4$ (mol wt 1376.65): C, 34.90; H, 6.88; N, 2.04. Found: C, 34.56; H, 7.17; N, 1.92.

$(Et_4N)_2[(\mu\text{-S-2-Bu})_6(CdBr)_4]$, as white crystals. The yield was 83%. Anal. Calcd. for $C_{40}H_{94}Br_4Cd_4N_2S_6$ (mol wt 1564.7.): C, 30.70; H, 6.06; N, 1.79. Found: C, 30.83; H, 5.71; N, 2.08.

$(Et_4N)_2[(\mu\text{-S-2-Bu})_6(ZnI)_4]$, as a white solid. The yield was 64%. Anal. Calcd. for $C_{40}H_{94}I_4N_2S_6Zn_4$ (mol wt 1564.65): C, 30.70; H, 6.06; N, 1.79. Found: C, 30.42; H, 6.34; N, 1.50.

$(Et_4N)_2[(\mu\text{-S-2-Bu})_6(CdI)_4]$, as white crystals. The yield was 68%. Anal. Calcd. for $C_{40}H_{94}Cd_4I_4N_2S_6$ (mol wt 1752.73): C, 27.41; H, 5.41; N, 1.60. Found: C, 27.28; H, 5.63; N, 1.69.

$(Et_4N)_2[(\mu\text{-SCH}_2\text{Ph})_6(ZnCl)_4]$. In this case, pentane was used to reduce the solubility instead of ether. The product was isolated as a white solid. The yield was 92%. Anal. Calcd. for $C_{58}H_{82}Cl_4N_2S_6Zn_4$ (mol wt 1402.94): C, 49.65; H, 5.89; N, 2.00. Found: C, 50.02; H, 5.87; N, 2.29.

$(Et_4N)_2[(\mu\text{-SCH}_2\text{Ph})_6(CdCl)_4]$. In this case, refrigeration was at -10 to -20 °C. The product was isolated as a white solid. The yield was 54%. Anal. Calcd. for $C_{58}H_{82}Cd_4Cl_4N_2S_6$ (mol wt 1591.02): C, 43.78; H, 5.20; N, 1.76. Found: C, 43.44; H, 4.98; N, 1.40.

$(Et_4N)_2[(\mu\text{-}SCH_2Ph)_6(ZnBr)_4]$, as a white solid. The yield was 89%. Anal. Calcd. for $C_{58}H_{82}Br_4N_2S_6Zn_4$ (mol wt 1580.74): C, 44.07; H, 5.23; N, 1.77. Found: C, 44.86; H, 5.29; N, 1.93.

$(Et_4N)_2[(\mu\text{-}SCH_2Ph)_6(CdBr)_4]$, as a white solid. The yield was 79%. Anal. Calcd. for $C_{58}H_{82}Br_4Cd_4N_2S_6$ (mol wt 1768.82): C, 39.38; H, 4.67; N, 1.58. Found: C, 40.02; H, 4.72; N, 1.56.

$(Et_4N)_2[(\mu\text{-}SCH_2Ph)_6(ZnI)_4]$. Here, pentane was used instead of ether. The product was a white solid. The yield was 84%. Anal. Calcd. for $C_{58}H_{82}I_4N_2S_6Zn_4$ (mol wt 1768.74): C, 39.38; H, 4.67; N, 1.58. Found: C, 39.56; H, 4.74; N, 1.75.

$(Et_4N)_2[(\mu\text{-}SCH_2Ph)_6(CdI)_4]$. Again pentane was used instead of ether. The product was a white foamy solid. The yield was 75%. Anal. Calcd. for $C_{58}H_{82}Cd_4I_4N_2S_6$ (mol wt 1956.82): C, 35.60; H, 4.22; N, 1.43. Found: C, 35.13; H, 4.14; N, 1.40.

Method B

The next two compounds were prepared in a different way from the above.

$(Et_4N)_2[(\mu\text{-}SEt)_6(CdBr)_4]$. Into a solution of $CdBr_2$ (1.1g, 4.0mmol) in EtOH (50mL) at 40°C, EtSH (0.50g, 8.1mmol) was added by stirring, followed by Et_3N (0.81g, 8.0mmol) and a solution of Et_4NBr (0.42g, 2.0mmol) in EtOH (5ml). A colorless solution was obtained, but a few minutes later a white precipitate was formed. When MeCN (5mL) was added to the mixture, the precipitate was dissolved. Cooling the resulting mixture in a refrigerator at about 0°C overnight, produced the white crystals, which were separated by filtration, washed with Et_2O, and dried in vacuo at room temperature. The yield was 1.0g (72%). Anal. Calcd. for $C_{28}H_{70}Br_4Cd_4N_2S_6$ (mol wt 1396.42): C, 24.08;

H, 5.05, N, 2.01. Found: C, 24.13; H, 5.00; N, 1.85.

$(Et_4N)_2[(\mu\text{-}SEt)_6(CdI)_4]$, was prepared analogously, as white crystals. The yield was 58%. Anal. Calcd. for $C_{28}H_{70}Cd_4I_4N_2S_6$ (mol wt 1584.42): C, 21.22; H, 4.45; N, 1.77. Found: C, 20.89; H, 4.11; N, 1.34.

Elemental microanalyses

All the analyses for C, H and N were carried out by Guelph Chemical Laboratories Ltd.

Nuclear magnetic resonance spectra

A Varian Gemini-200 spectrometer system was used to measure the ^1H and ^{13}C NMR spectra of the clusters of $(Et_4N)_2[(\mu\text{-}SAlk)_6(MX)_4]$ at ambient probe temperature. Solutions were in CD_3CN in 5 mm od NMR tubes. The ^2D resonance of the solvent, deuterated acetonitrile, was used as a field/frequency lock. The $CD_2\mathit{H}CN$ signal (δ_H = 1.93 ppm) and $\mathit{C}D_3CN$ signal (δ_C = 1.3 ppm) were used as internal references. For the reaction mixtures of $[(\mu\text{-}SPr^i)_6(CdX)_4]^{2-}$ with sulfur or selenium, ^{13}C NMR spectra were measured at ambient probe temperature on a Varian XL-200 spectrometer system with solutions in 10 mm od NMR tubes. No ^2D field/frequency lock was used. The $\mathit{C}H_2Cl_2$ signal (δ_C = 54.2 ppm) was used as an internal reference.

All the $^{111/113}Cd$ and ^{77}Se NMR spectra (with natural-abundance) were measured on a Varian XL-200 or -300 spectrometer system with solutions in 10 mm od NMR tubes. Again, no ^2D field-frequency lock was used (the field drift was < 1 Hz/day), at any temperature (ambient probe or reduced). The probe temperatures were calibrated using

a thermocouple probe in a stationary sample with an appropriate solvent. The reproducibility of $^{111/113}Cd$ or ^{77}Se chemical shifts was found to be ±1 ppm or 0.1 ppm. In a single session, chemical shift differences could usually be measured more precisely. The concentration unit of the samples was measured as the ratio of mole of solute to volume of solvent at ambient temperature. On both machines interference occurred to the part of the ^{113}Cd region, so many spectra were measured using ^{111}Cd. The sensitivity of ^{111}Cd is almost the same as that of ^{113}Cd at natural abundance. No primary isotope effect is expected, i.e. chemical shifts should be the same for both ^{111}Cd and ^{113}Cd. The external references were 0.1M $Cd(ClO_4)_2(aq)$ for $^{111/113}Cd$ and pure Me_2Se for ^{77}Se (all at ambient temperature). The reference frequencies on the XL-200 were 38.15, 42.41 and 44.37 MHz for ^{77}Se, ^{111}Cd and ^{113}Cd, respectively; on the XL-300 were 57.20, 63.59 and 66.53 MHz for ^{77}Se, ^{111}Cd and ^{113}Cd, respectively. The negative Overhauser effect was significant for $^{111/113}Cd$ in the Cd-SAlk complexes, therefore gated proton-decoupling was used, with the decoupler off for at least 80% of each duty cycle. Most of the $^{111/113}Cd$ NMR spectra were measured with the settings: acquisition time, 1 s; cycle time, 5 s; spectral window, 10 kHz; and tip angles, ca. 88° (for spectra at 213 K) and ca. 83° (for spectra at ambient probe temperature). For the mixtures of $[(\mu\text{-}SPr^i)_6(CdX)_4]^{2-}$ and sulfur or selenium, the settings for Cd NMR were: acquisition time, 0.6 s; cycle time, 4.6 s; spectral window, 2.5 kHz; tip angle, 83° (at ambient probe temperature). ^{77}Se NMR spectra were measured using continuous proton decoupling. For the species $[Cd_4(\mu_4\text{-}Se)(\mu\text{-}SPr^i)_{12}(CdX)_4]^{2-}$, $T_1(^{77}Se)$ appears to be ca. 20 s. In the final ^{77}Se NMR spectra of these species, measured on the XL-300 spectrometer at ambient probe temperature, the conditions were: acquisition time and cycle time, 1 s; spectral window, 10 kHz; and tip

angle, 18°.

Simulation of NMR Spectra

NMR spectra were simulated by using a version of LAOCOON3 adapted locally to run on a Victor 9000 computer as described in detail in Ref. [11].

X-ray Structure Determination

Single crystals of $(Et_4N)_2[\mu\text{-}SPr^i)_6(CdBr)_4]$ grown by diffusing diethylether into a acetone solution of the compound at 5 °C were found to be suitable for X-ray diffraction analysis, which was carried out by Dr. Vittal at the X-ray diffraction facilities of this department.

2.3 Results and Discussion

2.3.1 Synthesis

In this chapter, twenty-seven analytically pure Et_4N^+ salts have been isolated, including whole series (X = Cl~I) where R = Me, Et, 1-Pr, 1-Bu, 2-Pr, 2-Bu or benzyl; M = Zn or Cd. Most of the compounds were prepared in CH_2Cl_2 by *Method A* which is expressed by Equation [1*a*].

$$[1a] \quad 3\ M(SR)_2 + MX_2 + 2\ X^- \rightarrow [(\mu\text{-}SR)_6(MX)_4]^{2-}.$$

This reaction gives straightforward synthesis of a wide range of new adamantane-like clusters of zinc and cadmium containing bridging alkyl- or benzyl-thiolate ligands.

However, all attempts to isolate complexes (where the combination of R/M/X of the cluster was Me/Cd/Cl, Br or I; Bu^t/Zn or Cd/Br or I) failed, may be due to incomplete dissolution of starting materials. For the clusters with the combination Et/Zn/Cl or Br, the isolated product was spectroscopically but not analytically pure. For the clusters with Et/Cd/Br or I combination, *Method A* gives the expected product, but in relatively low yield (29 or 48%).

An alternative route (*Method B*) for the synthesis of $[(\mu\text{-SEt})_6(CdX)_4]^{2-}$ (X = Br or I) is shown in Equation [1*b*].

[1*b*] $4\ CdX_2 + 6\ EtSH + 6\ Et_3N \rightarrow [(\mu\text{-SEt})_6(CdX)_4]^{2-} + 6\ Et_3NH^+ + 4\ X^-$

The solvent used here is ethanol. The salt $(Et_4N)_2[(SEt)_6(ZnBr)_4]$ was obtained in a similar manner, but with the addition of Et_2O before cooling overnight. This salt was pure by ^1H and ^{13}C NMR, but did not give satisfactory elemental analyses.

A comparison of different methods of synthesis for $[(\mu\text{-ER})_6(MX)_4]^{2-}$ is interesting. Previously, $[(\mu\text{-SPh})_6(FeX)_4]^{2-}$ (X = Cl or Br)[12] and $[(\mu\text{-EPh})_6(HgX)_4]^{2-}$ [4] as well as $[(\mu\text{-SPr}^n)_6(MI)_4]^{2-}$ (M = Zn, Cd, or Hg)[4] have been synthesized by *method A* (eqn. 1a). There are some other ways to the cluster preparation, such as halogen oxidation of the parent anions $[(\mu\text{-EPh})_6(MEPh)_4]^{2-}$ (E = S or Se; M = Zn or Cd) with X_2 (X = Br or I) or $PhICl_2$[3], and group exchange reactions between $[(\mu\text{-EPh})_6(MEPh)_4]^{2-}$ (E = S or Se; M = Zn or Cd) and $R_nM'X$ (R_nM' = Ph_3Sn or MeHg; X = Cl, Br or I)[13]. The latter two preparative routes can not be applied in the present case because parent ions of the type $[(\mu\text{-SAlk})_6(MSAlk)_4]^{2-}$ have not yet been reported. The synthesis of $[(\mu\text{-SAlk})_6(MSAlk)_4]^{2-}$

was tried during the work for this thesis, but has not yet been brought to a successful conclusion.

In this chapter, the mixed-metal complexes $[(\mu\text{-SAlk})_6(CdX)_{4-n}(ZnX)_n]^{2-}$ and mixed-halide complexes of $[(\mu\text{-SAlk})_6(CdX)_{4-n}(CdX')_n]^{2-}$ were prepared in situ for NMR measurements. The statistical distributions of these species are exactly the same as that discussed in Section 1.6. The isolation of these mixed-metal or mixed-terminal compounds was not tried in this project.

2.3.2 NMR studies

(i) $[(\mu\text{-SR})_6(CdX)_4]^{2-}$

Proton and ^{13}C NMR are the very basic means for characterization of the new compounds, although they are not as important as metal NMR. All ^1H and ^{13}C data for the $(Et_4N)_2[(\mu\text{-SAlk})_6(MX)_4]$ series are listed in Table 2.1 & 2.2. Typical ^1H and ^{13}C NMR spectra (taking $(Et_4N)_2[(\mu\text{-SPr}^i)_6(CdCl)_4]$ as example) are shown in Fig. 2.1. In the proton NMR spectrum, first, there are shown four types of signals, indicating the existence of both Et and Pr^i groups; second, we could know which signal is which from their coupling modes (*e.g.* doublet of triplets and quartet for CH_3 and CH_2 in Et, and doublet and septet for CH_3 and CH in Pr^i); third, the signals could also be assigned by different intensities (*e.g.* CH_3 to CH is about 1:6 in Pr^i); finally, the intensity ratio of ethyl and isopropyl groups is about 8:6, allowing a first assessment of whether the isolated compounds are pure or not. The ^{13}C NMR spectrum tells us only that both ethyl and isopropyl groups occur in the isolated cluster. Signals in two regions are found for NEt and also for $SCHMe_2$. Signal assignment can be completed by comparison with

Table 2.1 ^{1}H NMR data for the anions in $(Et_4N)_2[(\mu\text{-}SR)_6(MX)_4]$ in CD_3CN at 295K.

			δ_H[a]				^3J(H-H)/Hz[b]		
R	X	M	H-1	H-2	H-3	H-4	1-2	2-3	3-4
Me[c,d]	Br	Zn	2.03				7.4		
Me[c,d]	I	Zn	2.00				7.3		
Et[c,d]	Cl	Zn	2.65	1.31			7.4		
Et[c,d]	Cl	Cd	2.68	1.33			7.3[e]		
Et[c,d]	Br	Zn	2.66	1.33			7.4		
Et[c,d]	Br	Cd	2.69	1.35			7.3		
Et[c,d]	I	Zn	2.66	1.34			7.4		
Et[c,d]	I	Cd	2.67	1.34			7.5		
1-Pr[c,d] I		Zn	2.61	1.74	0.90		7.4	7.3	
1-Pr[c,d] I		Cd	2.65	1.71	0.91		7.5	7.4	
2-Pr[c,d] Cl		Zn	1.41	3.29			6.7		
2-Pr[c,d] Cl		Cd	1.40	3.26			6.7[e]		
2-Pr[c,d] Br		Zn	1.44	3.36			6.8		
2-Pr[c,d] Br		Cd	1.41	3.35			6.7[e]		
2-Pr[c,d] I		Zn	1.47	3.48			6.8		
2-Pr[c,d] I		Cd	1.43	3.42			6.7		
1-Bu[c,d] I		Zn	2.63	1.73	1.33	0.87	7.4	7.5	7.3
1-Bu[c,b] I		Cd	2.66	1.71	1.34	0.87	≈7.4[e]	7.4	7.3
2-Bu[c,d]	Cl	Zn	1.41	3.06	1.75	0.88	6.8	[f]	7 3

Table 2.1 (Contd)

2-Bu[c,d]	Cl	Cd	1.39	3.06	1.75	0.90	6.7	[f]	7.3
2-Bu[c,d]	Br	Zn	1.45	[g]	1.80	0.89	6.8	[f]	7.3
2-Bu[c,d]	Br	Cd	1.41	[g]	1.75	0.90	6.7	[f]	7.3
2-Bu[c,d]	I	Zn	1.49	3.26	1.85	0.89	6.8	[f]	7.4
2-Bu[c,d]	I	Cd	1.43	3.22	1.78	0.90	6.8	[f]	7.3
CH_2Ph[d,h]	Cl	Zn	3.88[i]						
CH_2Ph[d,h]	Cl	Cd	3.88[i]						
CH_2Ph[d,h]	Br	Zn	3.89[i]						
CH_2Ph[d,h]	Br	Cd	3.86[i]						
CH_2Ph[d,h]	I	Zn	3.89[i]						
CH_2Ph[d,h]	I	Cd	3.84[i]						

[a] ±0.01 ppm.

[b] ±0.1 Hz.

[c] For Et_4N^+, δ_H = 3.17±0.01 and 1.20±0.01, for H-1 and H-2, respectively.

[d] For Et_4N^+, ^3J(H-H) = 7.3±0.1 Hz, $^3J(^{14}N\text{-}H)$ = 1.9±0.1 Hz.

[e] Not well resolved in the resonance of H-1.

[f] Not well resolved.

[g] δ_H = 3.1-3.2; this signal overlaps the multiplet from H-1 of Et_4N^+.

[h] For Et_4N^+, δ_H = 3.06±0.02 and 1.12±0.02, for H-1 and H-2, respectively.

[i] H-α; the phenyl resonance occurs at δ_C = 7.1-7.6.

Table 2.2 ^{13}C NMR data for $(Et_4N)_2[(\mu\text{-}SR)_6(MX)_4]$ in CD_3CN at 295 K

			δ_C[a]					
R	X	M	C-1[b]	C-2[b]	C-3[b]	C-4[b]	C-1[c]	C-2[c]
Me	Br	Zn	10.5				53.1	7.7
Me	I	Zn	11.6				53.1	7.8
Et	Cl	Zn	23.3	19.8			53.1	7.7
Et	Cl	Cd	23.4	21.7			53.1	7.8
Et	Br	Zn	23.7	19.7			53.1	7.8
Et	Br	Cd	23.7	21.6			53.1	7.8
Et	I	Zn	24.6	19.5			53.0	7.7
Et	I	Cd	24.5	21.2			53.2	7.8
1-Pr	I	Zn	32.2	27.6	14.0		53.2	7.7
1-Pr	I	Cd	32.2	29.6	14.1		53.1	7.8
2-Pr	Cl	Zn	29.1	35.0			53.2	7.7
2-Pr	Cl	Cd	30.4	34.9			53.2	7.7
2-Pr	Br	Zn	28.9	35.6			53.1	7.7
2-Pr	Br	Cd	30.2	35.2			53.0	7.7
2-Pr	I	Zn	28.6	36.8			53.1	7.7
2-Pr	I	Cd	30.1	35.9			53.0	7.7
1-Bu	I	Zn	36.3	29.8	22.8	14.0	53.1	7.8
1-Bu	I	Cd	38.4	29.7	22.9	14.0	53.3	7.8
2-Bu	Cl	Zn	25.4	41.0	34.9	12.6	53.0	7.7
2-Bu	Cl	Cd	27.0	41.0	36.3	12.7	53.2	7.7

Table 2 2 (Contd)

2-Bu	Br	Zn	25.6	41.9	34.9	12.7	53 2	7.7
2-Bu	Br	Cd	27.2	41.5	36.3	12.8	53.2	7.7
2-Bu	I	Zn	25.5	43.2	34.7	12.8	53.2	7.7
2-Bu	I	Cd	27.3	42.2	36.1	12.9	53.2	7.7
CH_2Ph	Cl	Zn	32.4[d]				53.2	7.7
CH_2Ph	Cl	Cd	32.5[d]				53.1	7.7
CH_2Ph	Br	Zn	32.7[d]				53.2	7.7
CH_2Ph	Br	Cd	33.0[d]				53.2	7.7
CH_2Ph	I	Zn	33.3[d]				53.2	7.8
CH_2Ph	I	Cd	33.4[d]				53.2	7.8

[a] Estimated error ±0.1 ppm.

[b] Thiolate carbons.

[c] Carbons of Et_4N^+. $^1J(^{13}C\text{-}^{14}N) = 3\pm0.2$ Hz.

[d] α-carbon. Aromatic carbons fall in the range δ_C = 127-145.

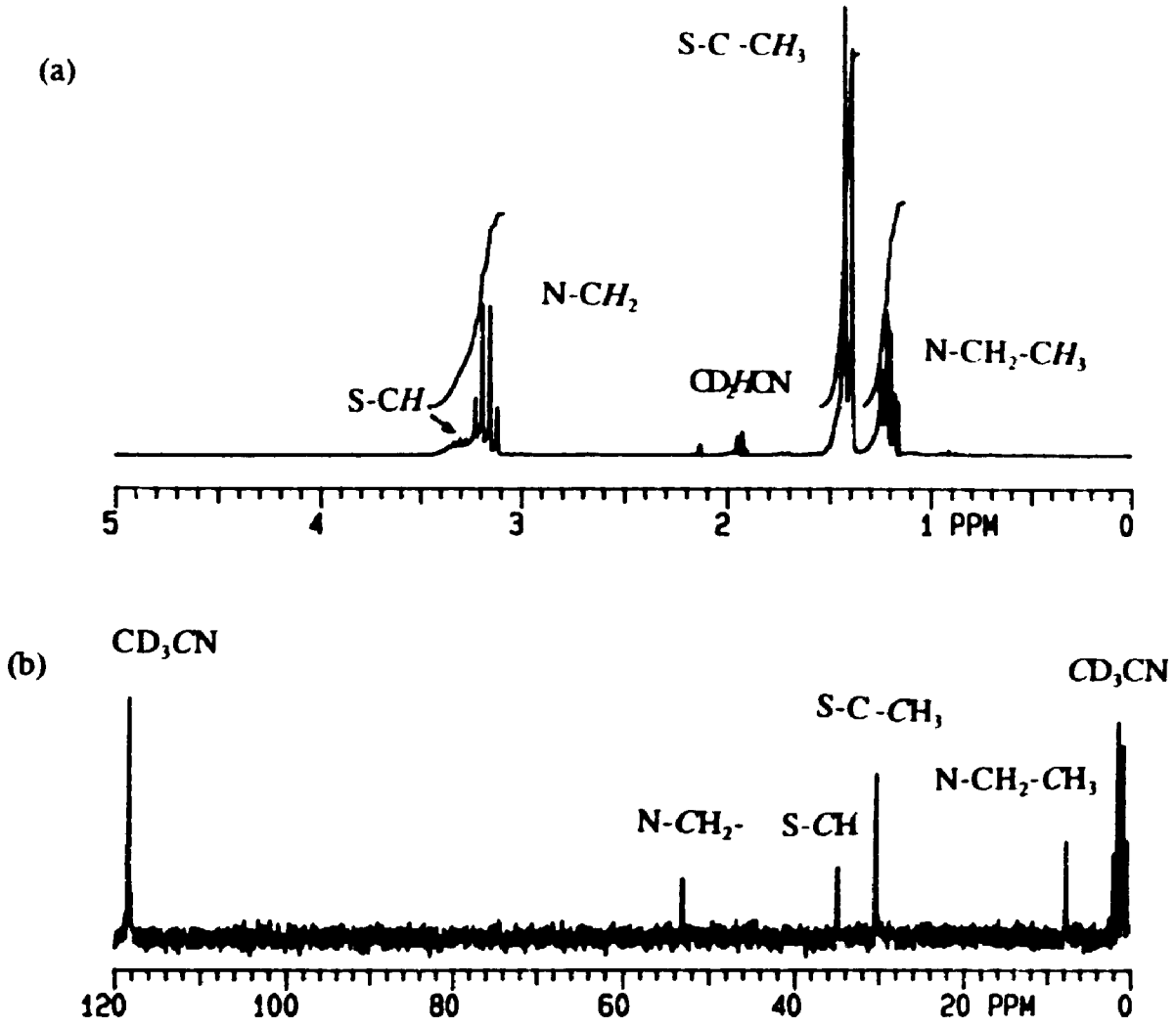

Figure 2.1 (a) ^{1}H and (b) ^{13}C NMR spectrum of $(Et_4N)_2[(\mu\text{-}SPr^i)_6(CdCl)_4]$ in CD_3CN at ambient probe temperature.

other known ^{13}C NMR spectra

The chemical shifts of $^{111,113}Cd$ (hereinafter in this chapter indicated by just Cd) NMR for the new clusters, $[(\mu\text{-SAlk})_6(CdX)_4]^{2-}$, are included in Table 2.3 (n = 0). When the alkyl group is kept the same, Cd nuclear shielding varies with X in the order I > Br > Cl For example, when R = 2-Pr at room temperature, the δ_{Cd} = 588, 566 and 529 ppm for Cl, Br and I, respectively. This order (called the Normal Halogen Dependence[14]) has been found for $[CdX_4]^{2-}$ [15] and $[(\mu\text{-EPh})_6(CdX)_4]^{2-}$ (E = S or Se)[3]. On the other hand, if the halogen is kept constant, the variation of Cd chemical shift with the R on SR is in the order: primary alkyl ≥ benzyl > secondary alkyl > phenyl[3]. For instance, for a given halogen (I) at room temperature, the δ_{Cd} value with different R in ppm shows that 568 (Et) ≈ 563 (1-Pr) ≈ 562 (1-Bu) ≈ 560 (Bz) > 531 (2-Bu) ≈ 529 (2-Pr) > 501[3] (Ph). The same order has been observed previously for $[Cd(SR)_4]^{2-}$ in water[16]. In addition, the chemical shift is very temperature-dependent. As can be seen from Table 2.3, these metal chemical shifts show changes of -0.14 to -0.25 ppm/K, which are of comparable size to the -0.2 ppm/K found[17,18] for $[(\mu\text{-SPh})_6(CdSPh)_4]^{2-}$. The Normal Halogen Dependence for the values of $\Delta\delta_{Cd}(T_R,T_A)$ (= δ_{Cd}(Reduced Temp) - δ_{Cd}(Ambient Temp)) is also observed here, *i.e.* for a constant R, the $\Delta\delta_{Cd}$ varies with I > Br > Cl.

Due to the statistical distribution of isotopes (see Section 1.5), two-bond coupling (^{113}Cd-S-^{111}Cd) is expected in this type of cluster $[(\mu\text{-SAlk})_6(CdX)_4]^{2-}$. Some of the clusters, such as $[(\mu\text{-SPr}^i)_6(CdX)_4]^{2-}$ (X = Cl or Br), give particularly narrow lines in their Cd NMR spectra even at ambient probe temperature, allowing the expected satellites to be seen. The cluster $[(\mu\text{-SPr}^i)_6(CdI)_4]^{2-}$ and the series $[(\mu\text{-SBz})_6(CdX)_4]^{2-}$ (X = Cl,Br,I) show this coupling only at reduced temperature. Table 2.4 includes these ^2J values, and

Table 2 3 Cadmium chemical shifts[a] of some complexes $[(\mu\text{-SR})_6(CdX)_{4-n}(ZnX)_n]^{2-}$ in CH_2Cl_2[b]

			δ_{Cd}[a]			
R	X	Temp (K)	n = 0	n = 1	n = 2	n = 3
Et[c]	Cl	293[d]	607			
		233	619			
	Br	292	595	593	590	588
	I	293	568	564	559	554
		256	576	571	566	560
2-Pr	Cl	296	588	584	580	575
		217[e]	602	597	592	585
	Br	294	566	561	556	550
		214[e]	583	574	567	560
	I	295	529	518	509	501
		218[e]	548	533	519	510
2-Bu	Cl	292	588	584	579	573
		215[e]	601[d]			
	Br	293	568	562	556	550
		215[e]	582	573	565	559
	I	292	531	519	510	502
		215[e]	548[d]			
1-Pr	I	294	563	558	554	549
		213[f]	578	571	564	557

Table 2 3 (Contd)

1-Bu	I	293	562	557	552	548
		215	578	572	565	558
$PhCH_2$	Cl	292	594[g]			
		215[e]	605	604	603	600
	Br	293	584	582	580	578
		215[e]	596	594	592	590
	I	293	560	556	552	547
		215	576			
Ph	I	260	---------- ≈518[h] ---------			

[a] Relative to external 0.1 M $Cd(ClO_4)_2$ (aq) at 293±1 K, for solutions containing 0.05 mol/L of solvent at ambient temperature, except as noted. Reproducibility ± 1 ppm.

[b] Except where noted otherwise.

[c] In MeCN.

[d] Concentration 0.025 mol/L of solvent.

[e] Average position of several closely-spaced resonances (see text).

[f] Data from Ref. 4, for solutions having 0.06 mol/L of solvent.

[g] Broad unresolved signals occur in Cd_4:Zn_4 mixtures.

[h] Separate signals not resolved.

Table 2 4 Two-bond ^{111}Cd-^{113}Cd coupling constants [a]

Complex	$^2J(^{111}Cd\text{-}S\text{-}^{113}Cd)$ (Hz)[b]
$[(\mu\text{-}SPr^i)_6(CdCl)_4]^{2-}$	22[c]
$[(\mu\text{-}SPr^i)_6(CdBr)_4]^{2-}$	28[d]
$[(\mu\text{-}SPr^i)_6(CdI)_4]^{2-}$	44
$[(\mu\text{-}SPr^i)_6(CdBr)_3(ZnBr)]^{2-}$	32
$[(\mu\text{-}SPr^i)_6(CdBr)_2(ZnBr)_2]^{2-}$	36
$[(\mu\text{-}SCH_2Ph)_6(CdCl)_4]^{2-}$	24
$[(\mu\text{-}SCH_2Ph)_6(CdBr)_4]^{2-}$	32
$[(\mu\text{-}SCH_2Ph)_6(CdI)_4]^{2-}$	44
$[(\mu\text{-}SCH_2Ph)_6(CdCl)_3(ZnCl)]^{2-}$	26
$[(\mu\text{-}SCH_2Ph)_6(CdCl)_2(ZnCl)_2]^{2-}$	35

[a] For solutions in CH_2Cl_2 at 215±3 K.

[b] Estimated error ±1 Hz.

[c] $^2J = 20 \pm 1$ Hz at 292 K.

[d] $^2J = 26 \pm 1$ Hz at 293 K.

some other values found in mixed-metal clusters as well. Comparing to those ^2J values (44 - ca.56 Hz) found in species with the $(\mu\text{-SPh})_6Cd_4$ cage[3,13,18,19], only for the iodides does the ^2J (44 Hz) of the alkyl- and benzyl-thiolate clusters overlap the range of that found for the benzenethiolate clusters. As can be seen from Table 2.4, for a given R, the coupling size depends on the terminal halogen in the order Cl < Br < I. This halogen dependence of $^2J(^{113}Cd\text{-}S\text{-}^{111}Cd)$ has been found previously for $[(\mu\text{-SePh})_6(CdX)_4]^{2-}$ [3,13].

In our Cd NMR experiment at reduced temperature, closely-spaced multiple lines are observed for some clusters $[(\mu\text{-SR})_6(CdX)_4]^{2-}$ (R = 2-Pr, 2-Bu or Bz; X = Cl, Br or I). For example, the spectrum of $[(\mu\text{-SBz})_6(CdI)_4]^{2-}$ in CH_2Cl_2 at 213 K consists of a major signal at $\delta_{Cd} = 575._7$, with a strong shoulder at $\delta_{Cd} = 575._9$. These two lines have identical $^{111}Cd\text{-}^{113}Cd$ satellite splitting. It seems that in these cases the multiple signals are observed due to slowing of inversion at sulfur, or, more likely, to restricted S-C bond rotation. The molecular structure of $[(\mu\text{-SPr}^i)_6(CdBr)_4]^{2-}$ (see below) shows evidence of disorder from rotation about most of the S-C bonds.

(ii) $[(\mu\text{-SR})_6(CdX)_{4-n}(ZnX)_n]^{2-}$

In the Cd NMR spectra of newly prepared solutions containing mixtures of $[(\mu\text{-SAlk})_6(CdX)_4]^{2-}$ and the analogous $[(\mu\text{-SAlk})_6(ZnX)_4]^{2-}$ in various ratios, a total of four lines, which correspond to the cluster species Cd_4, Cd_3Zn, Cd_2Zn_2, and $CdZn_3$, are observed. The spectrum of $[(\mu\text{-SPr}^i)_6(CdBr)_{4-n}(ZnBr)_n]^{2-}$ as a typical example is shown in Fig. 2.2. The observation of these four cadmium signals gives us an indirect suggestion that Zn_4 cluster exists in the solution, since the zinc cluster can not be detected directly. It also shows that the metal redistribution in solution is rapid on the preparative time scale

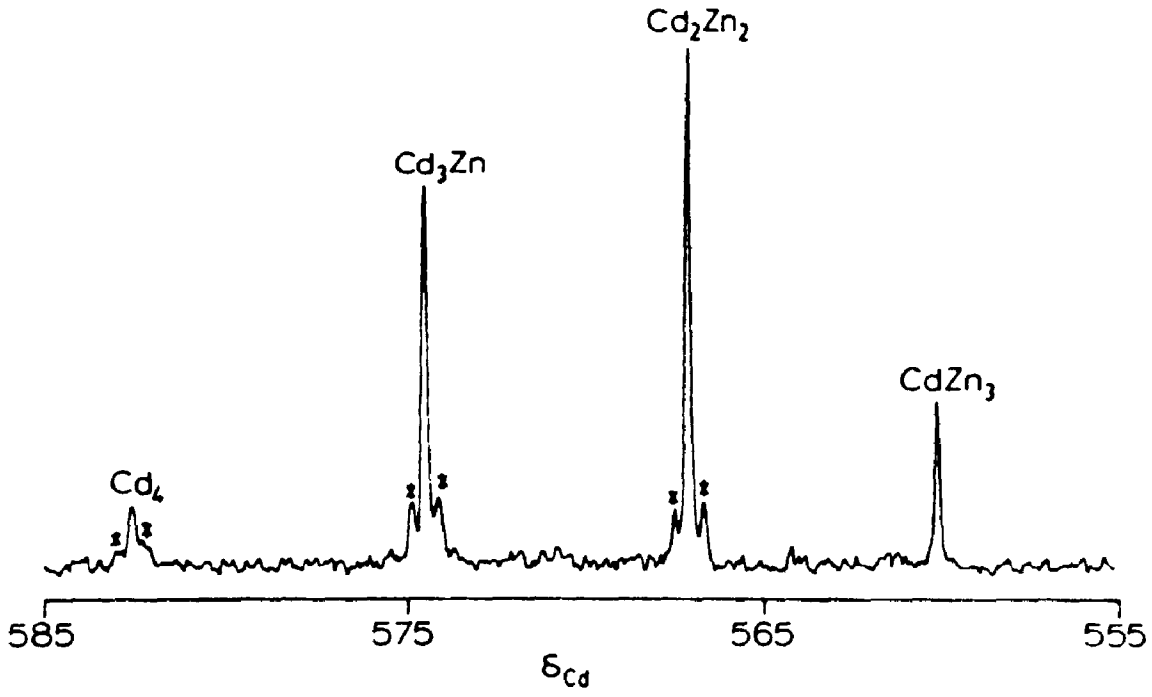

Figure 2.2 44.37 MHz 113-Cd NMR spectrum of a mixture with $[(\mu\text{-}SPr^i)_6(Cd Br)_4]^{2-}$: $[(\mu\text{-}SPr^i)_6(Zn Br)_4]^{2-}$ = 1:1 in CH_2Cl_2 at 215 K.[20] * indicates Cd satellite.

but slow on the NMR time scale (at reduced temperature). The equilibrium equation has been described in Section 1.6. Another expression of these equilibrium mixtures is shown in Eqn. [2].

[2] $[(\mu\text{-SAlk})_6(CdX)_4]^{2-} + [(\mu\text{-SAlk})_6(ZnX)_4]^{2-} \rightleftharpoons [(\mu\text{-SAlk})_6(CdX)_{4-n}(ZnX)_n]^{2-}$

In many cases, when the starting ratio of Cd and Zn is 1:1, the intensity ratio of four lines is close to 1:3:3:1 (see Fig. 2.2 as an example). This observation suggests that the metal redistribution here is close to a statistical process. In a previous NMR study of $[(\mu\text{-SPh})_6(CdSPh)_4]^{2-}$:$[(\mu\text{-SPh})_6(ZnSPh)_4]^{2-}$, $[(\mu\text{-SPh})_6(CdSPh)_{4-n}(ZnSPh)_n]^{2-}$ was found to occur only for n = 0 and 1 in DMF[7a] and only for n = 0-2 in acetone[7b].

Generally, the cadmium signals observed at reduced temperature are relatively sharper than those at ambient temperature. However, in some cases the lines are still sharp enough at ambient temperature to separate four signals. When this is so, it is evident that metal exchange at ambient temperature is slow on the NMR time scale also.

In two cases, R/X = Pr^{i}S/Br and $PhCH_2$/Cl, the Cd NMR spectra of $[(\mu\text{-SR})_6(CdX)_{4-n}(ZnX)_n]^{2-}$ at reduced temperature are sufficiently sharp to allow observation of the satellites. As for the parent clusters (n = 0), the satellites are caused by $^2J(^{113}Cd\text{-}S\text{-}^{111}Cd)$, but are expected only for n = 0-2 (see Figure 2.2 as an example). These couplings have been given in Table 2.4. For both series it is found that the coupling magnitude of $^2J(^{113}Cd\text{-}S\text{-}^{111}Cd)$ depends on n values in the order 2 > 1 > 0.

As discussed in Section 2.3.2(i) for the clusters with n = 0, the $\Delta\delta_{Cd}(T_R,T_A)$ values for the clusters with n = 1 or 2 show the halide influence, but for the clusters with n =

3, this influence is too weak to see. However, the $\Delta\delta_{Cd}(T_R,T_A)$ values of the n = 3 species are definitely smaller than that of the n = 0 species. For example, in the Pr^i/I series, $\Delta\delta_{Cd}(T_R,T_A)$ = 19 (n = 0) > 9 (n = 3). This observation suggests that when more zinc atoms replace the cadmium positions in cluster skeleton, the chemical shift of the remaining cadmium is not as temperature-sensitive as that of its parent cluster.

Another interesting parameter arising from the Cd NMR properties of the mixed-metal species is $\Delta\delta_{Cd}(0,3)$ (= $\delta_{Cd}(n = 0) - \delta_{Cd}(n = 3)$). This shows the properties of halogen dependence, alkylthiolate dependence and temperature dependence. As can be calculated from the data in Table 2.3, the $\Delta\delta_{Cd}(0,3)$ varies with X in the order I > Br > Cl, with R in the order secondary alkyl > primary alkyl, and with T in the order reduced T > ambient T. For example, if the combination R/T = Pr^i/295±1K is kept the same, the $\Delta\delta_{Cd}(0,3)$ value with a variable X are 28, 16, and 13 ppm for I, Br, and Cl, respectively. Similarly, if X/T = I/295±1K are constants and R is a variable, the $\Delta\delta_{Cd}(0,3)$ values are 28 (R = Pr^i) > 14 (R = Pr^n); and if R/X = Pr^i/I are constants and T is a variable, the $\Delta\delta_{Cd}(0,3)$ values are 38 (T = 218K) > 28 (T = 295K).

As can be seen from Table 2.3, in some cases, such as Pr^i/I/218K, the four lines are not equally spaced. The pattern of chemical shifts here shows a non-linear, second order dependence on the number of Zn atoms in the adamantanoid skeleton. Generally, the $\Delta\delta_{Cd}(n,n+1)$ values for $[(\mu\text{-SAlk})_6(CdX)_{4-n}(ZnX)_n]^{2-}$ are significantly larger than that (1.5 ppm) observed for $[(\mu\text{-SPh})_6(CdSPh)_{4-n}(ZnSPh)_n]^{2-}$ [7b]. From the Cd NMR measurement of the mixture of $[(\mu\text{-SPh})_6(CdI)_4]^{2-}$ and $[(\mu\text{-SPh})_6(ZnI)_4]^{2-}$, separate signals are not observed for the different n = 0-3 clusters of the series $[(\mu\text{-SPh})_6(CdI)_{4-n}(ZnI)_n]^{2-}$ (Table 2.3). This result suggests that the differences in $\Delta\delta_{Cd}(0,3)$ between the

alkylthiolate clusters and the benzenethiolate clusters are dominated by bridging rather than terminal ligands. Therefore, it shows the significance again for the study of alkylthiolate clusters, because benzenethiolate can not typify all thiolates, at least for Cd NMR spectroscopic purposes.

The Cd NMR data of all the cluster species $[(\mu\text{-SR})_6(CdX)_{4-n}(ZnX)_n]^{2-}$ with different alkylthiolates or halides have been included in Table 2.3.

(iii) $[(\mu\text{-SPr}^i)_6(CdX)_{4-n}(CdX')_n]^{2-}$

When we finished the study of mixed metal system, we thought it of interest to study the mixed halide clusters $[(\mu\text{-SAlk})_6(CdX)_{4-n}(CdX')_n]^{2-}$. The isopropyl was chosen just because of the relatively sharp signals of Cd-SPr^i clusters. In this chapter, the Cd NMR spectra of $[(\mu\text{-SPr}^i)_6(CdX)_4]^{2-}$: $[(\mu\text{-SPr}^i)_6(CdX')_4]^{2-}$ mixtures (X/X' = Cl/Br,Cl/I,Br/I) have been measured. The Cd NMR data are listed in Table 2.5 and a typical spectrum is shown in Fig. 2.3. This is the first time such a complete series has been studied.

At ambient probe temperature, only two broad lines are observed from a solution containing a mixture of $[(\mu\text{-SPr}^i)_6(CdX)_4]^{2-}$ and $[(\mu\text{-SPr}^i)_6(CdX')_4]^{2-}$. The chemical shifts of these two lines are close to but not simply equal to those of the parent complexes. However, it is clear that one signal is in the region for Cd attached directly to X (Cd-X), the other in the region for Cd attached directly to X' (Cd-X'). Actually, the chemical shifts are the weighted average of those of Cd_4X_4, Cd_4X_3X', $Cd_4X_2X'_2$, $CdXX'_3$ in the region Cd-X and the weighted average of those of $Cd_4X'_4$, $Cd_4X'_3X$, $Cd_4X'_2X_2$, $CdX'X_3$ in the region Cd-X'.

Due to the relatively slow exchange of X and X' between clusters at reduced

Table 2.5 Cadmium chemical shifts of $[(\mu\text{-SPr}')_6(CdX)_{4-n}(CdX')_n]^{2-}$ [a] (X,X' =Cl,Br,I)

				δ_{Cd} [b]	
				$(\mu\text{-SR})_3CdX$	$(\mu\text{-SR})_3CdX'$
X	X'	Temp(K)	n	kernel	kernel
Cl	Br	292[c]		588	570
		215[d]	0	601.1	
			1	600.2	585.8
			2	599.5	584.8
			3	598.6	583.7
			4		582.6
Cl	I	293[c]		587	535
		215[d]	0	601.0	
			1	599.0[e]	560.0,559.7
			2	596.9[f]	555.4
			3	594.4[g]	551.4
			4		547.8
Br	I	294[c]		567	532
		215[d]	0	582.5	
			1	580.7	555.0
			2	578.9[h]	552.5
			3	577.2[h]	550.1
			4		547.7

Table 2 5 (contd.)

[a] Produced in situ in $[(\mu\text{-SPr}^i)_6(CdX)_4]^{2-}$:$[(\mu\text{-SPr}^i)_6(CdX')_4]^{2-}$ mixtures. $[Cd_4]_{total}$, in mol/L of solvent at ambient probe temperature, were: 0.1 for X/X' = Cl/Br, and 0 05 for X/X' = Cl/I and Br/I.

[b] Relative to external 0.1 M $Cd(ClO_4)_2$ (aq) at 293±1 K.

[c] Average values; at ambient probe temperature, additional fine structure is not well resolved.

[d] See text

[e] ^2J(Cd-Cd) ≈ 25 Hz.

[f] ^2J(Cl-*Cd*-S-*Cd*-I) = 25±1 Hz.

[g] ^2J(Cl-*Cd*-S-*Cd*-I) ≈ 33 Hz.

[h] ^2J(Br-*Cd*-S-*Cd*-I) = 34±1 Hz.

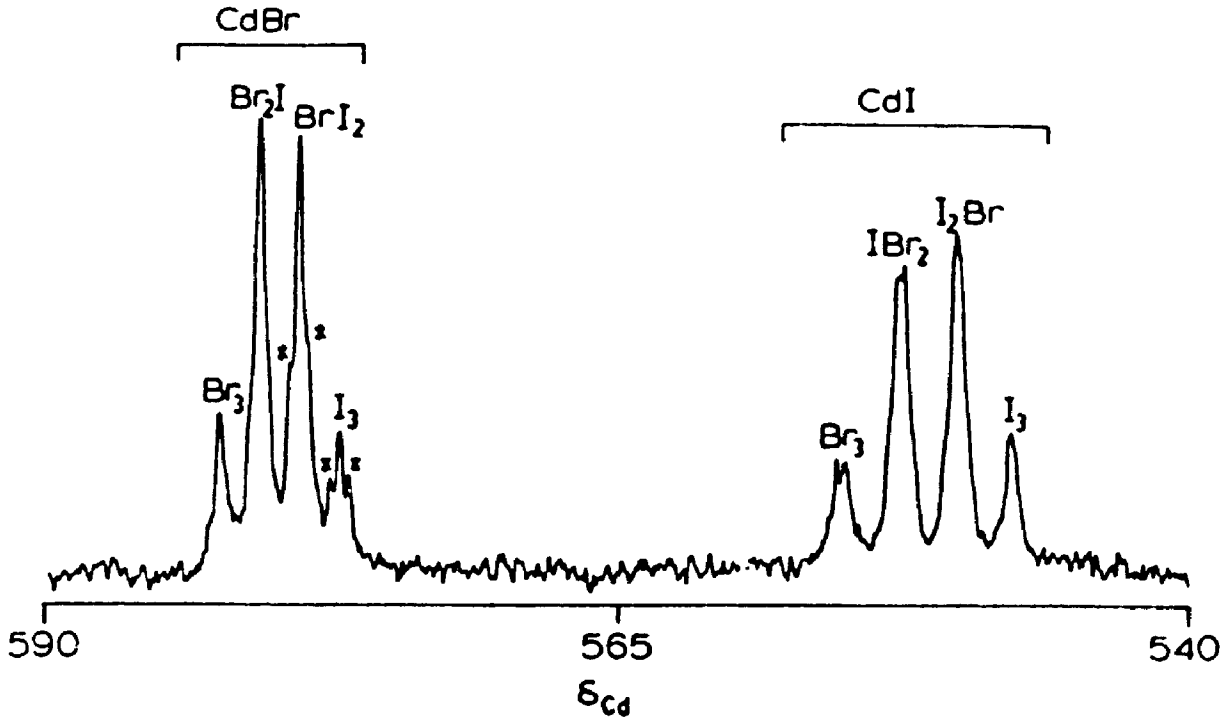

Figure 2.3 42.41 MHz 111-Cd NMR spectrum of a mixture with $[(\mu\text{-SPr}^i)_6(Cd\mathit{Br})_4]^{2-}$: $[(\mu\text{-SPr}^i)_6(Cd\mathit{I})_4]^{2-}$ = 1:1 in CH_2Cl_2 at 215 K.[20] * indicates Cd satellite.

temperature, additional fine structure is observed with two groups of signals, each containing four lines. These lines are corresponding to the species of Cd_4X_4, Cd_4X_3X', $Cd_4X_2X'_2$, $CdXX'_3$ in the region Cd-X and $Cd_4X'_4$, $Cd_4X'_3X$, $Cd_4X'_2X_2$, $CdX'X_3$ in the region Cd-X'. The equilibrium equation has been shown in Section 1.6. The assignment for these lines is completed by comparison to their parent signals and by the variation of the signal intensities as the X/X' ratio is changed. For example, Figure 2.3 shows the ^{111}Cd NMR spectrum of a 1:1 mixture of $[(\mu\text{-}SPr^i)_6(CdBr)_4]^{2-}$ and $[(\mu\text{-}SPr^i)_6(CdI)_4]^{2-}$ in CH_2Cl_2 at 215 K. In Fig. 2.3, the most deshielded signal has the same chemical shift as the cluster $[(\mu\text{-}SPr^i)_6(CdBr)_4]^{2-}$. Therefore this line must come from the parent cluster and the cadmium kernel here defines S_3CdBr. Then the logical analysis is that the next three signals are due to the kernel $S_2S'CdBr$ (S' stands for that S bridging between Cd-I and Cd-Br; see Section 1.6 for details), SS'_2CdBr, and S'_3CdBr in sequence. Also as can be seen from Fig. 2.3, the intensity ratio between Cd-Br and Cd-I regions is about 1:1, and in each region the intensity ratio of four signals is close to 1:3:3:1. This result suggests that the halide exchange between the two parent clusters is a close-to-statistical process. This random distribution process is also true of the Cl/Br and Cl/I cases. Furthermore, the results suggest that the cadmium chemical shifts of the clusters are sensitive not only to the directly attached halide but also to the halides three bonds away.

As can be seen in Table 2.5, when X in Cd_4X_4 is replaced by a heavier halide X', the remaining Cd in Cd-X are shielded. Conversely, if X is replaced by a lighter X', the substitution of Cd_4X_4 causes deshielding. The more the number of X'-substitutions, the larger the magnitude of the effect that is observed. It is not surprising to find that in Cd NMR data, the largest changes per substitution are observed in the series [(μ-

$SPr^i)_6(CdCl)_{4-n}(CdI)_n]^{2-}$, where introduction of each I^- causes an average change of -2.2 ppm in δ_{Cd}(Cd-Cl) and introduction of each Cl^- causes an average change of 4 ppm in δ_{Cd}(Cd-I).

In the mixed-halide system, two-bond cadmium coupling is expected. The ^2J here is different from that in the parent clusters, in that chemical inequivalence is involved. For example, when the cluster is $Cd_4X_2X'_2$, the Cd-X and Cd-X' are chemically inquivalent. Therefore, ^{111}Cd-X is coupled not only to neighbouring ^{113}Cd-X but also to neighbouring $^{111/113}$Cd-X'. Details of this phenomenon have been discussed in Section 1.6. In our NMR spectra, some ^2J values are observed when the lines are sharp enough. The coupling data are included in the footnotes of Table 2.5.

In the study of mixed terminal ligands, since the study of the SPr^i-bridged clusters gave us a satisfactory result, the clusters with other SAlk-bridged groups were not tried. In contrast to the results found for the SAlk system, only two broad signals were observed for the series $[(\mu\text{-SePh})_6(CdBr)_{4-n}(CdI)_n]^{2-}$ [3] at 260K. Separate signals have been observed for $[(\mu\text{-EPh})_6(CdEPh)_{4-n}(CdNCE')_n]^{2-}$ (E = S or Se, E' = O or S) at 213K[13], although the separations are not as good as that in this study.

Experiments involving mixed *bridging* ligands have been tried for $[(\mu\text{-SPr}^i)_{6-n}(\mu\text{-SBz})_n(CdI)_4]^{2-}$ and $[(\mu\text{-SPr}^i)_{6-n}(\mu\text{-SBu}^n)_n(CdI)_4]^{2-}$, but the systems are more complicated and the spectra are not well resolved.

2.3.3 Crystal structure of $(Et_4N)_2[(\mu\text{-SPr}^i)_6(CdBr)_4]$

The result of the crystal structure analysis of $(Et_4N)_2[(\mu\text{-SPr}^i)_6(CdBr)_4]$ is consistent with the NMR results for series involving $[(\mu\text{-SPr}^i)_6(CdBr)_4]^{2-}$. It proves that the

adamantane-like clusters $[(\mu\text{-SAlk})_6(CdX)_4]^{2-}$ exist in the solid state, as well as in solution. The crystal structure of the salt contains a well-separated anion and two cations. The structure of the $Cd_4Br_4(S\text{-}C_1)_6$ skeleton of the anion $[(\mu\text{-SPr}^i)_6(CdBr)_4]^{2-}$ (hereinafter indicated by **1**) is shown in Figure 2.4. This is the first example of an adamantanoid $(\mu\text{-SAlk})_6M_4$ cage that has been characterized crystallographically for M = zinc group elements. Selected interatomic distances and angles are presented in Table 2.6.

As can be seen from Table 2.6, the range of non-bonded Cd...Cd distances is 4.052(3)-4.138(3) Å, values which are smaller than those of 4.149(3)-4.439(3) Å reported for $[(\mu\text{-SPh})_6(CdSPh)_4]^{2-}$, **2**, as the $(Et_4N^+)(Et_3HN)^+$ salt[8], or 4.161(1)-4.167(1) Å reported for $[(\mu\text{-SPh})_6(CdBr)_4]^{2-}$, **3**, as the Me_4N^+ salt[3]. The range of Cd-S bond lengths in **1** is 2.512(7)-2.555(7) Å, comparable to 2.533(3)-2.603(3) Å in **2**, and 2.541(3)-2.565(3) Å in **3**. However, the range of Cd-Br bond lengths in **1** is 2.590(4)-2.608(4) Å, values which are larger than the 2.559(3)-2.565(2) Å observed for **3**, which may be due to the substituent influence of the bulky isopropyl groups. The range of Cd-Cd-Cd angles in **1** is 59.21-60.05° which indicates that the skeleton Cd_4 is close to a tetrahedron. The range of Cd-S-Cd angles in **1** is 106.1-109.4°, less than those of 109.1(1)-118.0(1)° and 109.4(1)-110.2(2)° in **2** and **3**, respectively. A large variation, 93.8-123.1°, in S-Cd-S angles is observed which indicates a large distortion of the adamantane-like skeleton. This range is close to that found in **2** (91.5-118.8°), and larger than that observed in **3** (104.5-117.1°).

There is no crystallographically-imposed symmetry in **1**. As was mentioned in Chapter 1, the adamantanoid cage $[(\mu\text{-SR})_6M_4]$ can exist as four configurational isomers, depending on the relative orientations of the R substituents at the pyramidal sulfur atoms

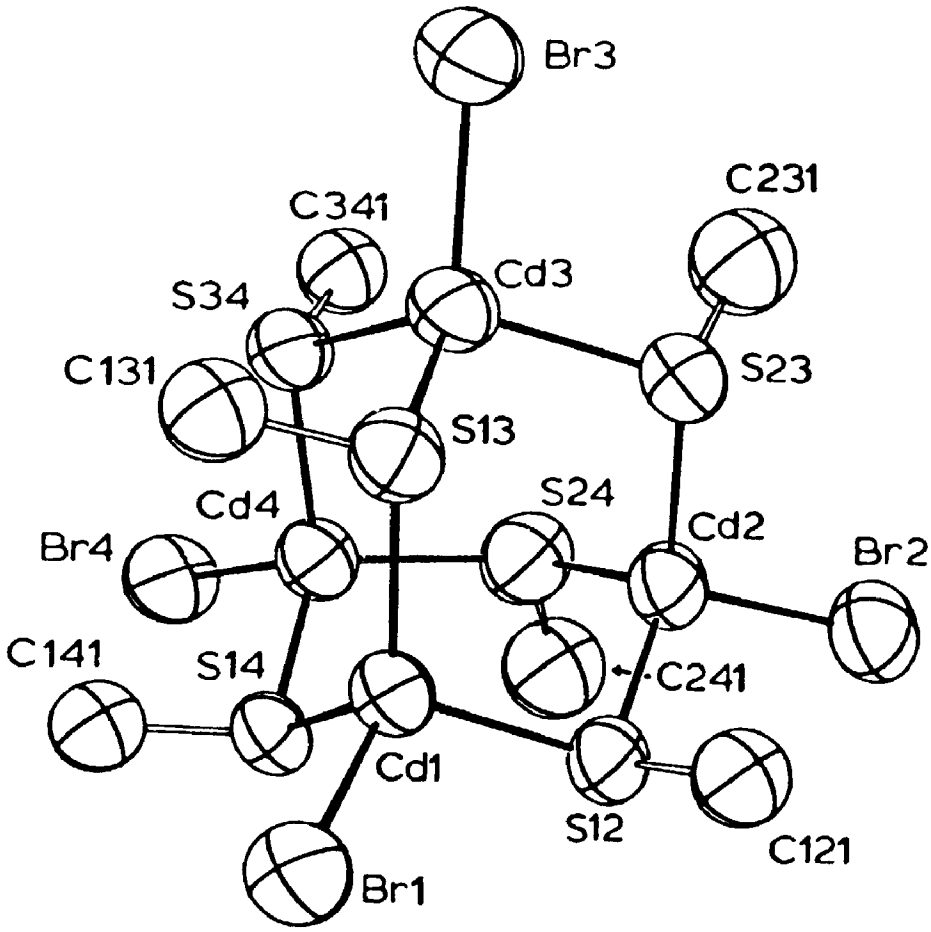

Figure 2.4 Perspective view of the anion $[(\mu\text{-}SPr^{i})_6(CdBr)_4]^{2-}$. For clarity, the methyl groups of the thiolate have been omitted.[20]

Table 2.6 Selected Interatomic Distances(Å) and Angles(deg) for $[(\mu\text{-SPr}^i)_6(CdBr)_4]^{2-}$

		Cd...Cd	
Cd(1)...Cd(2)	4.067(3)	Cd(1)...Cd(3)	4.138(3)
Cd(1)...Cd(4)	4.058(3)	Cd(2)...Cd(3)	4.052(3)
Cd(2)...Cd(4)	4.064(3)	Cd(3)...Cd(4)	4.063(3)
		S...S	
S(12)...S(13)	4.224(3)	S(12)...S(14)	3.711(3)
S(12)...S(23)	4.124(3)	S(12)...S(24)	4.231(3)
S(13)...S(14)	4.416(3)	S(13)...S(23)	3.812(3)
S(13)...S(34)	4.081(3)	S(14)...S(24)	4.172(3)
S(14)...S(34)	4.297(3)	S(23)...S(24)	4.073(3)
S(23)...S(34)	4.438(3)	S(24)...S(34)	3.919(3)
		Cd-Br	
Cd(1) - Br(1)	2.593(4)	Cd(2) - Br(2)	2.590(4)
Cd(3) - Br(3)	2.595(4)	Cd(4) - Br(4)	2.608(4)
		Cd-S	
Cd(1) - S(12)	2.525(7)	Cd(2) - S(12)	2.534(8)
Cd(1) - S(13)	2.533(8)	Cd(3) - S(13)	2.537(8)
Cd(1) - S(14)	2.555(7)	Cd(4) - S(14)	2.523(8)
Cd(2) - S(23)	2.528(8)	Cd(3) - S(23)	2.537(8)
Cd(2) - S(24)	2.527(9)	Cd(4) - S(24)	2.519(8)
Cd(3) - S(34)	2.512(7)	Cd(4) - S(34)	2.526(8)

Table 2.6 (contd.)

		Br-Cd-S	
S(12)-Cd(1)-Br(1)	111.6(2)	S(13)-Cd(1)-Br(1)	109.4(2)
S(14)-Cd(1)-Br(1)	107.4(2)	S(12)-Cd(2)-Br(2)	109.3(2)
S(23)-Cd(2)-Br(2)	108.2(2)	S(24)-Cd(2)-Br(2)	109.3(2)
S(13)-Cd(3)-Br(3)	113.7(2)	S(23)-Cd(3)-Br(3)	103.7(2)
S(34)-Cd(3)-Br(3)	110.7(2)	S(14)-Cd(4)-Br(4)	105.8(2)
S(24)-Cd(4)-Br(4)	114.3(2)	S(34)-Cd(4)-Br(4)	106.6(2)
		S-Cd-S	
S(13)-Cd(1)-S(12)	113.2(2)	S(14)-Cd(1)-S(12)	93.8(2)
S(14)-Cd(1)-S(13)	120.4(3)	S(23)-Cd(2)-S(12)	109.1(2)
S(24)-Cd(2)-S(12)	113.4(3)	S(24)-Cd(2)-S(23)	107.3(3)
S(23)-Cd(3)-S(13)	97.4(3)	S(34)-Cd(3)-S(13)	107.8(2)
S(34)-Cd(3)-S(23)	123.1(3)	S(24)-Cd(4)-S(14)	111.7(3)
S(34)-Cd(4)-S(14)	116.7(2)	S(34)-Cd(4)-S(24)	101.9(3)
		Cd-S-Cd	
Cd(2)-S(12)-Cd(1)	107.0(3)	Cd(3)-S(13)-Cd(1)	109.4(2)
Cd(4)-S(14)-Cd(1)	106.1(2)	Cd(3)-S(23)-Cd(2)	106.3(3)
Cd(4)-S(24)-Cd(2)	107.3(3)	Cd(4)-S(34)-Cd(3)	107.5(3)

Table 2 7 Correlation of S.. S distances and S-Cd-S angles in **1-3**[a]

	1	**2**	**3**
S...S Distances (Å)			
a-a	4.416, 4.438	4.316, 4.434	4.334
mean	4.43(2)	4.38(8)	4.334(0)
a-e	3.919 - 4.297	3.939 - 4.224	4.028 - 4.157
mean	4.14(12)	4.11(10)	4.09(9)
e-e	3.711, 3.812	3.695, 3.750	4.046
mean	3.76(7)	3.72(4)	4.046(0)
S-Cd-S Angles (deg)			
a-a	120.4, 123.1	114.7, 118.4	117.1
mean	121.7(19)	116.6(26)	117.1(0)
a-e	101.9 - 116.7	99.9 - 110.8	104.5 - 109.6
mean	110.1(46)	107.0(37)	107.4(32)
e-e	93.8, 97.4	91.5, 93.5	105.2
mean	95.6(25)	92.5(14)	105.2(0)

[a] See text for the corresponding clusters of **1-3**.

in the four $M_3(SR)_3$ rings. As can be seen in Fig 2.4, the six isopropyl groups adopt the configuration of Isomer III (C_1 symmetry). Thus the four six-membered M_3S_3 rings are [aae, aae, aee, aee]. This configuration has two axial-axial interactions, which is the minimum possible number. Both the S...S distances and the S-Cd-S angles should reflect the nature of the interaction (a-a, a-e or e-e) involved[1]. The S .S distances and the S-Cd-S angles for **1**, **2** and **3** are grouped in Table 2.7. As can be seen in Table 2.7, both parameters follow the order, a-a > a-e > e-e, which is also the order to the indication of their interactions. In addition, when only the a-a interaction is considered, the S...S distances and S-Cd-S angles in **1** are larger than those found in **2** and **3**. This may be due to the bulkiness of the substituent, isopropyl, in **1**.

2.3.4 Reaction of $[(\mu\text{-SPr}^i)_6(CdX)_4]^{2-}$ with sulfur and selenium

A study of the reaction of $[(\mu\text{-SPh})_6(MSPh)_4]^{2-}$ (M = Cd or Zn) with E'_8 (E' = S or Se) has been carried out and it has been shown that the decametallo-complex $[M_6(\mu_3\text{-}E')_4(\mu_2\text{-SPh})_{12}(MSPh)_4]^{2-}$ is formed according to Equation [3][21a].

[3] $$5\ [(\mu\text{-SPh})_6(MSPh)_4]^{2-} + 8\ E' \rightarrow 2\ [M_6(\mu_3\text{-}E')_4(\mu_2\text{-SPh})_{12}(MSPh)_4]^{4-} + 16\ Ph_2S_2 + 2\ SPh^-$$

The question now is what the result will be for the reaction with E' if the bridging ligands are changed to alkylthiolates instead of phenyl-thiolates/selenolates and the terminal ligands are changed to halides instead of chalcogenates in the starting tetranuclear clusters. In our experiment, the clusters $[(\mu\text{-SPr}^i)_6(CdX)_4]^{2-}$ (X = Cl, Br or I) are chosen

as the starting materials for the investigation, because they give sharp Cd NMR signals at ambient probe temperature (see above - Section 2.3.2).

At room temperature, sulfur or selenium dissolves readily in the CH_2Cl_2 solution of $[(\mu\text{-SPr}^i)_6(CdX)_4]^{2-}$. All the ^{77}Se and ^{111}Cd NMR spectra were measured at ambient probe temperature. The NMR results are included in Table 2.8. A typical ^{111}Cd NMR spectrum is shown in Figure 2.5a. This is for a mixture in which $[(\mu\text{-SPr}^i)_6(CdI)_4]^{2-}$: red-Se = 1 : 0.5. As can be seen in Fig. 2.5a, there are two additional signals (509 and 621 ppm) with equal intensity but the Cd_4 parent signal (531 ppm) is still a major one. For convenience of signal analysis, the less shielded signal (621 ppm) is arbitrarily assigned to Cd_A, and the more shielded one (509 ppm) is assigned to Cd_B. The chemical shift of Cd_B signal is close to that of parent signal. Also it shows a similar halogen dependence to that of $[(\mu\text{-SPr}^i)_6(CdX)_4]^{2-}$ by comparison of the data in Table 2.3 and Table 2.8. This result indicates that the species of Cd_B has a similar coordination environment about Cd as the parent cluster does, *i.e.* the Cd is four-coordinate and one ligand is probably a halide. The Cd_A signal is relatively far away from the parent signal, but it is still in the range of four-coordinate cadmium species. As can be seen from Table 2.8, the Cd_A kernel is little sensitive to the change of halide but relatively sensitive to the change of chalcogen. These observations suggest that Cd_A may coordinate directly with a chalcogenide ion, but not directly with a halide.

Besides the difference in chemical shifts for Cd_A and Cd_B, both Cd resonances show slightly different coupling modes. The contribution of satellites is mainly due to the cadmium isotopes of chemically inequivalent cadmiums (more details about this and selenium contribution will be discussed later). As can be seen from Fig. 2.5a and Table

Table 2.8 ^{111}Cd and ^{77}Se NMR data for $[(Cd_A)_4(\mu_4\text{-}E')(\mu_2\text{-}SPr')_{12}(Cd_BX)_4]^{2+}$ in CH_2Cl_2 at 294±1 K.[a]

E'	X	$\delta_{Cd}(Cd_A)$[a,b]	$\delta_{Cd}(Cd_B)$[a,b]	δ_{Se}[c]	$^2J(Cd\text{-}Cd)_{ave}$[d,e]	$^1J(Cd\text{-}Se)$[d]
S	Cl[f]	645	570		38	
	Br[f]	645	553		39	
	I[g]	642	518		41	
Se	Cl[h]	628	556	-613.6	35	73
	Br[h]	626	539	-610.6	37	74
	I[i]	621	508	-607.4	40	73

[a] See Fig. 2.6 for labelling.

[b] Relative to external 0.1 M $Cd(ClO_4)_2(aq)$ at 293±1 K.

[c] Relative to external pure Me_2Se at 295±1 K.

[d] Estimated error ±1 Hz.

[e] $^2J(^{111}Cd_A\text{-}S\text{-}^{111}Cd_B)$ and $^2J(^{111}Cd_A\text{-}S\text{-}^{113}Cd_B)$ were not resolved (see text).

[f] In a mixture where $[Cd_4]_{initial}$ = 0.05 mol/L of solvent and Cd_4:S = 1:1.

[g] In a mixture where $[Cd_4]_{initial}$ = 0.2 mol/L of solvent and Cd_4:S = 1:0.67.

[h] In a mixture where $[Cd_4]_{initial}$ = 0.1 mol/L of solvent and Cd_4:Se = 1:0.5.

[i] In a mixture where $[Cd_4]_{initial}$ = 0.2 mol/L of solvent and Cd_4:Se = 1:0.5.

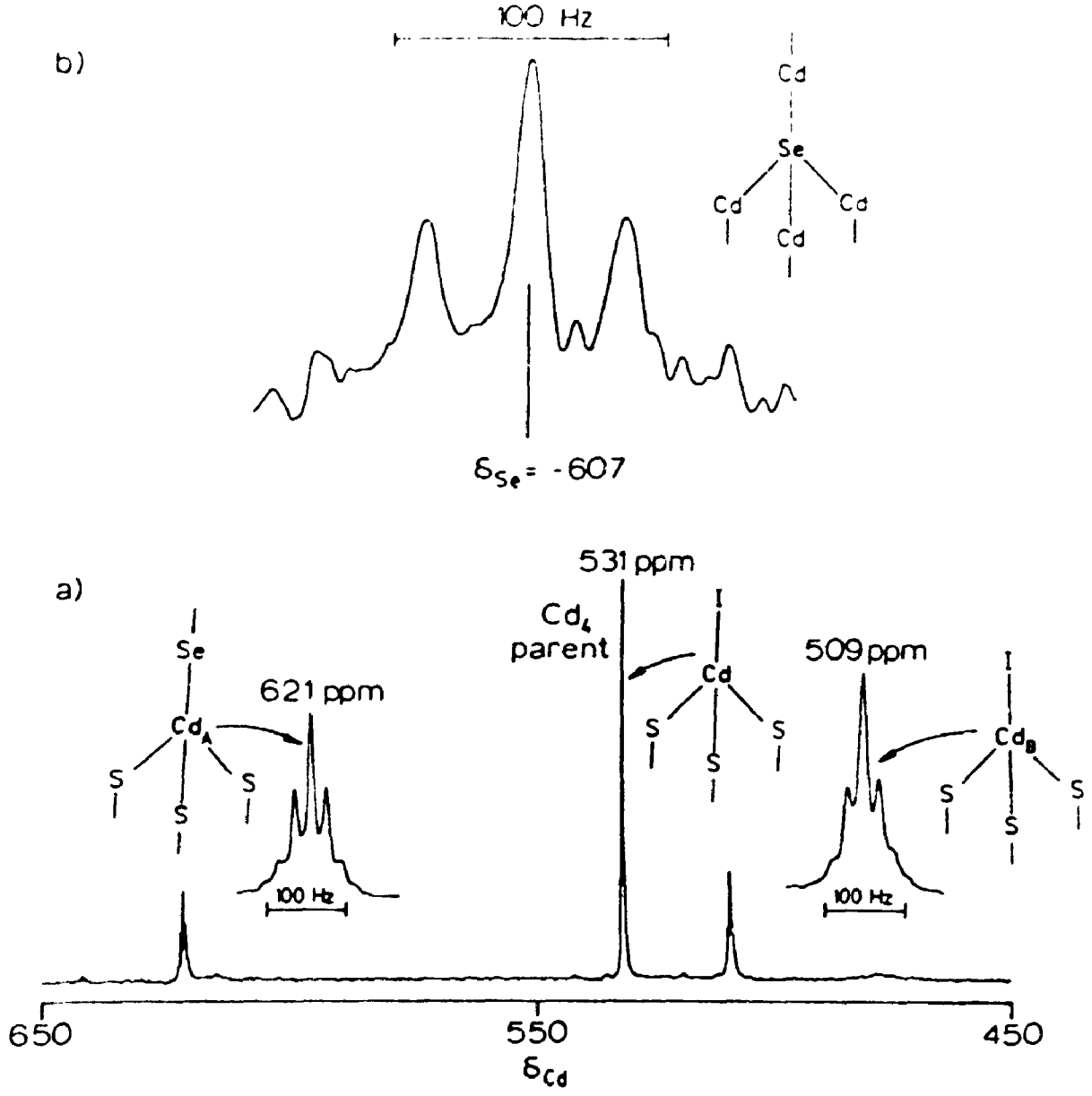

Figure 2.5 NMR spectra of Cd/Se-Containing Species in a 1.0.5 mixture of $[(\mu\text{-}SPr^i)_6(CdI)_4]^{2-}$ and red Se in CH_2Cl_2 at 295 K. (a) 42.41 MHz 111-Cd NMR spectrum. (b) 57.20 MHz 77-Se NMR spectrum.[20]

2.8, the magnitude of the major satellite separation is about 40 Hz. By comparison with the data in Table 2.4, this is clearly a two-bond cadmium-cadmium coupling. Therefore, Cd_A and Cd_B must be linked by one or more bridging groups The most probable bridging ligands here are thiolates. On the basis of these findings mentioned above (and the ^{77}Se NMR, as well as the signal simulations shown later), the high frequency signal in Figure 2.5a is assigned to the kernel $(\mu\text{-Se})Cd_A(\mu\text{-SPr}')_3$ while the other one is assigned to $ICd_B(\mu\text{-SPr}')_3$. The assignments to the other cases are made in a similar manner.

A ^{77}Se resonance is also observed for the mixture of the parent cluster and red-Se. The ^{77}Se NMR data of the new species have been included in Table 2.8. As an example, a partial ^{77}Se NMR spectrum of the mixture $[(\mu\text{-SPr}')_6(CdI)_4]^{2-}$: red-Se = 1 : 0.5 is shown in Figure 2.5b (there is an additional signal from $(Pr'S)_2Se$; see discussion below). As can be seen from Fig. 2.5b and Table 2.8, first, the signal positions (-613.6, -610.6 and -607.4 ppm for Cl, Br and I, respectively) are comparable to known values for Se^{2-} (δ_{Se} = -511 for 0.5 M $(NH_4)_2Se$ in D_2O[21b], δ_{Se} = -490 for hexagonal CdSe in the solid state[22], δ_{Se} = -731 for $[Cd_6(\mu_3\text{-Se})_4(\mu\text{-SPh})_{12}(CdI)_4]^{4-}$ in DMF[23]). Second, the coupling constants (73, 74 and 73 Hz for Cl, Br and I, respectively) are comparable to those known values observed for $^1J(^{111/113}Cd\text{-}^{77}Se)$ in $[(\mu\text{-SePh})_6(CdX)_4]^-$ clusters[3,13] (58, 80 and 120 for Cl, Br and I, respectively), which means that Se^{2-} is directly attached to cadmium. Third, both chemical shifts and coupling constants of the three new species are insensitive to the halides, which indicates that Se^{2-} is relatively far away from halides and therefore it coordinates with Cd_A rather than with Cd_B. The analysis results for the ^{77}Se NMR spectra are consistent with the assignments for Cd_A in ^{111}Cd NMR spectra.

From the ^{111}Cd and ^{77}Se NMR analysis discussed above, now we can assume that

the new species is $[(Cd_A)_4(\mu_4\text{-}E')(\mu_2\text{-}SPr^i)_{12}(Cd_BX)_4]^{2-}$ (abbreviated as Cd_8) with the skeleton shown in Fig. 2.6. A similar skeleton occurs in $[Zn_4(\mu_4\text{-}Cl)(SPh)_{12}(ZnSPh)_4]^{-}$ [24]. Very lately, while our own study was in progress, a very similar series $[Cd_4(\mu_4\text{-}E')(\mu\text{-}EPh)_{12}(CdX)_4]^{2-}$ (E, E' = S, Se, Te; X = halide or EPh^-) was reported and shown to have this structure also[25]. As well, such a skeleton has been found in $^3_\infty[\{SCd_8(S\text{-}2\text{-}Bu)_{12}\}(CN)_{4/2}]$ [26] in the solid state.

As can be seen from Fig. 2.6, there are two types of cadmium sites, *i.e.* four Cd_A and four Cd_B kernels. Each Cd_B has one terminal X and three two-bond neighbouring Cd_A through the bridging thiolate. In the ^{111}Cd NMR spectra, Cd_B is coupled to both ^{111}Cd and ^{113}Cd from the three sites A, because sites A and B are chemically different. The Cd_B may also be coupled through three-bonds to ^{77}Se and through four-bonds to $^{113}Cd_B$, but these couplings are expected to be too small to be considered. In our real spectra, the two-bond couplings of $^{111}Cd_{B/A}$-$^{111}Cd_{A/B}$ and $^{111}Cd_{B/A}$-$^{113}Cd_{A/B}$ are not resolved. Assuming that site B is ^{111}Cd, the isotope population of site A can be calculated by the formula mentioned in Section 1.5. The populations of $^0Cd_3$, $^{111,113}Cd^0Cd_2$, $^{111,113}Cd_2{}^0Cd$, and $^{111,113}Cd_3$ on three Cd_A are 0.4217, 0.4219, 0.1407 and 0.0156, separately. It can be seen that the major coupling contributions come from the first three combinations. The same analysis can be used to the coupling which happens on site A by the three Cd_B nuclei that are two bonds away. But two more couplings must be considered here. One is the $^1J(^{111}Cd_A\text{-}^{77}Se)$, for which the coupling probability is directly from its natural abundance, 7.58%. The other is $^2J(^{111}Cd_A\text{-}^{113}Cd_A)$, for which the probabilities of isotope combinations of $^{0,111}Cd_3$, $^{113}Cd^{0,111}Cd_2$, $^{113}Cd_2{}^{0,111}Cd$, and $^{113}Cd_3$ on the other three Cd_A are 0.6754, 0.2831, 0.0396, and 0.0018, respectively. Because of their low probabilities, the

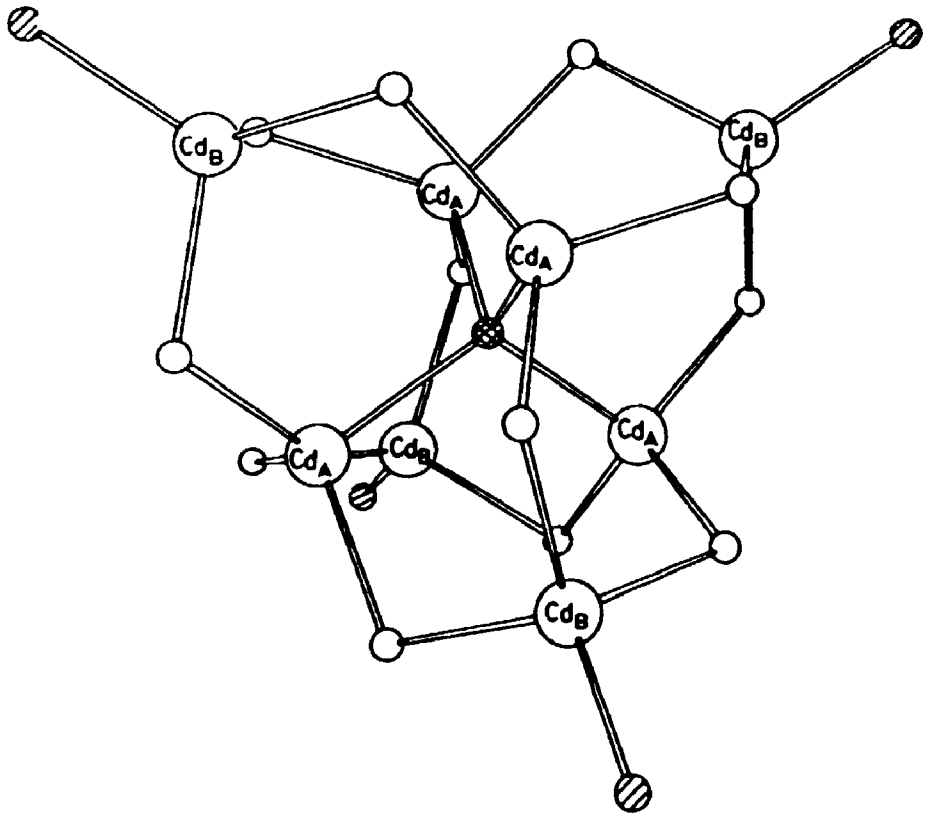

(○ = sulfur (of thiolate); ◐ = halide; ◉ = chalcogenide)

Figure 2.6 The skeleton of $[(Cd_A)_4(\mu_4\text{-}E')(\mu_2\text{-}SPr')_{12}(Cd_BX)_4]^{2-}$. [20]

last two combinations can be neglected. Furthermore, the magnitudes of $^2J(^{111}Cd_A\text{-}^{113}Cd_A)$ and $^2J(^{111}Cd_A\text{-}^{111/113}Cd_B)$ are close and therefore these two types of two-bond couplings can not be resolved either. Finally, ^{77}Se is expected to be coupled to $^{111/113}Cd$ in site A, but not to $^{111/113}Cd$ in the more distant site B. The populations of $^0Cd_4$, $^{111/113}Cd^0Cd_3$, $^{111/113}Cd_2{}^0Cd_2$, and $^{111/113}Cd_3{}^0Cd$ are 0.3162, 0.4219, 0.2110, and 0.0469, respectively.

Taking into account appropriate statistics discussed above, the ^{111}Cd and ^{77}Se NMR spectra of Figure 2.5 can be simulated using the Cd_8 structure with $^1J(^{111}Cd\text{-}^{77}Se) = 73$ Hz, $^2J(^{111}Cd_{B/A}\text{-S-}^{111/113}Cd_{A/B}) = {}^2J(^{111}Cd_A\text{-S-}^{113}Cd_A) = 40$ Hz, and empirical linewidths. The good matches between the observed and simulated spectra are shown in Figure 2.7. Based on these facts, now we can conclude that reaction of $[(\mu\text{-SPr}')_6(CdX)_4]^{2-}$] with sulfur or selenium really does produce the new and larger cluster $[Cd_4(\mu_4\text{-E}')(SPr')_{12}(CdX)_4]^{2-}$.

Although the Cd_8 cluster has been proved as a major product of the reaction of Cd_4 with S or Se, the stoichiometry of this reaction is still not certain at this point. However, in some cases (E' = S, X = Cl, Br, or I), colourless, crystalline materials were formed in the mixtures over several hours at ambient probe temperature. These crystals were isolated easily and finally shown to contain only Et_4N^+ by ^1H NMR. A single crystal was obtained from the case of E' = S, X = Br. X-ray analysis showed the product to be $(Et_4N)_2[CdBr_4]$[27]. When E' = Se, no crystalline material was formed, but a yellow oil was separated which again showed only the ^1H NMR resonances of Et_4N^+.

We have known that S or Se as an oxidant in the reaction is finally converted to S^{2-} or Se^{2-}. Therefore during the reaction there must be something oxidized. To complete the study on the reaction of Cd_4 and S or Se stoichiometrically, ^{13}C NMR was used as an additional probe. The ^{13}C NMR data of isopropyl in the clusters Cd_4 and Cd_8 are given

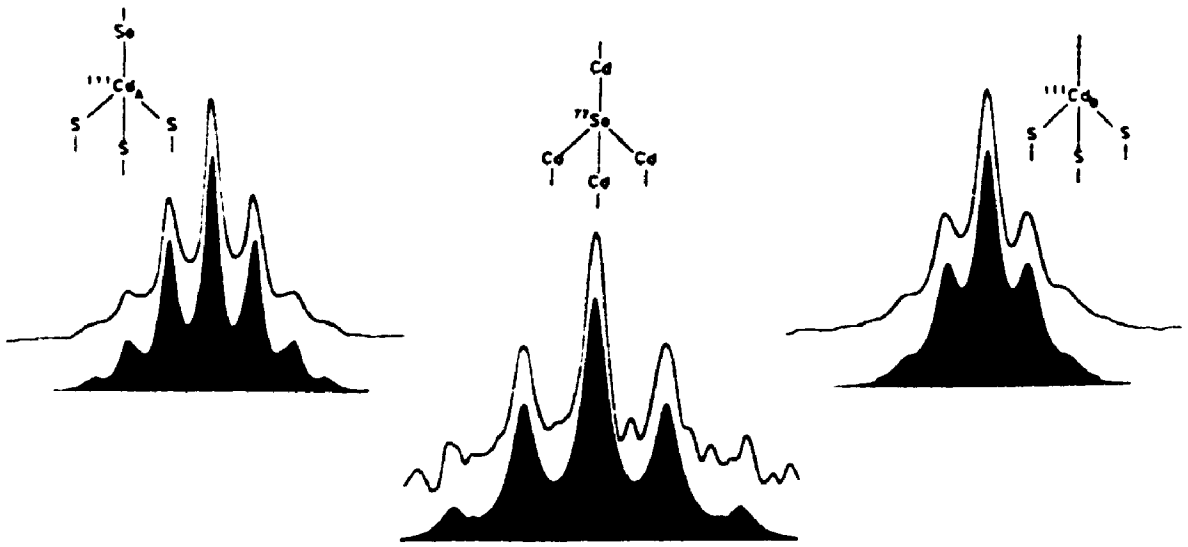

Figure 2.7. Observed and (below) simulated NMR spectra of $[(Cd_4(\mu_4\text{-}Se)(\mu\text{-}SPr^i)_{12}(CdI)_4]^{2-}$. [20]

Table 2.9 ^{13}C NMR data for $[(\mu\text{-}SPr^i)_6(CdX)_4]^{2-}$ and $[(Cd_A)_4(\mu_4\text{-}E')(\mu_2\text{-}SPr^i)_{12}(Cd_BX)_4]^{2-}$ in CH_2Cl_2 at 294±1 K[a]

		$\delta_C(Pr^i$ in $Cd_4)$		$\delta_C(Pr^i$ in $Cd_8)$	
E'	X	CH_3	CH	CH_3	CH
S	Cl	30.1	34.5	30.0[b]	34.9[c]
S	Br	30.2	34.9	30.0[d]	35.1[e]
S	I	30.1	35.5	29.9	35.7
Se	Cl	30.1	34.6	30.0	35.0
Se	Br	30.2	34.9	30.0	35.2[f]
Se	I	30.1	35.7	29.9	36.4

[a] The Cd_8 complex was formed *in situ* from the Cd_4 complex and E' (see text). The starting concentration of Cd_4 complex was 0.05-0.1 mol/L of CH_2Cl_2.

[b] $^3J(C,Cd) = 10.8 \pm 0.2$ Hz.

[c] $^2J(C,Cd) = 8.0 \pm 0.2$ Hz.

[d] $^3J(C,Cd) = 9.5 \pm 0.2$ Hz.

[e] $^2J(C,Cd) = 7.9 \pm 0.2$ Hz.

[f] $^2J(C,Cd) = 7.8 \pm 0.2$ Hz.

in Table 2.9. More importantly, the ^{13}C NMR spectra show that when sulfur is used as the oxidant, the oxidized isopropylthiolate is converted not only to Pr^{i}SSPr^i (δ_C = 22.3 (CH_3), 41.4 (CH)), but also to Pr^{i}SSSPr^i (δ_C = 22.2, 41.8) and Pr^{i}SSSSPr^i (δ_C = 22.4, 42.1), even if Cd_4 is still present. When selenium is used as the oxidant, the oxidized thiolate converted to $(Pr^iS)_2Se$ (δ_C = 23.5 (CH_3), 41.2(CH); δ_{Se} = 602), which is proved by comparison with an original sample of the Se(II) dithiolate.

Based on the preceding information, the reaction stoichiometry is finally given in Equation [4].

[4] $$7\ [(\mu\text{-}SPr^i)_6(CdX)_4]^{2-} + (3+3x)\ E' \rightarrow$$
$$3\ [Cd_4(\mu_4\text{-}E')(\mu\text{-}SPr^i)_{12}(CdX)_4]^{2-} + 3\ Pr^iSE'_xSPr^i + 4\ CdX_4^{2-}$$
$$(X = Cl, Br, I;\ E' = S,\ x \approx 1\ (ave);\ E' = Se,\ x = 1)$$

As can be seen from Fig. 2.5, the reaction of Cd_4 with Se is not very straight forward. The parent Cd_4 is still the major species in the solution. It is also true for all the other cases. It seems that the Cd_8 cluster initially forms then reacts with additional S or Se, so that the Cd_8 complex dies away while the starting Cd_4 still exists. Attempts to identify the new complexes formed from Cd_8 have so far not been successful yet.

2.4 Conclusions

Although the adamantanoid cages of $(\mu\text{-}SPh)_6M_4$ for zinc-group elements are well established, remarkably little attention has been paid to analogues of the type of $(\mu\text{-}SAlk)_6M_4$. A wide range of new adamantane-like clusters $(Et_4N)_2[(\mu\text{-}SAlk)_6(MX)_4]$ (M

= Zn or Cd; X = Cl, Br, or I) has been prepared by self-assembly method. In total, twenty-seven new clusters have been isolated and confirmed by microanalysis and NMR. The mixed-metal clusters $[(\mu\text{-SAlk})_6(CdX)_4(ZnX)_{4-n}]^{2-}$ (X = Cl, Br or I) and mixed-halide clusters $[(\mu\text{-SPr}')_6(CdX)_n(CdX')_{4-n}]^{2-}$ (X/X' = Cl/Br, Cl/I, or Br/I) have been measured by Cd NMR. In total, more than eighty cluster species in solution have been characterized by metal NMR.

As can be seen from the NMR results of the parent clusters, $[(\mu\text{-SR})_6(CdX)_4]^{2-}$, the Cd chemical shift varies with X in the order Cl > Br > I, and varies with R in the order primary alkyl ≥ benzyl > secondary alkyl > phenyl. The Cd chemical shift also depends on the temperature in the order reduced T > ambient T. These properties of chemical shift variations have also been found in their corresponding halide-exchange or metal-exchange mixtures.

From the Cd NMR result of metal-mixed clusters $[(\mu\text{-SAlk})_6(CdX)_4(ZnX)_{4-n}]^{2-}$, the four signals (n = 1 - 4) confirm the existence of both Cd_4 and Zn_4 parent clusters in solution, and the intensity ratio 1 : 3 : 3 : 1 when equimolar amounts of Zn and Cd are present, shows that the metal redistribution occurs close to statistically. The effect of zinc substitution on the cadmium chemical shift is generally larger for SAlk clusters than for SPh analogues.

Halide-exchange has been demonstrated successfully for the first time, in $[(\mu\text{-SPr}')_6(CdX)_n(CdX')_{4-n}]^{2-}$. From the NMR fine structure following halide redistribution, it is revealed that the halide exchange occurs close to statistically, and the distribution of halide at one terminal site influences the Cd nuclear shielding at the other positions. In principle, the heavier the halides, the more the Cd nuclear shielding.

Carbon-13, ^{77}Se and ^{111}Cd NMR have been used to study the reaction of $[(\mu\text{-}SPr^i)_6(CdX)_4]^{2-}$ with sulfur and selenium. The result shows that the larger clusters $[Cd_4(\mu_4\text{-}E')(\mu\text{-}SPr^i)_{12}(CdX)_4]^{2-}$ are formed in solution, although the reactions do not proceed to completion. The formation of the Cd_8 clusters is supported by simulated NMR spectra.

Finally, the crystal structure of $(Et_4N)_2[(\mu\text{-}SPr^i)_6(CdBr)_4]$ has been determined. This is the first example of an adamantane-like $(\mu\text{-}SAlk)_6M_4$ cage which has been characterized crystallographically for M = zinc group elements. The NMR study of the Cd_4 cluster series with alkylthiolate as bridging ligands is strongly supported by the findings of this crystal structure.

In brief, the results presented here show that the chemistry of Cd_4 clusters with alkylthiolates as bridging ligands is really different from that of those with phenylthiolates in many aspects, such as variation of cadmium nuclear shielding, the exchange of metals or terminal ligands, *etc.*

2.5 References

1 I.G. Dance, *Polyhedron*, 5 (1986) 1037.

2. P.J. Blower and J.R. Dilworth, *Coord. Chem. Rev.*, 76 (1987) 121.

3 P.A.W. Dean, J.J. Vittal and N.C. Payne, *Inorg. Chem.*, 26 (1987) 1683.

4. P.A.W. Dean and V. Manivannan, *Inorg. Chem.*, 29 (1990) 2997.

5. J.J. Vittal, P.A.W. Dean and N.C. Payne, *Can. J. Chem.*, 70 (1992) 792.

6. P.A.W. Dean and J.J. Vittal, in *Metallothioneins*, M.J. Stillman, C.F. Shaw III, and K.T. Suzuki, eds., VCH press, New York, 1992, Ch.14.

7. (a) I.G. Dance, *Austral. J. Chem.*, 38 (1985) 1745; (b) P.A.W. Dean and J.J. Vittal, *Inorg. Chem.*, 25 (1986) 514.

8. K.S. Hagen and R.H. Holm, *Inorg. Chem.*, 23 (1984) 418.

9. D.C. Bradley and C.H. Marsh, *Chem. and Ind.*, (1967) 361.

10. J.L Kice, T.W.S. Lee, and S. Pan, *J. Am. Chem. Soc.*, 102 (1980) 4448; J.L. Kice and H. Slebocka-Tilk, *J. Am. Chem. Soc.*, 104 (1982) 7123.

11. P.A.W. Dean, J.J. Vittal, and M.H. Trattner, *Inorg. Chem.*, 26 (1987) 4245.

12. D. Coucouvanis, M. Kanatzidis, E. Simhon and N.C. Baenziger, *J. Am. Chem. Soc.*, 104 (1982) 1874.

13. P.A.W. Dean and J.J. Vittal, *Can. J. Chem.*, 66 (1988) 2443.

14 C.J. Jameson and J. Mason, in *Multinuclear NMR*, Edited by J.Mason. Plenum Press, New York, 1987, p.69 *et seq.*

15. R. Colton and D. Dakternieks, *Austral. J. Chem.*, 33 (1980) 2405.

16 G.K. Carson, P.A.W. Dean and M.J. Stillman, *Inorg. Chim. Acta*, 66 (1982) 37.

17 I G. Dance, *Inorg. Chim. Acta*, 108 (1985) 227.

18. P.A.W. Dean and J.J. Vittal, *J. Am. Chem. Soc*, 106 (1984) 6436

19. I.G. Dance and J.K. Saunders, *Inorg. Chim. Acta*, 96 (1985) L71

20. P.A.W. Dean, J.J. Vittal, and Y. Wu, *Can. J. Chem*, 70 (1992) 779.

21. (a) I.G. Dance, A. Choy, and M.L. Scudder, *J. Am. Chem. Soc.*, 106 (1985) 6285.
(b) J.D. Odom, W H. Dawson, and P.D. Ellis, *J. Am. Chem. Soc.*, 101 (1979) 5815.

22. W. Koch, O. Lutz, and A. Nolle, *Z. Physik.* A289 (1978) 17.

23. P.A.W. Dean and V. Manivannan, Unpublished results.

24. I.G. Dance, *Austral. J. Chem.*, 38 (1985) 1391.

25. G.S.H. Lee, K.J. Fisher, D.C. Craig, M.L. Scudder, and I.G. Dance, *J. Am. Chem. Soc.*, 112 (1990) 6435.

26. I.G. Dance, R.G. Garbutt, I. Ma, and M.L. Scudder, Unpublished work quoted in ref. [25].

27. P.A.W. Dean, Y. Wu, J.J. Vittal, and N.C. Payne, Unpublished results.

CHAPTER 3 STUDIES ON CADMIUM CLUSTERS $[(\mu\text{-ER})_6(CdPPh_3)_n(Cd)_{4-n}]^{2+}$

3.1 Introduction

In the last chapter (Ch. 2) anions of the type $[(\mu\text{-SAlk})_6(MX)_4]^{2-}$ have been discussed. Now we are interested in what would happen if the X (= halides) were changed to the neutral ligands L (= phosphines). Could new Cd_4 clusters be formed? In the solid state or in solution? Could the new clusters (if they are formed) be formulated $[(\mu\text{-SAlk})_6(ML)_4]^{2+}$? What are the properties (especially NMR and structure) of the new clusters? As a terminal ligand, is phosphine better than halide? With these questions, we started the research of this chapter.

In the area of tetranuclear M-phosphine clusters, we note that the mercury clusters, such as $[(\mu\text{-ER})_6(HgL)_4]^{2+}$ (E = S or Se; R = Alk or Ph; L = tertiary phosphine or arsine)[1], are well known; their synthesis and NMR spectra have been reported. Similarly, $[(\mu\text{-TePh})_6(HgPR'_3)_{3 \text{ or } 4}(Hg)_{1 \text{ or } 0}]^{2+}$ (R' = Ph, 4-C_6H_4Me or 4-C_6H_4Cl)[2] have been described. The Cd-phosphine clusters are little known, however except that ^{77}Se and ^{113}Cd NMR data have been given for $[(\mu\text{-EPh})_6(CdPPh_3)_4]^{2+}$ (E = S, Se) in $CHCl_3$[3]. The studies had never been extended to the alkylthiolate series when this chapter work is started. We also note that in many cases the properties of cadmium clusters may not be parallel to the mercury analogues, e.g. $[(\mu\text{-ER})_6(CdX)_4]^{2-}$ (ER = SePh, SPh or SAlkyl; X = Cl, Br or I) are quite stable at ambient temperature[4-6] whereas the Hg_4 analogues dissociate.[6]

In this chapter, we try to prove the existence of this type of cadmium cluster in the solid state and in solution. Furthermore, we try to discover how the coordination properties of Cd are influenced by variation of the SR ligands. For these purposes,

several new compounds with the adamantanoid cage have been isolated, and multi-NMR spectra have been measured for several systems $Cd(PPh_3)_2(ClO_4)_2$:$Cd(ER)_2$:PPh_3 (ER = SePh, SPh or SAlkyl). To allow a better interpretation of the NMR spectra of the tetranuclear clusters formed in these systems, the ^{111}Cd NMR for mononuclear system of $Cd(PPh_3)_n(ClO_4)_2$ (n = 2-4) and ^{31}P and ^{111}Cd NMR for $[Cd(PPh_3)_n(OPPh_3)_{4-n}]^{2+}$ (n = 2,3) have been studied for the first time. The results show that the tetranuclear Cd-phosphine clusters are of the general type $[(\mu\text{-}ER)_6(CdPPh_3)_n(Cd)_{4-n}]^{2+}$. In addition, several *open* tetranuclear complexes $[Ph_3PCd(\{\mu\text{-}ER\}CdPPh_3)_3]^{5+}$ have been found in solution as the by-products of the study. Finally, an x-ray diffraction has been carried out for $[(\mu\text{-}SPr^i)_6(CdPPh_3)_2(CdOClO_3)_2]$.EtOH and the structure confirms the synthetic and NMR results.

3.2 Experimental

Materials and General Procedures

All starting materials were from commercial sources and were used as received. An exception is PPh_3 which was recrystallized from absolute EtOH. The compounds $Cd(ER)_2$ (E = S, R = *n*-Pr, *i*-Pr, *n*-C_5H_{11} (*n*-Pe), *c*-C_6H_{11} (Cy), or Ph; E = Se, R = Ph) were prepared by literature methods.[5,7] $OPPh_3$ was prepared by $KMnO_4$ oxidation of PPh_3 in Me_2CO.[8] $Cd(PPh_3)_2(ClO_4)_2$ was prepared by literature method[9a] but the initial product was usually contaminated with $Cd(PPh_3)_3(ClO_4)_2$, as indicated by reduced temperature ^{31}P NMR. Purification was performed by addition of Et_2O to a dilute solution of the crude product in CH_2Cl_2. The isolated crystals proved pure by ^{31}P NMR. [**CAUTION!** Since perchlorate salts of metal complexes with organic ligands are known

to be explosive[9b], they should be prepared in small amounts, usually not more than one gram, each time.] All solvents used in synthesis or in the preparation of NMR samples were dried over 3A molecular sieves and deoxygenated by sparging with Ar. All syntheses and preparations of NMR samples were carried out under an atmosphere of Ar or N_2.

Synthesis

$Cd_4(SePh)_6(PPh_3)_4(ClO_4)_2$. A mixture of $Cd(PPh_3)_2(ClO_4)_2$ (0.418g, 0.5 mmol), $Cd(SePh)_2$ (0.637g, 1.5 mmol) and PPh_3 (0.262g, 1.0 mmol) at molar ratio 1:3:2 in CH_2Cl_2 (5 mL) was stirred for 20 min. A small amount of insoluble gelatinous material was removed by filtration. Et_2O (5 mL) was added to this filtrate to give an oil-like product on the bottom. After refrigeration of the mixture at about 0°C overnight, the upper layer liquid was removed. The remaining oil was shaken with a further portion of Et_2O (5 mL) and refrigerated for several days. A white solid product was formed, then separated by filtration, washed with Et_2O and dried in vacuo; yield 0.70 g (53 %). Anal. Calcd. for $C_{108}H_{90}Cd_4Cl_2O_8P_4Se_6$ (mol wt 2634.11): C, 49.25; H 3.44. Found, C, 48.83; H, 3.28. ^1H NMR ($CDCl_3$): δ_H 6.8-7.5 (phenyl H).

$Cd_4(SPh)_6(PPh_3)_4(ClO_4)_2$. The synthesis was the same as above, with a 1:3:2 mixture of the appropriate reactants, except that the volume of CH_2Cl_2 was 10 mL and the addition of Et_2O was a single 6-mL portion, then the mixture was refrigerated overnight and a white crystalline product was resulted; yield 51 %. Anal. Calcd for $C_{108}H_{90}Cd_4Cl_2O_8P_4S_6$ (mol wt 2352.71): C, 55.14, H, 3.86. Found: C, 54.76; H, 3.76. ^1H NMR ($CDCl_3$): δ_H 6.6-7.5 (phenyl H).

$Cd_4(SPr^n)_6(PPh_3)_3(ClO_4)_2$. The synthesis followed that of $Cd_4(SPh)_6(PPh_3)_4(ClO_4)_2$, with a 1:3:2 mixture of the appropriate reactants, except that only 2.5 mL of Et_2O was used. The product was a white solid, which was shown to be a *tris*(phosphine) complex by microanalysis and NMR; yield 74 %. Anal. Calcd. for $C_{72}H_{87}Cd_4Cl_2O_8P_3S_6$ (mol wt 1886.31): C, 45.85; H, 4.65. Found: C, 45.13; H, 4.66. ^1H NMR ($CDCl_3$): δ_H 0.53 (t, -C*H*$_3$), 1.26 (m, -C*H*$_2$-), 2.38 (t, -S-C*H*$_2$-), 7.3-7.6 (phenyl H).

$Cd_4(SPr^i)_6(PPh_3)_2(ClO_4)_2$. The procedure was the exactly same as that used for $Cd_4(SPh)_6(PPh_3)_4(ClO_4)_2$, with a 1:3:2 mixture of the appropriate reactants. The white solid product was a *bis*(phosphine) complex, as shown by microanalysis and NMR; yield 43 %. Anal. Calcd for $C_{54}H_{72}Cd_4Cl_2O_8P_2S_6$ (mol wt 1623.96): C, 39.94; H, 4.47. Found: C, 39.66; H, 5.06. ^1H NMR (CD_3CN): 1.28 (d, -C*H*$_3$), 3.22 (m, -C*H*=); 7.4-7.5 (phenyl H). A reactant ratio of 1:3:0 gave the same product, as shown by ^1H, ^{31}P and ^{111}Cd NMR.

$Cd_4(SCy)_6(PPh_3)_2(ClO_4)_2$. A mixture of $Cd(PPh_3)_2(ClO_4)_2$ (0.42 g, 0.50 mmol) and $Cd(SCy)_2$ (0.51 g, 1.5 mmol) in CH_2Cl_2 (5 mL) was stirred for about 1 h. until it dissolved completely. Addition of Et_2O (3 mL) and refrigeration overnight gave a white microcrystalline solid. The product was separated, washed, and dried as described above; yield 0.75g (80 %). Anal. Calcd for $C_{72}H_{96}Cd_4Cl_2O_8P_2S_6$ (mol wt 1864.41): C, 46.38, H, 5.19. Found: C, 46.24; H, 5.37. ^1H NMR (CD_3CN): δ_H 0.9-2.8 (-C_6H_{11}), 7.4-7.6 (phenyl H). If the ratio of reactants was changed to 1:3:2, the same product was obtained (confirmed by ^1H, ^{31}P, and ^{111}Cd NMR).

NMR Spectra

Proton NMR samples were prepared in situ by dissolving a solid product in a suitable deuterated solvent in a standard 5 mm od NMR tube. The spectra were measured at ambient probe temperature using a Varian Gemini-200 spectrometer system. The ^{2}D resonance of the solvent was used as a field/frequency lock and signals from the solvent were used as internal references ($\delta_H(CHCl_3$ in $CDCl_3) = 7.24$; $\delta_H(CD_2HCN$ in $CD_3CN) = 1.93$).

All other NMR (^{31}P, ^{77}Se, $^{111/113}Cd$) samples were prepared in situ also, but by dissolving starting reactants (or a product in some cases) in CH_2Cl_2 (or $CHCl_3$ in some cases) in a standard 10 mm od NMR tube, using (mass of solute)/(volume of solvent at ambient temperature) as the concentration unit. The spectra were measured using a Varian XL-200 spectrometer system operating without a ^{2}D field/frequency lock (drift < 0.03 ppm/day), as described in previous papers from these laboratories.[1,2,5] The cadmium spectra for the system $Cd(PPh_3)_2(ClO_4)_2$: $3Cd(SPr^i)_2$: $xPPh_3$ (x = 0-2) were measured initially using the ^{113}Cd nuclide[10,11]. Because of these initial spectra containing a number of artifacts in the region of interest, subsequently the ^{111}Cd nuclide[10,11] was studied instead. No primary isotope effect is expected in our NMR experiments, i.e. both ^{111}Cd and ^{113}Cd nuclei should have the same chemical shifts. 85 % H_3PO_4, 0.1 M $Cd(ClO_4)_2$ (aq) and pure Me_2Se (all at ambient probe temperature) were used as external references for ^{31}P, ^{77}Se and ^{111}Cd, respectively. Reproducibility of δ_P, δ_{Cd} and δ_{Se} between sessions was found to be ±0.1, ±1, and ±0.1 ppm or better. In a single spectrum, signal separations, δ_{Cd}, are thought to be measurable to ± 0.1 ppm or better. Probe temperatures

were calibrated using a thermocouple probe in a stationary sample of the appropriate solvent.

Simulation of NMR spectra was as described in Ch. 2.

X-ray Structure Determination.

The single crystals obtained by diffusion of Et_2O into the solution of $Cd_4(SPr^i)_6(PPh_3)_2(ClO_4)_2$ in $CHCl_3$ were found to be suitable for X-ray diffraction analysis which was carried out by Drs. Payne and Vittal of this department.

Elemental Microanalyses

All the microanalyses for C and H were carried out by Guelph Chemical Laboratories Ltd.

3.3 Results and Discussion

3.3.1 Synthesis

Mixtures of $Cd(PPh_3)_2(ClO_4)_2$, $Cd(ER)_2$ and PPh_3 in 1:3:2 ratio are soluble in CH_2Cl_2 although $Cd(PPh_3)_2(ClO_4)_2$ is not very soluble alone and $Cd(ER)_2$ is almost insoluble. This indicates that reaction occurs between the three reactants. From the resulting colorless solution, compounds with the general formula $Cd_4(ER)_6(PPh_3)_n(ClO_4)_2$ can be isolated for ER = SPh or SePh, n = 4; for ER = SPr^n, n = 3; and for ER = SPr^i or SCy, n = 2. The reactions follow Eqn. [1]

[1] $Cd(PPh_3)_2(ClO_4)_2 + 3\ Cd(ER)_2 + 2\ PPh_3 \rightarrow Cd_4(ER)_6(PPh_3)_n(ClO_4)_2 + (4 - n)\ PPh_3$

(n = 2-4)

The isolation of compounds depends on the solubility of that specific species in solution. Since the phosphine is very soluble in CH_2Cl_2, in some cases it remains in solution while the clusters with n < 4 are isolated. The compound $Cd_4(SPe^n)_6(PPh_3)_4(ClO_4)_2$ exists in a 1:3:2 mixture, as proved by ^{31}P and ^{111}Cd NMR, but high solubility prevent the isolation of this or any other compound of the type $Cd_4(SAlk)_6(PPh_3)_4(ClO_4)_2$. The bis(phosphine) compounds (ER = SPr^i or SCy) were isolated from 1:3:0 mixtures also. It seems that for ER = SPr^i or SCy, the tetranuclear clusters with n = 2 are more stable or less soluble than those with n = 3 or 4, no matter whether the starting ratio is 1:3:2 or 1:3:0. The results from NMR spectroscopy and an x-ray analysis suggest that all these tetranuclear complexes have a adamantanoid skeleton, in which each cadmium is four-coordinate, and coordination of ClO_4^- is general when *n* < 4. Therefore, all the products are probably best formulated as $[(\mu\text{-}ER)_6(CdPPh_3)_n(CdOClO_3)_{4-n}](ClO_4)_{n-2}$. To date, isolated cadmium clusters of this type have not been reported anywhere else. The isolated mercury analogues are known only for *n* = 4, *e.g.* $[(\mu\text{-}EPh)_6(HgPPh_3)_4](ClO_4)_2$ (E = S or Se)[1], and *n* = 3, *e.g.* $[(\mu\text{-}TePh)_6(Hg)(HgPPh_3)_3](ClO_4)_2$[2]. The isolation and NMR spectra of clusters with *n* = 2 are reported the first time. The zinc analogues are not known so far; the necessary starting compound $Zn(PPh_3)_2(ClO_4)_2$ has not been reported.

3.3.2 NMR spectra

(i) The complexes $[Cd(PPh_3)_n]^{2+}$ (n = 2-4) and $[Cd(PPh_3)_n(OPPh_3)_{4-n}]^{2+}$ (n = 2,3)

Although ^{31}P NMR data of the mononuclear complexes $[Cd(PPh_3)_n]^{2+}$ were reported by earlier workers[9a], $^{111/113}Cd$ NMR spectra have not been described. This the first report of the Cd NMR spectra of $[Cd(PPh_3)_n]^{2+}$. However, ^{31}P NMR results in our experiments are in agreement with the previous work.[9a]

$Cd(PPh_3)_2(ClO_4)_2$ was taken as a starting material in our study. It is suggested by ^{31}P and ^{111}Cd NMR that $Cd(PPh_3)_2(ClO_4)_2$ is converted completely into $[Cd(PPh_3)_3]^{2+}$ by addition of one mole PPh_3, though results for the synthesis of $Cd(PPh_3)_2(ClO_4)_2$ (see Experimental Section) show that $[Cd(PPh_3)_3]^{2+}$ must dissociate in solution. Attempts to prepare $[Cd(PPh_3)_4]^{2+}$ by adding 1 mole PPh_3 to $[Cd(PPh_3)_3]^{2+}$ in solution show that the reaction does not occur stoichiometrically. Therefore, an excess of PPh_3 is required to convert the majority of $[Cd(PPh_3)_3]^{2+}$ into $[Cd(PPh_3)_4]^{2+}$. From ^{111}Cd NMR spectra measured at reduced temperature, the species of $[Cd(PPh_3)_n]^{2+}$ (n = 2, 3 or 4) are easily identified by the one-bond coupling ^{111}Cd-^{31}P. The coupling patterns are a triplet, quartet and pentet for n = 2, 3 and 4, respectively. Since ^{111}Cd NMR spectra of $[Cd(PPh_3)_n]^{2+}$ are relatively simple, they are not shown here, but NMR data for these complexes are listed in Table 3.1. As can be seen from Table 3.1, the chemical shifts of $[Cd(PPh_3)_n]^{2+}$ vary with n in the order $2 < 3 < 4$, while $^1J(P,Cd)$ values vary with n in the order $2 > 3 > 4$. The similar sequence of δ_{Cd} and $^1J(P,Cd)$ has been reported for $[Cd(PBu_3)_n]^{2+}$ (n = 1-3)[12a] and same sequence of δ_{Cd} has been observed for $[Cd(SP\{2\text{-}C_6H_4Me\}_3)_n]^{2+}$ (n = 2-4)[12b].

Table 3.1 ^{31}P and ^{111}Cd NMR Data for Some Mononuclear Complexes of Cadmium in CH_2Cl_2 [a]

Complex	$\delta_P(PPh_3)$ [b] (ppm)	$\delta_P(OPPh_3)$ [b] (ppm)	δ_{Cd} [c] (ppm)	$^1J(^{31}P\text{-}^{111}Cd)$ [d] (Hz)	$^2J(P^{31}\text{-}Cd)$ [e] (Hz)	$^3J(^{31}P\text{-}^{31}P)$ [f] (Hz)
$[Cd(PPh_3)_2]^{2+}$ [g]	10.7		249	2195		
$[Cd(PPh_3)_3]^{2+}$ [g]	10.1		431	1503		
$[Cd(PPh_3)_4]^{2+}$ [g]	10.3		467[h]	1106		
$[Cd(PPh_3)_2(OPPh_3)_2]^{2+}$ [i]	8.8	43.5	375	2013	23[j]	5[j]
$[Cd(PPh_3)_3(OPPh_3)]^{2+}$ [i]	8.4	44.2	465	1470	50	5

[a] At 213 K and [Cd] = 0.05 mol/L, except as noted.

[b] Relative to external 85 % H_3PO_4; reproducibility better than ±0.1 ppm.

[c] Relative to external 0.1 M $Cd(ClO_4)_2$ (aq); reproducibility better than ±1 ppm.

[d] Estimated error ±5 Hz.

[e] Average coupling, separate couplings to ^{111}Cd and ^{113}Cd were not resolved. Estimated error ± 2 Hz

Table 3.1 (Continued)

[f] Estimated error ±1 Hz.

[g] ^{31}P NMR data for $[Cd(PPh_3)_n]^{-}$ (n = 2-4) have been reported earlier.[9a]

[h] In a solution where $[Cd(PPh_3)_2]^{2+}$ PPh_3 = 1:6.

[i] In a mixture where $[Cd(PPh_3)_2]^{2+}$:$OPPh_3$ = 1.2 and [Cd] = 0.10 mol/L. Cd^{2+}:$OPPh_3$ complexes are formed also

[j] At 183 K; this coupling is not observed at 213 K.

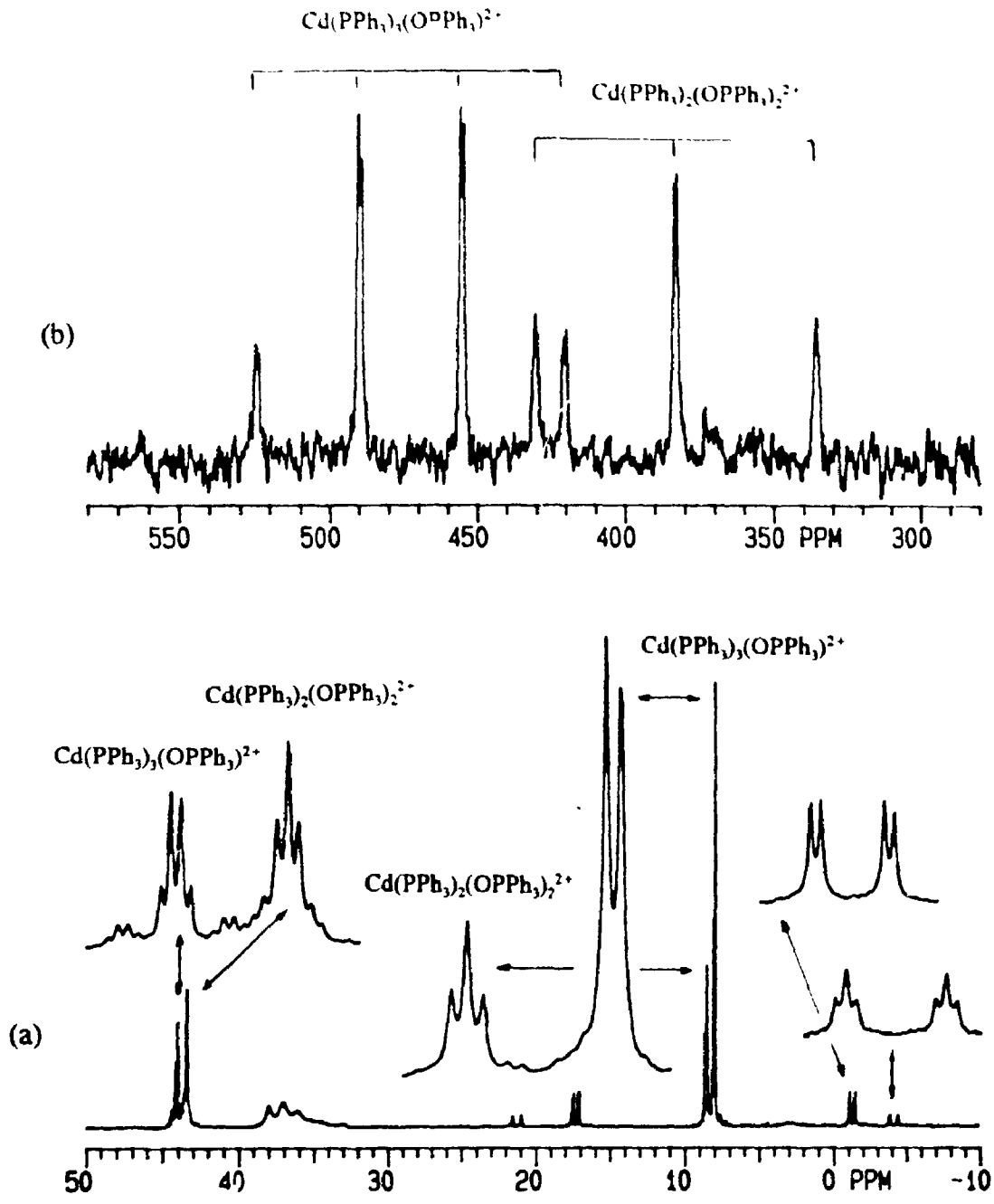

Figure 3.1 NMR spectra of a mixture containing $Cd(PPh_3)_2(ClO_4)_2$:$OPPh_3$ = 1:2 in CH_2Cl_2 at 183K, showing the formation of $Cd(PPh_3)_2(OPPh_3)_2$ and $Cd(PPh_3)_3(OPPh_3)$: (a) 80.98-MHz ^{31}P NMR spectrum, (b) 42.41-MHz ^{111}Cd NMR spectrum.

In solutions of the $[Cd(PPh_3)_n]^{2+}$ complexes and in some of the mixtures described below, trace amounts of ternary Cd(II):PPh_3 $OPPh_3$ complexes appear to be formed, presumably as a result of adventitious O_2[13]. Only one series of mixed phosphine · phosphine oxide complexes of Cd has been described earlier, $CdX_2(PCy_3)(OPCy_3)$ (X = Cl-I)[14]. The ternary Cd(II):PPh_3:$OPPh_3$ species was investigated using a 1:2 mixture of $Cd(PPh_3)_2(ClO_4)_2$ and $OPPh_3$ in CH_2Cl_2. The major ternary complexes, $[Cd(PPh_3)_3(OPPh_3)]^{2+}$ and $[Cd(PPh_3)_2(OPPh_3)_2]^{2+}$ with intensity ratio ca. 8:7, are readily identified by their first order ^{31}P and ^{111}Cd NMR NMR spectra (see Fig. 3.1). In Fig. 3.1a, ^{31}P resonances (with Cd satellites) in the more shielded region correspond to coordinated PPh_3. The doublet (coupled by one $OPPh_3$) with smaller $^1J(^{31}P,^{111/113}Cd)$ is assigned to $[Cd(PPh_3)_3(OPPh_3)]^{2+}$, and the triplet (coupled by two $OPPh_3$) with larger ^1J value is assigned to $[Cd(PPh_3)_2(OPPh_3)_2]^{2+}$. Their Cd satellites also show the same coupling mode (see the enlarged bands). In the less shielded region (43-45 ppm), the two ^{31}P signals are due to coordinated $OPPh_3$. The triplet (coupled by two PPh_3) comes from $[Cd(PPh_3)_2(OPPh_3)_2]^{2+}$, while the quartet (coupled by three PPh_3) comes from $[Cd(PPh_3)_3(OPPh_3)]^{2+}$. Both $OPPh_3$ signals show the $^2J(P,Cd)$ coupling. Besides the major products of $[Cd(PPh_3)_3(OPPh_3)]^{2+}$ and $[Cd(PPh_3)_2(OPPh_3)_2]^{2+}$, the mixture of $Cd(PPh_3)_2(ClO_4)_2$ and $OPPh_3$ contains no other PPh_3 (free or coordinated), but the formation of binary Cd^{2+}:$OPPh_3$ is observed by resonances in the region 35-39 ppm, deshielded relative to the signal of free $OPPh_3$ ($\delta_P(OPPh_3)$ = 28.5), as expected from earlier work.[15] In Fig. 3.1b, the ^{111}Cd spectrum is relatively simple which consists of a triplet and a quartet. The latter also shows the fine structure (each component is a doublet, caused by ^2J(Cd-O-P)). The NMR data have been included in Table 3.1.

As can be seen from Table 3.1, in the $[Cd(PPh_3)_n(OPPh_3)_{4-n}]^{2+}$ (n = 2-4) series, the chemical shift of $[Cd(PPh_3)_3(OPPh_3)]^{2+}$ is larger than that of $[Cd(PPh_3)_2(OPPh_3)_2]^{2+}$, but close to that of $[Cd(PPh_3)_4]^{2+}$. However, their $^1J(^{31}P\text{-}^{111}Cd)$ values definitely vary with n in the order 2 > 3 > 4, *i.e.* the more the number of PPh_3 ligands, the less the $^1J(^{31}P\text{-}^{111}Cd)$ values. Since *P* as a donor atom is softer than *O*, ^1J may be used as an indication of the ratio of soft:hard donors in the complexes. In addition, it can be seen that the ^1J values of $[Cd(PPh_3)_2]^{2+}$ and $[Cd(PPh_3)_2(OPPh_3)_2]^{2+}$ are close, although the latter has two more hard donors. A similar observation applies to $[Cd(PPh_3)_3]^{2+}$ and $[Cd(PPh_3)_3(OPPh_3)]^{2+}$ also. This suggests that ^1J is mainly influenced by the number of PPh_3 ligands and that the Cd in $[Cd(PPh_3)_2]^{2+}$ or $[Cd(PPh_3)_3]^{2+}$ is probably four-coordinated. From the ^1J analysis discussed above, the PPh_3 complexes may be better formulated $[Cd(PPh_3)_2(OClO_3)_2]$ and $[Cd(PPh_3)_3(OClO_3)]^+$.

(ii) The Systems $Cd(PPh_3)_2(ClO_4)_2$:$Cd(SR)_2$:PPh_3 (R = Pr^i or Cy)

The properties of these two systems are identical in their most important details and therefore the NMR study is described here for the SPr^i complexes. ^{31}P and ^{113}Cd NMR spectra for 1:3:x mixtures in CH_2Cl_2 at ambient probe temperature are broad and poorly resolved. However at 213 K these spectra are much better resolved. They are shown in Figures 3.2 and 3.3. When x = 2, the ^{31}P NMR spectrum shows a major signal at 0.9 ppm with $^{111/113}Cd$ satellites, $^1J(^{31}P\text{-}^{111/113}Cd)_{Ave} \approx 1143$ Hz (Fig. 3.2a). The corresponding ^{113}Cd NMR spectrum shows a doublet (623 ppm) with $^1J(^{31}P\text{-}^{113}Cd)$ = 1164±5 Hz (Fig. 3.3a). The cadmium chemical shift (623 ppm) is in the region for four-coordinate cadmium, *e.g.* the CdS_3Cl kernel in $[(\mu\text{-}SPr^i)_6(CdCl)_4]^{2-}$ has δ_{Cd} = 602 ppm at

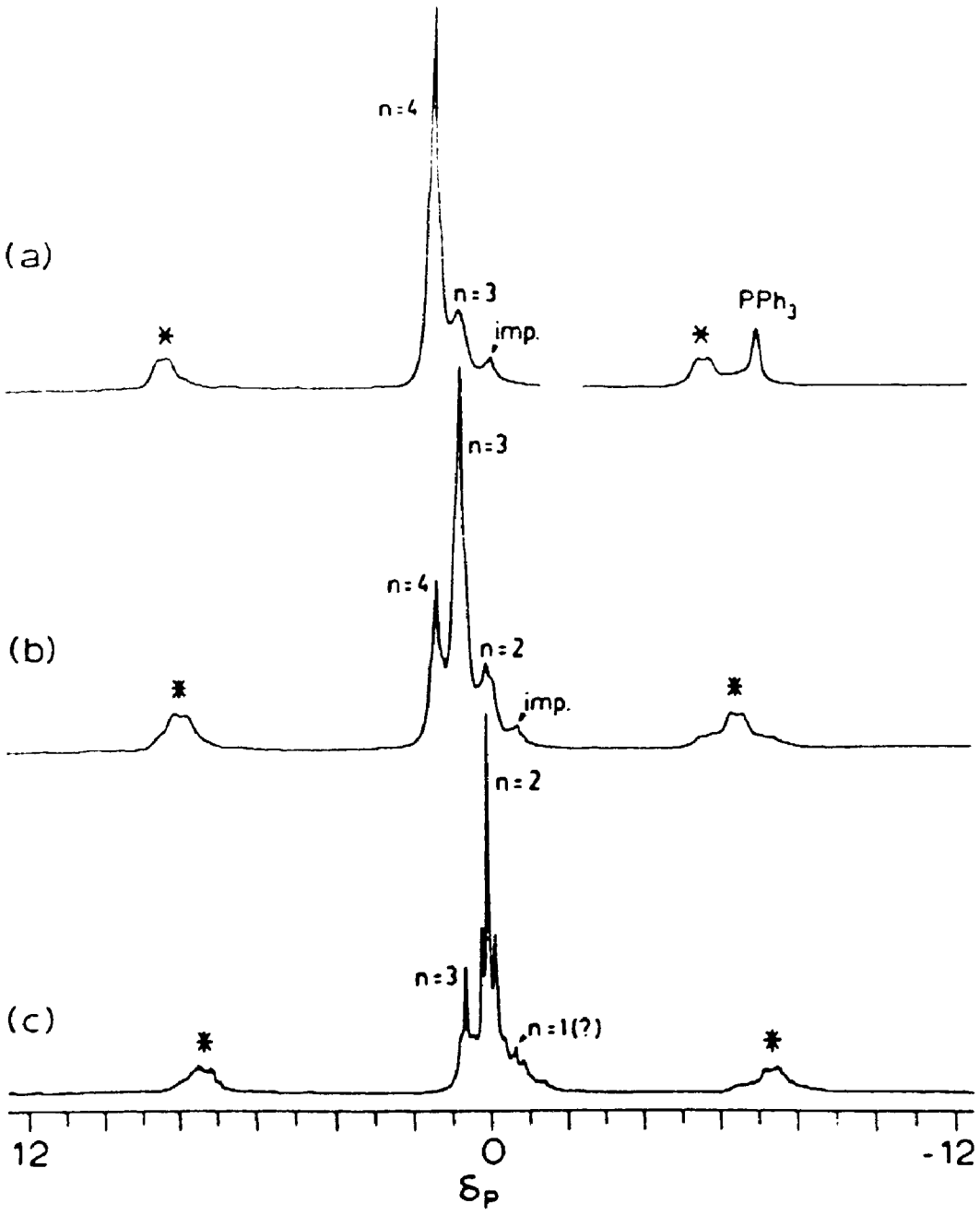

Figure 3.2 80.98-MHz ^{31}P NMR spectra of $Cd(PPh_3)_2(ClO_4)_2$:$Cd(SPr^i)_2$:PPh_3 mixtures in CH_2Cl_2 at 213 K, showing the formation of $[(\mu\text{-}SPr^i)_6(CdPPh_3)_n(Cd)_{4-n}]^{2+}$. $Cd(PPh_3)_2(ClO_4)_2$:$Cd(SPr^i)_2$:PPh_3 = (a) 1:3:2; (b) 1:3:1; (c) 1:3:0. Starred signals are $^{111/113}Cd$ satellites.[14]

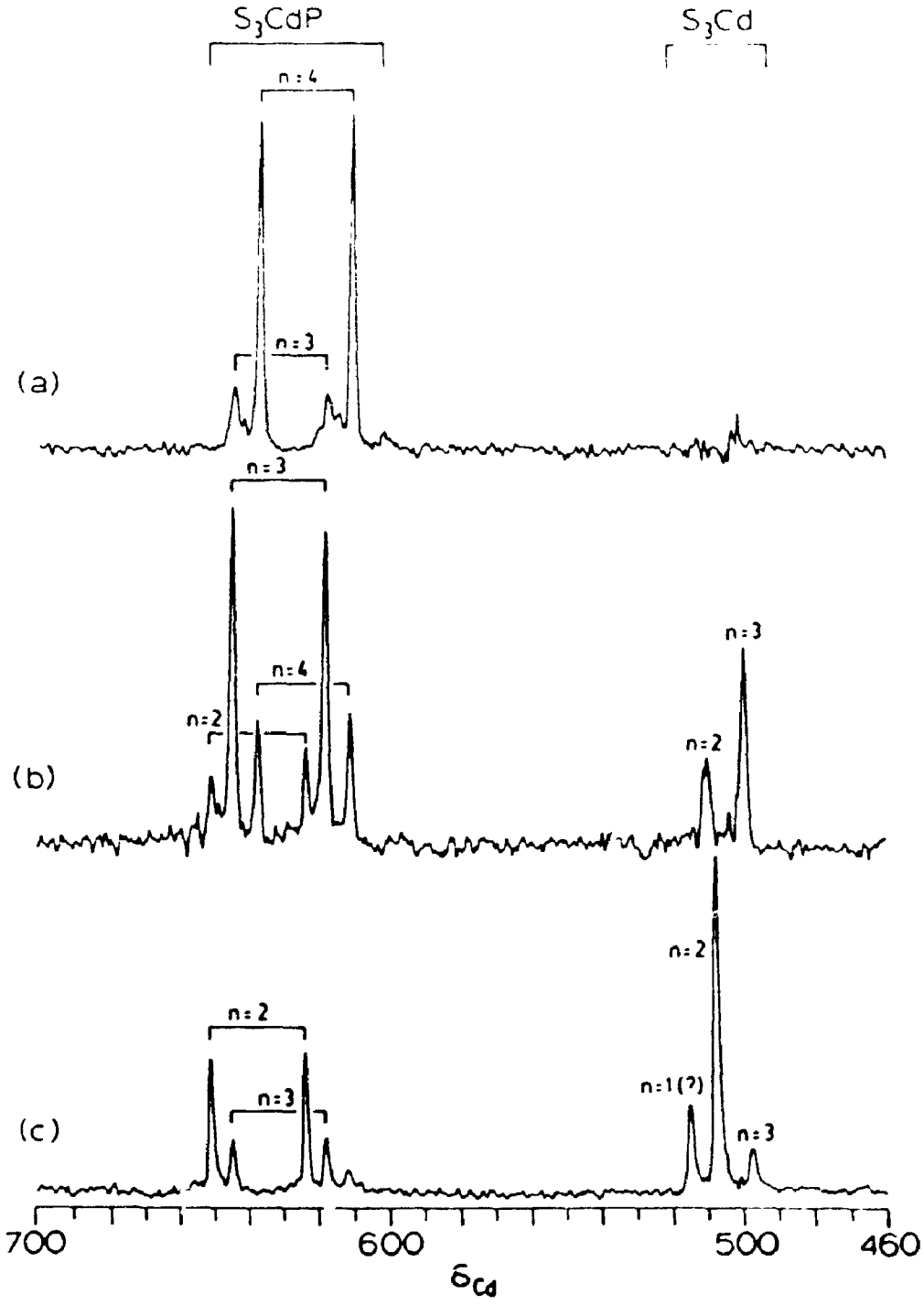

Figure 3.3 44.37-MHz ^{113}Cd NMR spectra of $Cd(PPh_3)_2(ClO_4)_2$:$Cd(SPr^i)_2$:PPh_3 mixtures in CH_2Cl_2 at 213 K, showing the formation of $[(\mu\text{-}SPr^i)_6(CdPPh_3)_n(Cd)_{4-n}]^{2+}$. $Cd(PPh_3)_2(ClO_4)_2$:$Cd(SPr^i)_2$:PPh_3 = (a) 1:3:2; (b) 1:3:1; (c) 1:3:0.[14]

217 K in CH_2Cl_2[5], and the magnitude of ^1J is similar to that for $[Cd(PPh_3)_4]^{2+}$ (1106 Hz in Table 3.1), suggesting that cadmium is coordinated by four soft donors. From the observation that the cadmium signal is a doublet, one (and only one) of these four soft donors is a phosphine. Since it is known that one ligand is a PPh_3, the other three must be SPr^i. According to this analysis, we can conclude that $[(\mu\text{-}SPr^i)_6(CdPPh_3)_4]^{2+}$ with the adamantanoid skeleton **I** (see Fig. 3.4) is formed as a major species in the 1:3:2 mixture.

In Fig. 3.2a, it also can be seen that there is a free PPh_3 signal at -6.8 ppm, and two weak signals at 0.7 and 0.0 ppm which are close to that of $[(\mu\text{-}SPr^i)_6(CdPPh_3)_4]^{2+}$ and are most probably due to $[(\mu\text{-}SPr^i)_6(Cd)(CdPPh_3)_3]^{2+}$ and $[(\mu\text{-}SPr^i)_6(Cd)_2(CdPPh_3)_2]^{2+}$. This suggests that $[(\mu\text{-}SPr^i)_6(CdPPh_3)_4]^{2+}$ cluster is appreciably dissociated, according to the Eqns. [2a] and [2b].

[2a] $[(\mu\text{-}SPr^i)_6(CdPPh_3)_4]^{2+} \rightleftharpoons [(\mu\text{-}SPr^i)_6(Cd)(CdPPh_3)_3]^{2+} + PPh_3$

[2b] $[(\mu\text{-}SPr^i)_6(CdPPh_3)_4]^{2+} \rightleftharpoons [(\mu\text{-}SPr^i)_6(Cd)_2(CdPPh_3)_2]^{2+} + 2\ PPh_3$

In the corresponding ^{113}Cd NMR spectrum (Fig. 3.3a), the signal of a *tris*(phosphine) cluster is observed, but the signal of the *bis*(phosphine) species is not. Therefore, the weak ^{31}P signal at 0.0 ppm in Fig. 3.2a is labelled *impurity*.

When x = 1, the signal of the *tris*(phosphine) complex (0.7 ppm) becomes major in the ^{31}P NMR spectrum (Fig. 3.2b). This resonance clearly has $^{111/113}Cd$ satellites ($^1J_{Ave} \approx$ 1166 Hz, which is in the same region as that of $[(\mu\text{-}SPr^i)_6(CdPPh_3)_4]^{2+}$). The corresponding ^{113}Cd NMR spectrum shows this species consisting of a doublet (δ = 631 ppm), in the same region as that of $[(\mu\text{-}SPr^i)_6(CdPPh_3)_4]^{2+}$, and a singlet that is in a more

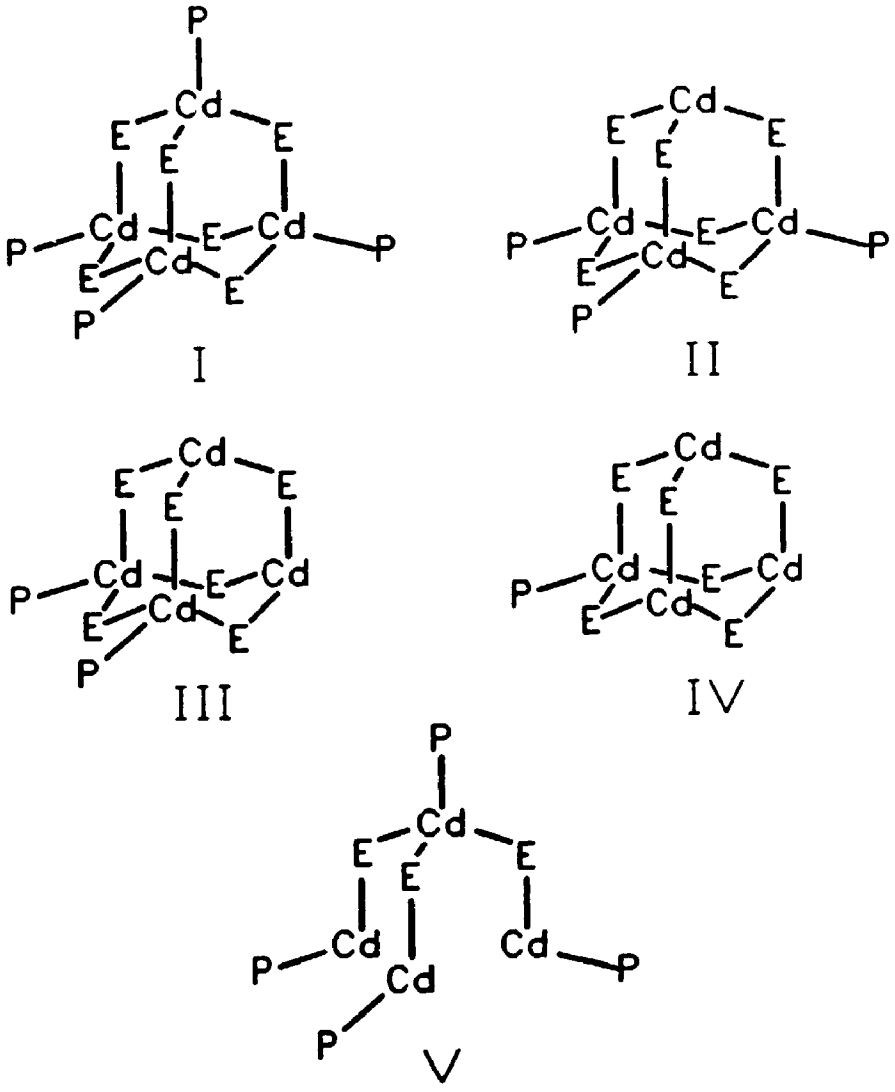

Figure 3.4 The chart showing different Cd_4 skeletons.[14]

shielded region (δ = 499 ppm) In addition, the intensity ratio of the doublet and the singlet is roughly 3.1. Following the logic discussed above, this species is assigned to the n = 3 cluster $[(\mu\text{-SPr}^i)_6(CdPPh_3)_3(Cd)]^{2+}$, with the skeleton II (Fig. 3.4), and the singlet in the ^{113}Cd NMR spectrum is due to the PPh_3-free site. The δ_{Cd} (499 ppm) of the CdS_3 kernel in the cluster is smaller than the values found for planar three-coordinate Cd in $Cd(SR)_3^-$ (δ_{Cd} = 577-568)[16]. It is possible that the cadmium is three-coordinate but *pyramidal* in order to fit into the adamantanoid skeleton, or that ClO_4^- is coordinated at this site to fit into the tetrahedral coordination. The latter possibility is supported by that relatively large ClO_4^- concentration dependence of δ_{Cd} for the PPh_3-free site (several ppm) compared with that for the PPh_3-bound site (≤1 ppm), as well as by the crystal structure of $[(\mu\text{-SPr}^i)_6(CdPPh_3)_2(CdOClO_3)_2]$ given below. The equilibrium coordination of ClO_4^- to the phosphine-free site can be shown in Eqn. [3].

[3] $S_3Cd + ClO_4^- = S_3CdOClO_3^-$

Therefore, the major species at the 1:3:1 starting ratio may be better assigned to $[(\mu\text{-SPr}^i)_6(CdPPh_3)_3(CdOClO_3)]^+$.

Figs. 3.2b and 3.3b also show that $[(\mu\text{-SPr}^i)_6(Cd)(CdPPh_3)_2]^{2+}$ is in equilibrium with $[(\mu\text{-SPr}^i)_6(CdPPh_3)_4]^{2+}$ and $[(\mu\text{-SPr}^i)_6(Cd)_2(CdPPh_3)_2]^{2+}$ (and probably $[(\mu\text{-SPr}^i)_6(Cd)_3(CdPPh_3)]^{2+}$). The dissociation can be expressed by Eqn. [4].

[4] $2\,[(\mu\text{-SPr}^i)_6(Cd)(CdPPh_3)_3]^{2+} = [(\mu\text{-SPr}^i)_6(CdPPh_3)_4]^{2+} + [(\mu\text{-SPr}^i)_6(Cd)_2(CdPPh_3)_2]^{2+}$

When x = 0, $[(\mu\text{-SPr}^i)_6(Cd)_2(CdPPh_3)_2]^{2+}$ becomes major, as can be seen from Figs 3.2c and 3.3c. The signal of this major species in the ^{31}P NMR spectrum (Fig 3.2c) shows the same general pattern as for the other Cd_4 species. In its ^{113}Cd NMR spectrum (Fig 3.3c), this major species shows signals in two regions, as seen before in Fig 3.3b The intensity ratio of two regions is about 1:1, suggesting that the two types of cadmium kernels are in the same number. The isolated pure $Cd_4(SPr^i)_6(PPh_3)_2(ClO_4)_2$ gives identical spectra. The major species at 1:3.0 starting ratio is assigned to $[(\mu\text{-SPr}^i)_6(CdPPh_3)_2(Cd)_2]^{2+}$, with skeleton III (Fig. 3.4).

As can be seen from the ^{31}P NMR spectrum (Fig. 3.2c), there is a weak signal of $[(\mu\text{-SPr}^i)_6(CdPPh_3)_3(Cd)]^{2+}$. The same species is observed from the ^{113}Cd NMR spectrum (Fig. 3.3c), too. If this *tris*(phosphine) species comes from the dissociation of the *bis*(phosphine) complex, there must be another species with less phosphine. This species is most probably $[(\mu\text{-SPr}^i)_6(CdPPh_3)(Cd)_3]^{2+}$, with structure IV (Fig. 3.4). However, it is not the major component of any mixture solution and its complete ^{113}Cd NMR spectrum could never be observed, therefore this assignment is tentative. The major ^{31}P NMR signal in Fig. 3.2c shows a splitting pattern, which is due to $^3J(^{31}P\text{-}^{111/113}Cd)$. The couplings $^3J(^{31}P\text{-}^{111/113}Cd)$ and sometimes $^4J(^{31}P\text{-}^{31}P)$ are better resolved when $CHCl_3$ is used as solvent, but use of this solvent changes the results for $Cd(PPh_3)_2(ClO_4)_2$:$Cd(SR)_2$ mixtures (see below). Details of the NMR spectra of $[(\mu\text{-SPr}^i)_6(CdPPh_3)_n(Cd)_{4-n}]^{2+}$ are included in Table 3.2.

Beside the couplings discussed above, two-bond Cd-Cd coupling is possible As can be seen from Fig. 3.4, although the four cadmiums are chemically equivalent in structure I, they are not in II - IV. When ^{113}Cd NMR spectra are measured, $^2J(^{113}Cd\text{-}$

Table 3.2 ^{31}P and $^{111,113}Cd$ NMR Data for $[(\mu\text{-ER})_6(Cd_APPh_3)_n(Cd_B)_{4-n}]^{2-}$.[a]

ER	*n*	δ_P[b]	δ_{Cd_A}[c]	δ_{Cd_B}[c,d]	$^1J(^{31}P\text{-}^{111}Cd)$[e]	$^3J(^{31}P\text{-}Cd)$[f]	$^4J(^{31}P\text{-}^{31}P)$[g]
SPr[i]	1[h]	-0.7	'	514	'	≈30[h,j]	'
	2	0.0	636	507	1164	29[j]	'
	3	0.7	631	499	1141	21[j,k],23[k,l]	6[k]
	4	0.9	623		1117	20[k,l]	6[k]
SCy	2	-2.0	637	510	1134	28[j]	'
	3	-1.0	630	504	1115	'	'
	4	-0.7	621		1094	20[l]	6
SPh	1[h]	9.7	'	'	'	27[j]	'
	2[h]	8.8	'	'	'	27[j]	'
	3	8.0	604	450	1503	≈23[j],15[l]	5
	4	7.4	597		1514	16[l]	5
SePh	2[h]	7.0	'	'	'	'	'
	3	5.6	577	508	1236	23[j],23[l]	'
	4[m]	4.3	568		1260	19[l]	7
SPr[n]	2[h]	'	662	522	≈1200	[o]	'
	3	-1.8	657	517	1168	16[l,n,p]	7[k]
	4	-1.7	651		1154	18[l,n]	7[n]
SPe[n,q]	3	-2.4	658	516	1157	'	'
	4	-2.0	652		1136	18[l]	6

Table 3.2 (Continued)

[a] In CH_2Cl_2 at 213 K except as noted. Constituents were mixed to give a Cd_4 concentration of 0.05 mol/L of solvent at ambient temperature

[b] Reproducibility ±0.1 ppm or better

[c] From ^{113}Cd NMR spectrum for E = SPr^i, ^{111}Cd NMR spectra in all other cases (see Experimental); reproducibility ±1 ppm or better

[d] These resonances show significant composition dependence. Typical values are shown.

[e] Estimated error ±5 Hz.

[f] Average coupling; separate couplings to ^{113}Cd and ^{111}Cd were not resolved. Estimated error ±2 Hz.

[g] Estimated error ±1 Hz.

[h] Tentative assignment.

[i] Not observed.

[j] $^3J(^{31}P\text{-}Cd_B)$.

[k] In $CHCl_3$ at 213 K.

[l] $^3J(^{31}P\text{-}Cd_A)$.

[m] δ_{Se} = -96.8±0.2; $^1J(^{77}Se\text{-}Cd)_{Ave}$ = 142±2 Hz; $^2J(^{31}P\text{-}^{77}Se)$ = 27±1 Hz

[n] At 193 K.

[o] Could not be measured with certainty.

[p] From the ^{111}Cd NMR spectrum. $^3J(^{31}P\text{-}Cd_B)$ could not be measured with certainty.

[q] Pe^n = n-C_5H_{11}.

^{111,113}Cd) is expected in structure II - IV, and even in structure I, $^{2}J(^{113}Cd\text{-}^{111}Cd)$ could be expected. In fact, this two-bond coupling has not been observed, perhaps because it is too small to be seen in our experiments.

When $Cd(PPh_3)_2(ClO_4)_2$:$Cd(SPr^i)_2$ = 1:<3 in CH_2Cl_2, the starting materials still dissolve easily. From the solutions, complicated ^{31}P and ^{111}Cd NMR spectra are observed. At a 1:1 ratio (Fig. 3.5), the complexes existing in the mixture solution include some known species, $[(\mu\text{-}SPr^i)_6(CdPPh_3)_n(Cd)_{4-n}]^{2+}$ (n = 2 and possibly 1), $Cd(PPh_3)_2^{2+}$, and $Cd(PPh_3)_3^{2+}$, and two additional unknown species. One of these latter two has a weak ^{31}P resonance with δ_P = 9.0 (singlet) and $^{1}J(^{31}P\text{-}^{111}Cd)$ = 2162±5 Hz. The ^{1}J coupling of this species is very close to those of $[Cd(PPh_3)_2]^{2+}$ and $[Cd(PPh_3)_2(OPPh_3)_2]^{2+}$ (see Table 3.1), and therefore the species must have two soft donor atoms attached to Cd. Since the two donor ligands could not be the same, *i.e.* the species could not be either $[Cd(PPh_3)_2]^{2+}$ (different δ_P and ^{1}J values) or $Cd(SPr^i)_2$ (no ^{31}P signal and in any case of insufficient solubility), it may be $[Pr^iSCdPPh_3]^+$. Unfortunately, no cadmium resonance could be observed. Thus the assignment of this species is tentative. The second species gives a relatively strong ^{31}P NMR signal with δ_P = 5.8 (singlet), $^{1}J(^{31}P\text{-}^{111}Cd)$ = 1728±5 Hz, and δ_{Cd} = 461 (doublet). The ^{1}J value is closest to those of $[Cd(PPh_3)_3]^{2+}$ and $[(Cd(PPh_3)_3(OPPh_3)]^{2+}$ (see Table 3.1), therefore, the species may have three soft donor atoms. However from the ^{111}Cd NMR spectrum each Cd has only one PPh_3 attached. Accordingly, it is tentatively characterized as $[(\mu\text{-}SPr^i)CdPPh_3]_m^{m+}$. This type of complex is feasible, especially when m = 3. Then it forms a six-membered ring with three Cd, three bridging S and three terminal P, which is a possible precursor to the adamantanoid complexes. At a 1:2 ratio, the NMR results show that the major species in CH_2Cl_2

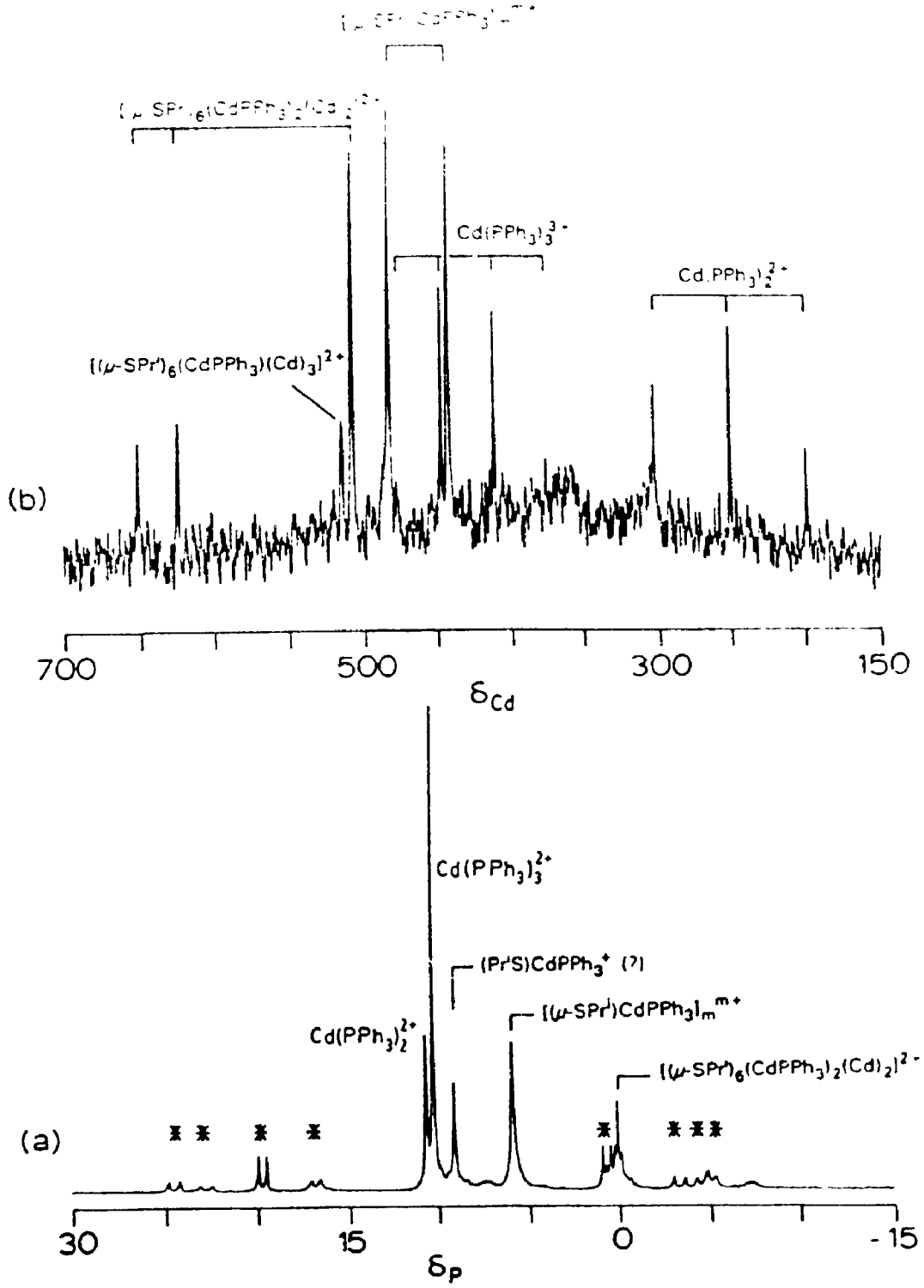

Figure 3.5 NMR spectra of a mixture containing $Cd(PPh_3)_2(ClO_4)_2$:$Cd(SPr^i)_2$ = 1:1 in CH_2Cl_2 at 213K. (a) 80.98-MHz ^{31}P NMR spectrum (starred signals are $^{111/113}Cd$ satellites); (b) 42.41-MHz ^{111}Cd NMR spectrum.[14]

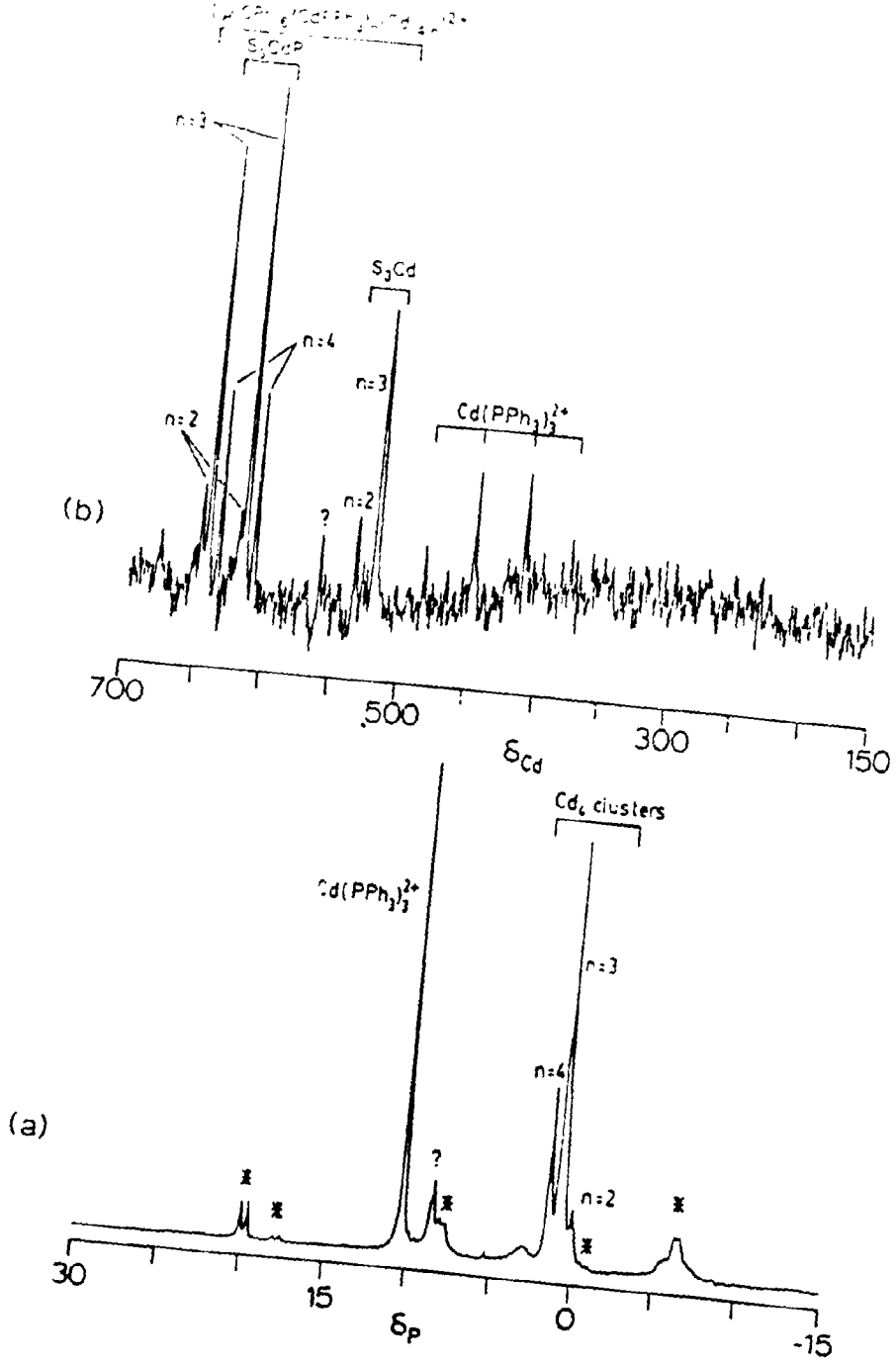

Figure 3 6 NMR spectra of a mixture containing $Cd(PPh_3)_2(ClO_4)_2$:$Cd(SPr^i)_2$ = 1:1 in $CHCl_3$ at 213K. (a) 80.98-MHz ^{31}P NMR spectrum (starred signals are $^{111/113}Cd$ satellites); (b) 42.41-MHz ^{111}Cd NMR spectrum.[14]

solution are $[(\mu\text{-SPr}^i)CdPPh_3]_m^{m+}$ and $[(\mu\text{-SPr}^i)_6(Cd)_2(CdPPh_3)_2]^{2+}$, as well as small amounts of $[(\mu\text{-SPr}^i)_6(Cd)(CdPPh_3)_3]^{2+}$ and $[(\mu\text{-SPr}^i)_6(Cd)_3(CdPPh_3)]^{2+}$.

If the solvent is changed to $CHCl_3$, the NMR results for the mixture solution of $Cd(PPh_3)_2(ClO_4)_2$ and $Cd(SPr^i)_2$ at 1:1 ratio do not show any species of $[Pr^iSCdPPh_3]^+$ or $[(\mu\text{-SPr}^i)CdPPh_3]_m^{m+}$ but instead show mainly Cd_4 clusters and $Cd(PPh_3)_4^{2+}$. Since the assignments of the ^{31}P and ^{111}Cd NMR spectra are clearly shown in Fig. 3.6, no more discussion will be given here. However, the result suggests that the solvent could affect the formation of complexes in some circumstances. (also see below)

The NMR properties of $[(\mu\text{-SCy})_6(CdPPh_3)_n(Cd)_{4-n}]^{2+}$ system in CH_2Cl_2 are very similar to that of SPr^i series, except that the proposed species $[CySCdPPh_3]^+$ is not observed. However, for the expected species $[CySCdPPh_3]_m^{m+}$ with δ_P = 5.3 (singlet), $^1J(^{31}P\text{-}^{113})$ = 1720±5 Hz, and δ_{Cd} = 471 (doublet) has been observed. To save space here, the ^{31}P and ^{111}Cd NMR spectra are not given, but the NMR data are included in Table 3.2.

(iii) The systems $Cd(PPh_3)_2(ClO_4)_2$:$Cd(EPh)_2$:PPh_3 (E = S or Se)

The behaviours of these two systems are almost parallel in all respects, thus the discussion here is restricted to the SPh series. The mixtures of these starting reactants of $Cd(PPh_3)_2(ClO_4)_2$:$Cd(SPh)_2$:PPh_3 at 1:3:x (x = 0-2) ratio are not completely dissolved in CH_2Cl_2, especially at 1:3:0 (relatively more white solid in the NMR tube). However, their supernatant liquid spectra were measured by ^{31}P and ^{111}Cd NMR, and the spectra are shown in Figs. 3.7 and 3.8.

When x = 2 (see Figs. 3.7a and 3.8a), the cluster $[(\mu\text{-SPh})_6(CdPPh_3)_4]^{2+}$ exists as the only species in solution. The spectra of the isolated cluster are the same as those of

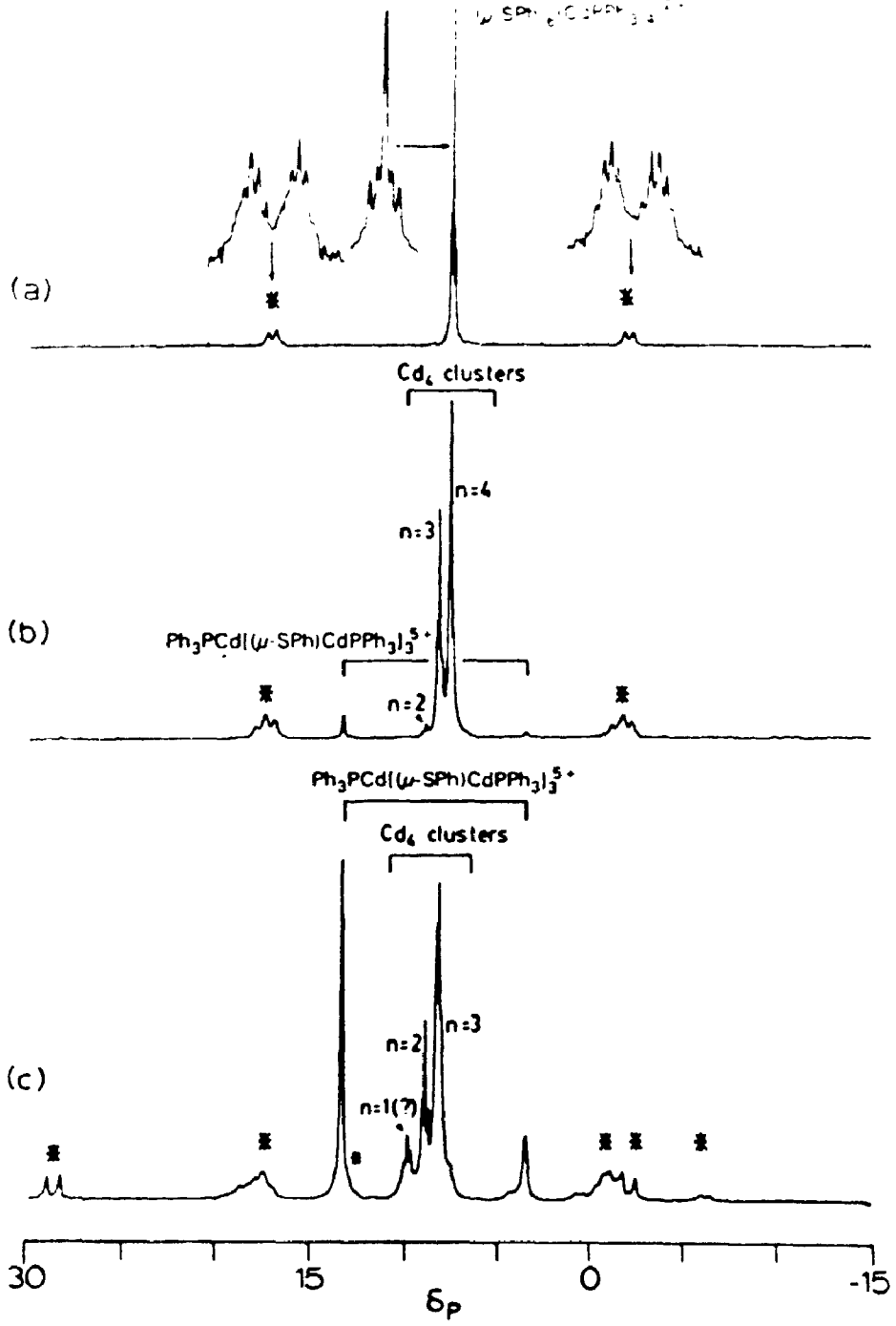

Figure 3.7 80.98-MHz ^{31}P NMR spectra of the supernatant liquid from $Cd(PPh_3)_2(ClO_4)_2$: $Cd(SPh)_2$: PPh_3 mixtures in CH_2Cl_2 at 213 K, showing the formation of $[(\mu\text{-}SPh)_6(CdPPh_3)_n(Cd)_{4-n}]^{2+}$ and $[PPh_3Cd(\{\mu\text{-}SPh\}CdPPh_3)_3]^{5+}$. $Cd(PPh_3)_2(ClO_4)_2$: $Cd(SPh)_2$: PPh_3 = (a) 1:3:2 (isolated solid); (b) 1:3:1; (c) 1:3:0. Starred signals are $^{111/113}Cd$ satellites.[14]

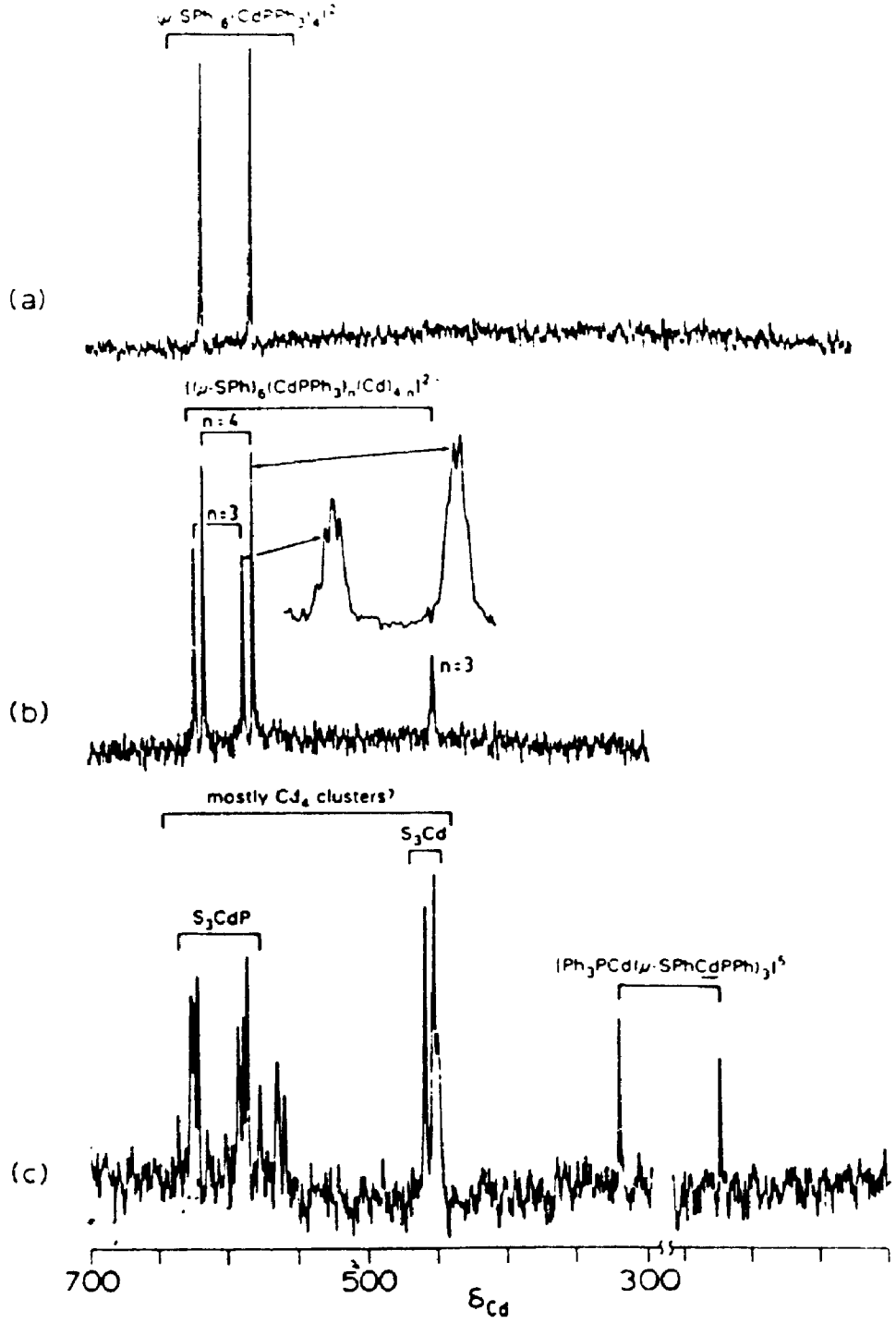

Figure 3.8 42.41-MHz ^{111}Cd NMR spectra of the supernatant liquid from $Cd(PPh_3)_2(ClO_4)_2$: $Cd(SPh)_2$: PPh_3 mixtures in CH_2Cl_2 at 213 K, showing the formation of $[(\mu\text{-}SPh)_6(CdPPh_3)_n(Cd)_{4-n}]^{2+}$ and $[Ph_3PCd(\{\mu\text{-}SPh\}CdPPh_3)_3]^{5+}$. $Cd(PPh_3)_2(ClO_4)_2$: $Cd(SPh)_2$: PPh_3 = (a) 1:3.2 (isolated solid); (b) 1:3.1; (c) 1:3:0.[14]

the 1 3 2 mixture. This cluster (n = 4), as well as some other clusters (n < 4; see below) is assigned in the same way as the SPr' analogues discussed above. In the ^{111}Cd NMR spectrum, the signal is a doublet caused by $^{1}J(^{31}P\text{-}^{111}Cd)$. This one-bond coupling, as well as $^{1}J(^{31}P\text{-}^{113}Cd)$, is also observed in the corresponding ^{31}P NMR spectrum as satellites. The ^{31}P NMR signals (central or satellite bands) are particularly sharp for this species, allowing us to see the couplings $^{3}J(^{31}P\text{-}^{111/113}Cd)$ and $^{4}J(^{31}P\text{-}^{31}P)$. Note that the ^{3}J here is an average value, because the separate couplings to ^{111}Cd and ^{113}Cd are not resolved.

The analysis of these couplings is relatively complicated. The most abundant isotopomer of Cd_4 is $^{0}Cd_3{}^{111/113}Cd$ with probability 0.4219 (the method of calculation can be seen in Section 1.5). For the central band in the ^{31}P NMR spectrum, the ^{3}J intensity is mainly caused by one $^{111/113}$Cd and the ^{4}J is mainly caused by one ^{31}P atom which connects to $^{111/113}$Cd directly. For the ^{111}Cd or ^{113}Cd satellites, the ^{4}J coupling is contributed by three ^{31}P atoms which attach to ^{0}Cd directly. The enlarged bands of these Cd satellite splitting in Fig. 3.7a is severely distorted, suggesting that the $^{0}Cd_2{}^{111/113}Cd_2$ species (with probability 0.2110) may need to be considered.

When x = 1 (see Figs. 3.7b and 3.8b), the expected species (n = 3) is observed, but it is not dominant in solution. The signal of the n = 4 cluster is more intense. The apparent non-stoichiometry may be due to the fact that the three reactants are not completely dissolved in solution. Since the assignments of the ^{31}P and ^{111}Cd NMR spectra are clearly shown in Figs. 3.7b and 3.8b, no more discussion will be given. However, it is worth mentioning that fine structure from $^{3}J(^{31}P\text{-}^{111}Cd)$ couplings is observed in ^{111}Cd NMR spectrum. The signals of the n = 3 cluster show coupling to two phosphines

(triplet) and the signals of the n = 4 cluster show coupling to three distant phosphines (quartet).

When x = 0 (see Figs. 3.7c and 3.8c), the species $[(\mu\text{-SPh})_6(CdPPh_3)_n(Cd)_{4-n}]^{2+}$ (n = 3, 2, and probably 1) are identified from the ^{31}P spectrum but not from ^{111}Cd NMR spectrum. The NMR data of these Cd_4 clusters have been included in Table 3.2. However, at the 1:3:0 ratio, there is clearly a new type of complex formed, as shown by both the ^{31}P and the ^{111}Cd NMR spectra (Figs. 3.7c and 3.8c). To identify this new species, a mixture of $Cd(PPh_3)_2(ClO_4)_2$:$Cd(SPh)_2$ = 1:1 in CH_2Cl_2 was tried. The two reactants are completely dissolved. The ^{31}P and ^{111}Cd NMR spectra (Fig. 3.9) show that the new species is almost the only one in the solution. As can be seen from the ^{31}P NMR spectrum (Fig. 3.9a), there are two signals with intensity ratio about 3:1. Let them be labelled as P_A and P_B. The P_A signal is less shielded at position of 13.1 ppm and with relatively large satellite splitting, $^1J(^{31}P\text{-}^{111}Cd)$ = 2443 Hz. The P_B signal is at 3.3 ppm and with 1531 Hz $^{31}P\text{-}^{111}Cd$ coupling. It also can be seen that the P_A signal is a doublet while P_B is a quartet, with a splitting magnitude aroud 4 Hz which is in the usual range of four-bond coupling, $^4J(^{31}P\text{-}^{31}P)$. The splitting pattern of P_B shows the coupling $^3J(^{31}P\text{-}Cd)$ also. In the corresponding ^{111}Cd NMR spectrum (Fig. 3.9b), there are two doublets at 290 and 604 ppm. Both must correspond to Cd with one attached PPh_3. Then from the coupling patterns and signal intensities[17] of these two types of cadmium, they can be assigned to Cd_A attached P_A and Cd_B attached to P_B, respectively.

Comparison of $\delta(Cd_A)$ (290 ppm) and $^1J(^{31}P\text{-}^{111}Cd_A)$ (2443 Hz) with those values for $Cd(PPh_3)_2^{2+}$ and $Cd(PPh_3)_2(OPPh_3)_2^{2+}$ in Table 3.1 suggests that Cd_A is attached to two soft donors. Since it has already been shown that one ligand is phosphine, the other must

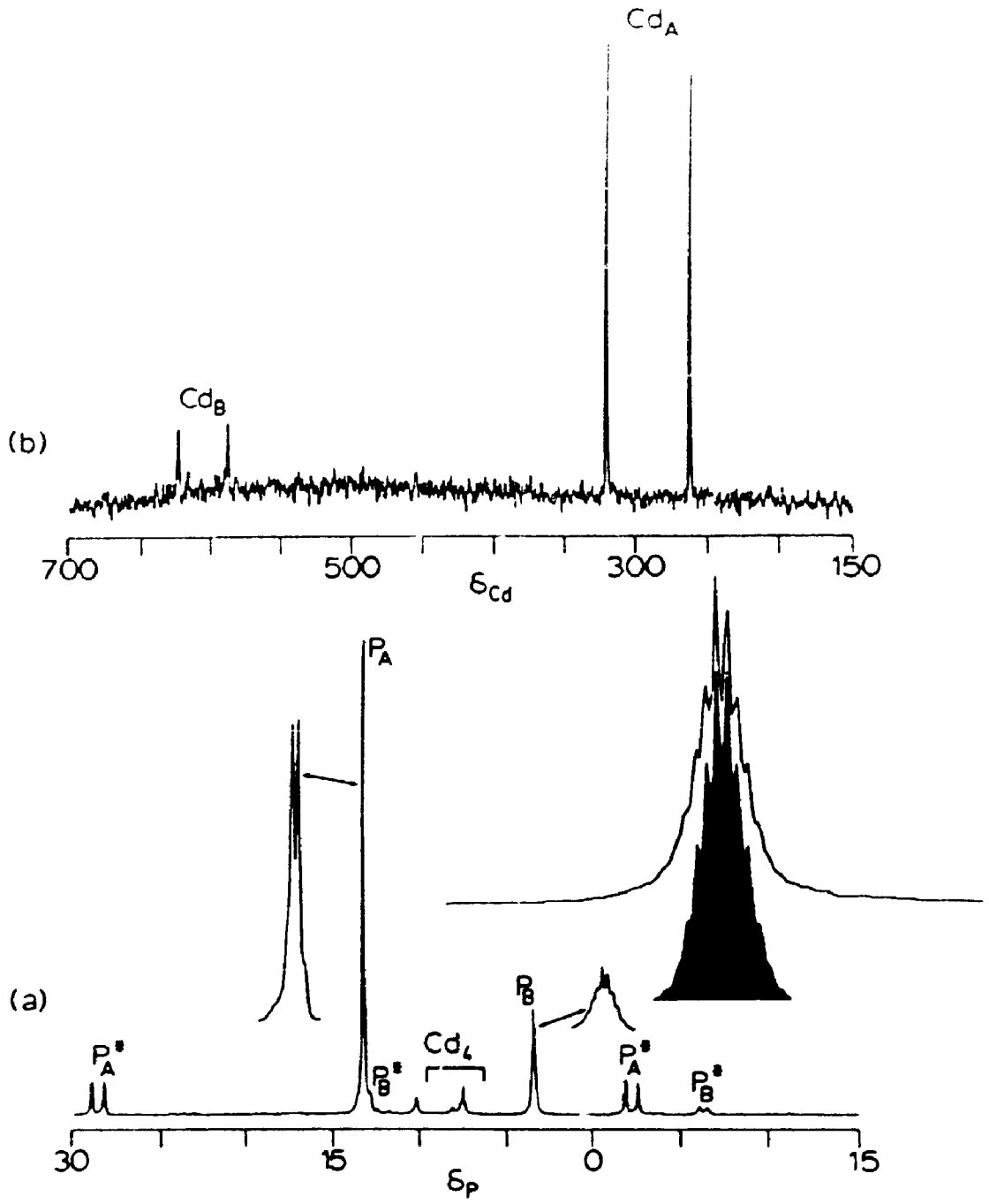

Figure 3 9 NMR spectra of a mixture containing $Cd(PPh_3)_2(ClO_4)_2$:$Cd(SPh)_2$ = 1:1 in CH_2Cl_2 at 213 K, showing the formation of $[Ph_3P_BCd_B(\{\mu\text{-}SPh\}Cd_AP_APh_3)_3]^{5+}$. (a) 80.98-MHz ^{31}P NMR spectrum with simulation inset (starred signals are $^{111/113}$ Cd satellites); (b) 42.41-MHz ^{111}Cd NMR spectrum.[14]

be phenylthiolate, indicating a SCd_AP_A kernel. On the other hand, when $\delta(Cd_B)$ (604 ppm) and $^1J(^{31}P\text{-}^{111}Cd_B)$ (1531 Hz) are compared with the data for $[(\mu\text{-}SPh)_6(CdPPh_3)_n(Cd)_{4-n}]^{2+}$ in Table 3.2, it is evident that Cd_B must have a $S_3Cd_BP_B$ kernel. These two kernels are not independent or separate complexes in solution, because the P_A signal shows coupling to one P_B, while P_B shows coupling to three P_A. Therefore, they must be connected together as one complex, and the only possible connecting ligand is SPh. Considering all the information obtained from ^{31}P and ^{111}Cd NMR spectra (see Table 3.3), we conclude that the new complex can be formulated to $[Ph_3P_BCd_B(\{\mu\text{-}SPh\}Cd_AP_APh_3)_3]^{5+}$ with the skeleton **V** (see Fig. 3.4). The new species, an *open* complex, is of a type that has not been described previously. The significance of this finding is that such an open species is another type of precursor to the adamantanoid system. NMR data for this type of open complexes are given in Table 3.3.

The P_B signal is simulated using $^4J(^{31}P\text{-}^{31}P) = 4Hz$ and $^3J(^{31}P\text{-}Cd_A) = 16Hz$, and it is inset in Fig. 3.9a. The similarity of the real signal and the simulated one supports the above assignment for this open complex.

It is interesting that the open complex is not formed when the solvent is changed to $CHCl_3$. The reason is not certain, but it may be related to the trace amount of EtOH which is a stabilizer in $CHCl_3$. In $CHCl_3$ at the 1:1 ratio, the ^{31}P and ^{111}Cd NMR results show that the major species are $[(\mu\text{-}SPh)_6(CdPPh_3)_4]^{2+}$ and $Cd(PPh_3)_3^{2+}$. The assignments of these two complexes are clearly shown in Fig. 3.10, thus no more discussion will be given.

The system of $Cd(PPh_3)_2(ClO_4)_2$:$Cd(SePh)_2$:PPh_3 has the same behaviour as the SPh analogue judging by its ^{31}P and ^{111}Cd NMR spectra. In addition, further

Table 3 3 ^{31}P and ^{111}Cd NMR Data for $[PPh_3Cd_B(\{\mu\text{-}ER\}Cd_APPh_3)_3]^{5+}$ in CH_2Cl_2 at 213 K

ER	δ_{PA}[a]	δ_{PB}[a]	δ_{CdA}[b]	δ_{CdB}[b]	$^1J(^{31}P\text{-}^{111}Cd_A)$[c]	$^1J(^{31}P\text{-}^{111}Cd_B)$[c]	$^3J(^{31}P\text{-}Cd_A)$[d,e]	$^3J(^{31}P\text{-}Cd_B)$[d,e]	$^4J(^{31}P\text{-}^{31}P)$[d]
SPh	13.1	3.3	290	604	2443	1531	16	9	4
SePh[f]	11.8	1 1	281	580	2300	1278	19	10	5
SPr[n]	11.1	-0 3	326	650	2273	1116	19	9	4
SPe[n]	10.4	-0.4	323	651	2260	1109	20	9	4

[a] Reproducibility ±0.1 pm or better.

[b] Reproducibility ±1 pm or better.

[c] Estimated error ±5 Hz.

[d] Estimated error ±1 Hz.

[e] Average coupling; separate couplings to ^{111}Cd and ^{113}Cd were not resolved.

[f] $\delta_{Se} = -71.2\pm0.2$; $(^2J(^{31}P_A\text{-}^{77}Se)+ {}^2J(^{31}P_B\text{-}^{77}Se)) = 52\pm2$ Hz. $^1J(^{77}Se\text{-}^{111}Cd_{A/B}$ could not be measured with certainty.

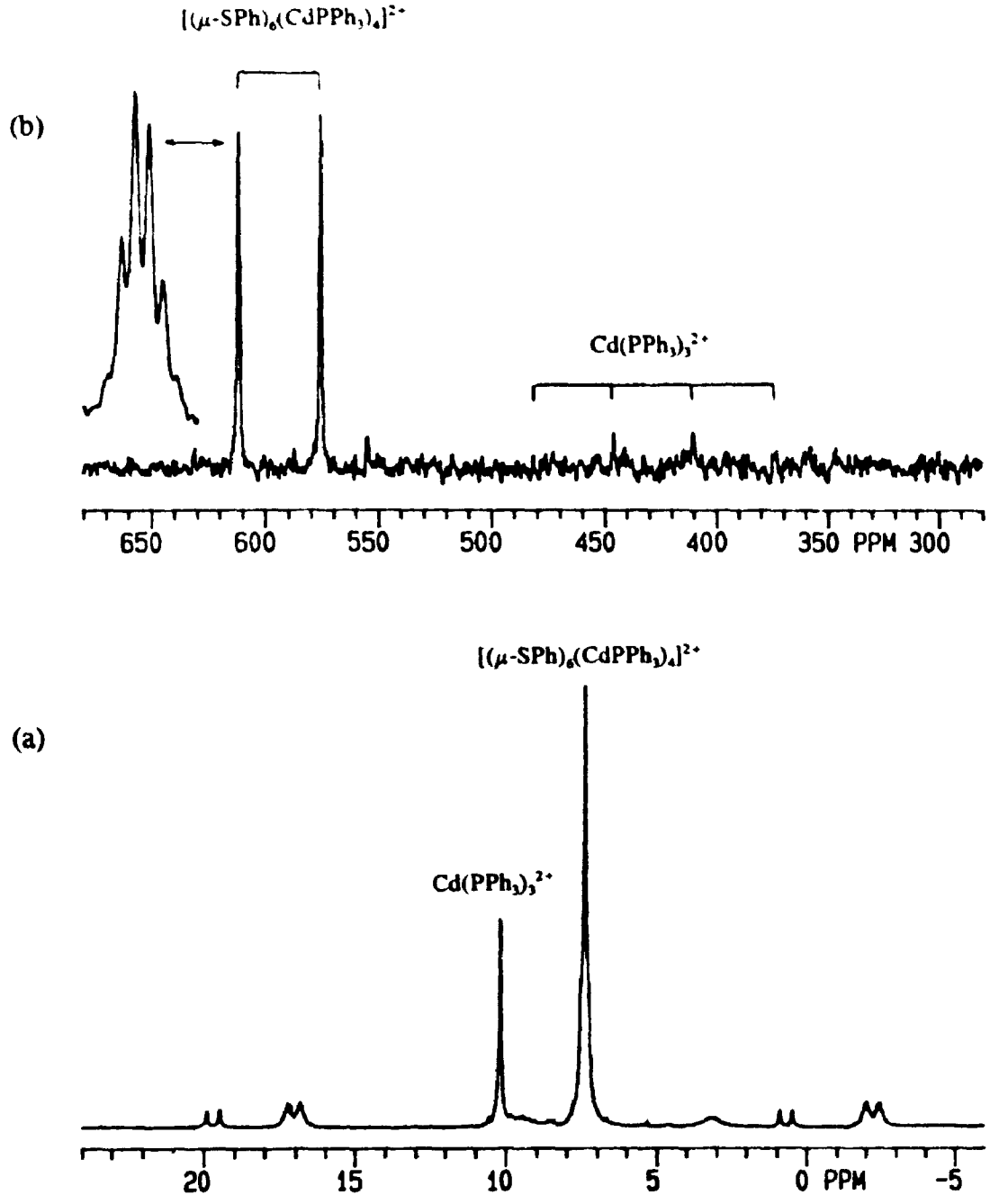

Figure 3.10 NMR spectra of a mixture containing $Cd(PPh_3)_2(ClO_4)_2$:$Cd(SPh)_2$ = 1:1 in $CHCl_3$ at 213K. (a) 80.98-MHz ^{31}P NMR spectrum; (b) 42.41-MHz ^{111}Cd NMR spectrum.

characterization is possible by ^{77}Se NMR, and agreement with the ^{31}P and ^{111}Cd NMR results is achieved. All the NMR data for $[(\mu\text{-SePh})_6(CdPPh_3)_n(Cd)_{4-n}]^{2+}$ are included in Table 3.2 and those for $[Ph_3PCd(\{\mu\text{-SePh}\}CdPPh_3)_3]^{5+}$ in Table 3.3.

(iv) The systems $Cd(PPh_3)_2(ClO_4)_2$:$Cd(SR)_2$:PPh_3 (R = Pr^n or Pe^n)

The NMR behaviour of these two systems is very similar to those of EPh analogues. Therefore, no more detailed discussion will be given. However, there is a notable difference between SR (R = Pr^n or Pe^n) and EPh (E = S or Se) systems. The *open* tetranuclear complexes persist in both CH_2Cl_2 and $CHCl_3$, when they contain the primary alkylthiolates as the bridging ligands. NMR data in CH_2Cl_2 for the $[(\mu\text{-SR})_6(CdPPh_3)_n(Cd)_{4-n}]^{2+}$ clusters are included in Table 3.2 and those for the $[Ph_3PCd(\{\mu\text{-SR}\}CdPPh_3)_3]^{2+}$ *open* complexes in Table 3.3.

3.3.3 Enhanced solubility of $Cd(ER)_2$ ($Cd(ER)_2/Cd(PPh_3)_2^{2+} > 3$)

As noted above, the compounds $Cd(ER)_2$ are poorly soluble in CH_2Cl_2, but they partially or completely solubilized when $Cd(PPh_3)_2(ClO_4)_2$ exists in solution. In general, the smaller the $Cd(ER)_2/Cd(PPh_3)_2(ClO_4)_2$ ratio, the easier the solubilization of $Cd(ER)_2$. The formation of $[(\mu\text{-ER})_6(CdPPh_3)_2(Cd)_2]^{2+}$ needs $Cd(ER)_2/Cd(PPh_3)_2(ClO_4)_2 = 3:1$, but in some cases, significantly more $Cd(ER)_2$ can be dissolved, *i.e.* $Cd(ER)_2/Cd(PPh_3)_2(ClO_4)_2 > 3$. When the concentration of $Cd(PPh_3)_2(ClO_4)_2$ is 0.05 M, the $Cd(ER)_2/Cd(PPh_3)_2(ClO_4)_2$ ratios that can be reached at room temperature are approximately 3, 4, 6, 4, 4, and >12 for ER = SPh, SePh, SPr^n, SPr^i, SPe^n and SCy, respectively. The enhanced solubility of $Cd(ER)_2$ indicates that some reactions must be

happening between $Cd(ER)_2$ and $Cd(PPh_3)_2(ClO_4)_2$. Unfortunately, the chemistry of these reactions is not very certain, because we have been unable to isolate or otherwise characterize the $Cd(ER)_2$-rich species occurring in these solutions. For higher $Cd(ER)_2/Cd(PPh_3)_2(ClO_4)_2$ ratios, at least, they may be related to the recently-characterized[18] $6Hg(SCy)_2.HgBr_2$.

3.3.4 Structure of $[(\mu\text{-}SPr^i)_6(CdPPh_3)_2(CdOClO_3)_2].EtOH$

The crystal structure consists of well-separated molecules of $[(\mu\text{-}SPr^i)_6(CdPPh_3)_2(CdOClO_3)_2]$ and EtOH. The ethanol here must come from $CHCl_3$ which contains 0.75% EtOH as a stabiiizer. The solvent molecules are disordered and will not be discussed further. The adamantane-like skeleton of $[(\mu\text{-}SPr^i)_6(CdPPh_3)_2(CdOClO_3)_2]$ is shown in Fig. 3.11. Selected bond distances and angles are tabulated in Table 3.4. As can be seen from Fig. 3.11, each Cd atom is attached to three bridging S atoms while each S atom bridge two Cd atoms. The four Cd atoms are at the corners of a distorted tetrahedron (Cd...Cd distances: 3.801(3)-4.188(3) Å; Cd-Cd-Cd angles: 56.3(1)-64.4(1)°) and the six S atoms at the corners of a distorted octahedron (geminal S...S distances: 3.992(3)-4.439(3) Å). The tetrahedral coordination geometry of the cadmium is completed by three bridging SR and one terminal PPh_3 (or $OClO_3$). The most important information is that the crystal structure confirms both the occurrence of the $(\mu\text{-}SR)_6Cd_4$ cage and the coordination of ClO_4^- that was proposed from the metal NMR data discussed above. As well, this is only the second structural analysis of a $(\mu\text{-}SAlk)_6Cd_4$ cage (the first one is in Ch. 2).

As described in Ch. 1, isomerism can be produced by the disposition of the R groups in a $(\mu\text{-}ER)_6M_4$ cage. The configuration of $[(\mu\text{-}SPr^i)_6(CdPPh_3)_2(CdOClO_3)_2]$ is that

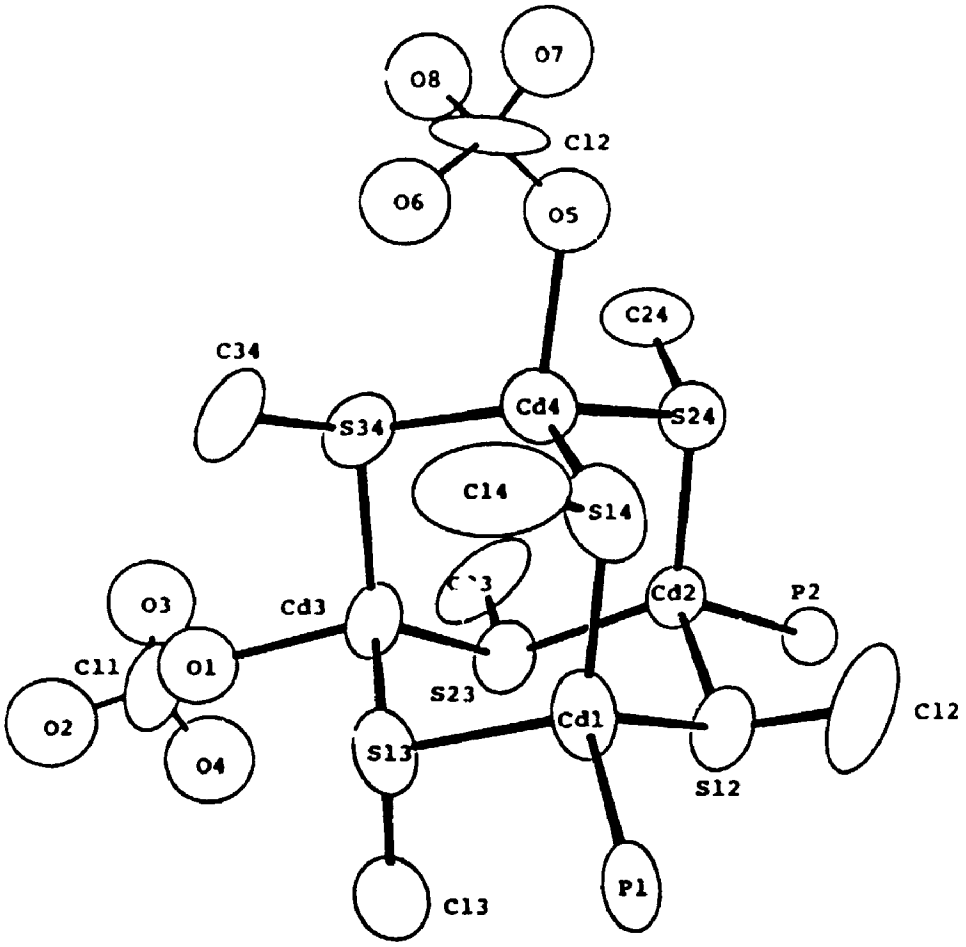

Figure 3.11 A view of the adamantane-like skeleton in $[(\mu\text{-SPr}^{i})_6(CdPPh_3)_2(CdOClO_3)_2]$.[14]

Table 3.4. Bond Distances (Å) and Angles (°) for $[(\mu\text{-SPr}^i)_6(CdPPh_3)_2(CdOClO_3)_2]$ EtOH

Bond distances

Cd(1)-P(1)	2.643(5)	Cd(2)-P(2)	2.656(4)
Cd(1)-S(12)	2.525(5)	Cd(2)-S(12)	2.542(5)
Cd(2)-S(13)	2.527(5)	Cd(3)-S(13)	2.513(6)
Cd(1)-S(14)	2.544(7)	Cd(4)-S(14)	2.459(6)
Cd(2)-S(23)	2.520(5)	Cd(3)-S(23)	2.508(5)
Cd(2)-S(24)	2.523(5)	Cd(4)-S(24)	2.549(5)
Cd(3)-S(34)	2.502(6)	Cd(4)-S(34)	2.504(6)
Cd(3)-O(1)	2.309(17)	Cd(3)-O(1a)	2.375(18)
Cd(4)-O(5)	2.356(9)	P-C mean	1.799(8)

Bond angles

S-Cd-P

S(12)-Cd(1)-P(1)	110.1(2)	S(13)-Cd(1)-P(1)	107.4(2)
S(14)-Cd(1)-P(1)	110.4(2)	S(12)-Cd(2)-P(2)	104.8(2)
S(23)-Cd(2)-P(2)	104.9(2)	S(24)-Cd(2)-P(2)	115.4(2)

S-Cd-S

S(13)-Cd(1)-S(12)	108.2(2)	S(14)-Cd(1)-S(12)	107.6(2)
S(14)-Cd(1)-S(13)	113.1(2)	S(23)-Cd(2)-S(12)	104.1(2)
S(24)-Cd(2)-S(12)	105.6(2)	S(24)-Cd(2)-S(23)	120.4(2)

Table 3 4 (Contd)

S(23)-Cd(3)-S(13)	112.9(2)	S(34)-Cd(3)-S(13)	114.4(2)
S(34)-Cd(3)-S(23)	115.3(2)	S(24)-Cd(4)-S(14)	108.1(2)
S(34)-Cd(4)-S(14)	126.9(2)	S(34)-Cd(4)-S(24)	107.5(2)

O-Cd-S

O(1) -Cd(3)-S(13)	93.2(5)	O(1) -Cd(3)-S(23)	115.6(4)
O(1) -Cd(3)-S(34)	103.0(5)	O(1a)-Cd(3)-S(13)	122.5(5)
O(1a)-Cd(3)-S(23)	98.1(5)	O(1a)-Cd(3)-S(34)	91.5(6)
O(5) -Cd(4)-S(14)	110.2(7)	O(5) -Cd(4)-S(24)	91.9(4)
O(5) -Cd(4)-S(34)	106.7(7)		

Cd-S-Cd

Cd(2)-S(12)-Cd(1)	111.5(2)	Cd(3)-S(13)-Cd(1)	104.5(2)
Cd(4)-S(14)-Cd(1)	101.3(2)	Cd(3) -S(23)-Cd(2)	100.4(2)
Cd(4)-S(34)-Cd(3)	98.8(2)	Cd(4) -S(24)-Cd(2)	104.0(2)

Cℓ-O-Cd

Cℓ(1)-O(1) -Cd(3)	132.0(12)	Cℓ(1) -O(1a)-Cd(3)	126.1(13)
Cℓ(2)-O(5) -Cd(4)	124.6(9)	Cℓ(2a)-O(5) -Cd(4)	108.4(12)

of Isomer III which is the same as that of $[(\mu\text{-SPr}^i)_6(CdBr)_4]^{2-}$ described in chapter 2 Therefore, the conformation of the Pr^i groups at S in the four Cd_3S_3 chairs is [aae,aae,aee,aee], an arrangement that has two a-a interactions (the minimum number) between substituents. The a-a interactions in the $(\mu\text{-SPr}^i)_6Cd_4$ cage lead to distortions of Cd_4 from ideal tetrahedral geometry and of S_6 from ideal octahedral geometry, as discussed for $[(\mu\text{-SPr}^i)_6(CdBr)_4]^{2-}$. The distortion of the Cd_4S_6 skeleton is reflected by the S-Cd-S angles and geminal S...S distances in $[(\mu\text{-SPr}^i)_6(CdPPh_3)_2(CdOClO_3)_2]$. Since the distortions are similar to those discussed in details for $[(\mu\text{-SPr}^i)_6(CdBr)_4]^{2-}$ (see chapter 2), no more discussion will be given here.

3.4 Conclusions

In this chapter, new clusters $[(\mu\text{-ER})_6(CdPPh_3)_n(Cd)_{4-n}]^{2+}$ have been studied, as well as some possible precursors to the adamantanoid cage system. Compared with their halide-terminal analogues (Ch. 2), the Cd-phosphine clusters have the features of phosphine-free terminal sites in this system, which suggests that the coordination capability of halide is larger than that of phosphine when they are acting as terminal ligands to Cd.

Five new adamantane-like clusters $[(\mu\text{-ER})_6(CdPPh_3)_n(Cd)_{4-n}](ClO_4)_2$ have been isolated with n = 2 for ER = SPr^i and SCy, n = 3 for ER = SPr^n, and n = 4 for ER = SPh and SePh. More than twenty cluster species have been produced from mixtures of $Cd(PPh_3)_2(ClO_4)_2$: $Cd(ER)_2$: PPh_3 (ER = SPr^i, SCy, SPh, SePh, SPr^n, SPe^n) and characterized by multi-NMR (^{31}P, $^{111/113}Cd$, ^{77}Se). For a better understanding of the NMR spectra of these tetranuclear clusters, ^{111}Cd NMR spectra for mononuclear complexes

$Cd(PPh_3)_n(ClO_4)_2$ (n = 2-4) and the ^{31}P and ^{111}Cd NMR for $[Cd(PPh_3)_n(CdOPPh_3)_{4-n}]^{2+}$ (n = 2,3) have been measured for the first time. The NMR results suggest that all the tetranuclear complexes have the adamantanoid skeleton in solution and in all tetranuclear cases there is probably an equilibrium coordination of ClO_4^- at the PPh_3-free cadmiums. Therefore, this type of cluster is better formulated $[(\mu\text{-}ER)_6(CdPPh_3)_n(CdOClO_3)_{4-n}](ClO_4)_{n-2}$.

Some possible precursors to the adamantanoid cage have been found by ^{31}P and ^{111}Cd NMR spectra using 1:1 mixtures of $Cd(PPh_3)_2(ClO_4)_2$ and $Cd(ER)_2$. For ER = SPh, SePh, SPr^n and SPe^n in CH_2Cl_2 and for SPr^n and SPe^n in $CHCl_3$, the *open* complexes $[Ph_3PCd(\{\mu\text{-}ER\}CdPPh_3)_3]^{5+}$ are formed cleanly. For ER = SPr^i and SCy in CH_2Cl_2, the *ring* complexes $[(\mu\text{-}SR)CdPPh_3]_m^{m+}$ have been observed as a minor species. If m = 3, the complex with a six-membered ring is another type of possible precursor to the adamantanoid cage.

In addition, the structure of $[(\mu\text{-}SPr^i)_6(CdPPh_3)_2(CdOClO_3)_2]$.EtOH was determined by single crystal X-ray analysis at -40°C. This is the first example showing that the terminal PPh_3-free site of CdS_3 can be coordinated by η^1-ClO_4^- to maintain the tetrahedral coordination structure, and the second example of a $(\mu\text{-}SAlk)_6Cd_4$ cage.

3.5 References

1. P.A.W. Dean, J.J. Vittal, and M.H. Trattner, *Inorg. Chem* , 26 (1987) 4245
2. P.A.W. Dean, V. Manivannan, and J.J. Vittal, *Inorg. Chem.*, 28 (1989) 2360.
3. P.A.W. Dean and J.J. Vittal, In *Metallothionein*, M.J. Stillman, C.F. Shaw III, and K.T. Suzuki, Eds., VCH, New York, 1992, Chapter 14.
4. P.A.W. Dean, J.J. Vittal, N.C. Payne, *Inorg. Chem.*, 26 (1987) 1683
5. P.A.W. Dean, J.J. Vittal, and Y. Wu, *Can. J. Chem.*, 70 (1992) 779.
6. P.A.W. Dean and V. Manivannan, *Inorg. Chem.*, 29 (1990) 2997.
7. (a) D.C. Bradley, and C.H. Marsh, *Chem. Ind.*, (1967) 361. (b) I.G. Dance, R.G. Garbutt, D.C. Craig, and M.L. Scudder, *Inorg. Chem.*, 26 (1987) 4057.
8. K. Isslieb and A. Brack, *Z. Anorg. Allgem. Chem.*, 277 (1954) 258.
9. (a) R.G. Goel and N.K. Jha, *Can. J. Chem.*, 59 (1981) 3267. (b) W.C. Wolsey, *J. Chem. Educ.*, 50 (1973) A335. *Chem. Eng. News*, 61 (Dec. 5, 1983) 4; 41 (July 8, 1963) 47.
10. Cadmium-111 and -113 are both spin-1/2 nuclei. They have similar receptivities, e.g. the receptivities relative to ^{13}C, D^c, are 6.97 and 7.67, respectively.[11]
11. R.K. Harris, *Nuclear Magnetic Resonance Spectroscopy*, Pitman, London, (1983) p. 230.
12. (a) D. Dakternieks and C.L. Rolls, *Inorg. Chim. Acta*, 105 (1985) 213. (b) P.A.W. Dean, *Can. J. Chem.*, 59 (1981) 3221.
13. R.G. Goel, W.P. Henry, and N.K. Jha, *Inorg. Chem.*, 21 (1982) 2551.
14. P.A.W. Dean, N.C. Payne, J.J. Vittal, and Y. Wu, *Inorg. Chem.*, 32 (1993) 4632.
15. P.A.W. Dean and G.K. Carson, *Can. J. Chem.*, 61 (1982) 1800.

16 (a) E S. Gruff and S.A. Koch, *J. Am. Chem. Soc.*, 112 (1990) 1245. (b) R.A. Santos, E.S. Gruff, S.A. Koch, and G.S. Harbison, *J. Am. Chem. Soc.*, 113 (1991) 469

17. Presumably RF saturation prevents this ratio from having the expected value of three.

18. T. Alsina, W. Clegg, K.A. Fraser, and J. Sola, *J. Chem. Soc., Chem. Commun.*, (1992) 1010.

CHAPTER 4 STUDIES ON MERCURY CLUSTERS $[(\mu\text{-SAlk})_{6-m}(\mu\text{-X})_m(HgX)_4]^{2-}$

4.1 Introduction

As discussed in Chapter 2[1], $[(\mu\text{-SAlk})_6(MX)_4]^{2-}$ (X = Cl-I) are well-established and isolable for zinc and cadmium. Now the following questions arise: (1) Do the mercury analogues exist in solution? (2) Are they isolable? (3) Are these complexes more or less stable than their zinc or cadmium analogues in solution or in the solid state? (4) What are their NMR spectroscopic and structural properties?

In the area of adamantane-like clusters of mercury, *cations* of the type $[(\mu\text{-SR})_6(HgL)_4]^{2+}$ (L = PR'_3 or AsR'_3) have been isolated[2] and very lately the crystal structure of $[(\mu\text{-SPh})_6(HgPPh_3)_4](ClO_4)_2.2CHCl_3$ has been determined[3]. It is known that the properties of clusters with terminal phosphines are much different from those of clusters with terminal halides (see Ch.2 and 3). Thus, *anions* of the type $[(\mu\text{-SAlk})_6(HgX)_4]^{2-}$ (X = halides) are of interest and might provide models for the mercury-binding site in mercury metallothioneins.[4] However, no isolation of such alkylthiolato-complexes with terminal halides has been reported. At the start of this work there was only evidence from NMR that adamantanoid anions $[(\mu\text{-SR})_6(HgX)_4]^{2-}$ (R = Ph or Pr") exist in solution at reduced temperature (213K).[5] Since these complexes dissociate at ambient probe temperature, the isolation of them was expected to be difficult. The nature of the dissociation products is not known with certainty. Tentatively, it has been suggested[5] that dissociation products of the SPh-complexes contain both SPh and X, while those of the SPr"-complexes are HgX_4^{2-} and $Hg(SPr")_2$.

The initial purpose of this work was to try to isolate some representative compounds with anions of formula $[(\mu\text{-SAlk})_6(HgX)_4]^{2-}$, to characterize a more extensive series of this type of clusters in solution, to investigate further the dissociation products of these species, and to get at least one representative single crystal structure. During the course of this study we not only completed the project mentioned above, but also discovered a new family of adamantanoid complexes of Hg(II), a very exciting result that had not been considered. The new family of mercury clusters has both halides and thiolates in bridging positions, $[(\mu\text{-SR})_{6-m}(\mu\text{-X})_m(HgX)_4]^{2-}$ (m = 1 or 2). To our knowledge the only analogues of this type of complex reported to date are $[(\mu\text{-EPh})_{6-m}\ (\mu\text{-I})_m(CdI)_4]^{2-}$ (E = S or Se), which have only been identified in solution by ^{77}Se and ^{113}Cd NMR.[6] An X-ray analysis of $(Ph_4P)_2[Hg_4(SEt)_5Br_5]$ which confirms the existence of such a type of mercury complexes, will be presented in this chapter.

4.2 Experimental

Materials and General Procedures

All starting materials were from commercial sources and were used as received. The compounds $Hg(SR)_2$ (R = Et, Pr^n, Pr^i, Bu^n, Cy) were prepared by the literature method.[7] This method is very straightforward. One molar equivalent of $Hg(CN)_2$ and two molar equivalents of HSR were mixed in EtOH at about 30°C. When the mixtures were cooled at 0°C, the white crystalline products were obtained in high percentage yields (ca. 90 %). All solvents used in synthesis or in the preparation of NMR samples were dried over 3A molecular sieves and were deoxygenated by sparging with Ar. All

syntheses of clusters and preparations of NMR samples were performed under an atmosphere of Ar.

Synthesis

$(Bu^n_4N)_2[Hg_4(SEt)_6Br_4]$. A mixture of $HgBr_2$ (0.108 g, 0.30 mmol), $Hg(SEt)_2$ (0.291 g, 0.90 mmol) and Bu^n_4NBr (0.193 g, 0.60 mmol), *i.e.* molar ratio 1:3:2, was dissolved in CH_2Cl_2 (2 mL) at room temperature after 10 min stirring. Et_2O (4 mL) was added to this colorless solution. After refrigeration at about 0°C for 3 h, the upper liquid layer was removed by pipette. A second portion of Et_2O (4 ml) was added to the remaining syrup, and the new mixture then refrigerated overnight. The white solid was isolated by filtration, washed by Et_2O and dried under vacuum at room temperature for 2 h; yield 0.30 g (51 %). Anal. Calcd. for $C_{44}H_{102}Br_4Hg_4N_2S_2$ (mol wt 1973.63): C, 26.78; H, 5.21; N, 1.42. Found: C, 26.49; H, 5.42; N, 1.32.

Prepared in a same manner (with the appropriate change of the three reactants) were:

$(Bu^n_4N)_2[Hg_4(SEt)_6I_4]$, as a white solid; yield 46 %. Anal. Calcd. for $C_{44}H_{102}Hg_4I_4N_2S_6$ (mol wt 2161.62): C, 24.45; H, 4.76; N, 1.30. Found: C, 24.95; H, 4.66; N, 1.15.

$(Bu^nN)_2[Hg_4(SPr^i)_6Br_4]$, as white crystals; yield 76 %. Anal. Calcd. for $C_{50}H_{114}Br_4Hg_4N_2S_6$ (mol wt 2057.77): C, 29.18; H, 5.58; N, 1.36. Found: C, 28.98; H, 5.37; N, 1.56.

$(Bu^n_4N)_2[Hg_4(SPr^i)_6Cl_4]$, as white crystals; yield 53 %. Anal. Calcd. for $C_{50}H_{114}Cl_4Hg_4N_2S_6$ (mol wt 1879.96): C, 31.94; H, 6.11; N, 1.49. Found: C, 31.62; H, 6.30; N, 1.89.

$(Ph_4P)_2[Hg_4(SEt)_6Br_4]$. This compound was prepared in a manner similar to $(Bu^n_4N)_2[(Hg_4(SEt)_6Br_4]$, except that the white crystals were formed directly after the first addition of Et_2O and subsequent refrigeration overnight. Yield 97 %. Anal. Calcd. for $C_{60}H_{70}Br_4Hg_4P_2S_6$ (mol wt 2167.50): C, 33.25; H, 3.25. Found: C, 32.90; H, 2.95.

$(Et_4N)_2[Hg_4(SBu^n)_6I_4]$. This compound was prepared as white crystals from a mixture of HgI_2, $Hg(SBu^n)_2$ and Et_4NI in the molar ratio 1:3:2, following the procedure used for $(Ph_4P)_2[Hg_4(SEt)_6Br_4]$; yield 79 %. Anal. Calcd. for $C_{40}H_{94}Hg_4I_4N_2S_6$ (mol wt 2105.49): C, 22.82; H, 4.50; N, 1.33. Found: C, 22.60; H, 4.55; N, 1.36.

$(Et_4N)_2[Hg_4(SEt)_6Cl_4]$. A mixture of $HgCl_2$ (0.109 g, 0.40 mmol), $Hg(SEt)_2$ (0.387 g, 1.2 mmol) and $Et_4NCl.H_2O$ (0.147 g, 0.80 mmol) in CH_2Cl_2 (6 mL) was stirred at room temperature for 3 h. A small amount of insoluble material was removed by filtration, then Et_2O (6 mL) was added. The white crystals that formed after refrigeration of the mixture overnight were separated by decantation, washed with Et_2O and dried in vacuum at room temperature; yield 0.35 g (56 %). Anal. Calcd. for $C_{28}H_{70}Cl_4Hg_4N_2S_6$ (mol wt 1571.40): C, 21.40; H, 4.49; N, 1.78. Found: C, 21.35; H, 4.18; N, 1.83.

$(Ph_4P)_2[Hg_4(SEt)_5I_5]$. This compound was prepared as white crystals from a mixture of HgI_2 (0.60 mmol), $Hg(SEt)_2$ (1.0 mmol) and Ph_4PI (0.8 mmol) in CH_2Cl_2 (3 mL), following the procedure used for $(Ph_4P)_2[Hg_4(SEt)_6Br_4]$; yield 0.94 g (97 %). Anal. Calcd. for $C_{58}H_{65}Hg_4I_5P_2S_5$ (mol wt 2421.28): C, 28.77; H, 2.71. Found: C, 28.87; H, 2.40.

$(Ph_4P)_2[Hg_4(SPr^i)_5I_5]$. This compound was prepared as white crystals from a mixture of HgI_2 (1 mmol), $Hg(SPr^i)_2$ (3 mmol) and Ph_4PI (2 mmol) in CH_2Cl_2 (5 mL), following the procedure used for $(Ph_4P)_2[Hg_4(SEt)_5I_5]$; yield 49 %. Anal. Calcd. for $C_{63}H_{75}Hg_4I_5P_2S_5$ (mol wt 2491.41): C, 30.37; H, 3.03. Found: C, 30.18; H, 3.05.

Prepared in a same manner were:

$(Bu^n_4N)_2[Hg_4(SPr^i)_5I_5]$, as white crystals; yield 51 %. Anal. Calcd. for $C_{47}H_{107}Hg_4I_5N_2S_5$ (mol wt 2306.64): C, 24.47; H, 4.68, N, 1.21. Found: C, 24.74; H, 4.67; N, 1.21.

$(Ph_4P)_2[Hg_4(SPr^i)_5Br_5]$, as white crystals; yield 56 %. Anal. Calcd. for $C_{63}H_{75}Br_5Hg_4P_2S_5$ (mol wt 2256.41): C, 33.54; H, 3.35. Found: C, 33.71; H, 3.25.

$(Bu^n_4N)_2[Hg_4(SPr^i)_5Cl_5]$. This compound was prepared as white crystals from a mixture of $HgCl_2$, $Hg(SPr^i)_2$ and $Bu^n_4NCl.xH_2O$ in a 3:5:4 ratio, following the procedure used for $(Et_4N)_2[Hg_4(SEt)_6Cl_4]$; yield 24 %. Anal. Calcd. for $C_{47}H_{107}Cl_5Hg_4N_2S_5$ (mol wt 1840.37): C, 30.67; H, 5.87; N, 1.52. Found: C, 31.10; H, 5.69; N, 1.70.

$(Et_4N)_2[Hg_4(SPr^i)_5Cl_5]$. This compound was prepared as white crystals from a mixture of $HgCl_2$, $Hg(SPr^i)_2$ and $Et_4NCl.H_2O$ in a 3:5:4 ratio, following the procedure used for $(Et_4N)_2[Hg_4(SEt)_6Cl_4]$; yield 31 %. Anal. Calcd. for $C_{31}H_{75}Cl_5Hg_4N_2S_5$ (mol wt 1615.87): C, 23.04; H, 4.68; N, 1.73. Found: C, 22.95; H, 4.30; N, 1.92.

$(Ph_4P)_2[Hg_4(SBu^n)_4I_6]$. This compound was prepared as white crystals from a mixture of HgI_2, $Hg(SBu^n)_2$ and Ph_4PI in a 1:1:1 ratio, following the procedure used for $(Ph_4P)_2[Hg_4(SEt)_5I_5]$; yield 87 %. Anal. Calcd. for $C_{64}H_{76}Hg_4I_6P_2S_4$ (mol wt 2599.28): C, 29.57; H, 2.95. Found: C, 30.06; H, 2.87.

The evidence for the presence of preceding compounds and the stoichiometry of their appropriate constituents (cation and SR^-) was obtained by ^1H and ^{13}C NMR at ambient probe temperature. As well, the authenticity of the new clusters was confirmed by comparison of the reduced temperature ^{199}Hg NMR spectra of isolated products with those of analogous formed in situ (see Section 4.3). Some other attempted preparations of this type of clusters are mentioned below.

$(Ph_4P)_2[Hg_4(SPr^i)_4Br_6]$. This compound was obtained as a foamy white solid from a mixture of $HgBr_2$, $Hg(SPr^i)_2$ and Ph_4PBr in a 1:1:1 ratio, following the same procedure used for $(Ph_4P)_2[Hg_4(SBu^n)_4I_6]$. The product was pure by ^1H, ^{13}C and ^{199}Hg NMR but did not give satisfactory microanalytical results. Anal. Calcd. for $C_{60}H_{68}Br_6Hg_4P_2S_4$ (mol wt 2661.17): C, 31.87; H, 3.03. Found: C, 31.22; H, 2.60.

$(Ph_4P)_2[Hg_4(SEt)_4Br_6]$. This compound was obtained as white crystals from a mixture of $HgBr_2$, $Hg(SEt)_2$ and Ph_4PBr in a 3:5:4 ratio, following the procedure used for $(Ph_4P)_2[Hg_4(SEt)_5I_5]$. The product had a satisfactory microanalytical result for the Br_6 - compound but it was proved to be a mixture of Br_6-/Br_5-compounds (ca. 1:1) by ^1H, ^{13}C and ^{199}Hg NMR. Anal. Calcd. for $C_{56}H_{60}Br_6Hg_4P_2S_4$ (mol wt 2205.06): C, 30.50; H, 2.74. Found: C, 30.33; H, 2.61.

$(Ph_4P)_2[Hg_4(SEt)_5Br_5]$. This compound was obtained from the recrystallization of $(Ph_4P)_2[Hg_4(SEt)_6Br_4]$ (50 mg) in $CHCl_3$ (2 mL) and Et_2O (2 mL) at room temperature for two days. The crystalline product contained a crystal was suitable for crystallography (see below) and in addition was characterized by ^1H NMR and microanalysis. Anal. Calcd. for $C_{58}H_{65}Br_5Hg_4P_2S_5$ (mol wt 2186.28): C, 31.86; H, 3.00. Found: C, 32.10; H, 2.58.

In most cases the clusters undergo dissociation in solution at ambient probe temperature (see Section 4.3 for details). When Et_2O was layered onto a dilute CH_2Cl_2 solution of crude $(Et_4N)_2[Hg_4(SEt)_6Br_4]$ (this compound was pure by ^1H and ^{13}C NMR, but elemental analysis was not obtained) at room temperature, a very poorly soluble crystalline product was obtained. X-ray analysis (determination of the unit cell parameters) proved this product to be $(Et_4N)_2[HgBr_4]$. Similarly, when recrystallizations of $(Ph_4P)_2[Hg_4(SEt)_6Br_4]$ from CH_2Cl_2/Et_2O at room temperature and of $(Et_4N)_2[Hg_4(SBu^n)_6I_4]$ from $CHCl_3/Et_2O$ at room temperature were attempted, the resulting products were shown to be mononuclear complexes, $(Ph_4P)_2[HgBr_4]$ and $(Et_4N)_2[HgI_4]$, respectively, from their unit cell parameters. However, when the recrystallization of crude $[(Et_4N)_2[Hg_4(SPr^n)_6I_4]$ (prepared in the same way as the Bu^nS^- analogue, but containing about 10 % $[(Et_4N)_2[Hg_4(SPr^n)_5I_5]$ (proved by ^1H, ^{13}C and ^{199}Hg NMR)) from Et_2O/CH_2Cl_2 was attempted at room temperature, the crystalline product obtained, proved to be $(Et_4N)_2[Hg_2(SPr^n)I_5]$ from ^1H NMR and by the complete X-ray analysis (see below)

NMR Spectra

Samples were prepared in situ for ^1H and ^{13}C NMR by dissolving an isolated product in a suitable deuterated solvent in a 5 mm od NMR tube. The spectra were measured by using a Varian Gemini-200 spectrometer system at ambient probe temperature. The ^2D resonances of the solvents were used as field/frequency locks. For ^1H NMR the internal references are those δ_H = 1.93, 7.24 and 2.04 for $CD_2\mathit{H}CN$, $C\mathit{H}Cl_3$ and $(CD_3)(CD_2\mathit{H})CO$, respectively, and for ^{13}C NMR the internal references are those δ_C = 1.3, 77.0 and 29.8 for $\mathit{C}D_3CN$, $\mathit{C}DCl_3$ and $(\mathit{C}D_3)_2CO$, respectively

Cadmium-111 and ^{199}Hg NMR spectra[8,9] were measured as described in Ch.2 and previous papers,[5,10] with samples in 10 mm od NMR tubes. For ^{111}Cd and ^{199}Hg, samples were referenced to external 0.1 M $Cd(ClO_4)_2$(aq) and pure $HgMe_2$, respectively, at ambient probe temperature by sample interchange. ^{111}Cd nucleus (as opposed to slightly more sensitive[8] ^{113}Cd) was observed to decrease problems with artifacts when measuring Cd NMR spectra using our Varian XL-200 or -300 spectrometer systems.[10] No primary isotope effect is expected. Later ^{199}Hg NMR spectra were measured using a Varian Gemini-200 spectrometer system, because the old XL-200 was replaced in our department. For ^{111}Cd, the frequencies at the reference were 42.41 and 63.59 MHz on the XL-200 and XL-300 spectrometers, respectively. For ^{199}Hg, the corresponding frequencies were 35.83, 35.84 and 53.72 MHz on the XL-200, Gemini-200 and XL-300 spectrometers, respectively.

X-ray Structure Determinations

The crystals of $[(C_6H_5)_4P]_2[Hg_4Br_5(SC_2H_5)_5]$ and $[(C_2H_5)_4N]_2[Hg_2I_5(S\text{-}n\text{-}C_3H_7)]$ (see above for the synthesis) were examined by Dr. Vittal using the X-ray diffraction facilities of this department.

Elemental Microanalyses

All analyses were performed by Guelph Chemical Laboratories Ltd.

4.3 Results and Discussion

4.3.1 Synthesis

At a 1:3:2 molar ratio of HgX_2:$Hg(SR)_2$:$(Cat^+)X$, complexes $[Hg_4(SR)_6X_4]^{2-}$ were isolated for the following representative combinations of Cat^+/R/X: Et_4N^+/Et/Cl; Et_4N^+/Bu^n/I; $Bu^n_4N^+$/Et/I, Br; $Bu^n_4N^+$/Pr^i/Br, Cl; Ph_4P^+/Et/Br. The reactions follow eqn [1].

[1] $$HgX_2 + 3\ Hg(SR)_2 + 2\ X^- \longrightarrow [Hg_4(SR)_6X_4]^{2-}$$

However, in some cases, at the 1:3:2 ratio of reactants, complexes of $[Hg_4(SR)_5X_5]^{2-}$ are the isolated product (Cat^+/R/X: Ph_4P^+/Pr^i/I, Br; $Bu^n_4N^+$/Pr^i/I). An equilibrium such as eqn. [2] may exist in solution.

[2] $$3\ HgX_2 + 9\ Hg(SR)_2 + 6\ X^- \rightleftharpoons 2\ [Hg_4(SR)_5X_5]^{2-} + 4\ Hg(SR)_2 + 2\ X^-$$

$$\downarrow\uparrow$$

$$3\ [Hg_4(SR)_6X_4]^{2-}$$

At the ratio of 1:3:2, the isolation of $[Hg_4(SR)_5X_5]^{2-}$ clusters depends on the cation properties. For example, if the cation is Ph_4P^+, the salts Ph_4PX and $(Ph_4P)_2[Hg_4(SR)_6X_4]$ are relatively more soluble in solution than their Et_4N^+ analogues; thus the $[Hg_4(SR)_5X_5]^{2-}$ clusters may isolated as their Ph_4P^+ salts according to the eqn. [2]. (Note: $Hg(SR)_2$ is extremely soluble in CH_2Cl_2). The properties of SR and X may influence the isolation, as well. In general, the solubility of the salts with R = Pr^i is larger than those with Et or

Bu^n, and solubilities change with X in the order: I > Br > Cl. This may explain why, when R = Pr^i and X = I, $[Hg_4(SR)_5X_5]^{2-}$ clusters are always isolated instead of $[Hg_4(SR)_6X_4]^{2-}$. Of course, anions of the stoichiometry $[Hg_4(SR)_5X_5]^{2-}$ can also be isolated from 3:5:4 molar ratios of HgX_2:$Hg(SR)_2$:$(Cat^+)X^-$ (*e.g.* Cat^+/R/X = Ph_4P^+/Et/I; Et_4N^+/Pr^i/Cl; and $Bu^n{}_4N^+$/Pr^i/Cl), as expected from eqn. [3].

[3] $3\ HgX_2 + 5\ Hg(SR)_2 + 4\ X^- \longrightarrow 2\ [Hg_4(SR)_5X_5]^{2-}$

In addition, recrystallization of $(Ph_4P)_2[Hg_4(SEt)_6Br_4]$ gives $(Ph_4P)_2[Hg_4(SEt)_5Br_5]$ (perhaps following eqn. [2]) in a form suitable for x-ray analysis (the crystal structure will be described below).

At a 1:1:1 molar ratio of HgX_2:$Hg(SR)_2$:$(Ph_4P^+)X^-$, the complexes of $(Ph_4P)_2[Hg_4(SBu^n)_4I_6]$ and $(Ph_4P)_2[Hg_4(SPr^i)_4Br_6]$ are isolated analytically and spectroscopically pure, respectively (see eqn. [4]).

[4] $HgX_2 + Hg(SR)_2 + X^- \longrightarrow 1/2\ [Hg_4(SR)_4X_6]^{2-}$

Following eqn. [4], the isolation of other $[Hg_4(SR)_4X_6]^{2-}$ as Ph_4P^+ salts (R = Pr^i, X = I; R = Et, X = I or Br) has been tried, but the pure compounds have never been isolated, which might be due to a solubility problem. At this 1:1:1 ratio, the reactants are not completely dissolved or a new white precipitate formed (when R = Et), although the $[Hg_4(SEt)_4X_6]^{2-}$ species could be examined in solution by ^{199}Hg NMR. On the other hand, $[Hg_4(SPr^i)_4I_6]^{2-}$ may be too soluble to be isolated (even at the 3:1:2 molar ratio of

HgX_2:$Hg(SR)_2$:Ph_4PX, the reactants are all dissolved). Isolation of the complex $(Ph_4P)_2[Hg_4(SBu)_3I_7]$ has been attempted also, but the solubility of the reactants (too low) was the major problem for its synthesis.

As mentioned above for the preparation of $(Ph_4P)_2[Hg_4(SEt)_4Br_6]$, this $(\mu\text{-}X)_2$ compound is isolated from a solution containing 3:5:4 molar ratio of reactants, and it is contaminated by the $(\mu\text{-}X)$ compound. Thus it suggests that the equilibrium eqn. [4b] may exist in solution.

$$[4b] \quad 6\ HgX_2 + 10\ Hg(SR)_2 + 8\ X^- \rightleftharpoons 3\ [Hg_4(SR)_4X_6]^{2-} + 4\ Hg(SR)_2 + 2\ X^-$$

$$\downarrow\uparrow$$

$$4\ [Hg_4(SR)_5X_5]^{2-}$$

Under different conditions (see Experimental), attempted recrystallizations for $(Et_4N)_2[Hg_4(SEt)_6Br_4]$, $(Ph_4P)_2[Hg_4(SEt)_6Br_4]$ and $(Et_4N)_2[Hg_4(SBu^n)_6I_4]$ give the mono-mercury salts $(Et_4N)_2[HgBr_4]$, $(Ph_4P)_2[HgBr_4]$ and $(Et_4N)_2[HgI_4]$, separately. This type of dissociation reaction may follow eqn. [5], since $Hg(SR)_2$ is very soluble and remains in solution.

$$[5] \quad [Hg_4(SR)_6X_4]^{2-} \rightleftharpoons [HgX_4]^{2-} + 3\ Hg(SR)_2$$

Another attempted recrystallization of crude $(Et_4N)_2[Hg_4(SPr^n)_6I_4]$ (see Experimental) gave $(Et_4N)_2[Hg_2(SPr^n)I_5]$ containing a novel dimeric anion. This is another type of dissociation

which may follow eqn. [6]. The structure of the new binuclear complex will be described below.

[6] $[Hg_4(SPr^n)_5I_5]^{2-} = [Hg_2(SPr^n)I_5]^{2-} + 2\ Hg(SPr^n)_2$

The preceding discussion suggests that at or near room temperature there is dissociation of $[Hg_4(SR)_6X_4]^{2-}$ to give a variety of possible products (a tetranuclear cluster with a (μ-X) ligand, a binuclear complex, or a mononuclear complex). The one that is isolated depends on which is least soluble in the circumstances.

In this chapter, mixed-metal solutions of $[(\mu\text{-SAlk})_6(HgX)_{4-n}(MX)_n]^{2-}$ (M = Zn, Cd) are prepared in situ for NMR measurement. If the mixtures start with a 1:1 ratio of Hg_4:M_4 and follow statistical redistributions, the fractional populations of $Hg_{4-n}M_n$ (n = 0-4) will be similar to those of the Cd_nZn_{4-n} system which have been discussed in section 1.6. Therefore, no more discussion will be given here. No attempt was made in our experiments to isolate these mixed-metal complexes.

4.3.2 NMR studies

(i) $[(\mu\text{-SR})_6(HgX)_4]^{2-}$

Proton and ^{13}C NMR data of $[Hg_4(SAlk)_6X_4]^{2-}$ are listed in Table 4.1 (m = 0). The spectra are very similar to those of the zinc or cadmium analogues (see Ch.2), and therefore none of them is shown here. However, these spectra also allow a first assessment of whether the isolated compounds are pure or not.

Table 4.1 ^{1}H and ^{13}C NMR Data for the Anions in $(Cat)_2[(\mu\text{-}SR)_{6-m}(\mu\text{-}X)_m(HgX)_4]$ at Ambient Probe Temperature.[a,b]

Cat^{+} [b]	X	R	m	Solvent	δ_H[c]				δ_C[d]			
					H_1	H_2	H_3	H_4	C_1	C_2	C_3	C_4
$Bu^n_4N^+$	I	Et	0	CD_3CN	2.96	1.36			28.2	21.1		
$Bu^n_4N^+$	Br	Et	0	CD_3CN	3.01	1.36			27.5	21.3		
Ph_4P^+	Br	Et	0	$CDCl_3$	3.08	1.32			26.8	21.1		
Et_4N^+	Cl	Et	0	$CDCl_3$	3.17	1.40			25.0	22.0		
$Bu^n_4N^+$	Br	Pr^i	0	CD_3CN	3.70	1.43			38.6	29.9		
$Bu^n_4N^+$	Cl	Pr^i	0	CD_3CN	3.64	1.40			37.6	30.1		
Et_4N^+	I	Bu^n	0	CD_3CN	2.94	1.70	1.40	0.88	38.2	29.2	22.6	14.1
Ph_4P^+	I	Et	1	$CDCl_3$	3.02	1.34			27.7	20.8		
Ph_4P^+	Br	Et	1	$CDCl_3$	3.13	1.38			[e]			
Ph_4P^+	I	SPr^i	1	$CDCl_3$	3.73	1.42			36.8	30.5		
$Bu^n_4N^+$	I	SPr^i	1	CD_3CN	3.73	1.42			39.2	29.8		
Ph_4P^+	Br	SPr^i	1	$CDCl_3$	3.76	1.40			38.4	29.7		

Table 4.1 (Continued)

Et_4N^+	Cl	SPr^i	1	$CDCl_3$	3.87	1.49			38.5	29.8		
$Bu^n_4N^+$	Cl	SPr^i	1	$CDCl_3$	3.89	1.50			38.4	29.8		
Ph_4P^+	I	SBu^n	2	$(CD_3)_2CO$	3.07	1.75	1.46	0.90	38.3	33.0	22.5	14.1
Ph_4P^{+f}	Br	SPr^i	2	$CDCl_3$	3.86	1.46			39.4	29.1		
Ph_4P^{+g}	Br	SEt	2	$CDCl_3$	3.13	1.36			27.3	27.3		

[a] The anions are appreciably dissociated at this temperature (see text).

[b] For Et_4N^+ in $CD_3CN(CHCl_3)$: δ_H 1.21(*1.35*) (m, H_2)), 3.17(*3.40*) (q, H_1)); δ_C 7.7(*8.1*) (C_2), 53.0(*53.1*) (C_1). For $Bu_{4n}N^+$ in $CD_3CN(CHCl_3)$: δ_H 0.96(*0.99*) (t, H_4)), 1.36(*1.45*) (m, H_3)), 1.60(*1.65*) (m, H_2)), 3.09(*3.28*) (m, H_1)); δ_C 13.8(*13.8*) (C_4), 20.3(*19.9*) (C_3), 24.3(*24.3*) (C_2), 59.3(*59.2*) (C_1). For Ph_4P^+ in $CHCl_3$: δ_H ca 7.5-8.0; δ_C 117.4 (C_1, ^1J(P-C) = 89 Hz), 134.5 ($C_{2,6}$, ^2J(P-C) = 11 Hz), 130.9 ($C_{3,5}$, ^3J(P-C) = 13 Hz), 135.8 (C_4, ^4J(P-C) = 3 Hz). For Ph_4P^+ in $(CD_3)_2CO$: δ_H ca 7.8-8.1; δ_C 135.7 ($C_{2,6}$, ^2J(P-C) = 10 Hz), 131.4 ($C_{3,5}$, ^3J(P-C) = 13 Hz), 136.4 (C_4, ^4J(P-C) = 3 Hz), C_1 not obs.

[c] Relative to the solvent residual signals with δ_H as follows: CHD_2CN, 1.93; $CHCl_3$, 7.24; $(CD_3)(CHD_2)CO$, 2.04.

[d] Relative to the solvent signals with δ_C as follows: CD_3CN, 1.3; $CDCl_3$, 77.0; $(CD_3)_2CO$, 29.8.

Table 4.1 (Continued)

[e] Not measured.

[f] This compound gave unsatisfactory elemental analytical results but was pure by ^{1}H, ^{13}C and ^{199}Hg NMR.

[g] This compound gave satisfactory elemental analytical results but was not pure by ^{1}H, ^{13}C and ^{199}Hg NMR.

Mercury-199 NMR spectra of $[Hg_4(SR)_6X_4]^{2-}$ were measured using a sample of pure isolated compound or a sample prepared in situ. Some of ^{199}Hg NMR data for clusters $[(\mu\text{-}SR)_6(HgX)_4]^{2-}$ are included in Table 4.2. The ^{199}Hg NMR spectra of $[Hg_4(SR)_6X_4]^{2-}$ at reduced temperature show generally a single line which is consistent with the formulation $[(\mu\text{-}SR)_6(HgX)_4]^{2-}$ of skeleton I (see fig. 4.1). An exception is that when R = Pr^i or Cy, the spectra show two additional weaker lines at reduced temperature that are due to $[(\mu\text{-}SR)_5(\mu\text{-}X)(HgX)_4]^{2-}$ (see Fig. 4.4a and discussion below). However, the single line spectrum of $[(\mu\text{-}SR)_6(HgX)_4]^{2-}$ can be obtained by adding excess X^-. The exact equilibrium reaction that produces this result is not very clear. It may follow eqn. [2b], shown below. In this case, increasing the concentration of X^- pushes the equilibrium to the left side.

[2b] $3\ [(\mu\text{-}SR)_6(HgX)_4]^{2-} \rightleftharpoons 2\ [(\mu\text{-}SR)_5(\mu\text{-}X)(HgX)_4]^{2-} + 4\ Hg(SR)_2 + 2\ X^-$

As can be seen from Table 4.2, the nuclear shielding of mercury shows the Normal Halogen Dependence[11], *i.e.* I > Br > Cl, as is found for the analogous clusters of cadmium also. For example, when R = Pr^i and T = 213K, the chemical shifts for I, Br and Cl are: -905, -655 and -537, respectively. The chemical shifts also depend on the bridging thiolate. For a constant halogen, δ_{Hg} varies with R in the order primary alkyl > secondary alkyl, which is the same as found in Chapter 2 for cadmium systems. For example, at 213K, when X = Br, the chemical shifts of ^{199}Hg with R in the order : Et (-602) ≈ Bu (-607) > Pr^i (-655). If the values of δ_{Hg} for $[(\mu\text{-}SR)_6(HgX)_4]^{2-}$ in Table 4.2 are combined with earlier data[5] and some other data in this chapter (Table 4.3, n =

Table 4.2 NMR Data for $[(\mu\text{-SR})_6(HgX)_4]^{2-}$ in CH_2Cl_2

R	X	δ_{Hg}[a]	
		Temp/K = 213	295
Et	I	-828	-1096
	Br	-602	-804
	Cl	-497	-721
2-Pr	I	-905	-1229
	Br	-655	-948
	Cl	-537	-774
1-Bu	I	-839	not obs.
	Br	-607	-848

[a] Relative to pure $HgMe_2$ at 295 K

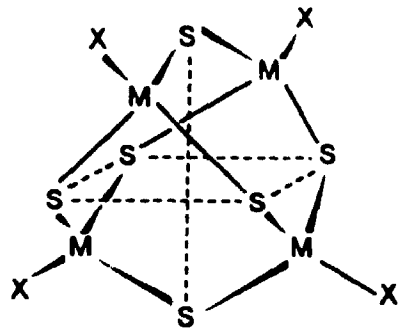

(I)

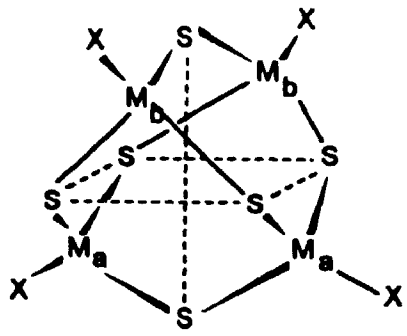

(II)

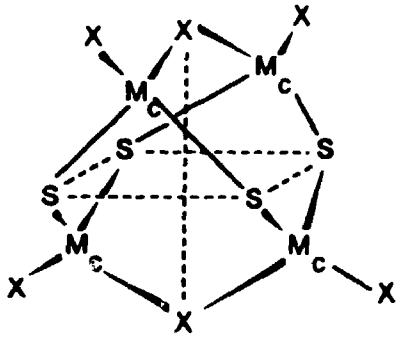

(IIIa)

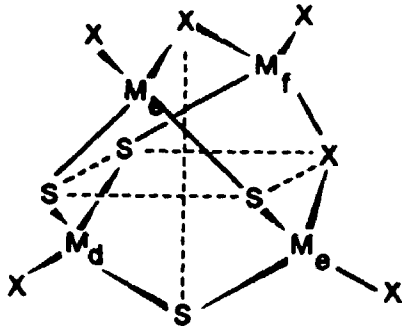

(IIIb)

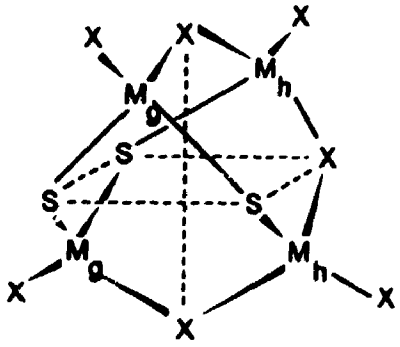

(IVa)

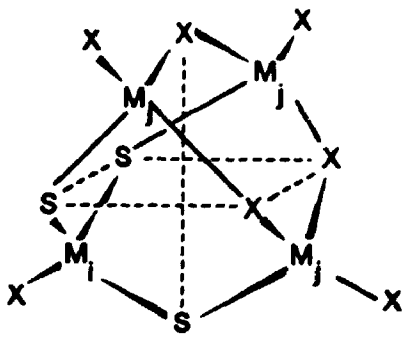

(IVb)

Fig 4.1 Skeletons for the clusters $[(\mu\text{-SR})_{6-m}(\mu\text{-X})_m(HgX)_4]^{2-}$ (m = 0-3)

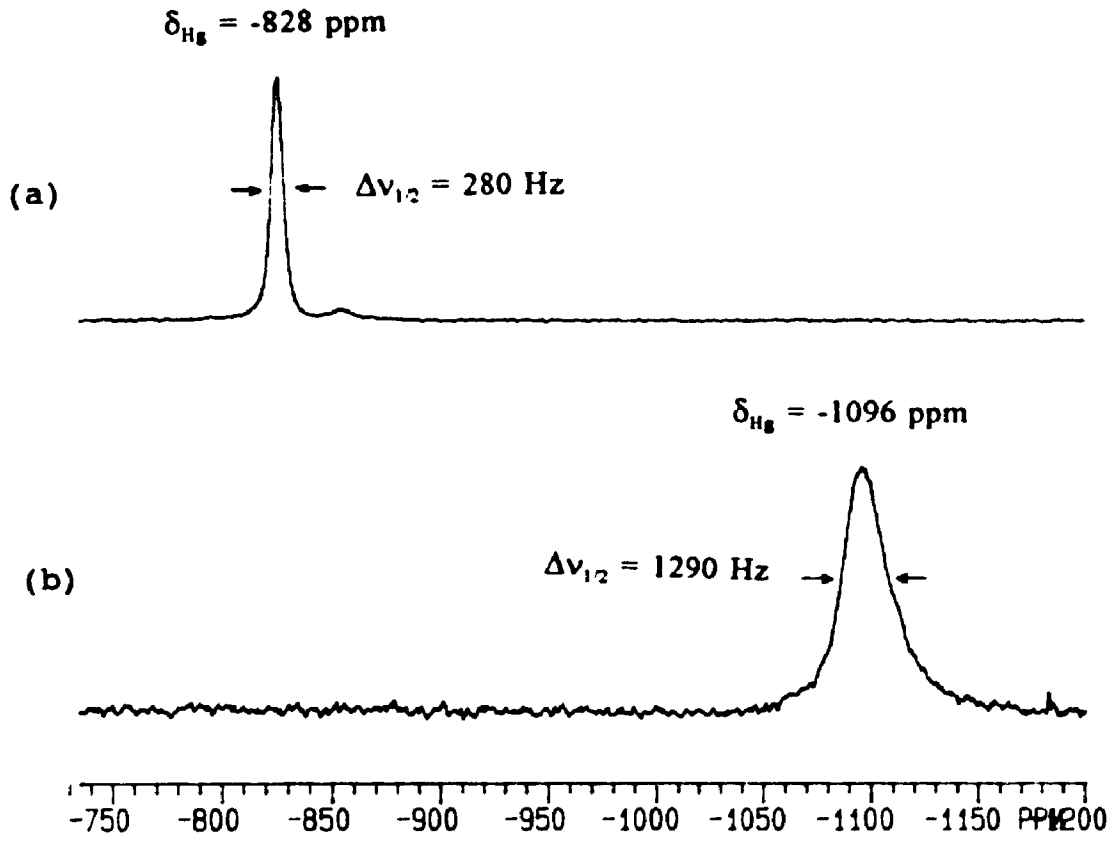

Fig. 4.2 ^{199}Hg NMR spectra of $[(\mu\text{-}SEt)_6(HgI)]^{2-}$ in CH_2Cl_2 at (a) 213K; (b) 295K.

0; and Table 4.4, m = 0; all shown later), the variation of δ_{Hg} with ER is found to be in the order: SEt ≈ SPr^n ≈ SBu^n > SPr^i ≈ SCy > SPh > SePh > TePh.

In addition, the chemical shifts are influenced by temperature. When the temperature is raised, the ^{199}Hg NMR spectra of all of the $[(\mu\text{-SR})_6(HgX)_4]^{2-}$ become significantly shielded and broaden. In some cases no signals can be observed at room temperature. For example, the δ_{Hg} of $[(\mu\text{-SEt})_6(HgI)_4]^{2-}$ is -828ppm with $\nu_{1/2}$ = 280Hz at 213K, but -1096 ppm with $\nu_{1/2}$ = 1290Hz at 295K (Table 4.2 and Fig. 4.2). The difference here (293 ppm) is quite large compared to that found for the cadmium analogue (583ppm (at 218K) - 566ppm (at 294K) = 17ppm, see Table 2.4). However, for the same mercury cluster at 183K, δ_{Hg} is -810ppm (see Table 4.4, shown later). The δ_{Hg} difference between 183K and 213K is only 18ppm. Therefore, it is not certain that the chemical shift of mercury at 293K represents the real cluster $[(\mu\text{-SPr}^i)_6(HgBr)_4]^{2-}$ or the dissociation product. Earlier, it has been suggested that such a big change between 213K and 295K is indicative of dissociation.[5] In our experiments a range of products has been isolated at higher temperatures (*e.g.* 273K) from solutions having the correct stoichiometry for $[(\mu\text{-SR})_6(HgX)_4]^{2-}$. These results provide additional circumstantial evidence for cluster dissociation.

(ii) $[(\mu\text{-SR})_6(HgX)_{4-n}(MX)_n]^{2-}$ (M = Zn or Cd)

In this project, ^{199}Hg NMR spectra of mixed-metal solutions of $[(\mu\text{-SR})_6(HgX)_4]^{2-}$ with the known[10] Zn_4 and Cd_4 analogues were measured to prove that the single line ^{199}Hg NMR spectra are indeed due to $[(\mu\text{-SR})_6(HgX)_4]^{2-}$ (not other species, such as mononuclear complexes $[Hg(SR)_3X]^{2-}$). For such a mixed-metal system $[(\mu\text{-SR})_6(HgX)_{4-n}$

$(MX)_n]^{2-}$ (M = Zn or Cd), a total of four ^{199}Hg NMR resonances are expected, corresponding to a total of four Hg-containing species (n = 0-3) On the other hand, a total of four $^{111/113}$Cd NMR resonances are expected also when M = Cd, corresponding to n = 1-4. From our measured ^{199}Hg and ^{111}Cd NMR spectra, all expected metal signals are indeed observed. Therefore, the formulation of $[(\mu\text{-SR})_6(HgX)_4]^{2-}$ for those complexes isolated or prepared in situ (see above) is proved. The structures of these mixed-metal clusters have been discussed in Section 1.6 and shown in Fig. 1 4. Metal NMR data for the various complexes $[(\mu\text{-SR})_6(HgX)_{4-n}(MX)_n]^{2-}$ are included in Table 4 3 and typical examples of ^{199}Hg and ^{111}Cd NMR spectra are shown in Figs. 4 3 and 4 4.

In the ^{199}Hg NMR spectra of Hg_4/Zn_4 mixtures (*e.g.* Fig. 4 3a), the intensity ratio of four signals is normally about 1:3:3:1, corresponding to the process shown in eqn. [7].

[7] $\quad 8\ Hg_4 + 8\ Zn_4 \rightleftharpoons Hg_4 + 4\ Hg_3Zn + 6\ Hg_2Zn_2 + 4\ HgZn_3 + Zn_4$

This is the result expected if the redistribution occurs statistically (see Section 1 6 for details). Mixtures of Hg_4/Cd_4 normally redistribute statistically also as confirmed by both ^{199}Hg and ^{111}Cd NMR (*e.g.* Figs. 4.3b and 4.4a). Most ^{199}Hg NMR spectra of Hg_4/M_4 are similar to Figs. 4.3a and 4.3b, but it is still worthwhile to indicate that in some cases redistribution appears not to occur statistically. This may be due to solubility problems or one kind of species may indeed be more stable than the others in solution

As can be seen from Figs. 4.3 and 4.4 and Table 4.3, increasing substitution of Zn for Hg in $[(\mu\text{-SR})_6(HgX)_4]^{2-}$ causes increasing shielding of the ^{199}Hg signal of the remaining mercury nuclei (Fig. 4 3a). That is also true of $^{111/113}$Cd for Cd_4/Zn_4 mixtures

Table 4.3 NMR Data for $[(\mu\text{-SR})_6(HgX)_{4-n}(MX)_n]^{2-}$ (M = Zn,Cd) in CH_2Cl_2 [a]

R	X	M	*n*	δ_{Hg} [b]	δ_{Cd} [c]	$^2J(^{111}Cd\text{-}^{199}Hg)$ [d]
Et	I	Zn	0	-830		
			1	-844		
			2	-858		
			3	-873		
		Cd	0	-828		
			1	-811	571	142
			2	-794	575	140
			3	-776	579	[e]
			4		584	
	Br	Zn	0	-602		
			1	-610		
			2	-615		
			3	-618		
		Cd	0	-602		
			1	-592	594	
			2	-581	599	111[f]
			3	-570	603	113[f]
			4		607	
Pr[i]	I	Zn	0	-904		
			1	-946		

Table 4.3 (Continued)

R	X	M	*n*	δ_{Hg}[b]	δ_{Cd}[c]	$^2J(^{111}Cd\text{-}^{199}Hg)$[d]
			2	-984		
			3	-1005		
		Cd	0	-905		
			1	-889	534	146
			2	-869	538	139
			3	-848	543	119
			4		549	
	Br	Zn	0	-657		
			1	-678		
			2	-695		
			3	-714		
		Cd	0	-654		
			1	-647	572	96
			2	-638	575	104
			3	-627	579	116
			4		583	
Bu^n	I	Zn	0	-839		
			1	-855		
			2	-873		
			3	-892		
		Cd	0	-840		

Table 4 3 (Continued)

R	X	M	*n*	δ_{Hg} [b]	δ_{Cd} [c]	$^{2}J(^{111}Cd\text{-}^{199}Hg)$ [d]
			1	-823	566	153[f]
			2	-806	570	144
			3	-789	574	131
			4		578	

[a] Data measured at 213 K and concentration (at room temperature) = 0.05 mol/L of solvent, except as noted.

[b] Relative to external pure $HgMe_2$ at 295±1 K; reproducibilty ±1 ppm.

[c] Measured as ^{111}Cd relative to external $Cd(ClO_4)_2$ (0.1M, aq) at 293±1 K; reproducibilty ±1 ppm.

[d] Estimated error 5 Hz.

[e] Not well resolved.

[f] At 193 K.

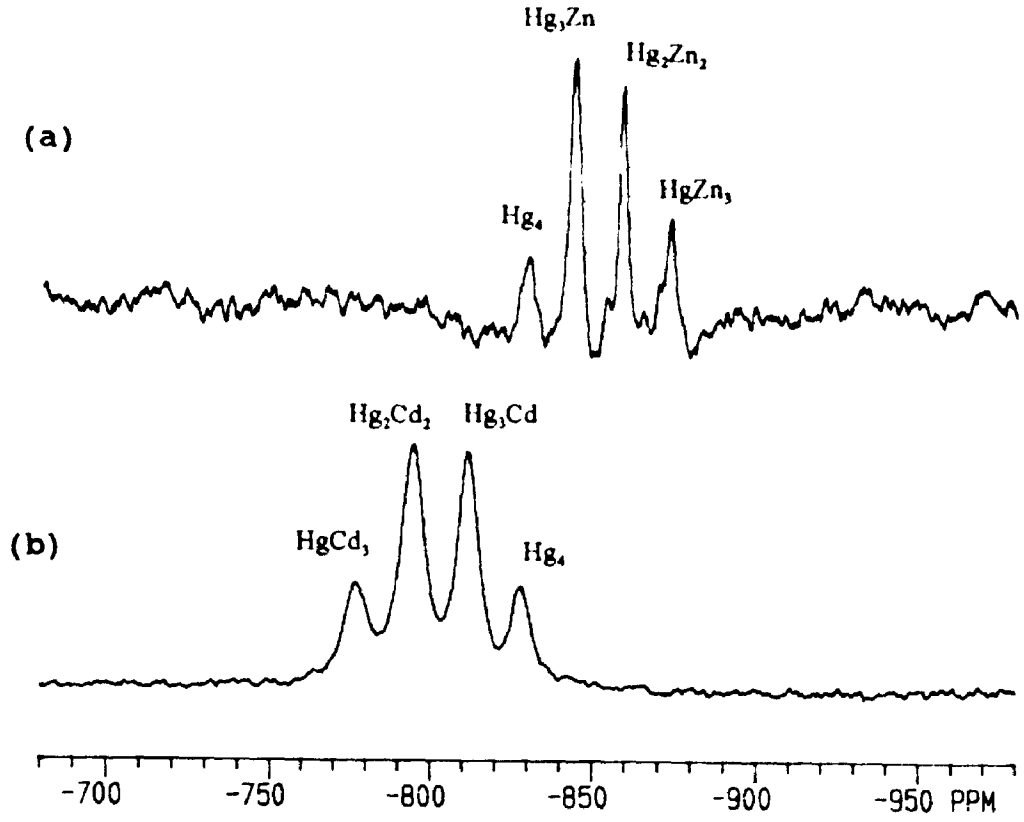

Fig. 4.3 ^{199}Hg NMR spectra of $[(\mu\text{-}SEt)_6(HgI)_{4-n}(MI)_n]^{2-}$ in CH_2Cl_2 at 213K, (a) M = Zn; (b) M = Cd.

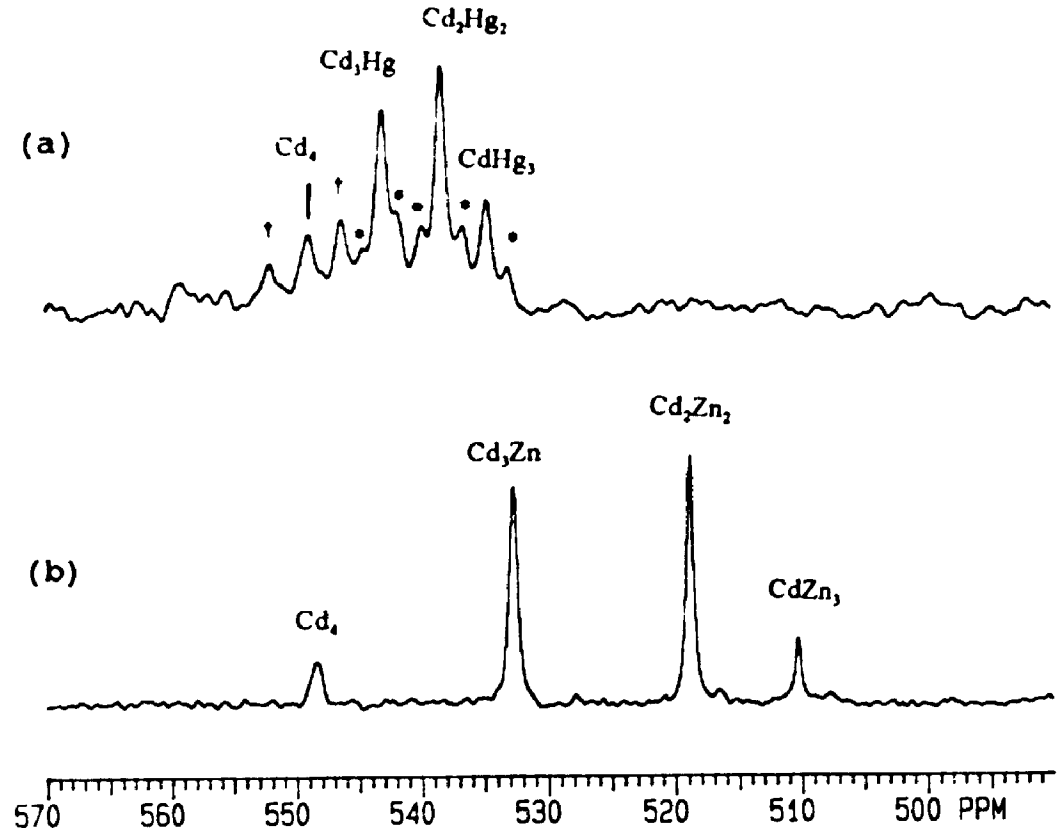

Fig. 4 4 ^{111}Cd NMR spectra of $[(\mu\text{-}SPr^i)_6(CdI)_{4-n}(MI)_n]^{2-}$ in CH_2Cl_2, (a) M = Hg, at 213K; (b) M = Zn, at 218K.

* Satellites due to $^2J(^{111}Cd\text{-}^{199}Hg)$. † Unknown signal.

(Fig. 4.4b, and see Chapter 2 for details). The more the Zn substitution for Cd, the more the shielding of the cadmium signal for the remaining Cd nuclei. But for Hg_4/Cd_4 mixtures, increasing substitution of Cd for Hg produces increasing *de*shielding of ^{199}Hg signal (Fig. 4.3b). On the other hand, increasing substitution of Hg for Cd still results in increasing shielding of $^{111/113}Cd$ (Fig. 4.4a). These observations are general for all Hg_4/M_4 mixtures (Table 4.3).

As can be seen from Table 4.3, the chemical shifts between adjacent Hg signals do not have to be equally spaced. This depends on the properties of the substituting metals, bridging ligands, and terminal ligands. For example, when R = Pr^i, X = I, and M = Zn, the values of $\Delta_{0,1}$ ($\Delta_{0,1}$ stands for $\delta_{n-0} - \delta_{n-1}$), $\Delta_{1,2}$ and $\Delta_{2,3}$ are 42, 38 and 21ppm, respectively; while the corresponding changes when M = Cd are 16, 20 and 21 ppm, respectively. From Table 4.3, it is evident that the properties of halogen dependence and thiolate dependence can also be seen here from ^{199}Hg chemical shift change between the parent Hg_4 species and those M-substituted species (M = Zn or Cd). In general, the magnitude of substitution effect varies with X in the order I > Br, and with R in the order Pr^i > *n*-alkyl. For example, if R = Pr^i and M = Zn, when X = I, $\Delta_{0,3}$ = 101ppm; while when X = Br, $\Delta_{0,3}$ = 57ppm. On the other hand, if X = I and M = Zn, when R = Pr^i, $\Delta_{0,3}$ = 101ppm; while when R = Et, $\Delta_{0,3}$ = 43ppm.

For the clusters $[(\mu\text{-}SR)_6(HgX)_4]^{2-}$ discussed above, the four Hg atoms are chemically equivalent, and thus no $^2J(^{199}Hg\text{-}^{199}Hg)$ is expected. However, it is different for the mixed-metal system $[(\mu\text{-}SR)_6(HgX)_{4-n}(MX)_n]^{2-}$. When the substituting metals are Cd, the two-bond $^{111/113}Cd\text{-}^{199}Hg$ coupling is expected. Some of these couplings have been observed, particularly from ^{111}Cd NMR spectra where the signals are relatively sharper.

These ^2J values are included in Table 4.3. When the substituting metals are Zn, of course no $^2J(^{67}Zn\text{-}^{199}Hg)$ coupling is expected, because ^{67}Zn is a quadrupolar nucleus and relaxes rapidly. As can be seen from Table 4.3, the $^2J(^{111}Cd\text{-}^{199}Hg)$ values are influenced by X in the order I > Br. As well the ^2J values are affected by *n* values. It is interesting that ^2J varies with *n* in the order 1 > 2 > 3 when X = I, but in the order 3 > 2 > 1 when X = Br.

It may be worthwhile to mention here that mixtures of terminal ligands have been tried also. The ^{199}Hg NMR spectra show the expected two groups of signals corresponding to Hg-X and Hg-X', but the fine structure from different $[(\mu\text{-SR})_6(HgX)_{4-n}(CdX')_n]^{2-}$ are not well resolved (see Sections 1.6 and 2.3.2(ii) for details). The reason for this is not clear.

(iii) $[(\mu\text{-SR})_{6-m}(\mu\text{-X})_m(HgX)_4]^{2-}$ (m = 1 or 2)

As we mentioned above in Section 4.3.2(i), the measured ^{199}Hg NMR spectra for $[Hg_4(SPr^i)_6X_4]^{2-}$ show an additional weak signal in a more shielded region. At first, this was puzzling. Tentatively it was thought that it might be due to a "terminal-empty" species, such as $[(\mu\text{-}SPr^i)_6(HgX)_3(Hg)]^{2-}$ [12]. In practice, the signal is diminished as expected from the tentative explanation when more halide is added to the solution. (Actually, this is due to a process which has been shown in eqn. [2b].) However, other evidence, particularly the X-ray analysis of $(Ph_4P)_2[(\mu\text{-SEt})_5(\mu\text{-Br})(HgBr)_4]$, points to its being due to a new kind of cluster with one halide as bridging ligand.

Proton and ^{13}C NMR spectra are measured for all isolated $[(\mu\text{-SR})_{6-m}(\mu\text{-X})_m(HgX)_4]^{2-}$ (m = 1 or 2) clusters and all these data have been listed in Table 4.1. The

difference from those parent clusters (m = 0) is only that the ^1H signals of R group are relatively weaker when m = 1 or 2. The intensity ratio of cation:SR^- can be used as an estimate of the stoichiometry. The evidence in support of the new complexes comes from elemental analysis and, more importantly, ^{199}Hg NMR measurement.

Mercury-199 NMR spectra have been measured for various $[(\mu\text{-}SR)_{6-m}(\mu\text{-}X)_m(HgX)_4]^{2-}$ (m = 1 or 2; isolated or prepared in situ). The data are listed in Table 4 4. Spectra of the system $HgBr_2$:$Hg(SPr^i)_2$:$(Ph_4P)Br$ (particularly well resolved) are shown in Fig. 4.5. A lot of structural information about the *m* = 1 clusters can be obtained by the analysis of Fig. 4.5b. First, the spectrum consists of two major signals (-649 and -863 ppm): one is very close to that of parent $[(\mu\text{-}SR)_6(HgBr)_4]^{2-}$, and the other is more shielded. This indicates that there are two types of Hg kernels: one is HgS_3Br, and the other is probably HgS_2Br_2. For the convenience of spectrum analysis, here let the less shielded signal be assigned to Hg_a and the more shielded one to Hg_b. Second, the two major lines have the approximately equal intensity, which suggests that Hg_a and Hg_b have the same number of atoms in the complex. Third, both signals show satellite splitting with coupling magnitude 533±5 Hz. The coupling pattern here must be due to ^{199}Hg-^{199}Hg coupling, and in the adamantane-like skeleton it is a two-bond coupling. Based on the analysis above, the major species shown in Fig. 4.5b is considered to be $[(\mu\text{-}SR)_5(\mu\text{-}Br)(HgBr)_4]^{2-}$ with the skeleton **II** in Fig. 4.1. From this model, one bridging Br causes two types of chemically inequivalent Hg with equal numbers (two Hg_a and two Hg_b), and consequently two-bond Hg-Hg coupling becomes possible.

The formulation and assignment is also confirmed by a ^{199}Hg NMR spectrum obtained without ^1H decoupling. As can be seen from Fig. 4.6a, there is a triplet splitting

Table 4.4 ^{199}Hg NMR Data for $[(\mu\text{-}SR)_{6-m}(\mu\text{-}X)_m(HgX)_4]^{2-}$ in CH_2Cl_2 at 183 K[a]

R	X	δ_{Hg}			
		m = 0	m = 1		m = 2
			Hg_a[b]	Hg_b[b]	
Cy[c]	I	-880	-887	-1306	-1342
	Br	-642	-652	-858	-894[d,e]
	Cl	-527	-534[d]	-694[d]	[f]
Pr^i	I[g]	-887	-884	-1340	-1370
	Br[g]	-643	-649[h]	-863[h,i]	-896
	Cl[j]	-528	-534	-693	-722
Et	I[g]	-810	-842	-1240	-1320[d,k]
	Br[g]	-587	-618	-822	-904[d]
	Cl[j]	-482	-517[d]	-690[d]	[f]
Bu^n	I[g]	-821	-857	-1224	-1312

[a] Relative to external pure $HgMe_2$ at 295±1 K; reproducibilty ±1 ppm. Concentration (at room temperature) 0.05 mol/L of solvent, except as noted.

[b] See structure II.

[c] Cation: $Bu^n{}_4N^+$.

[d] In a mixture solution prepared in situ, insoluble white material was present.

[e] $[(\mu\text{-}SCy)_5(\mu\text{-}Br)(HgBr)_4]^{2-}$:*trans*-$[(\mu\text{-}SCy)_4(\mu\text{-}Br)_2(HgBr)_4]^{2-} \approx 1:1$.

[f] Insufficient solubility for ^{199}Hg NMR.

Table 4.4 (*Continued*)

[g] Cation: Ph_4P^+.

[h] $^2J(Hg_a\text{-}Hg_b) = 533\pm5$ Hz.

[i] $^3J(Hg_b\text{-}S\text{-}C\text{-}H) \approx 102$ Hz (see Fig. 4.6 and discussion below).

[j] Cation: Ph_4As^+.

[k] $[(\mu\text{-}SEt)_5(\mu\text{-}I)(HgI)_4]^{2-}$:*trans*-$[(\mu\text{-}SEt)_4(\mu\text{-}I)_2(HgI)_4]^{2-} \approx 2:1$.

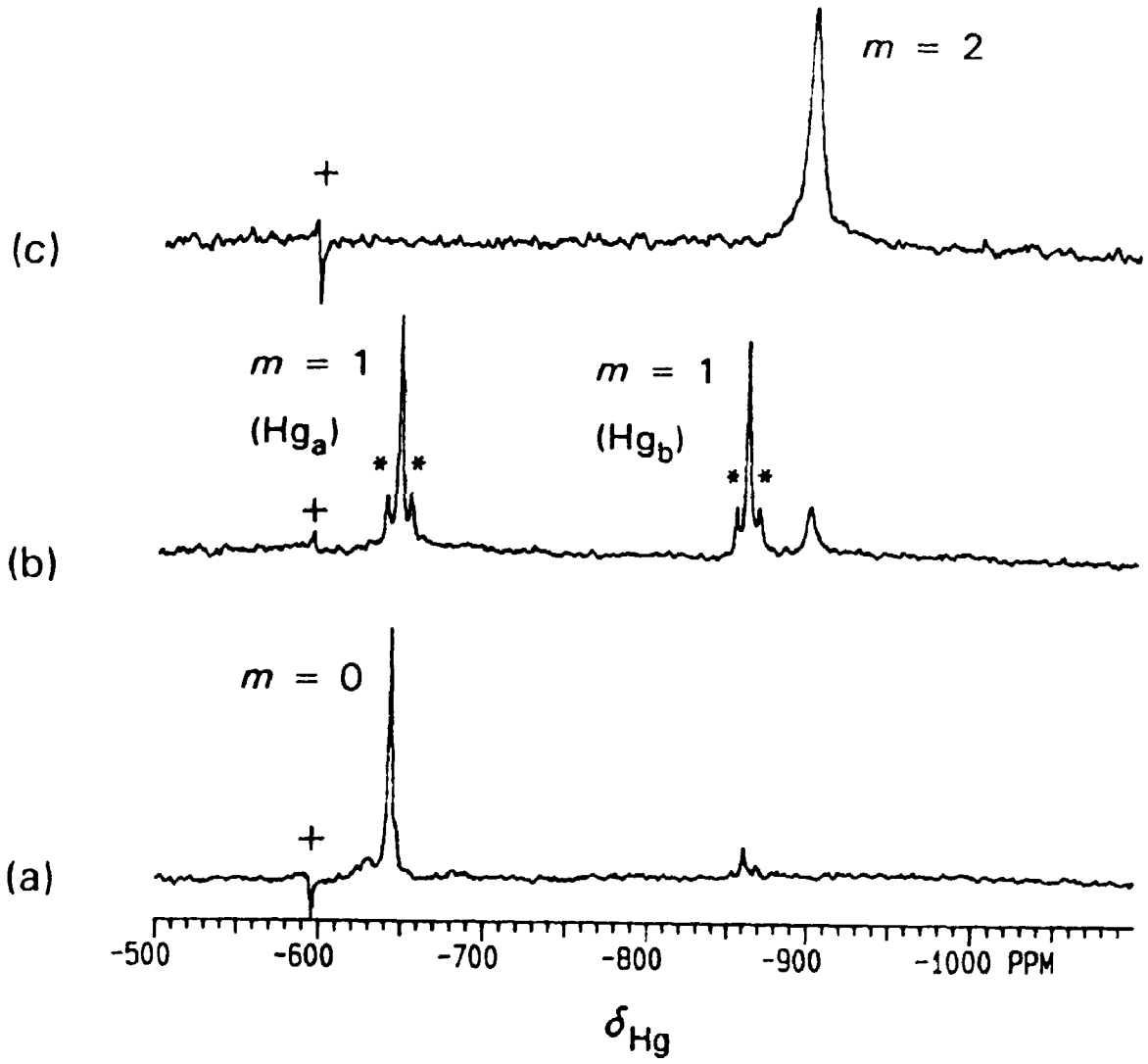

Fig. 4.5 ^{199}Hg-{^{1}H} NMR Spectra of $HgBr_2$:$Hg(SPr^i)_2$:$(Ph_4P)Br$ Mixtures in CH_2Cl_2 at 183 K, showing the formation of $[(\mu\text{-}SPr^i)_{6-m}(\mu\text{-}Br)_m(HgBr)_4]^{2-}$, (a) m = 0; (b) m = 1; (c) m = 2. * = ^{199}Hg satellite; + = artifact. [13]

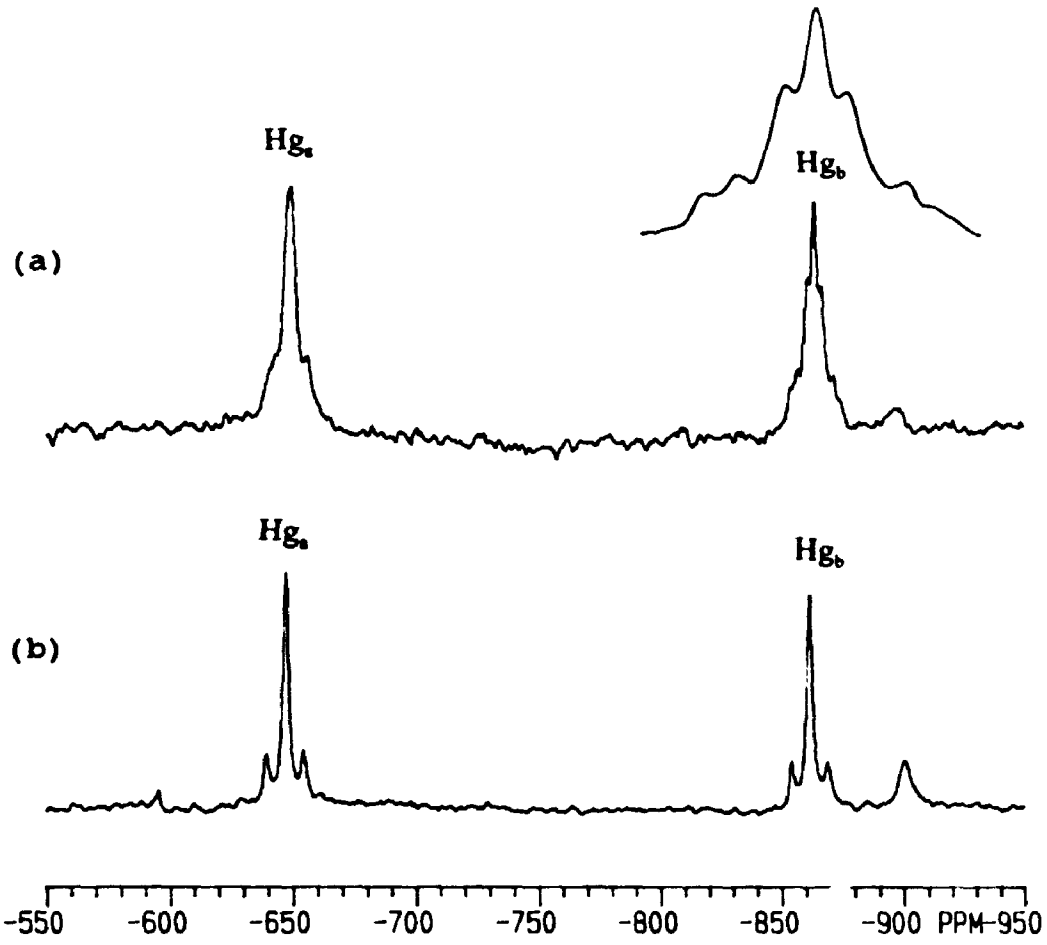

Fig. 4.6 ^{199}Hg NMR spectra of $[(\mu\text{-SPr}^i)_5(\mu\text{-Br})(HgBr)_4]^{2-}$ in CH_2Cl_2 at 183 K, (a) without proton decoupling; (b) with proton decoupling (same spectrum of Fig. 4.5b; shown here for comparison).

for the resonance of Hg_b, which is due to ^3J(Hg-S-C-H) and indicates two attached SPr^i ligands. In addition, the assignment for Hg_a and Hg_b is supported by the known ^{199}Hg NMR data of $Hg(SR)_4^{2-}$ [14a] and HgX_4^{2-} [14b]. For example, the δ_{Hg} for $Hg(SPr^i)_4^{2-}$ is -275 ppm at 297K which has been converted from Ref. [14a] by using $\delta_{Hg}(HgMe_2$, external) = δ_{Hg}(0.1M $Hg(ClO_4)_2$, external) - 2253 ppm, and for $HgBr_4^{2-}$ is -1817 ppm at 163 K which has been converted from Ref. [14b] by using $\delta_{Hg}(HgMe_2$, external) = δ_{Hg}(1M $HgPh(MeCO_2)$, external) - 1437 ppm. According to these two values of $Hg(SPr^i)_4^{2-}$ and $HgBr_4^{2-}$, we could assume that the Hg shielding with different kernels is in the order: $S_3HgBr > S_2BrHgBr > SBr_2HgBr$, and based on first order additivity of substituent effects, the δ_{Hg} of these three kernels should fall in the three approximate regions of -660, -1050 and -1430 ppm, respectively. In the real spectrum of $[(\mu\text{-}SPr^i)_5(\mu\text{-}Br)(HgBr)_4]^{2-}$, the δ_{Hg} of site Hg_a is -649 ppm which is in good with the estimated value, but the δ_{Hg} of site Hg_b is -863 ppm which is only half way to the estimated value (-1050 ppm). However, this is not surprising, because the chemical shift may not show first order additivity of substituent effects. Although there is a relatively large difference between real and estimated values of $\delta(Hg_b)$, the correct *sequence* is still shown. Therefore the assignments for Hg_a and Hg_b are quite reasonable.

It can be seen from Table 4.4, that in $[(\mu\text{-}SR)_5(\mu\text{-}X)(HgX)_4]^{2-}$, both ^{199}Hg signals show the property of NHD[11], *i.e.* mercury nuclear shielding varies with X in the order I > Br > Cl. It is interesting that the separation of the two signals shows the same order also. For example, if R = Pr^i and m = 1, the δ_{Hg}(X = I) = (-884) - (-1340) = 465 ppm is larger than δ_{Hg}(X = Br) = (-649) - (-863) = 214 ppm. The property of NHD has been found for the $^{111/113}$Cd nucleus in $[(\mu\text{-}SPh)_6(CdX)_4]^{2-}$ (X = SPh, Cl, Br, or I) system[15].

When the terminal SPh is replaced by halides, the Cd shielding varies in the order I > Br > Cl. Thus it is reasonable that when the bridging μ-SR is replaced by μ-X, the same sequence occurs for Hg shielding in our $[(\mu\text{-SR})_{6-m}(\mu\text{-X})_m(HgX)_4]^{2-}$ system.

In Fig. 4.5b(m = 1), besides two strong lines (due to Hg_a and Hg_b), there is an extra weak line at the most shielded position (due to $[Hg_4(SR)_4X_6]^{2-}$ species). More experiments were carried out in which reduced temperature ^{199}Hg NMR spectra of $[Hg_4(SR)_4X_6]^{2-}$ were measured using isolated material or material produced in situ (eqn. [4]). These give just one ^{199}Hg NMR line (Table 4.4 and Fig.4.5c). This resonance is adjacent to that of Hg_b of $[(\mu\text{-SR})_5(\mu\text{-X})(HgX)_4]^{2-}$ (Fig.4.5b), indicating the same kernel S_2XHgX if we neglect the slight difference between Hg_b and Hg_c (see Fig. 4.1, skeletons II and IIIa). For clusters $[(\mu\text{-SR})_4(\mu\text{-X})_2(HgX)_4]^{2-}$, there are two possible structures (cis and trans; see IIIa and IIIb). In the trans-structure, all four Hg atoms are identical, with same coordination environment. Thus the ^{199}Hg NMR should show only one line, as found experimentally. If the cluster had structure IIIb, there should be three kinds of mercury: Hg_d, Hg_e and Hg_f. The chemical shifts for Hg_d is expected to occur in the same region as that for Hg_a. Similarly, the Hg_e is close to Hg_b or Hg_c. The Hg_f has a new kernel SX_2HgX, and the chemical shift should be at more shielded position than the others, perhaps in the range of -1000 to -1400 ppm for R = Pr^i and X = Br (see discussion above about $Hg(SPr^i)_4^{2-}$ and $HgBr_4^{2-}$). The intensity ratio of these three signals should be 1:2:1. In no experiments have the ^{199}Hg NMR signals for Hg_d and Hg_f ever been observed. Therefore, we have confidence in assigning the ^{199}Hg NMR singlet to *trans*-$[(\mu\text{-SR})_4(\mu\text{-X})_2(HgX)_4]^{2-}$, with structure IIIa.

It is not certain yet why the clusters $[(\mu\text{-SR})_4(\mu\text{-X})_2(HgX)_4]^{2-}$ prefer to form the trans-structure. For random distribution, the two bridging halides could be either in cis- or in trans-form and the probability of formation of the cis-structure should be larger than that of trans. The ratio is calculated to be 4:1 (see Section 1.6 for calculation details). Thus the trans-structure must have special stability. However, no such a trans-cluster of zinc group metals has been crystallographically determined. Single crystal growth has been tried during this work, but with no success yet. Two *similar* trans structures are crystallographically characterized. They both involve compounds of group III metals: $[(\mu\text{-SMe})_4(\mu\text{-S})_2(GaI)_4]$ [16] and $[(\mu\text{-SMe})_4(\mu\text{-S})_2(AlI)_4]$ [17]. In these, the two bridging S^{2-} ligands take opposite positions in the adamantanoid skeleton, forming the trans-structure. There is no other suitable crystal structure for illustrating our proposed structure.

4.3.3 Crystal structures

(i) $(Ph_4P)_2[(\mu\text{-SEt})_5(\mu\text{-Br})(HgBr)_4]$

This crystal structure determination confirms the existence of the halide-bridged clusters which have been identified by synthesis and multi-NMR also. The crystal structure has well-separated anion and cations. The geometry of PPh_4^+ cations is not important here and thus will not be discussed further. The structure of the anion $[(\mu\text{-SEt})_5(\mu\text{-Br})(HgBr)_4]^{2-}$ is shown in Fig. 4.7. Selected bond distances and angles are listed in Table 4.5.

As can be seen from Fig. 4.7 and Table 4.5, the structure of the anion is adamantane-like, but distorted. As well as five S atoms taking the bridging positions as usual, one Br atom also occupies such a position, which is the infomation most wanted.

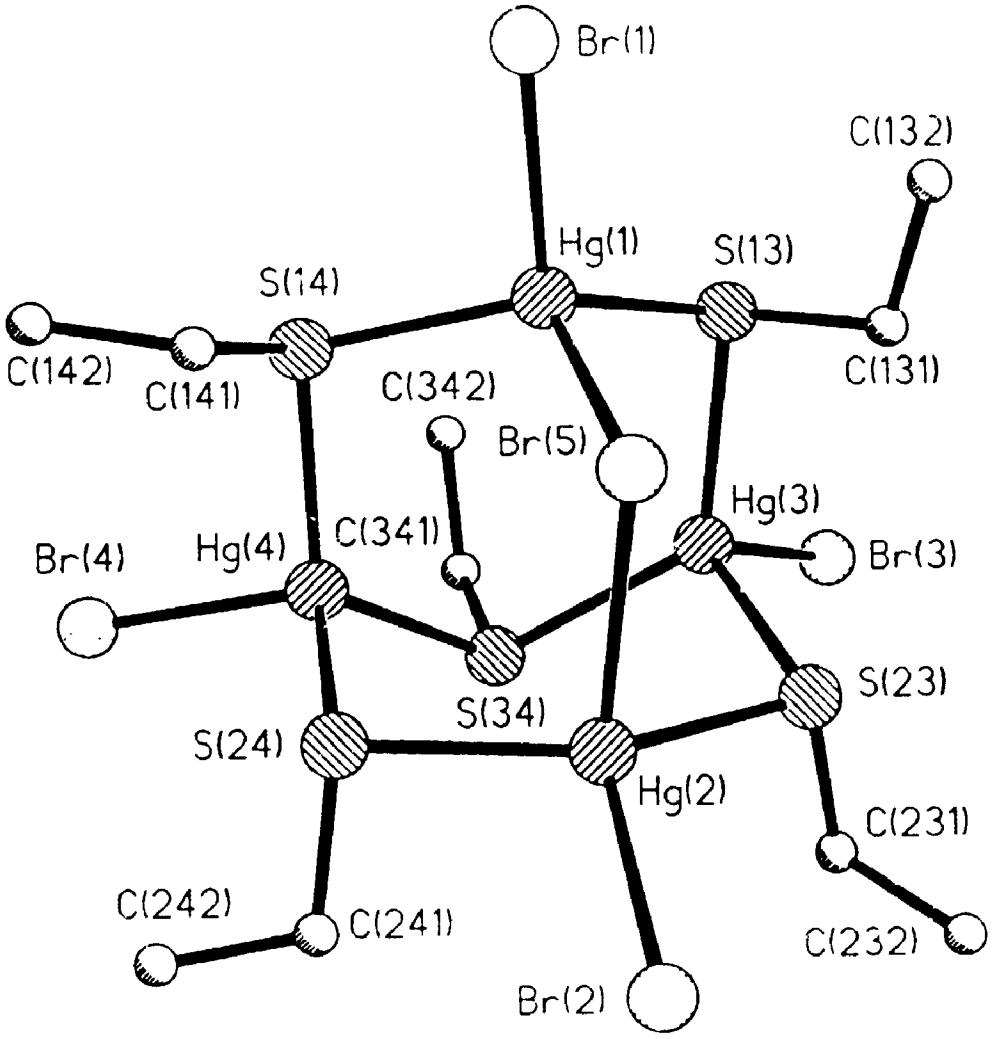

Fig 4 7 The structure of $[(\mu\text{-SEt})_3(\mu\text{-Br})(HgBr)_4]^{2-}$ in $(Pn_4P)_2[(\mu\text{-SEt})_3(\mu\text{-Br})(HgBr)_4]$[13]

Table 4 5 Selected Bond Distances (Å) and Angles (°) in $(Ph_4P)_2$ $[(\mu\text{-}SEt)_3(\mu\text{-}Br)(HgBr)_4]$

Hg(1)-Br(1)	2.628(5)	Hg(2)-Br(2)	2.643(5)
Hg(3)-Br(3)	2.619(5)	Hg(4)-Br(4)	2.616(5)
Hg(1)-Br(5)	2.733(6)	Hg(2)-Br(5)	2.902(7)
Hg(1)-S(13)	2.467(11)	Hg(1)-S(14)	2.483(11)
Hg(2)-S(23)	2.408(15)	Hg(2)-S(24)	2.435(13)
Hg(3)-S(13)	2.518(12)	Hg(3)-S(23)	2.573(15)
Hg(3)-S(34)	2.497(12)	Hg(4)-S(14)	2.518(12)
Hg(4)-S(24)	2.611(14)	Hg(4)-S(34)	2.492(13)
S(13)-C(131)	1.804(10)	S(14)-C(141)	1.805(10)
S(23)-C(231)	1.795(10)	S(24)-C(241)	1.804(10)
S(34)-C(341)	1 804(10)		

Br(5) -Hg(1)-Br(1)	96.5(2)	Br(5) -Hg(2)-Br(2)	111.3(2)
S(13) -Hg(1)-Br(1)	115.7(3)	S(13) -Hg(1)-Br(5)	107.9(3)
S(14) -Hg(1)-Br(1)	105.1(3)	S(14) -Hg(1)-Br(5)	111.6(3)
S(23) -Hg(2)-Br(2)	108 3(4)	S(23) -Hg(2)-Br(5)	91.7(5)
S(24) -Hg(2)-Br(2)	101 6(3)	S(24) -Hg(2)-Br(5)	93.5(5)
S(13) -Hg(3)-Br(3)	107 2(3)	S(23) -Hg(3)-Br(3)	113.1(4)
S(34) -Hg(3)-Br(3)	102.4(3)	S(14) -Hg(4)-Br(4)	103.8(3)

Table 4.5 (Continued)

S(24) -Hg(4)-Br(4)	111.4(3)	S(34) -Hg(4)-Br(4)	108 7(3)
S(14) -Hg(1)-S(13)	118.0(4)	S(24) -Hg(2)-S(23)	145 3(5)
S(23) -Hg(3)-S(13)	104.0(6)	S(34) -Hg(3)-S(13)	126 0(4)
S(34) -Hg(3)-S(23)	104.4(5)	S(24) -Hg(4)-S(14)	103 0(5)
S(34) -Hg(4)-S(14)	120.3(4)	S(34) -Hg(4)-S(24)	109.5(5)
Hg(2) -Br(5)-Hg(1)	100.0(2)	Hg(3) -S(13)-Hg(1)	100 5(4)
Hg(4) -S(14)-Hg(1)	103.5(4)	Hg(3) -S(23)-Hg(2)	101.6(5)
Hg(4) -S(24)-Hg(2)	97.9(5)	Hg(4) -S(34)-Hg(3)	105.9(5)
C(131)-S(13)-Hg(1)	101.5(17)	C(131)-S(13)-Hg(3)	98.6(10)
C(141)-S(14)-Hg(1)	100.1(12)	C(141)-S(14)-Hg(4)	103.9(19)
C(231)-S(23)-Hg(2)	104.3(20)	C(231)-S(23)-Hg(3)	98.3(15)
C(241)-S(24)-Hg(2)	96.4(17)	(24 --S(24)-Hg(4)	110.8(19)
C(341)-S(34)-Hg(3)	101.3(17)	C(341)-S(34)-Hg(4)	106.4(17)

Each of four Hg atoms has a tetrahedral coordination kernel: half have HgS_3Br kernels and half have HgS_2Br_2 kernels. Configurational isomerism is possible (see Section 1.3 for details) in $[(\mu\text{-SEt})_5(\mu\text{-Br})(HgBr)_4]^{2-}$, although there are only five SR bridging ligands. In this crystal structure, the configuration of the R groups on the S atoms is [aae, aee, ae, ae], which is a quasi-isomer III. If the μ-Br is substituted by μ-SR, the configuration goes back to isomer III, *i.e.* [aae, aee, aae, aee].

The $Hg\text{-}Br_t$ distances (2.616 - 2.645(5) Å) in this tetranuclear cluster are comparable to the terminal Br-Hg distances (2.542 - 2.650(5) Å)[18,19] reported for the mononuclear complex $[HgBr_4]^{2-}$. The unsymmetrical $Hg\text{-}Br_{br}$ distances of 2.733(6) and 2.902(7) Å are somewhat longer than the $Hg\text{-}Br_t$ distances. An analogous result is found in $(Et_4N)_2[(\mu\text{-I})(\mu\text{-SPr})(HgI_2)_2]$ (see below). The range of the $Hg\text{-}S_{br}$ distances is from 2.408(15) to 2.611(14) Å, that of the Hg...Hg distances is from 3.807(3) to 4.319(3) Å, that of the S-Hg-S angles is from 103.0(5) to 145.3(5)°, and that of the Hg-S-Hg angles is from 97.9(5) to 105.9(5)°. All these range variations for $[(\mu\text{-SEt})_5(\mu\text{-Br})(HgBr)_4]^{2-}$ are larger than those for $[(\mu\text{-SPh})_6(HgPPh_3)_4]^{2+}$ [3] (2.523(5) - 2.616(5) Å, 4.293(1) - 4.390(1) Å, 98.4(2) - 110.6(2)°, and 113.2(2) - 117.2(2)°, respectively). Thus, larger distortion from the ideal adamantanoid skeleton occurs in the new cluster, which is due to the introduction of one bridging Br atom into the adamantanoid core.

(ii) $(Et_4N)_2[(\mu\text{-I})(\mu\text{-SC}_3H_7)(HgI_2)_2]$

The crystal structure consists of discrete anion and cations. A skeletal view of the dimeric anion, with selected bond distances and angles, is given in Fig. 4.8. Three significant points about this structure are particularly noteworthy. First, the SPr^n prefers

Hg-I(1)	2 944(2)	Hg-I(2)	2 712(2)	Hg-I(3)	2 743(2)
Hg-S	2 530(7)				
S-C(1)	1 79(4)				
I(1)-Hg-I(2)	106 72(7)	I(1)-Hg-I(3)	102 82(7)	I(2)-Hg-I(3)	119 66(7)
I(1)-Hg-S	95 7(2)	I(2)-Hg-S	115 6(2)	I(3)-Hg-S	112 3(2)
Hg-I(1)-Hg^a	74 96(6)	Hg-S-Hg^a	90 2(3)	Hg-S-C(1)	100 8(10)
S-C(1)-C(2)	111(3)				

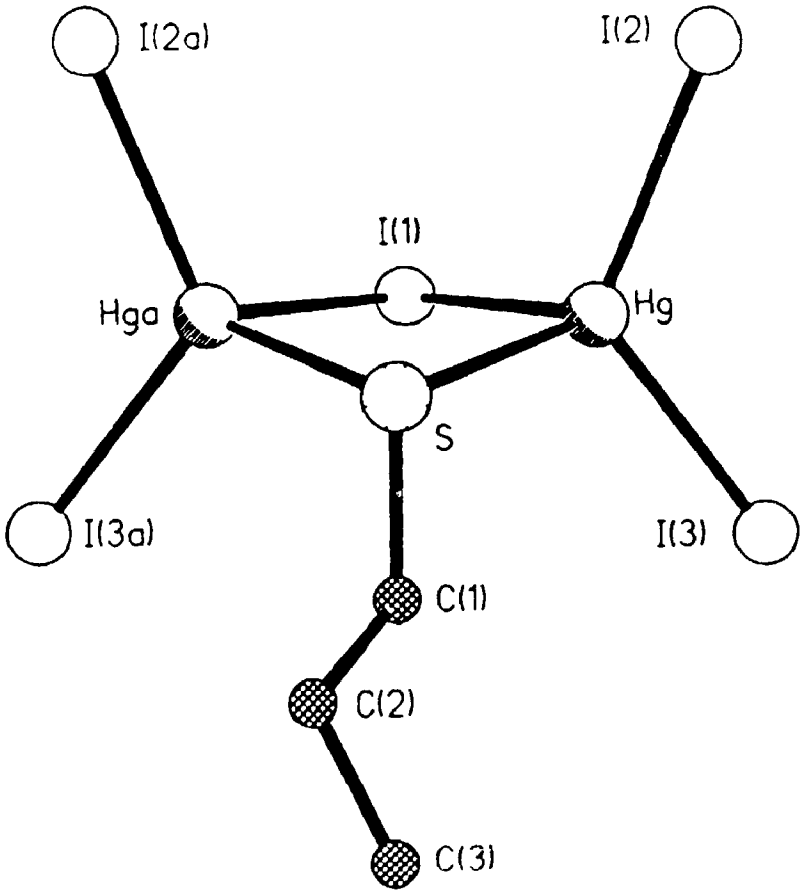

Fig. 4 8 A view of $[(\mu\text{-SPr})(\mu\text{-I})(HgI_2)_2]^{2-}$ in $(Et_4N)_2[(\mu\text{-SPr})(\mu\text{-I})(HgI_2)_2]$ with selected bond distances (Å) and angles (°). [13]

to be a bridging as opposed to a terminal ligand. Second, the bond length of Hg-I_{br} is larger than that of Hg-I_t, as expected. Third, the four-member ring $Hg_2I_{br}S_{br}$ has a "butterfly" conformation, with a dihedral angle of 159.2° between the $HgI_{br}S_{br}$ and $Hg'I_{br}S_{br}$ planes. The formation of the dimer provides a better understanding of the cluster dissociation (see discussion above).

4.4 Conclusions

In this chapter, the anions $[(\mu\text{-SAlk})_6(HgX)_4]^{2-}$ have been studied in detail. Importantly, during the course of this work, a new series of clusters $[(\mu\text{-SAlk})_{6-m}(\mu\text{-X})_m(HgX)_4]^{2-}$ (m = 1 or 2) has been found. Overall, a total of 14 new clusters have been isolated microanalytically pure by the self-assembly method. This is the first report of the isolation of such clusters. The synthetic product is sensitive to the different conditions, such as cations, halides, solvents, concentrations, *etc.*

NMR, especially metal NMR, has proved very helpful for this study. For the non-halide-bridged series (m = 0), more than 40 species of formula $[(\mu\text{-SAlk})_6(HgX)_{4-n}(MX)_n]^{2-}$ (M = Zn or Cd) has been produced in situ and characterized by ^{199}Hg and (where appropriate) $^{111/113}Cd$ NMR. In this way a great deal of information about direction and quantity of mixed-metal clusters has been obtained relating to metal redistribution, substitution effects on the nuclear shielding, *etc.* In addition, the nature of the anions in isolated compounds has also been verified by these metal NMR results, *i.e.* confirmation has been obtained that the single ^{199}Hg resonance found for the parent compound really is due to the tetranuclear cluster. For the halide-bridged series (m = 1 or 2), the ^{199}Hg NMR results have shown that these novel species are stable in solution and that the

complex with m = 2 has the trans structure. It is observed that the more shielded signal corresponding to the HgS_2X_2 kernel indicates the presence of clusters with m = 1 or 2 The isolated compounds have again been authenticated by comparison of the identical ^{199}Hg NMR spectra found for the anion prepared in situ and that from the isolated product.

Finally, the structure of $(Ph_4P)_2[(\mu\text{-}SEt)_5(\mu\text{-}Br)(HgBr)_4]$ has been determined by the single crystal X-ray diffraction method. This is the first reported crystal structure of a $(\mu\text{-}ER)_5(\mu\text{-}X)M_4$ cage. In this compound, the tetranuclear anion contains a highly distorted adamantane-like core with five sulfur atoms and one bromine atom in the bridging positions. The ethyl groups attached to the sulfur atoms have the configuration of [aae, aee, ae, ae] which is a quasi-isomer III structure. As a bonus, another single crystal structure, that of $(Et_4N)_2[(\mu\text{-}SPr)(\mu\text{-}I)(HgI_2)_2]$ has been determined. The occurrence of this dinuclear anion may help provide a better understanding of the dissociation of the tetranuclear complexes.

4.5 References

1. P.A. W. Dean and J.J. Vittal, In *Metallothioneins*, M.J. Stillman, C.F. Shaw III, and K.T. Suzuki, Eds., VCH, New York, 1992, Chapter 14.
2. P.A.W. Dean, J.J. Vittal, and M.H. Trattner, *Inorg. Chem.*, 26, (1987) 4245
3. J.J. Vittal, P.A.W. Dean, and N.C. Payne, Unpublished results quoted in Ref. 1
4. M.J. Stillman, In *Metallothioneins*, M.J. Stillman, C.F. Shaw III, and K.T. Suzuki, Eds., VCH, New York, 1992, Chapter 4.
5. P.A.W. Dean and V. Manivannan, *Inorg. Chem.*, 29 (1990) 2997

6 P A W Dean and J.J Vittal, Unpublished results quoted in Ref. 1.

7 E Wertheim, *J. Am. Chem Soc.* 51 (1929) 3661.

8. For the nuclei ^{111}Cd, ^{113}Cd and ^{199}Hg, the percent natural abundances and receptivities relative to ^{13}C are 12.75 and 6.97, 12.26 and 7.67, and 16.84 and 5.57.[9]

9. R.K. Harris, *Nuclear Magnetic Resonance Spectroscopy*, Pitman, London, 1983, p 230 ff.

10. P.A.W. Dean, J.J. Vittal, and Y. Wu, *Can. J. Chem.* 70 (1992) 779.

11. R.G. Kidd, *Annu. Rep. NMR Spectrosc.* 10a (1980) 6.

12. P.A.W. Dean, V. Manivannan, and J.J. Vittal, *Inorg. Chem.*, 28 (1989) 2360.

13. P.A.W. Dean, J.J. Vittal, and Y. Wu, *Inorg. Chem.*, to be published.

14. (a) G.K. Carson, and P.A.W. Dean, *Inorg. Chim. Acta*, 66 (1982) 157. (b) R. Colton and D. Dakternieks, *Aust. J. Chem.* 33 (1980) 2405.

15. P.A.W. Dean, J.J. Vittal, and N.C. Payne, *Inorg. Chem.* 26 (1987) 1683. P.A.W. Dean and J.J. Vittal, *Can. J. Chem.* 66(1988) 2443.

16. A. Boardman, S.E. Jeffs, R.W.H. Small, and I.J. Worrall, *Inorg. Chim. Acta*, 83 (1984) L39

17. A. Boardman, R.W.H. Small, and I.J. Worrall, *Inorg. Chim. Acta*, 120 (1986) L23

18. X Bu, P. Coppens, and M.J. Naughton, *Acta Crystallogr., Sect. C: Cryst. Struct. Commun.*, C46 (1990) 1609.

19 I. Pabst, J.W. Bats, and H. Fuess, *Acta Crystallogr., Sect. B.*, B46 (1990) 503.

CHAPTER 5 STUDIES ON CADMIUM CLUSTERS $[(\mu\text{-ER})_{6-m}(\mu\text{-X})_m(CdX)_4]^{2-}$

5.1 Introduction

In the last chapter (Ch. 4), we have studied the system of $[(\mu\text{-SAlk})_{6-m}(\mu\text{-X})_m(MX)_4]^{2-}$ (M = Hg, m = 0-2). Now the remaining question is whether the analogues with M = Cd or Zn and m = 1 or 2 exist? If so, can the bridging ligand SAlk be extended to the more general ER (E = S, Se or Te; R = alkyl or phenyl)? Moreover, will the cadmium clusters in this series have the similar properties to the mercury analogues? For example, when m = 2, is it possible to get two halides in mutually cis positions in the adamantanoid skeleton? Obviously, this is an interesting area to be explored.

A wide range of zinc and cadmium clusters with m = 0 have been studied (Ref. [1-3], as well as Ch. 2 in this thesis). When m = 1 or 2, the only reported mixed-bridging clusters of this type are $[(\mu\text{-EPh})_{6-m}(\mu\text{-I})_m(CdI)_4]^{2-}$ (E = S or Se), which have been identified in acetone by ^{77}Se and ^{113}Cd NMR[4]. However, no isolation of this type of cage system (m = 1 or 2) has been reported. From the study of alkylthiolate clusters (see previous chapters and references therein), we know that there is no guarantee that *phenylthiolate* complexes can be representative of *alkylthiolate* analogues. Therefore, we need to know more about this type of cluster.

In this chapter, cadmium clusters $[(\mu\text{-ER})_{6-m}(\mu\text{-X})_m(CdX)_4]^{2-}$ (m = 0-2) have been studied. The ^{113}Cd NMR method is a particularly convenient probe for the investigation. The zinc analogues are difficult to characterize by multi-NMR, except that Cd NMR of Cd/Zn mixtures can be measured. In fact, when m = 1 or 2, the mixed-metal structures are much more complicated than when m = 0 (see Discussion part for details). Therefore,

the zinc series with m = 1 or 2 is not investigated in this chapter. However, the existence of cadmium clusters with mixed-bridging ligands have been proved. During this work 25 new compounds have been isolated analytically pure. Of these 14 have both halides and chalcogenates in bridging positions. The cluster behaviour in solution has been investigated by multi-NMR (^{77}Se and ^{113}Cd). Some different NMR properties have been found between the clusters of primary-alkylthiolates, secondary-alkylthiolates and phenylthiolates.

5.2 Experimental

Materials and General Procedures

The compounds $Cd(SR)_2$ (R = Et, Pr^n, Pr^i, Cy and Ph) were synthesized by an adaptation of the literature method[5] (see Ch. 2 for details). $Cd(SePh)_2$ was prepared by mixing MeOH solutions of $Cd(NO_3)_2.4H_2O$ and NaSePh in a glove bag under Ar. All other starting materials were from commercial sources and were used as received. All solvents for use in synthesis or in the preparation of NMR samples were dried over 3-A molecular sieves and de-oxygenated by sparging with Ar. All syntheses and preparations of NMR samples were carried out under an atmosphere of Ar.

Synthesis

$(Bu_4N)_2[Cd_4(SEt)_6I_4]$. A mixture of CdI_2 (0.055g, 0.15mmol), $Cd(SEt)_2$ (0.106g, 0.45mmol), and Bu_4NI (0.111g, 0.3?mmol) in CH_2Cl_2 (3ml) was stirred for 5min., producing a colorless solution with a small amount of white insoluble material, which was removed by decantation. This solution was layered with Et_2O (3ml), then cooled at about

0^0C overnight. The white crystals was isolated by decantation, washed with Et_2O, and dried under vacuum at room temperature; yield 0.205g (76%). Anal Calcd. for $C_{44}H_{102}Cd_4I_4N_2S_6$ (mol wt 1808.92): C, 29 22; H, 5.68; N, 1 55. Found: C, 28.90, H, 5.43; N, 1.50.

The preparations of the other compounds were carried out in an essentially similar manner. Depending on the individual case, stirring times of up to a few hours were necessary to get all three starting components dissolved, and/or a refrigeration time longer than one day was necessary to get a crystalline product. Also in some cases, after a period of stirring, there is no insoluble material at all in the mixture, while in other cases insoluble material remains no matter how long the mixture is stirred, and this must be removed by decantation or filtration. For the compounds with m = 1 and 2, the ratio of the three starting materials, CdX_2, $Cd(ER)_2$ and (cat)X, was changed to 3:5:4 and 1:1:1, respectively.

$(Ph_4P)_2[Cd_4(SEt)_6I_4]$, as white crystals; yield 82%. Anal. Calcd. for $C_{60}H_{70}Cd_4I_4P_2S_6$ (mol wt 2002.78): C, 35.98; H, 3.52. Found: C, 36.10; H, 3.30.

$(Bu_4N)_2[Cd_4(SEt)_6Br_4]$, as white crystals; yield 74%. Anal. Calcd. for $C_{44}H_{102}Br_4Cd_4N_2S_6$ (mol wt 1620.92): C, 32.60; H, 6.34; N, 1.73 Found: C, 32.37; H, 6.10; N, 2.07.

$(Ph_4P)_2[Cd_4(SEt)_6Br_4]$, as white crystals; yield 85%. Anal. Calcd for $C_{60}H_{70}Br_4Cd_4P_2S_6$ (mol wt 1814.78): C, 39.71; H, 3.89. Found: C, 39.56; H, 4 01.

$(Ph_4P)_2[Cd_4(SEt)_5I_5]$, as white crystals; yield 59%. Anal. Calcd for $C_{58}H_{65}Cd_4I_5P_2S_5$ (mol wt 2068.56): C, 33.68, H, 3.17. Found: C, 33.50; H, 2 87

$(Bu_4N)_2[Cd_4(SEt)_4I_6]$, as white crystals; yield 71%. Anal Calcd. for

$C_{40}H_{92}Cd_4I_6N_2S_4$ (mol wt 1940.49). C, 24.76, H, 4 78; N, 1.44. Found: C, 24 88; H, 4.56; H, 1 50

$(Ph_4P)_2[Cd_4(SPr^n)_6I_4]$, as white crystals; yield 68%. Anal. Calcd. for $C_{66}H_{82}Cd_4I_4P_2S_6$ (mol wt 2086 95). C, 37.99; H, 3.96. Found: C, 38.21; H, 4.01.

$(Et_4N)_2[Cd_4(SPr^n)_5I_5]$, as white crystals; yield 69%. Anal. Calcd. for $C_{31}H_{75}Cd_4I_5N_2S_5$ (mol wt 1720.40): C, 21.64; H, 4.39; N, 1.63. Found: C, 21.77; H, 4.39; N, 1.73.

$(Ph_4P)_2[Cd_4(SPr^i)_6I_4]$, as white crystals; yield 99%. Anal. Calcd. for $C_{66}H_{82}Cd_4I_4P_2S_6$ (mol wt 2086.95): C, 37.99; H, 3.96. Found: C, 37.65; H, 3.82.

$(Ph_4P)_2[Cd_4(SPr^i)_6Br_4]$, as white crystals; yield 80%. Anal. Calcd. for $C_{66}H_{82}Br_4Cd_4P_2S_6$ (mol wt 1898.95): C, 41.75; H, 4.35. Found: C, 41.51; H, 4.35.

$(Et_4N)_2[Cd_4(SPr^i)_5I_5]$, as white crystals; yield 93%. Anal. Calcd. for $C_{31}H_{75}Cd_4I_5N_2S_5$ (mol wt 1720.40): C, 21.64; H, 4.39; N, 1.63. Found: C, 21.30; H, 4.03; N, 1 65.

$(Bu_4N)_2[Cd_4(SPr^i)_5I_5]$, as white crystals; yield 89%. Anal. Calcd. for $C_{47}H_{107}Cd_4I_5N_2S_5$ (mol wt 1944.84): C, 29.03; H, 5.55; N, 1.44. Found: C, 28.69; H, 5.52; N, 1.44.

$(Et_4N)_2[Cd_4(SPr^i)_5Br_5]$, as white crystals; yield 90%. Anal. Calcd. for $C_{31}H_{75}Br_4Cd_5N_2S_5$ (mol wt 1485.40): C, 25.07; H, 5.09; N, 1.89. Found: C, 24.91; H, 4 76; N, 1 71.

$(Et_4N)_2[Cd_4(SPr^i)_4I_6]$, as white crystals; yield 79%. Anal. Calcd. for $C_{28}H_{68}Cd_4I_6N_2S_4$ (mol wt 1772.17): C, 18.98; H, 3.87; N, 1.58. Found: C, 18.98; H, 3.67; N, 1.70

$(Bu_4N)_2[Cd_4(SPr^i)_4I_6]$, as white crystals, yield 73% Anal Calcd for $C_{44}H_{100}Cd_4I_6N_2S_4$ (mol wt 1996 59): C, 26.47, H, 5.05, N, 1 40 Found C, 26 26, H, 4 70, N, 1.10.

$(Bu_4N)_2[Cd_4(SPr^i)_4Br_6]$, as white crystals, yield 94% Anal Calcd for $C_{44}H_{100}Br_4Cd_6N_2S_4$ (mol wt 1714.58) C, 30.82; H, 5 88; N, 1 63 Found C, 30 72, H, 5.56; N, 1.76.

$(Bu_4N)_2[Cd_4(SCy)_6Br_4]$, as white crystals; yield 47%. Anal Calcd for $C_{68}H_{138}Br_4Cd_4N_2S_6$ (mol wt 1945.47): C, 41.98; H, 7.15; N, 1 44 Found C, 41 80, H, 6.86; N, 1.20.

$(Bu_4N)_2[Cd_4(SCy)_5Br_5]$, as white crystals; yield 57%. Anal. Calcd. for $C_{62}H_{127}Br_5Cd_4N_2S_5$ (mol wt 1910.15): C, 38.99; H, 6.70; N, 1 47 Found C, 38.62; H, 6.55; N, 1.45.

$(Bu_4N)_2[Cd_4(SePh)_6I_4]$, as white crystals; yield 72% Anal. Calcd for $C_{68}H_{102}Cd_4I_4N_2Se_6$ (mol wt 2378.59): C, 34.34; H, 4.32; N, 1.18 Found C, 34 61, H, 4.30; N, 1.44.

$(Et_4N)_2[Cd_4(SPh)_6I_4]$. A mixture of CdI_2 (0.110g, 0.30mmol), $Cd(SPh)_2$ (0 298g, 0.90mmol), and Bu_4NI (0.154g, 0.60mmol) in CH_2Cl_2 (6ml) was stirred for 2 Hrs, producing a solution with two layers. To this solution, 6ml Et_2O was added The subsequent procedure was the same as described above. Yield of white crystals, 87% Anal. Calcd. for $C_{52}H_{70}Cd_4I_4N_2S_6$ (mol wt 1872.75): C, 33.35; H, 3.77, N, 1 50 Found C, 32.98; H, 3.64; N, 1.58.

Prepared in the same way were:

$(Et_4N)_2[Cd_4(SPh)_6Br_4]$, as white crystals, yield 94% Anal. Calcd for

$C_{52}H_{70}Br_4Cd_4N_2S_6$ (mol wt 1684.75). C, 37.07; H, 4.19, N, 1.66. Found: C, 37.18; H, 3.83, N, 1.27.

$(Et_4N)_2[Cd_4(SPh)_5I_5]$, as white crystals; yield 88%. Anal. Calcd. for $C_{46}H_{65}Cd_4I_5N_2S_5$ (mol wt 1890.49): C, 29.23; H, 3.47; N, 1.48. Found: C, 28.92; H, 3.35; N, 1.68.

$(Et_4N)_2[Cd_4(SPh)_5Br_5]$, as white crystals; yield 69%. Anal. Calcd. for $C_{46}H_{65}Br_5Cd_4N_2S_5$ (mol wt 1655.49): C, 33.37; H, 3.96; N, 1.69. Found: C, 33.28; H, 3.67; N, 1.60.

$(Et_4N)_2[Cd_4(SPh)_4I_6]$, as white crystals; yield 93%. Anal. Calcd. for $C_{40}H_{60}Cd_4I_6N_2S_4$ (mol wt 1908.23): C, 25.18; H, 3.17; N, 1.47. Found: C, 25.33; H, 3.33; N, 1.43.

$(Et_4N)_2[Cd_4(SPh)_4Br_6]$, as white crystals; yield 78%. Anal. Calcd. for $C_{40}H_{60}Br_6Cd_4N_2S_4$ (mol wt 1626.22): C, 29.54; H, 3.72; N, 1.72. Found: C, 29.90; H, 3.67; N, 1.57.

NMR Spectra

Proton and ^{13}C NMR spectra were obtained at ambient probe temperature using a Varian Gemini-200 spectrometer system with solutions in 5mm od NMR tubes. The ^2D resonances of the deuterated solvents were used as field/frequency locks. For ^1H NMR the solvent residuals were used as internal references (δ_H = 1.93 and 7.24 ppm for CD_2HCN and $CHCl_3$, respectively). For ^{13}C NMR the solvent signals were used similarly (δ_C = 1.3 and 77.0 ppm for CD_3CN and $CDCl_3$, respectively).

Natural-abundance ^{113}Cd and ^{77}Se NMR spectra were measured also using a Varian

Gemini-200 system, operating without a ^2D field/frequency lock (field drift < 0.03 ppm/day), with the samples in 10mm od NMR tubes. Samples were prepared using mass of solute : volume of solvent at ambient temperature as the concentration unit. The external references were 0.1M $Cd(ClO_4)_2$ (aq) and pure $SeMe_2$ (all at ambient probe temperature) for ^{113}Cd and ^{77}Se, respectively. The frequencies at references were 44.368 and 38.163 MHz for ^{113}Cd and ^{77}Se, respectively. Gated proton-decoupling was used for ^{113}Cd, with the decoupler off at least 80% of each duty cycle. Reproducibility of δ_{Cd} and δ_{Se} between sessions was ±1 and 0.1ppm or better. In a single session, reproducibility of δ_{Cd} is thought to be ±0.1ppm or better. Probe temperatures were calibrated using a thermocouple probe in a stationary sample of the appropriate solvent.

Elemental Microanalyses

All analyses were performed by Guelph Chemical Laboratories Ltd.

5.3 Results and Discussions

5.3.1 Synthesis

All the compounds were prepared in CH_2Cl_2 using CdX_2, $Cd(ER)_2$ and (Cat)X as starting materials. When m = 0, the self-assembly reaction follows the eqn [1]

[1] $$CdX_2 + 3\ Cd(ER)_2 + 2\ (Cat)X \rightarrow (Cat)_2[(\mu\text{-}ER)_6(CdX)_4]$$

This reaction gave isolable products very straightforwardly, as discussed in Ch. 2. While all the isolated compounds described in Ch. 2 had $Cat^+ = Et_4N^+$, the compounds tried here

have $Cat^+ = Bu_4N^+$ and Ph_4P^+, except when ER = SPh

When m = 1, the reaction follows eqn. [2]. In this case, choosing suitable

[2] $$1.5\ CdX_2 + 2.5\ Cd(ER)_2 + 2\ (Cat)X \rightarrow (Cat)_2[(\mu\text{-}ER)_5(\mu\text{-}X)(CdX)_4]$$

cations is important. For example, when $Cat^+ = Et_4N^+$, ER = SEt, and X = I or Br, the starting materials in the mixture solution were not dissolved completely, no matter how long it was stirred. This means that the reaction may not follow the stoichiometry of eqn. [2]. On the other hand, choice of a cation that gives too soluble a product may cause another kind of problem. For example, when $Cat^+ = Bu_4N^+$, ER = SPr^n, and X = I, the three components dissolved, but the isolated product was a syrup that was difficult to handle, and therefore not characterized further.

When m = 2, the reaction of three components was supposed to be eqn. [3].

[3] $$2\ CdX_2 + 2\ Cd(ER)_2 + 2\ (Cat)X \rightarrow (Cat)_2[(\mu\text{-}ER)_4(\mu\text{-}X)_2(CdX)_4]$$

For these compounds with m = 2, the same or even worse problems occurred as for the analogues with m = 1. For example, when $Cat^+ = Bu_4N^+$, almost all the products were syrups or sticky materials, except those with the ER/X combinations = SEt/I; SPr^i/I,Br. However, some representative complexes have been isolated with satisfactory microanalyses. All the isolated compounds in this project have been re-checked by their ^{113}Cd NMR, which are consistent with those spectra from three component solutions prepared in situ

5.3.2 NMR studies

(i) ER = SPr^i and SCy

As was described in Ch. 2 and Ch 3, the clusters with SPr^i or SCy are a special group (probably due to the bulky substituent), and the properties of these are usually different from those of the others. The ^{1}H and ^{13}C NMR data are listed in Tables 5.1 and 5.2. Typical ^{1}H NMR spectra are shown in Fig. 5.1. It can be seen from Fig 5.1 that the relative intensity of SPr^i protons decreases when the m value increases. The intensity ratio of SPr^i and Et_4N suggests that the isolated compounds have the expected formula. Comparing the ^{1}H NMR data in Table 5.1 to that in Table 2.2 (in Ch. 2), we find out that the δ_H values of the proton which is nearest to the S atom are varying with the m values in the order 2 > 1 > 0. For example , the δ_H values of -SC*H*= in SPr^i of complexes $(Et_4N)_2[(\mu\text{-}SPr^i)_{6-m}(\mu\text{-}I)_m(CdI)_4]$ in CD_3CN are 3.54, 3.51, and 3.42 ppm for m = 2, 1, and 0, respectively. This effect (δ_H varying with m) even influences the methyl protons in SPr^i, in the same order: m = 2 > 1 > 0 (e.g. 1.48, 1.46, and 1.42 ppm, when X = I). Of course, the effect should be reflected by δ_C also. Taking the same compounds as an example, from Tables 5.2 and 2.3, it can be seen that the δ_C values of -SCH= are 37.2, 36.8, and 35.9 ppm for m = 2, 1, and 0, respectively. It should be noted that all ^{1}H and ^{13}C NMR data are exchange-averaged.

All the samples for which ^{113}Cd NMR spectra were measured were prepared in situ in CH_2Cl_2 by mixing three components CdX_2, $Cd(ER)_2$, and Bu_4NX in the appropriate ratio according to eqns. [1] - [3]. For the system of ER = SPr^i or SCy, almost all the three components are dissolved in a period of stirring to produce a colorless solution, except for the SCy/Cl case at the 2:2:2 ratio. For interest, the 2:5 - 1:5 - 2 ratio of

Table 5 1 ^{1}H NMR Data for $(Cat)_2[(\mu\text{-}ER)_{6-m}(\mu\text{-}X)_m(CdX)_4]$ at ambient probe temperature[a,b]

					δ_H[c,d]		
Cat[e]	ER[e]	X	m	Solvent	H_α	H_β	H_γ
Bu_4N	SEt	I	0	$CDCl_3$	2.84	1.43	
Ph_4P	SEt	I	0	$CDCl_3$	2.71	1.29	
Bu_4N	SEt	Br	0	CD_3CN	2.71	1.36	
Ph_4P	SEt	Br	0	$CDCl_3$	2.72	1.27	
Ph_4P	SPr^n	I	0	CD_3CN	2.63	1.71	0.89
Ph_4P	SPr^i	I	0	$CDCl_3$	3.51	1.39	
Ph_4P	SPr^i	Br	0	$CDCl_3$	3.43	1.37	
Et_4N	SPh	I	0	CD_3CN	[f]		
Et_4N	SPh	Br	0	CD_3CN	[f]		
Bu_4N	SePh	I	0	CD_3CN	[g]		
Bu_4N	SCy	Br	0	$CDCl_3$	[h]		
Ph_4P	SEt	I	1	CD_3CN	2.72	1.38	
Et_4N	SPr^n	I	1	CD_3CN	2.67	1.74	0.92
Et_4N	SPr^i	I	1	CD_3CN	3.51	1.46	
Bu_4N	SPr^i	I	1	$CDCl_3$	3.64	1.53	
Et_4N	SPr^i	Br	1	CD_3CN	3.40	1.43	
Et_4N	SPh	I	1	CD_3CN	[f]		
Et_4N	SPh	Br	1	CD_3CN	[f]		
Bu_4N	SCy	Br	1	$CDCl_3$	[h]		

Bu_4N	SEt	I	2	CD_3CN	2.77	1.39
Et_4N	SPr^i	I	2	CD_3CN	3.54	1.48
Bu_4N	SPr^i	I	2	$CDCl_3$	3.66	1.54
Bu_4N	SPr^i	Br	2	$CDCl_3$	3.57	1.50
Et_4N	SPh	I	1	CD_3CN	[f]	
Et_4N	SPh	Br	1	CD_3CN	[f]	

[a] Reproducibility for δ_H is ±0.01 ppm, for ^3J is ±0.1 Hz.

[b] For Et_4N in CD_3CN: δ_H = 3.15 (q) and 1.19 (m); ^3J(H-H) = 7.3; $^3J(^{14}N\text{-}H)$ = 1.9. For Bu_4N in CD_3CN: δ_H = 3.07 (m), 1.60 (m), 1.35 (m), and 0.96 (t). For Bu_4N in $CDCl_3$: δ_H = 3.22 (m), 1.66 (m), 1.46 (m), and 1.01 (t). For Ph_4P in CD_3CN: δ_H = 7.6-8.0. For Ph_4P in $CDCl_3$: δ_H = 7.5-8.0.

[c] Relative to the solvent residual signals with δ_H as follows: CD_2HCN, 1.93, $CHCl_3$, 7.24 ppm.

[d] H_α = -S-C-*H*, H_β = -S-C-C-*H*, *etc.*

[e] When ER = SEt, the H_α signal is a quartet and H_β is a triplet; when ER = SPr^n, the H_α signal is a triplet, H_β is a multiplet, and H_γ is a triplet; when ER = SPr^i, the H_α signal is a septet and H_β is a doublet.

[f] 6.9 - 7.6 ppm (SPhenyl H).

[g] 6.9 - 7.7 ppm (SePhenyl H).

[h] The SCy signals are not well resolved, because of overlaping with Bu_4N

Table 5.2 ^{13}C NMR data for $(Cat)_2[(\mu\text{-}ER)_{6-m}(\mu\text{-}X)_m(CdX)_4]$ at ambient probe temperature[a,b]

					δ_C[c,d]		
Cat[+]	ER	X	m	Solvent	C_α	C_β	C_γ
Bu_4N	SEt	I	0	$CDCl_3$	24.2	21.0	
Ph_4P	SEt	I	0	$CDCl_3$	24.2	21.1	
Bu_4N	SEt	Br	0	CD_3CN	23.8	21.6	
Ph_4P	SEt	Br	0	$CDCl_3$	23.2	21.2	
Ph_4P	SPr^n	I	0	CD_3CN	31.9	29.6	14.1
Ph_4P	SPr^i	I	0	$CDCl_3$	36.0	29.9	
Ph_4P	SPr^i	Br	0	$CDCl_3$	34.5	30.1	
Et_4N	SPh	I	0	CD_3CN	[e]		
Et_4N	SPh	Br	0	CD_3CN	[e]		
Bu_4N	SePh	I	0	CD_3CN	[f]		
Bu_4N	SCy	Br	0	$CDCl_3$	[f]		
Ph_4P	SEt	I	1	CD_3CN	25.0	21.5	
Et_4N	SPr^n	I	1	CD_3CN	32.5	29.4	14.1
Et_4N	SPr^i	I	1	CD_3CN	36.8	30.1	
Bu_4N	SPr^i	I	1	$CDCl_3$	[g]	29.8	
Et_4N	SPr^i	Br	1	CD_3CN	[g]	30.3	
Et_4N	SPh	I	1	CD_3CN	[e]		
Et_4N	SPh	Br	1	CD_3CN	[e]		
Bu_4N	SCy	Br	1	$CDCl_3$	[f]		

Bu_4N	SEt	I	2	CD_3CN	25.5	21.1
Et_4N	SPr^i	I	2	CD_3CN	37.2	29.9
Bu_4N	SPr^i	I	2	$CDCl_3$	[g]	29.7
Bu_4N	SPr^i	Br	2	$CDCl_3$	35.5	30.0
Et_4N	SPh	I	1	CD_3CN	[e]	
Et_4N	SPh	Br	1	CD_3CN	[e]	

[a] Reproducibility for δ_C is ±0.1 ppm, for J(P-C) is ±1 Hz.

[b] For Et_4N in CD_3CN: δ_C = 53.1 and 7.7. For Bu_4N in CD_3CN: δ_C = 59.3, 24.3, 20.2, and 13.8. For Bu_4N in $CDCl_3$: δ_C = 59.1, 24.3, 19.9, and 13.9. For Ph_4P in CD_3CN: δ_C = 135.7 ($C_{2,6}$, ^2J(P-C) = 10), 131.2 ($C_{3,5}$, ^3J(P-C) = 13), 136.4 (C_4, ^4J(P-C) = 3), C_1 not obsd. For Ph_4P in $CDCl_3$: δ_C = 117.4 (C_1, ^1J(P-C) = 90), 134.4 ($C_{2,6}$, ^2J(P-C) = 10), 130.9 ($C_{3,5}$, ^3J(P-C) = 13), 135.9 (C_4, ^4J(P-C) = 3).

[c] Relative to the solvent residual signals with δ_C as follows: CD_3CN, 1.3, $CDCl_3$, 77.0 ppm.

[d] C_α = -S-*C*, C_β = -S-C-*C*, *etc.*

[e] $C_{2,6}$ = 126.1 - 126.3, $C_{3,5}$ = 129.2 - 129.3, C_6 = 134.3 - 134.9, C_1 not obsd

[f] Not measured.

[g] The signal is too weak to be assigned.

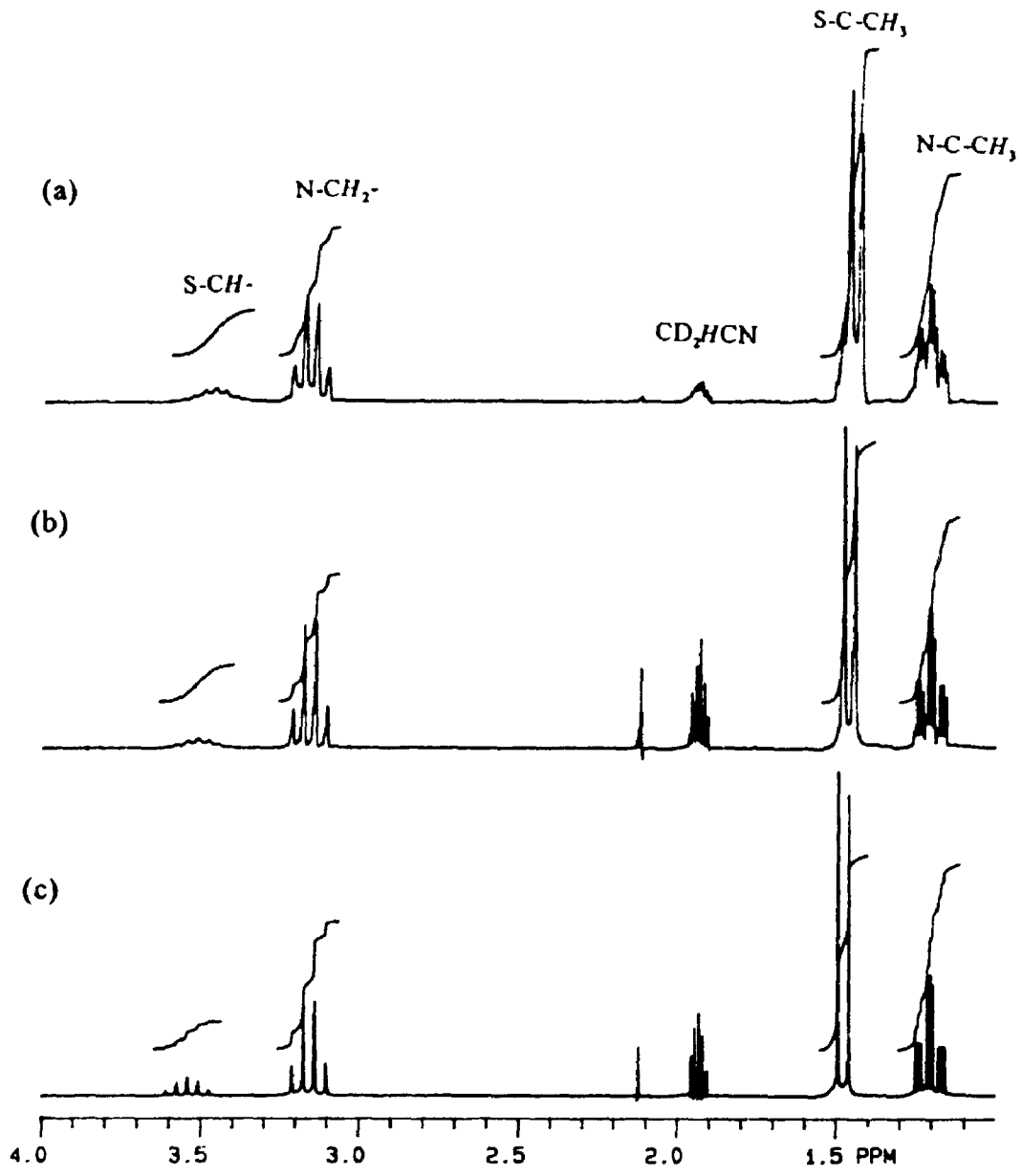

Fig 5.1 The ^1H NMR spectra of $(Et_4N)_2[(\mu\text{-}SPr^i)_{6-m}(\mu\text{-}I)_m(CdI)_4]$ in CD_3CN at ambient probe temperature, (a) m = 0; (b) m = 1; (c) m = 2. The signals at about 3.5 and 1.4 ppm are due to Pr^i protons; signals at 3.2 and 1.2 ppm due to Et protons; the others due to solvent.

starting materials was tried for ER = SPr^i, X = I or Br, but the three components are no longer completely dissolved, indicating that the species with m = 3 do not form cleanly. However, ^{113}Cd NMR spectra show that there may be a species with a $CdSX_3$ kernel in solution as a minor component (see discussion below). The signals of the species with m = 1 or 2 are relatively easy to observe in the reduced temperature spectra. At room temperature, when m = 1, the two signals (due to kernels of CdS_3X and CdS_2X_2) can not be observed and it is clear that site exchange is occurring. However, the signal of the species with m = 2 can be observed even at room temperature, although it is broad ($\nu_{1/2}$ ≈ 500 Hz). The ^{113}Cd NMR data for clusters $[(\mu\text{-ER})_{6-m}(\mu\text{-X})_m(CdX)_4]^{2-}$ are included in Table 5.3.

The signal assignments for the clusters with m = 1 or 2 are logically deduced by comparison of spectra at different ratios of starting materials. Since the details have been described in Ch. 4 for the mercury analogues, detailed discussion about signal assignment is omitted here. As can be seen from the data in Table 5.3, the ^{113}Cd chemical shifts for analogous complexes at a certain temperature shows the property of NHD,[6] *i.e.* σ_{Cd} varies with X in the order I > Br > Cl. For example, when ER = SPr^i, m = 1, and T = 183K, the δ_{Cd} values of CdS_2X_2 kernels are 441, 518, and 546 ppm for X = I, Br, and Cl, respectively. That is consistent with the result found in mercury analogues (Ch. 4) and all clusters of zinc, cadmium, and mercury with m = 0[4].

It can be seen that the δ_{Cd} values are temperature dependent, even for the cases of m = 1 or 2. In general, it is more temperature dependent for m = 2 species than for m = 0 species. For instance, if ER = SCy and X = I are kept the same, when m = 2, $\Delta_{183\text{-}293}$ = 449 - 408 = 41 ppm; while m = 0, $\Delta_{183\text{-}293}$ = 555 - 530 = 25 ppm. The NHD

Table 5 3 ^{113}Cd NMR Data for $[(\mu\text{-}ER)_{6-m}(\mu\text{-}X)_m(CdX)_4]^{2-}$ in CH_2Cl_2[a]

			δ_{Cd}[b]			
ER	X	T(K)	m = 0	m = 1		m = 2
				Cd_A	Cd_B	
SPr^i	I	293	532[c]	[d]		413
		213	550	555	437	440
		183	554	561	441	447[e]
	Br	293	569[c]	[d]		498
		213	584	585	514	517
		183	589	592	518	523[f]
	Cl	293	587	[d]		529
		213	602	603	544	547[g]
		183	606	607	546	548
SCy	I	293	530	[d]		408
		213	548	553	436	440[h]
		183	555	561	442	449[i]
	Br	293	568	[d]		496
		213	582	585	514	516
		183	587	592	518	523
	Cl	293	589	[d]		531
		213	602	605	544	545[j,k]
		183	607	610	547	551
CEt	I	293	565[c]	[d]		~ 450

		213	582	581	470	462[j,l]
		183	589	585	477	468[j,m]
	Br	293	"	"		"
		213	607	d		d
		183	613	611	537	537[j,o]
SPr[n]	I	293	"	d		d
		213	579	577	471	"
		183	584	579	475	465[j,p]
	Br	293	"	"		"
		213	605	603	532	530[j,q]
		183	610	608	536	532[j,r]
SPh	I	293	503	d		d
		213	524	518	426	418
		183	532	526	434	427
	Br	293	535	d		d
		213	554	550	494	d
		183	558	556	499	493
SePh	I	293	444	d		~ 331
		213	462	456	371	364
		183	471	466	381	373
	Br	293	493	d		d
		213	509	505	456	452[j,r]
		183	515	512	461	457[j,t]

[a] Data measured at concentration [Cd_4] = 0.05M; Cation: Bu_4N; Temp: ±1 K.

[b] Relative to external $Cd(ClO_4)_2$ (0.1M, aq.) at 293±1 K; reproducibility ±1 ppm, except as noted.

[c] 3 ppm difference from corresponding δ_{Cd} in Table 2.4.

[d] Not observed.

[e] At 1:1:1 ratio, two extra weak signals at 287 and 567 ppm

[f] At 1.1:1 ratio, two extra weak signals at 438 and 596 ppm.

[g] At 1:1:1 ratio, three extra signals at 450, 544, and 604 ppm.

[h] At 1:1:1 ratio, two extra weak signals at 241 and 477 ppm.

[i] At 1:1:1 ratio, four extra weak signals at 80, 251, 315, and 485 ppm.

[j] At 1:1:1 ratio, the three components not completely dissolved.

[k] At 1:1:1 ratio, two extra signals at 452 (strong) and 605 (weak).

[l] At 1:1:1 ratio, two extra weak signals at 254 and 574 ppm.

[m] At 1.1:1 ratio, four extra weak signals at 80, 263, 477, and 585 ppm.

[n] Not measured.

[o] At 1:1:1 ratio, three extra signals at 370, 611, and 613 ppm.

[p] At 1:1.1 ratio, five extra signals at 80, 261, 312, 475, and 579 ppm.

[q] At 1:1:1 ratio, five extra signals at 421, 364, 532, 603, and 605 ppm.

[r] At 1:1:1 ratio, four extra signals at 370, 426, 536, and 608 ppm.

[s] At 1:1:1 ratio, five extra signals at 314, 366, 456, 506, and 509 ppm.

[t] At 1.1:1 ratio, five extra signals at 317, 370, 406, 461, and 512 ppm.

property is also reflected by the temperature dependence. Still taking ER = SCy as an example, when m = 2, (449 - 408 = 41, X = I) > (523 - 496 = 27, X = Br) > (551 - 531 = 20; X = Cl). It is also interesting to point out that at any particular temperature, the chemical shift difference between m = 0 and m = 2 varies with halides in the order I > Br > Cl, too. For instance, when ER = SPr^i and T = 183K, it shows (554 - 447 = 107, X = I) > (589 - 523 = 66; X = Br) > (606 - 548 = 58; X = Cl). In fact, this property has reference to the chemical shifts of $Cd(SPr^i)_4^{2-}$ and CdX_4^{2-} (X = Cl, Br or I). Since the δ_{Cd} of $Cd(SPr^i)_4^{2-}$ is larger than that of CdX_4^{2-} and the δ_{Cd} of CdX_4^{2-} varies with X in the order I < Br < Cl (see Table 5.4), the $\Delta\delta_{Cd}$ between a given $Cd(SPr^i)_4^{2-}$ and various CdX_4^{2-} is of course in the order I > Br > Cl. Therefore, the $\Delta\delta_{Cd}$ between any two given kernels (such as CdS_3X and CdS_2X_2) should follow this order I > Br > Cl, if the first-order additivity can be assumed.

Typical ^{113}Cd NMR spectra for mixtures of $CdBr_2$:$Cd(SPr^i)_2$:Br^- at varying ratios are shown in Fig. 5.2. As can be seen from Fig. 5.2, the linewidth of the species with m = 1 or 2 (66 ~ 73 Hz) is broader than that of the corresponding species with m = 0 (26 Hz). This is true for all the other ER/X combinations also. Differently from the mercury analogues, no two-bond coupling of $^2J(Cd\text{-}Cd)$ has been observed in any species with m = 1. The reason may be the relatively broad signals combined with the relatively small values of ^2J. ^2J is expected to be in the range of 22 ~ 44 Hz (from Table 2.5, Ch. 2). From Fig. 5.2, it is interesting to see that the signal of the CdS_3Br kernel in $[(\mu\text{-}SPr^i)_6(CdBr)_4]^{2-}$ is more shielded than that in $[(\mu\text{-}SPr^i)_5(\mu\text{-}Br)(CdBr)_4]^{2-}$, and the signal of CdS_2Br_2 in trans-$[(\mu\text{-}SPr^i)_4(\mu\text{-}Br)_2(CdBr)_4]^{2-}$ is more *de*shielded than that in $[(\mu\text{-}SPr^i)_5(\mu\text{-}Br)(CdBr)_4]^{2-}$. This is true for all cadmium clusters containing SPr^i or SCy. For the

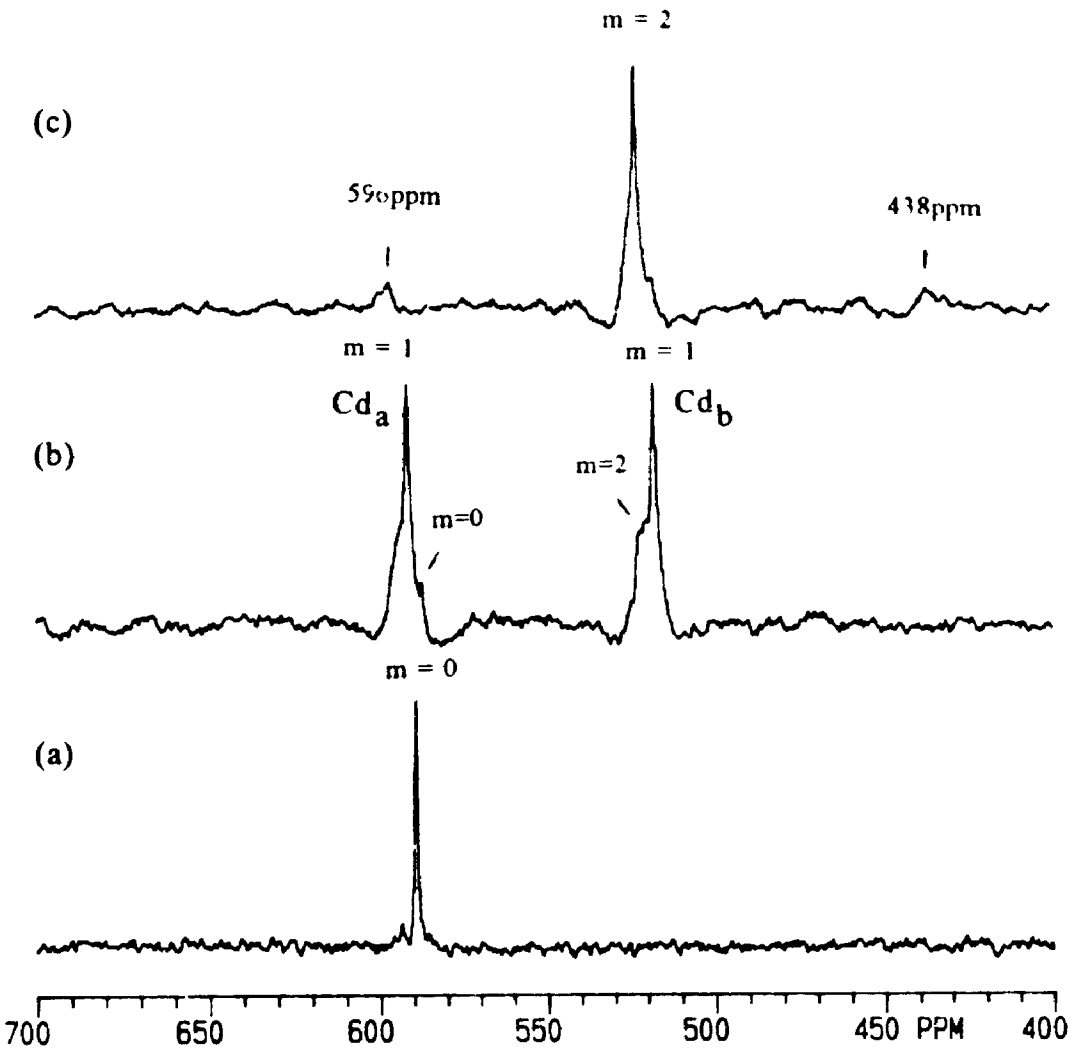

Fig. 5 2 ^{113}Cd NMR spectra of mixtures of $CdBr_2$. $Cd(SPr^i)_2$ · Bu_4NBr = (a) 1 : 3 : 2, (b) 1.5 : 2 5 : 2, (c) 2 : 2 · 2, in CH_2Cl_2 at 183K, showing the formation of $[(\mu\text{-}SPr^i)_{6-m}(\mu\text{-}Br)_m(CdBr)_4]^{2-}$, (a) m=0, (b) m=1, (c) m=2.

mercury analogues (see Table 4 4, Ch 4), the relative nuclear shieldings are the other way round, except when SR = SPr^i

When the starting ratio of three components is 1.5 : 2 5 : 2, the two major signals are due to the species $[(\mu\text{-SPr}^i)_5(\mu\text{-Br})(\text{CdBr})_4]^{2-}$ (see Fig. 5.2b). However, some weak signals indicate the existence of the clusters with m = 0 and 2 in equilibrium in solution. All the other spectra at the ratio 1.5 : 2 5 : 2 are similar. Therefore, the equilibrium eqn. [4] is possible in this case.

[4] $$2\ [(\mu\text{-ER})_5(\mu\text{-X})(\text{CdX})_4]^{2-} \rightleftharpoons [(\mu\text{-ER})_6(\text{CdX})_4]^{2-} + [(\mu\text{-ER})_4(\mu\text{-X})_2(\text{CdX})_4]^{2-}$$

When the mixture ratio is at 2:2:2 (or 1:1.1), in most cases the Cd NMR spectra show some extra signals besides the one major signal which has been assigned for trans-$[(\mu\text{-ER})_4(\mu\text{-X})_2(\text{CdX})_4]^{2-}$ species. For example, when ER = SPr^i, X = I, and T = 183K, there are two additional weak signals at 287 and 567 ppm, as well as the major signal at 447 ppm. (Note: the signal at 567 ppm is close to but different from that at 554 ppm which is due to m = 0 cluster and that at 561 ppm which is due to m = 1 cluster.) One possible explanation is that besides the trans-$[(\mu\text{-Pr}^i)_4(\mu\text{-I})_2(\text{CdI})_4]^{2-}$ species, a minor portion of the cis-species is formed in solution following the eqn. [5].

[5] $$\text{trans-}[(\mu\text{-ER})_4(\mu\text{-X})_2(\text{CdX})_4]^{2-} \rightleftharpoons \text{cis-}[(\mu\text{-ER})_4(\mu\text{-X})_2(\text{CdX})_4]^{2-}$$

The cis-structure can be seen in Fig. 4.1 IIIb, Ch. 4. In the cis-complex, two cadmiums still keep the kernel CdS_2X_2 which is similar to that in trans-, but one of the remaining

two has a CdS_3X kernel and the other a $CdSX_3$ kernel. Therefore, two extra signals would be expected, one close to that of the cluster with m = 0, the other more shielded than that of the signal from CdS_2X_2. For the convenience of comparison, some δ_{Cd} values of $Cd(SR)_{4-n}X_n^{2-}$, calculated assuming first-order additivity, are listed in Table 5.4. Since these species are somewhat different (mononuclear with two negative charges) and the data for the parent species are in a different solvent (water) and at a different temperature (308K), the real δ_{Cd} may deviate from that calculated by as much as a hundred ppm. Therefore, the experimental value of 287 ppm which is assigned to the $CdSI_3$ kernel is quite reasonable compared to the estimated one (194 ppm). Actually, the other known species with CdS_3I and CdS_2I_2 kernels have similar deviations (ca. 100 ppm) from calculated data.

A similar result is found for the SPr^i/Br case at 183K. As can be seen from Fig. 5.2c, there are two very weak signals at 438 and 596 ppm that may be due to the $CdSBr_3$ and CdS_3Br kernels in cis-$Cd_4S_4Br_6$. In addition, evidence for the $CdSX_3$ kernel is found in SPr^i/Cl/213K (at 450 ppm) and SCy/Cl/213K (at 452 ppm), too. In these last two cases, it is not certain whether the $CdSCl_3$ kernel is due to cis-$Cd_4S_4Cl_6$ or a more extensively halide-bridged cluster (such as $Cd_4S_3Cl_7$; see Fig. 4.1 IV for structural information) or a decomposition product (such as $CdSCl_3^{2-}$). However, in the more deshielded region (larger than 545 or 547 ppm), the observed signals are at the same position as that of m = 0 or 1 clusters. No other signal caused by cis-$Cd_4S_4Cl_6$ has been found. Therefore, the chemistry of such cases is presumably following the eqns [6] and [7].

Table 5.4 Some Reference and Assumed δ_{Cd} Values of $Cd(SR)_{4-n}X_n^{2-}$

R	X	n = 0[a]	n = 1[b]	n = 2[b]	n = 3[b]	n = 4[c]
Et	I	648	499	349	200	50
	Br	648	575	503	430	357
Pr^n	I	647	498	349	199	50
	Br	647	575	502	430	357
Pr^i	I	625	481	338	194	50
	Br	625	558	491	424	357
	Cl	625	579	533	487	441
Ph	I	583	450	317	183	50
	Br	583	527	470	414	357

[a] Data in water at 308K, from Ref. [7].

[b] Assumed species and values.

[c] Data in CH_2Cl_2 at 308K (from Ref. [8a]), using $\delta\{0.1M\ Cd(ClO_4)_2\} = \delta\{4.5M\ Cd(NO_3)_2\}$ - 49.4 ppm (from Ref. [8b]). Note: Data in DMSO at 303K (from Ref. [8c]) show the close values (44, 351, and 442 ppm for I, Br, and Cl, respectively).

[6] $2\,[(\mu\text{-ER})_4(\mu\text{-X})_2(CdX)_4]^{2-} \rightleftharpoons [(\mu\text{-ER})_5(\mu\text{-X})(CdX)_4]^{2-} + [(\mu\text{-ER})_3(\mu\text{-X})_3(CdX)_4]^{2-}$

[7] $3\,[(\mu\text{-ER})_4(\mu\text{-X})_2(CdX)_4]^{2-} \rightleftharpoons [(\mu\text{-ER})_6(CdX)_4]^{2-} + 2\,[(\mu\text{-ER})_3(\mu\text{-X})_3(CdX)_4]^{2-}$

Besides a signal from a possible $CdSX_3$ kernel, a weak signal at more a shielded position (80 ppm) has been found in the SCy/I/183K case Logically, this signal can be assigned to a species with the CdI_4 kernel, although it is not certain whether the CdI_4 kernel is due to a tetranuclear cluster (such as cis-$Cd_4S_2I_8$) or the monocadmium anion. In the same spectrum, the weak signal at 251 ppm is assigned to the $CdSI_3$ kernel, and the strong signal at 449 ppm is assigned to CdS_2I_2 kernel in trans-$Cd_4S_4I_6$, but two extra weak signals at 315 and 485 ppm could not be assigned. However, it is certain that two unknown signals are not due to tetranuclear cluster. Then they must be due to some other non-adamantanoid complexes (such as the larger clusters, non-tetrahedral coordination kernels, *etc.*).

For interest, we tried a Cd NMR measurement at 183K for the mixed-metal solution of $[Cd_4(SPr^i)_4Br_6]^{2-}$: $[Zn_4(SPr^i)_4Br_6]^{2-}$ at 1:1 ratio, prepared in situ The spectrum is expected to be more complicated than that of m = 0 analogues discussed in Ch 2. Theoretically, there should be six signals in total which represent six types of CdS_2Br_2 kernels in that trans-$(\mu\text{-Br})_2(\mu\text{-S})_4Cd_{4-n}Zn_n$ cluster (see Fig. 5.3a). The intensity ratio of total six signals should be 1 : (1 : 2) : (2 : 1) : 1 If the cis-$M_4S_4Br_6$ or a [illegible]ated equilibrium is considered (see Eqns. [5]~[7]), the analysis of Cd NMR spectrum would be more difficult. In the real spectrum (see Fig. 5 3b), there are two groups of signals The group of major signals is at the range of 510- 523 ppm that is thought to be the resonances due to CdS_2Br_2 kernels. There are six signals in this group, as we expected

(a)

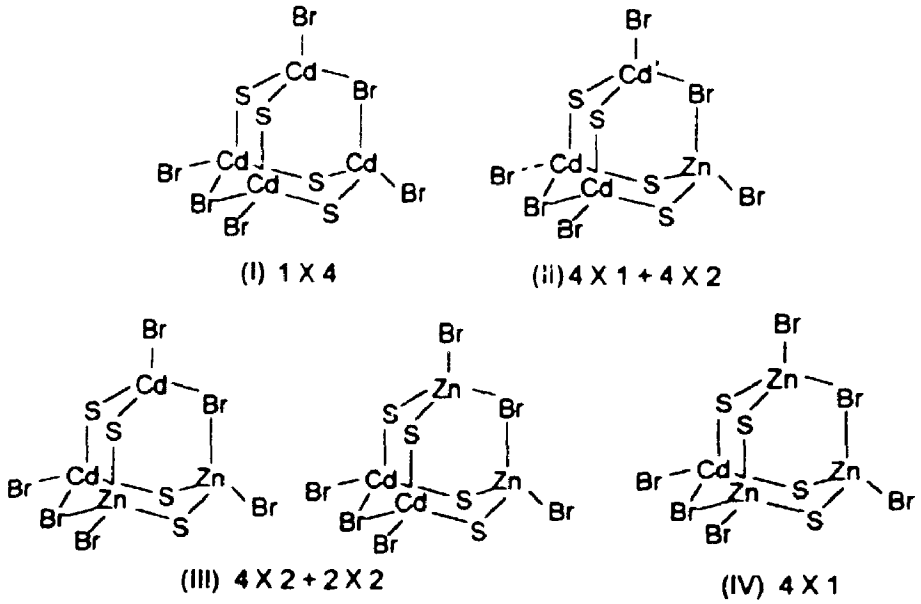

(b)

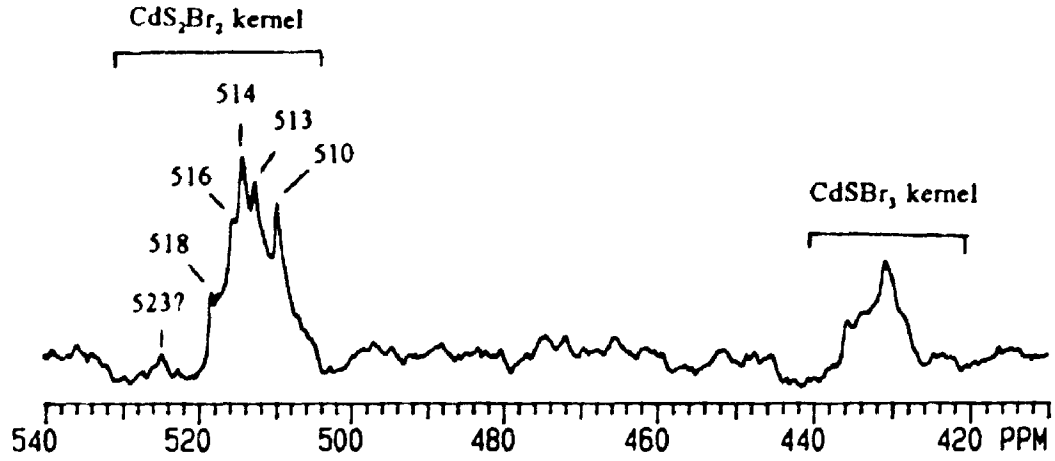

Fig 5.3 (a) The possible trans-$(\mu\text{-Br})_2(\mu\text{-S})_4(CdBr)_{4-n}(ZnBr)_n$ (n = 0~3) skeletons, showing six types of CdS_2Br_2 kernels with probabilities. (b) ^{113}Cd NMR spectrum of $[Cd_4(SPr^i)_4Br_6]^{2-}$: $[Zn_4(SPr^i)_4Br_6]^{2-}$ at 1:1 ratio in CH_2Cl_2, prepared in situ, and measured at 183K.

for trans-$M_4S_4Br_6$ structure, but the signal intensities do not have the expected statistical distribution. Lacking further experimental information, these signals can not be assigned The group of minor signals at about 426~438 ppm is thought to be due to Cd_3SBr_4 kernels, but the signals are not well separated. Because no other signal is observed around 589 ppm, we can not assign them to the cis-$M_4S_4Br_6$ in this situation Thus no more information can be obtained from this spectrum.

In summary, at a 1:1:1 ratio of CdX_2 : $Cd(SR)_2$ (R = Pr^i or Cy) : Bu_4NX, the major product is trans-$[Cd_4(SR)_4X_6]^{2-}$, but some other species may occur in solution as minor products, according to the equilibrium eqns. [5] - [7] Compared to the mercury analogues, the trans-$[Cd_4(SR)_4X_6]^{2-}$ looks not as stable as trans-$[Hg_4(SR)_4X_6]^{2-}$ at 183K, because of the formation of some other minor species. All the information of these minor signals in Cd NMR spectra have been included in the footnote of Table 5.3

(ii) ER = SEt and SPr^n

Samples for NMR were again prepared in situ. The solubility was not as good as that of clusters containing SPr^i. At 1:1:1 ratio, the three starting materials were not completely dissolved. The X = Cl clusters were not tried for either SEt or SPr^n systems, because of the poorer solubility expected. The ^{113}Cd NMR data of these two groups of clusters have been included in Table 5.3. The spectra look similar to those containing SPr^i or SCy groups: there is a single line due to the parent cluster (m = 0) at a 1:3:2 ratio, two major signals due to the cluster with m = 1 at a 1:5:2.5:2 ratio, and a major signal due to the trans-cluster with m = 2 at a 2:2:2 ratio (for X = I) When X = Br, at the same ratio 2:2:2, the trans-$Cd_4S_4Br_6$ signal becomes a minor one and other signals (due to

CdS_3Br and $CdSBr_3$ kernels) become stronger, which may be connected to the observation of poor solubility of the reactants

In these two series, the properties of halogen dependence and temperature dependence are the same to those in the series containing SPr^i or SCy as discussed above, but there is an interesting difference between the series with SEt or SPr^n and those with SPr^i or SCy, as can be seen by comparing the chemical shift tendency for different cadmium kernels. As can be seen from Table 5.3, the δ_{Cd} value of CdS_3X kernel in the cluster with m = 0 is larger than that of the same kernel but in the cluster with m = 1, and the δ_{Cd} value of CdS_2X_2 kernel in the cluster with m = 2 is smaller than that of the same kernel in the cluster with m = 1. For example, in the case of SEt/I/183K, 589 (m = 0) > 585 (m = 1, Cd_A), and 468 (m = 2) < 477 (m = 1, Cd_B). This nuclear shielding tendency is opposite to that in the SPr^i or SCy series, but consistent with that in the mercury analogues.

Again, at a 2:2:2 ratio, the signals of $CdSX_3$ kernels have been observed for the following ER/X/T combinations: SEt/I/213K (254 ppm), SEt/I/183K (263 ppm), SPr^n/I/183K (261 ppm), SPr^n/Br/213K (421 ppm), and SPr^n/Br/183K (426 ppm). The signals of CdX_4 kernels have been found for the following combinations: SEt/I/183K (80 ppm), SEt/Br/213K (364 ppm), SEt/Br/183K (370 ppm), SPr^n/I/183K (80 ppm), SPr^n/Br/213K (364 ppm), and SPr^n/Br/183K (370 ppm). Even from these data, we can see the properties of temperature and halogen dependence.

(iii) ER = SPh and SePh

The ^{113}Cd NMR data for clusters containing SPh or SePh and with X = I and Br

have been listed in Table 5.3. The ^{77}Se NMR spectra were also measured for the series with ER = SePh. Some NMR data have been reported for $[(\mu\text{-SePh})_{6-m}(\mu\text{-I})_m(CdI)_4]^{2-}$ (m = 0[2], 1[4] and 2[4]) in acetone. At a 1:1:1 ratio, the three starting materials were not completely dissolved for the SePh/Br case. The ^{77}Se NMR data are included in Table 5.5. Typical ^{77}Se NMR data are shown in Fig. 5.4.

As can be seen in Table 5.3, the ^{113}Cd NMR properties of halogen dependence, temperature dependence, and nuclear shielding tendency for EPh series are the same as that for SEt or SPr^n series. Moreover, at a 2:2:2 ratio, the signals of $CdEX_3$ kernels have been found for the following E/X/T combinations: Se/Br/213K (366 ppm), and Se/Br/183K (370 ppm). The signals of CdX_4 kernels have been observed for these combinations: Se/Br/213K (314 ppm) and Se/Br/183K (317 ppm). Comparison of data for all different ER clusters in Table 5.3 shows that the Cd chemical shift varies with ER in the order SEt ≈ SPr^n > SPr^i ≈ SCy > SPh > SePh, whether m = 1 (Cd_A or Cd_B) or m = 2. This order is obviously the same as that we discussed for cadmium clusters in chapters 2 and 3 and mercury clusters in Ch. 4, and consistent with the reported result[4].

For interest, the mixture at a 2.5 : 1.5 : 2 ratio of CdI_2 : $Cd(SPh)_2$: Bu_4NI was tried. The solids were not completely dissolved at this ratio. The ^{113}Cd NMR spectrum at 183K shows that as well as one major signal at 426 ppm assigned to CdS_2I_2 in trans-$Cd_4S_4I_6$, there are two signals with equal intensity at 282 and 418 ppm due to $CdSI_3$ and CdS_2I_2 kernels, respectively. One possible explanation to it is that the mer-$[(\mu\text{-SPh})_3(\mu\text{-I})_3(CdI)_4]^{2-}$ species may be formed in solution (see Fig. 4.1 IVa for structural details).

In the SePh series, the ^{77}Se NMR results are consistent with the corresponding ^{113}Cd NMR results in this chapter, and also with reported results[2,4]. At a 1:3:2 ratio of

Table 5.5 ^{77}Se NMR Data for $[(\mu\text{-SePh})_{6-m}(\mu\text{-X})_m(CdX)_4]^{2-}$ in CH_2Cl_2[a]

		δ_{Se}[b]			
X	T(K)	m = 0	m = 1		m = 2
			Se_A	Se_B	
I	293	-51.5	-51.7	-41.0	~ -35[c]
	213	-63.1[d]	-63.2[e]	-51.4[f]	-46.7
	183	-66.5[g]	-66.6[h]	-55.2[i]	-50.8
Br	293	-62.8	-62.7	-59.8	[j]
	213	-73.6[k]	-73.6[l]	-70.7[m]	[j]
	183	-76.7	-76.7	-74.3	[j]

[a] Data measured at concentration $[Cd_4]$ = 0.05M; Cation: Bu_4N; Temp: ±1 K.

[b] Relative to external pure $SeMe_2$ at 293±1 K; reproducibility ± 0.1 ppm.

[c] Broad line with $\nu_{1/2} \approx 380$ Hz.

[d] $^1J(^{77}Se\text{-}^{111/113}Cd) = 123 \pm 5$ Hz.

[e] $^1J(^{77}Se\text{-}^{111/113}Cd) = 124 \pm 5$ Hz.

[f] $^1J(^{77}Se\text{-}^{111/113}Cd) = 98 \pm 5$ Hz.

[g] $^1J(^{77}Se\text{-}^{111/113}Cd) = 120 \pm 5$ Hz.

[h] $^1J(^{77}Se\text{-}^{111/113}Cd) = 116 \pm 5$ Hz.

[i] $^1J(^{77}Se\text{-}^{111/113}Cd) = 90 \pm 5$ Hz.

[j] Not observed.

[k] $^1J(^{77}Se\text{-}^{111/113}Cd) = 86 \pm 5$ Hz.

[l] $^1J(^{77}Se\text{-}^{111/113}Cd) = 87 \pm 5$ Hz.

[m] $^1J(^{77}Se\text{-}^{111/113}Cd) = 78 \pm 5$ Hz.

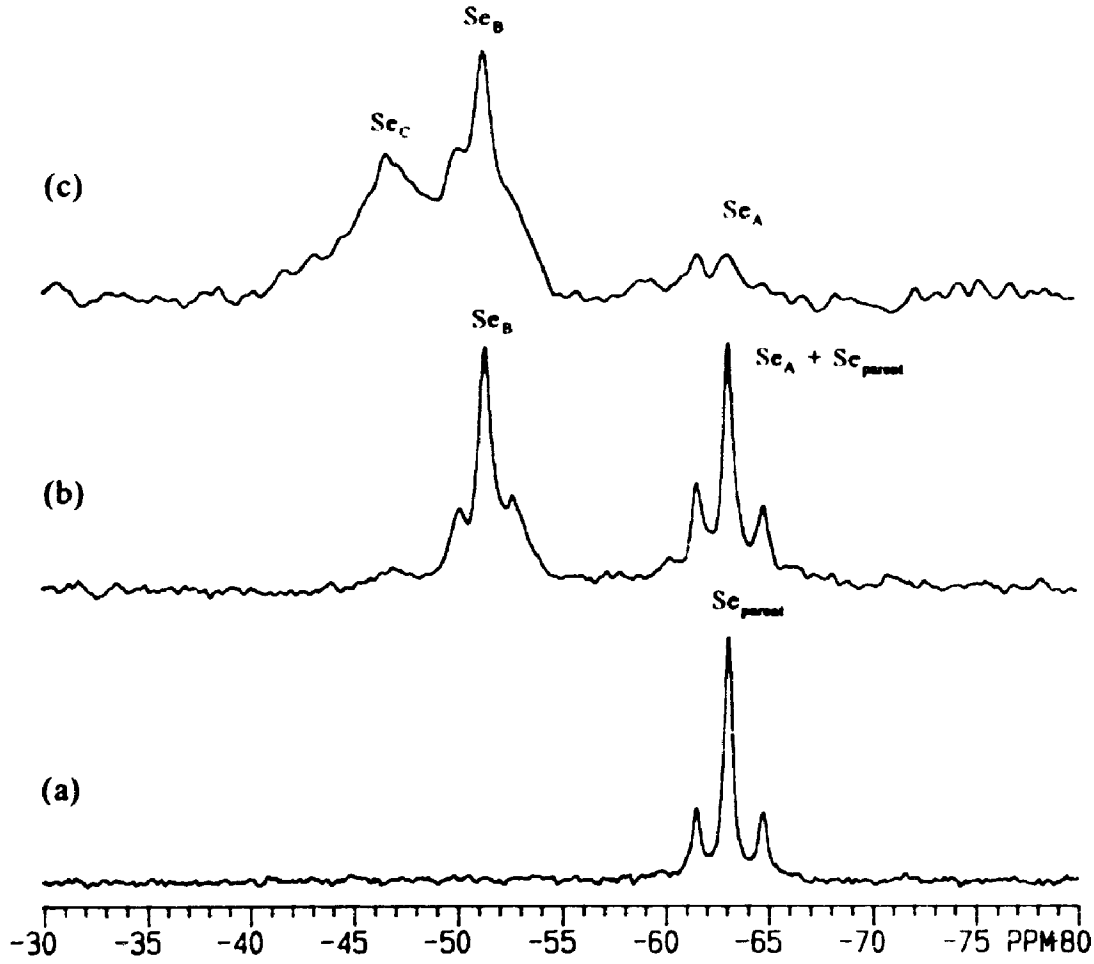

Fig. 5.4 ^{77}Se NMR Spectra of mixtures of CdI_2 : $Cd(SePh)_2$: Bu_4NI = (a) 1 : 3 : 2, (b) 1.5 : 2.5 . 2, (c) 2 : 2 : 2, in CH_2Cl_2 at 213K, showing the formation of $[(\mu\text{-}SePh)_{6-m}(\mu\text{-}I)_m(CdI)_4]^{2-}$. (See text for Se_A~Se_C labelling.)

CdX_2 $Cd(SePh)_2$ Bu_4NX (X = I or Br), there is a broad signal at ambient probe temperature, which turns sharp and shows satellites at reduced temperature (Fig. 5.4a). The one-bond coupling $^1J(^{77}Se\text{-}^{111/113}Cd)$ is about 123 Hz for X = I and 86 Hz for X = Br. The sizes of these couplings are consistent with those reported for $[Cd_4(SePh)_6I_4]^{2-}$ (120±10 Hz)[2,4], for $[Cd_4(SePh)_6Br_4]^{2-}$ (120 Hz[2] or 80±2 Hz[4]), and for bridging SePh of $[Cd_4(SePh)_{10}]^{2-}$ (165±3 Hz)[9], all in acetone.

At a 1.5 : 2.5 : 2 ratio, when X = I, two broad ^{77}Se signals at 293K represent the two types of SePh in the cluster. At reduced temperature (see Fig. 5.4b), fine structure has been observed for both types of SePh. The signal of Se_A (that without geminal μ-X) is at a position (-63 2 ppm) almost unchanged relative to that of m = 0 cluster (-63.1 ppm), with cadmium satellites (^1J = 124 Hz). The signal of Se_B (that with one geminal μ-X) is at a less shielded position (-51.4 ppm), with $^1J(^{77}Se\text{-}^{111/113}Cd)$ = 98 Hz. The intensity ratio of Se_A/Se_B is supposed to be 1:4 in the $Cd_4Se_5I_5$ cluster (see Fig. 4.1 II for structural information), but the observed ratio is roughly 1:1. The most likely explanation is that a portion of $Cd_4Se_6I_4$ cluster exists in this mixture solution and its $^{77}Se_{parent}$ signal overlaps the Se_A signal since these two signals are very close. In fact, the ^{113}Cd NMR spectrum for the same sample was measured, and it was shown that the quantity of $Cd_4Se_6I_4$ is about half to that of $Cd_4Se_5I_5$ species. Therefore, when this contribution is considered, the signal intensity at Se_A position should be the same as that at Se_B position. When X = Br at this ratio, the ^{77}Se NMR spectrum behaves in the similar manner to that when X = I (see Table 5.5)

At a 2:2:2 ratio, when X = I, room temperature spectrum shows a very broad ^{77}Se signal at about -35 ppm. At reduced temperature (Fig. 5.4c), the signal at -51.4 ppm is

known to be due to Se_B from $Cd_4Se_4I_6$, and the less shielded signal at -46.7 ppm is assigned to Se_C (that with two geminal μ-X) which may be from trans-$Cd_4Se_4I_6$. One-bond coupling was not found for the Se_C signal, because it is relatively broad and overlapped with the signal of Se_B. Presumably, this coupling constant should be smaller than that of Se_B-Cd (98 Hz) and Se_A-Cd (123 Hz), and deduced around 70 Hz. This may be another reason for why the Se_C-Cd coupling was not observed.

The ^{77}Se NMR spectrum at a 1:1.1 ratio should be just one signal, if only trans-$Cd_4Se_4I_6$ occurs in solution. However, the real spectrum shows two signals due to Se_B and Se_C, and the latter is a little bit weaker (the intensity integrals of two lines are close to 1:1). The corresponding ^{111}Cd NMR spectrum shows that the amount of m = 2 cluster is almost the same as that of m = 1 cluster in solution. Therefore, the intensity ratio of Se_B : Se_C is close to 1:1.

When X = Br at the same ratio of starting materials, no Se_C signal was observed even if at reduced temperature. Therefore, the cluster with m = 2 may not exist in the sample. The ^{77}Se NMR result is consistent with the corresponding ^{113}Cd NMR spectrum in which the trans-$Cd_4Se_4Br_6$ signal is very weak. The absence of trans-$Cd_4Se_4Br_6$ as a major species in the solution at 1:1.1 ratio may be due to the poor solubility at this ratio.

From metal NMR studies, we know that the clusters trans-$[(\mu\text{-}ER)_4(\mu\text{-}X)_2(CdX)_4]^2$ exist in the solution, but the existence of the corresponding cis-clusters is not certain. However, the ^{113}Cd NMR spectra have provided the evidence for the occurrence of $CdEX_3$ kernels in solution; these *may* come from cis-$[(\mu\text{-}ER)_4(\mu\text{-}X)_2(CdX)_4]^2$.

It is not common that halides behave as the bridging ligands in the tetracadmium clusters with the adamantane-like skeleton. Except for a preliminary NMR study[4] of [(μ-

$EPh)_{6-m}(\mu\text{-}I)_m(CdI)_4]^{2-}$ (E = S or Se; m = 1 or 2), no other such findings have been reported. However it is interesting to note that a zinc cluster with a fully halogen-bridged adamantane-like skeleton has been reported for $[(\mu\text{-}Cl)_6(ZnCl)_4]^{2-}$ [10], while halogen-bridged adamantanoid units, $[(\mu\text{-}X)_6(MX_{1/2})_4]^{2-}$, have been reported to occur in solid $ZnBr_2$[11], ZnI_2[12], and HgI_2[13], but not in any solid CdX_2.

5.4 Conclusions

In this chapter, the system of $[(\mu\text{-}ER)_{6-m}(\mu\text{-}X)_m(CdX)_4]^{2-}$ has been investigated. Complexes with ER = SAlk, m = 1 or 2 have been studied for the first time. Twenty-five new compounds have been successfully produced using the self-assembly method, and isolated analytically pure. These new compounds have covered a wide range of chalcogenates, ER (ER = SAlk, SPh or SePh) and halides, X (X = I, Br or Cl), and provided the evidence of their existence in solid state.

In the solution, the existence of these clusters has been confirmed by ^{77}Se and ^{113}Cd NMR. The metal NMR properties of these clusters are similar to those of their mercury analogues in some ways, such as halogen dependence, temperature dependence and chalcogen dependence; but are also different in other ways, such as nuclear shielding pattern. There also appear to be differences in stability in solution. In most cases, the clusters with m = 2 are proved to have the trans-$(\mu\text{-}X)_2$ structure, but in some cases there is evidence for cis-clusters or cis-/trans- equilibrium in solution. In some cases species with $CdSX_3$ or CdX_4 kernels occur, although they are minor species in solution; it is not certain whether these are due to adamantanoid clusters or dissociation/decomposition products. However, such tetrahedral coordination kernels with more than two halogens

were never found in the analogous mercury-containing systems

5.5 References

1. P.A.W. Dean and J J. Vittal, *Inorg. Chem.*, 24 (1985) 3722
2. P.A.W. Dean, J.J. Vittal, and N.C. Payne, *Inorg. Chem.*, 26 (1987) 1683
3. P.A.W. Dean, J.J. Vittal, and Y. Wu, *Can. J. Chem.*, 70 (1992) 779
4. P.A.W. Dean and J.J. Vittal, in *Metallothioneins*, M.J. Stillman, C F. Shaw III, & K.T. Suzuki, Eds., VCH, New York, 1992, chapter 14.
5. D.C. Bradley and C.H Marsh, *Chem. and Ind.*, (1967) 361.
6. R.G. Kidd, *Annu. Rep. NMR Spectrosc.*, 10a (1980) 6.
7. G.K. Carson, P.A.W. Dean, and M.J. Stillman, *Inorg. Chim. Acta*, 56 (1981) 59.
8. (a) R. Colton and D. Dakternieks, *Austr. J. Chem.*, 33 (1980) 2405. (b) G E Maciel and M. Borzo, *J. Chem. Soc., Chem. Comm.*, (1973) 394. (c) T Drakenberg, N. Bjork, and R. Portanova, *J. Phys. Chem.*, 82 (1978) 2423.
9. P.A.W. Dean and J.J. Vittal, *Can. J. Chem.*, 66 (1988) 2443.
10. F. Bottomley and S. Karslioglu, *J. C. S. Chem. Comm.*, (1991) 222
11. C. Chieh and M.A. White, *Z. Kristallogr*, 166 (1984) 189.
12. D. Schwarzenbach, *Z. Kristallogr.*, 128 (1969) 97.
13. P.H. Fourcroy, D. Carre, and J. Rivet, *Acta Crystallogr.*, B34 (1978) 3160

CHAPTER 6 SUMMARY AND CONCLUSIONS

As mentioned in the Introductory Chapter (Section 1.7), the major focus of this thesis is that of looking for new types of adamantane-like clusters and collecting NMR data for model complexes. The task has been accomplished by the isolation of 71 new compounds, by measurement of multinuclear magnetic resonance for more than one hundred clusters in solution, and, in a few cases, by obtaining single crystals suitable for X-ray analysis (The X-ray analyses were carried out by others.) As a result, three types of clusters have been discovered and studied in details. They are: (1) clusters with alkylthiolates as bridging ligands, formulated as $[(\mu\text{-SAlk})_6(MX)_4]^{2-}$ (M = Zn, Cd or Hg); (2) clusters with phosphines as terminal ligands, formulated as $[(\mu\text{-ER})_6(CdPPh_3)_{4-n}(Cd)_n]^{2+}$; and (3) clusters with halides as bridging ligands, formulated as $[(\mu\text{-ER})_{6-m}(\mu\text{-X})_m(MX)_4]^{2-}$ (M = Cd or Hg). The results in this thesis provide potential model data for studies on metallothioneins and other biological systems with metal-cysteine sites.[1]

6.1 Alkylthiolates as Bridging Ligands

Although clusters with phenylthiolate (PhS^-) are well established for all zinc-group elements,[2-9] very little attention has been paid to those with alkylthiolates as bridging ligands. Only one $(Et_4N)_2[(\mu\text{-SPr}^n)_6(CdI)_4]$ has been isolated previously.[6] As well, this compound and its zinc and mercury analogues were studied in solution.[6] The propylthiolate may not be representative of all alkylthiolates. In fact, the properties of clusters with primary alkylthiolates are different from those of clusters with secondary thiolates. Therefore, the study of a much wider series of $[(\mu\text{-SAlk})_6(MX)_4]^{2-}$ was warranted.

In my study of this type of cluster, $[(\mu\text{-SAlk})_6(MX)_4]^{2-}$, many significant results have been obtained. First, it has been proved that clusters with alkylthiolates as bridging ligands can exist in solution or in the solid state for a wide range of different alkylthiolates, Alk = Me, Et, 1-Pr, 2-Pr, 1-Bu, 2-Bu, Cy or CH_2Ph. All the zinc group elements (Zn, Cd, and Hg) form this type of cluster, and the halides can be Cl, Br, and I.

Second, the chemical shifts of $^{111/113}Cd$ or ^{199}Hg vary with the R group in SR in the order primary alkyl ≥ benzyl > secondary alkyl > phenyl, with X in the order Cl > Br > I, and with temperature in the order reduced T > ambient T. For the last two factors the relative ordering, but not the magnitude of the effects, is that found for the phenylthiolate analogues. (Note: the properties of chalcogen dependence, halogen dependence and temperature dependence of NMR spectra apply also to all the other clusters summarized later in Sections 6.2 and 6.3).

Third, the NMR study on metal-mixed clusters, $[(\mu\text{-SAlk})_6(MX)_{4-n}(M'X)_n]^{2-}$, shows that in general metal redistribution does occur rapidly for all mixtures of all alkylthiolate-bridged clusters, *i.e.* the four expected Cd or Hg signals are observed. In most cases, the redistribution occurs close to statistically. In contrast, for the case of the phenylthiolate analogues, such as $[(\mu\text{-SPh})_6(CdI)_{4-n}(ZnI)_n]^{2-}$, the spectra are not well resolved, *i.e.* four separate signals are not observed, and the redistribution is not statistical for $[(\mu\text{-SPh})_6(CdSPh)_{4-n}(ZnSPh)_n]^{2-}$, with signals being observed only for n = 0 and 1 in DMF[8] and for n = 0 - 2 in acetone[9]. For $[(\mu\text{-SAlk})_6(MX)_{4-n}(M'X)_n]^{2-}$, the Cd nuclear shielding varies with n in the order $0 < 1 < 2 < 3$ in the $Cd_{4-n}Zn_n$ or $Cd_{4-n}Hg_n$ mixture. The Hg nuclear shielding takes the same order as above in the $Hg_{4-n}Zn_n$ mixture, but reversed

order, *i.e.* 0 > 1 > 2 > 3, in the $Hg_{4-n}Cd_n$ mixture. The same results are found for all alkylthiolate cases and agree with data for the SPr^n complexes[6]

Fourth, it is the first time that metal NMR data have been obtained for a complete series of mixed-halide clusters, $[(\mu\text{-}SPr^i)_6(CdX)_{4-n}(CdX')_n]^{2-}$. The Cd NMR fine structure offers information about halide exchange, which is close to a statistical case. The Cd nuclear shielding of CdX (CdX') kernel of course varies with X (or X') in the order I > Br > Cl However it is also influenced slightly by the number of substituent X' (or X), *e.g.* when X is heavier than X', δ_{Cd} varies with *n* in the order 0 > 1 > 2 > 3 for CdX site, and 1 > 2 > 3 > 4 for CdX' site.

In addition, the reaction of $[(\mu\text{-}SPr^i)_6(CdX)_4]^{2-}$ with sulfur and selenium has been studied by ^{13}C, ^{77}Se and ^{111}Cd NMR. Evidence was found for the formation of larger clusters, $[Cd_4(\mu_4\text{-}E')(\mu_2\text{-}SPr^i)_{12}(CdX)_4]^{2-}$ (E' = S or Se: X = Cl, Br or I), in solution. At the same time, a similar result was reported by another research group.[10]

6.2 Phosphines as Terminal Ligands

This thesis has been concerned mainly with cadmium complexes. Some mercury analogues have been reported by previous work[5,11]. This is the first investigation of adamantane-like cadmium clusters with alkylthiolates as bridging ligands and phosphines as terminal ligands, $[(\mu\text{-}SAlk)_6(CdPPh_3)_4]^{2+}$, though preliminary NMR work on $[(\mu\text{-}EPh)_6(CdPPh_3)_4]^{2+}$ (E = S or Se) in $CHCl_3$ has been reported[12]. The significance of the current project is described below.

First, the cadmium clusters existing in CH_2Cl_2 solution are better labelled as $[(\mu\text{-}ER)_6(CdPPh_3)_{4-n}(CdOClO_3)_n]^{(2-n)+}$. Some of them are isolable, depending on the conditions.

The existence of this type of cadmium cluster has been confirmed by multi-NMR measurements, five isolated compounds and a representative crystal structure.

Second, in the case of ER = SPr^i or SCy, the clusters with n = 2 are easily formed and isolated, while in the case of ER = SPh or SePh, the complexes with n = 0 are easily isolable. The ease of formation of the complexes with ER = SPr^n or SPe^n falls between that for SPr^i and SPh. Therefore, the capability of coordinating PPh_3 in this type of cluster varies with R in the order secondary alkyl < primary alkyl < phenyl

Third, it is the first time that adamantanoid clusters of the zinc-group elements have been produced systematically with two (or less) strong donor ligands at the terminal positions. It was thought that four would be needed. Comparing the propensity of the Cd_4 complexes for terminal coordination of PPh_3 with that of mercury analogues[10,11] and of cadmium clusters with terminal halides[4,13,14], it is possible to suggest that the coordination capability of phosphine varies with M in order Hg > Cd, and is smaller than that of halides, at least in CH_2Cl_2, the solvent commonly used here.

Fourth, it is suggested by the crystal structure of $[(\mu\text{-SPr}^i)_6(CdPPh_3)_2(CdOClO_3)_2]$ that in such a type of cluster the phosphine-free cadmium site can be occupied by some other potential ligand(s) in the mixture solution, such as suitable anions from the starting materials, or solvent molecules with donor electron pairs[11].

In addition, a possible precursor, $[Ph_3PCd(\{\mu\text{-ER}\}CdPPh_3)_3]^{5+}$, to the adamantane-like clusters has been found by multi-NMR spectra in solution. This may allow us to get a better understanding of the process in which the adamantanoid clusters are formed

6.3 Halides as Bridging Ligands

This type of cluster is formulated as $[(\mu\text{-ER})_{6-m}(\mu\text{-X})_m(MX)_4]^{2-}$ (m = 1 or 2). The only previous data reported for clusters of this type are preliminary NMR results on ER = SPh or SePh, M = Cd, and X = I.[12] Clearly, much remained to be done in this area. The achievements described in this thesis are included below.

First, the existence of this type of cluster over a wide range of ER, *m*, X and M (ER = SAlk, SPh or SePh; *m* = 1 or 2; X = Cl, Br or I; M = Cd or Hg) has been proved for both solid state and solution. This is the first time that an NMR investigation has been made of mercury clusters of this type. Also this is the first time that the isolation of Cd and Hg clusters of this type has been reported.

Second, when m = 2, it has been found that the two halides prefer to take mutually trans-positions in all the mercury clusters and most of cadmium clusters. However, in some cadmium cases, the NMR evidence suggests the existence of the cis-$(\mu\text{-X})_2$ cluster in solution. Moreover, the existence of the MSX_3 or MX_4 kernel has been observed by metal NMR for M = Cd, but not for M = Hg.

Third, neither cadmium nor mercury clusters appear to form with m > 2. In most cases, when the starting reagent ratio is modified to provide for the synthesis of the clusters with $m \geq 3$, complete dissolution does not occur, suggesting that such clusters do not form. This means that as a bridging ligand, ER may be better than X, or that there is a limit to which the central $(\mu\text{-SR})_6M_4$ cage can be destablized by replacement of ER by X.

Finally, the first reported crystal structure of a $(\mu\text{-ER})_5(\mu\text{-X})M_4$ cage, in $(Ph_4P)_2[(\mu\text{-SEt})_4(\mu\text{-Br})(HgBr)_4]$, supports the existence of this type of cluster. As well, the finding

and X-ray analysis of $[(\mu\text{-SPr})(\mu\text{-I})(HgI_2)_2]^{2-}$ gives us a better understanding of cluster dissociation.

6.4 Suggestions for Future Work

There is scope for much further study in this area

6.4.1 Continuing studies on the system $[(\mu\text{-ER})_6(MPPh_3)_{4-n}(M)_n]^{2+}$

In this system, the clusters with M = Zn have never been studied. Presumably, the bond between zinc and the phosphine is readily cleaved. Therefore, the zinc clusters may or may not exist in CH_2Cl_2 (see Section 6.2). However, DMF can be tried as a solvent instead of CH_2Cl_2, because the mixture of starting materials commonly dissolves in DMF, and DMF is also a potential terminal ligand in such a mixture solution[111]. Phosphorus-31 NMR should be a good probe for this investigation.

It is interesting to see whether PPh_3 can be replaced by $E'PPh_3$ (E' = S or Se) Clusters of phosphine chalcogenides have been reported for M = Hg[15], but not for M = Cd or Zn. The difficulty here is probably the preparation of $M(E'PPh_3)_2(ClO_4)_2$ (M = Cd or Zn). A preliminary attempt at these syntheses has been made during the work for this thesis but suitable synthetic conditions have not been developed systematically.

In addition, no data are available for cadmium clusters in which PPh_3 is replaced by $AsPh_3$ or even PR'_3 (R' = Cy, 4-C_6H_4Cl, *etc.*). Since mercury analogues are known[10,11] with a variety of "soft" neutral ligands (except PCy_3), it may be possible to study these cadmium clusters in solution by NMR and even isolate them.

6.4.2 Continuing studies on the system $[(\mu\text{-ER})_{6-m}(\mu\text{-X})_m(MX)_4]^{2-}$ (m = 1 or 2)

The clusters with M = Zn have never been investigated. One reason may be that unlike Cd or Hg clusters there is no suitable metal NMR nucleus for use as a probe of the zinc clusters when E = S. However, If E = Se or Te, the structural information can be obtained by ^{77}Se or ^{125}Te NMR. Selenium-77 NMR has been applied successfully to the mixtures of $[(\mu\text{-SePh})_6Cd_4I_{4-x}X_x]^{2-}$ (X = Br or Cl; x = 0 - 4) in solution[16].

In the current work no strong evidence has been found for the species with $m \geq 3$. Solubility was a major problem. However only CH_2Cl_2 was tried as a solvent. Progress might be made by changing CH_2Cl_2 to another solvent, such as DMF. If so, the NMR spectra will be interesting.

6.4.3 Miscellaneous new systems

(1) Alkylthiolate as a terminal ligand

Clusters with alkylthiolates as both bridging and terminal ligands have been reported only for $M = Fe^{II}$ ($[Fe_4(SEt)_{10}]^{2-}$ [17]). The SAlk as a terminal ligand may not as stable as a halide or even phenylthiolate (clusters, $[M_4(SPh)_{10}]^{2-}$ (M = Zn or Cd), have been well characterized by x-ray analysis[18,19] and NMR spectra[20-24]), but it should still be possible to study some complexes of Zn^{II}, Cd^{II} or Hg^{II}. This is a worthwhile thing to try, because it provides a better model for the four-metal cysteinyl-bridged clusters that occurs in Zn or Cd -metallothionein.

(2) Dithiolate as a bridging ligand

Adamantane-like clusters containing *di*thiolates have never been reported for the zinc-group elements, though they are known for Cu and Ag[1] (see Section 1.1 also; they

are $[Cu_4(edt)_3]^{2-}$, $[Cu_4(pdt)_3]^{2-}$, $[Cu_4(S_2\text{-xyl})_3]^{2-}$, and $[Ag_4(S_2\text{-xyl})_3]^{2-}$) However, for the zinc-group elements, non-adamantanoid polymeric complexes with dithiolate have been reported, such as $[Hg_3(edt)_4]^{2-}$ [25], $[Hg_3(S_2\text{-xyl})_4]^{2-}$ [26] Therefore, the synthesis of adamantanoid clusters with dithiolate is a possibility. If the alkane-dithiolates, $^-S(CH_2)_nS^-$ (n = 2 - 4), prove too flexible to fix the cluster skeleton, a relatively rigid ligand, such as xylene-α,α'-dithiolate, $C_6H_4(CH_2S^-)_2$, or durene-α,α'-dithiolate, $(CH_3)_2C_6H_4(CH_2S^-)_2$, can be considered.

6.5 References

1. I. Dance, K. Fisher, and G. Lee, in *Metallothioneins*, M.J. Stillman, C.F. Shaw III, and K.T. Suzuki, eds., VCH, New York, 1992, Ch.13.
2. I.G. Dance, *Polyhedron*, 5 (1986) 1037.
3. P.J. Blower and J.R. Dilworth, *Coord. Chem. Rev.*, 76 (1987) 121.
4. P.A.W. Dean, J.J. Vittal, and N.C. Payne, *Inorg. Chem.*, 26 (1987) 1683.
5. P.A.W. Dean, J.J. Vittal, and M.H. Trattner, *Inorg. Chem.*, 26 (1987) 4245
6. P.A.W. Dean and V. Manivannan, *Inorg. Chem.*, 29 (1990) 2997.
7. J.J. Vittal, P.A.W. Dean, and N.C. Payne, *Can. J. Chem.*, 70 (1992) 792.
8. I.G. Dance, *Austral. J. Chem.*, 38 (1985) 1745.
9. P.A.W. Dean and J.J. Vittal, *Inorg. Chem.*, 25 (1986) 514.
10. G.S.H. Lee, K.J. Fisher, D.C. Craig, M.L. Scudder, and I.G. Dance, *J Am. Chem. Soc.*, 112 (1990) 6435.
11. P.A.W. Dean, V. Manivannan, and J.J. Vittal, *Inorg. Chem.*, 28 (1989) 2360.

12. P.A W Dean and J.J Vittal, in *Metallothioneins*, M.J. Stillman, C.F. Shaw III, and K.T. Suzuki, eds., VCH, New York, 1992, Ch.14.

13. P.A.W. Dean and J.J. Vittal, *Inorg. Chem.*, 24 (1985) 3722.

14. P.A.W. Dean, J.J. Vittal, and Y. Wu, *Can. J. Chem.*, 70 (1992) 779.

15. P.A.W. Dean and V. Manivannan, *Can. J. Chem.*, 68 (1990) 214.

16. P.A.W. Dean and J.J. Vittal, *Inorg. Chem.*, 26 (1987) 278.

17. K.S. Hagen and R.H. Holm, *Inorg. Chem.*, 23 (1984) 418.

18. K.S. Hagen and R.H. Holm, *Inorg. Chem.*, 22 (1983) 3171.

19. J.L. Hencher, M. Khan, F.F. Said, and D.G. Tuck, *Polyhedron*, 4 (1985) 1261.

20. K.S. Hagen, D.W. Stephan, and R.H. Holm, *Inorg. Chem.*, 21 (1982) 3928.

21. P.A.W. Dean and J.J. Vittal, *J. Am. Chem. Soc.*, 106 (1984) 6436.

22. I.G. Dance and J.K. Saunders, *Inorg. Chim. Acta*, 96 (1985) L71.

23. I.G. Dance, *Inorg. Chim. Acta*, 108 (1985) 227.

24. P.A.W. Dean and J.J. Vittal, *Can. J. Chem.*, 66 (1988) 2443.

25. G. Henkel, P. Betz, and B. Krebs, *J. Chem. Soc., Chem. Commun.*, (1985) 1498.

26. G. Henkel, P. Betz, and B. Krebs, *Inorg. Chim. Acta*, 134 (1987) 195.

APPENDIX Summary of Crystal Data and Experimental Details for Three Adamantanoid Clusters

Compound	$C_{34}H_{82}N_2Br_4Cd_4S_6$	$C_{54}H_{72}Cd_4Cl_2O_8P_2S_6 \cdot C_2H_5OH$	$C_{58}H_{65}Br_5Hg_4P_2S_5$
Formula weight	1480.6	1664.1	2186.3
Crystal system	Monoclinic	Monoclinic	Monoclinic
Space group	$P2_1/c$ (No. 14)	$P2_1/c$ (No. 14)	$C2/c$ (No. 15)
Cell dimensions			
a (Å)	24.079(3)	15.006(2)	46.599(5)
b (Å)	11.365(2)	16.250(2)	12.775(2)
c (Å)	22.561(3)	28.227(3)	25.582(3)
β (deg)	113.89(1)	98.79(1)	116.50(1)
Z	4	4	8
Cell volume ($Å^{-3}$)	5645(2)	6802(2)	13629(3)
Temperature, °C	23	-40(2)	23
Diffratometer	Enraf-Nonius CAD4F	Enraf-Nonius CAD4F	Enraf-Nonius CAD4F
Radiation, wavelength (Å)	CuKα, 1.5418	MoKα, 0.71073	CuKα, 1.5418
Filter/monochromator	Nickel prefilter	graphite monochromator	Nickel prefilter
Absorption coeff. (cm^{-1})	178.5	15.8	210.7
No. of observ., variables	2699($I > 2.5\sigma(I)$), 277	4756($I \geq 3\sigma(I)$), 394	3495($I \geq 3\sigma(I)$), 291
Final model; R_1 and R_2	0.0663, 0.0703	0.0778, 0.0884	0 0772, 0.0828